eman ta zabal zazu
Universidad del País Vasco
Euskal Herriko Unibertsitatea

# LIGNIN EXTRACTION, PURIFICATION AND DEPOLYMERIZATION STUDY

Ana Toledano Zabaleta

May 2012

© Servicio Editorial de la Universidad del País Vasco
Euskal Herriko Unibertsitateko Argitalpen Zerbitzua

ISBN: 978-84-9860-779-0
D.G. - L.G.: BI-142-2013

ESCUELA POLITÉCNICA DE SAN SEBASTIÁN
DONOSTIAKO ESKOLA POLITEKNIKOA
Departamento de Ingeniería Química y del Medio Ambiente
Ingeniaritza Kimikorako eta Ingurugiroko Saila

# LIGNIN EXTRACTION, PURIFICATION AND DEPOLYMERIZATION STUDY

**Memory by**
**ANA TOLEDANO ZABALETA**
**for the degree of**
**Doctor of Philosophy in RENEWABLE MATERIALS ENGINEER**

DIRECTOR: Dr. JALEL LABIDI

CO-DIRECTOR: Dr. LUIS SERRANO

Donostia-San Sebastián, 2012

# Summary

Petroleum reverses are depleting, fuel prices are increasing and the push of the environmental policies such as Kioto protocol are forcing the search for new biofuels, biomaterials and biochemicals. Lignocellulosic biomass seems to be a promising raw material for its transformation into the desirable aforementioned bioproducts in the so-called Biorefineries. Bearing this in mind, an entire biorefinery process is proposed in this thesis in order to add value to lignin stream by transforming lignin into simple phenolic monomeric compounds. Agricultural residues were considered as interesting candidates to be used as raw material in biorefinery processes because of their abundance and their low price. In that sense, olive tree pruning was used as raw material in the developed study.

Two lignin revalorization processes were proposed in this thesis to produce high-added value bulk chemicals. Revalorization process schemes were composed of three stages: lignin extraction, lignin purification and lignin depolymerization. Extraction and purification processes were the same for the two proposals. Lignin extraction was studied in the sense of the enhancement of lignin production as well as trying to extract lignin with optimum physicochemical properties for its valorization. To this end, different extraction methods were studied and the one that gave the best results was optimized. Purification process objective was to obtain specific lignin fractions with different characteristics so they can be used in their most adequate application. Different purification processes (differential precipitation and ultrafiltration) were considered with this purpose. Ultrafiltration was selected as the purification process that produced lignin fractions with different purity, specific molecular weight and defined physicochemical properties.

Finally, two catalytic pathways (hydrolysis and hydrogenolysis) were proposed for lignin revalorization into high value added bulk chemicals. Lignin hydrothermal depolymerization was studied in terms of screening the best catalyst (homogeneous catalysts) and of optimizing the reaction conditions (temperature and time). Comparatively, lignin hydrogenolytic depolymerization was also considered in order to reach the same goal. In this sense, different heterogeneous metallic catalysts and hydrogen donating solvents were proposed so as to improve simple phenolic compounds production. The optimized conditions of each depolymerization process were applied to define lignin fractions in order to study the influence of lignin properties on depolymerization reactions yields and to compare which catalytic proposal presented the best challenge for lignin revalorization.

## TABLE OF CONTENTS

**1. Introduction** 1

1.1 Motivation 3

1.2 Biomass as new renewable feedstock 4

1.3. Lignocellulosic biomass 7

1.3.1. Cellulose 9

1.3.2. Hemicelluloses 11

1.4. Lignin 12

1.4.1. Lignin applications 15

1.5. Olive tree pruning 19

1.6. Objective 21

1.7. References 23

**2. Lignin extraction study** 27

2.1. Introduction 29

2.1.1. Objective 33

2.2. Olive tree pruning lignin properties depending on the applied extraction process 33

2.2.1. Materials and methods 34

2.2.2. Liquid fractions characterization 36

2.2.3. Lignin characterization 37

2.2.4. Conclusions 48

2.3. Experimental design for organosolv extraction process optimization 49

2.3.1. Materials and methods 50

2.3.1.1. Lignin characterization 52

2.3.2. Experimental design results 53

2.3.3. Isolated lignins characterization 58

2.3.4. Conclusions 61

2.4. Lignin production from olive tree pruning 62

2.4.1. Organosolv olive tree pruning lignin production 63

2.4.2. Organosolv olive tree pruning lignin characterization 65

2.5. Conclusions 68

2.6. References 71

**3. Lignin purification-fractionation study** 75

3.1. Background 77

3.2. Membrane technology 81

3.2.1. Ultrafiltration 83

3.3. Materials and methods 85

3.4. Ultrafiltration results 87

3.4.1. Ultrafiltered lignin fractions characterization 88

3.5. Conclusions 94

3.6. References 96

**4. Lignin depolymerization by hydrolysis** 99

4.1. Introduction 101

4.1.1. Objective 104

4.2. Materials and methods 105

4.2.1. Products characterization 106

4.3. Effect of the base nature on lignin hydrothermal depolymerization 108

4.3.1. Effect on the oil yield and composition 108

4.3.2. Effect on char formation 113

4.3.3. Effect on residual lignin 114

4.3.4. Conclusions 119

4.4. Effect of reaction conditions on lignin hydrothermal depolymerization 120

4.4.1. Effect on the oil yield and composition 122

4.4.2. Effect on char formation 128

4.4.3. Effect on residual lignin 129

4.4.4. Conclusions 132

4.5. Process for lignin revalorization by hydrothermal depolymerization 133

4.5.1. Effect on the oil yield and composition 134

4.5.2. Effect on char formation 138

4.5.3. Effect on residual lignin 139

4.5.4. Ultrafiltration and hydrolysis as the pathway to 141

revalorize lignin
4.5.5. Conclusions 144
4.6. Improvement of lignin hydrothermal depolymerization 145
4.6.1. Effect on oil yield and composition 146
4.6.2. Effect on char formation 155
4.6.3. Effect on residual lignin 156
4.6.4. Conclusions 160
4.7. Hydrothermal lignin depolymerization conclusions 161
4.8. References 163

**5. Lignin depolymerization by hydrogenolysis** 169
5.1. Introduction 171
5.1.1. Objective 173
5.2. Materials and methods 174
5.2.1. Catalyst preparation and characterization 174
5.2.1.1. Catalyst characterization 175
5.2.2. Products characterization 177
5.3. Effect of the nature of the catalyst on lignin hydrogenolytic depolymerization 179
5.3.1. Materials and methods 180
5.3.2. Catalyst properties and characteristics 181
5.3.3. Effect on oil yield and composition 185
5.3.4. Effect on char formation 191
5.3.5. Effect on residual lignin 192
5.3.6. Conclusions 196
5.4. Effect of hydrogen-donor solvent on lignin hydrogenolytic depolymerization 197
5.4.1. Materials and methods 199
5.4.2. Effect on oil yield and composition 200
5.4.3. Effect on char formation 207
5.4.4. Effect on residual lignin 209
5.4.5. Conclusions 212
5.5. Process proposal for lignin revalorization by hydrogenolytic depolymerization 213
5.5.1. Materials and methods 214

5.5.2. Effect on oil yield and composition 214
5.5.3. Effect on residual lignin 219
5.5.4. Ultrafiltration and hydrogenolysis as the pathway to revalorize lignin 221
5.5.5. Conclusions 223
5.6. Hydrogenolysis depolymerization conclusions 224
5.7. References 226

**6. Conclusions, future work and publications** 231
6.1. Conclusions 233
6.2. Future work 238
6.3. List of publications and presentations 239
6.3.1. Publications 239
6.3.1.1. Scientific articles 239
6.3.1.2. Book chapter 243
6.3.2. Communications 244

**Appendix** 249
Appendix I 251
Appendix II 261
Appendix III 267

List of Figures 271
List of Tables 277

# 1. INTRODUCTION

## 1.1 Motivation

Fossil fuel reserves are running out, oil increasing prices (Figure 1.1), global warming is becoming a reality, waste recycling is becoming ever more costly and problematic, and unrelenting population growth will require more and more energy and consumer products (Octave et al 2009).

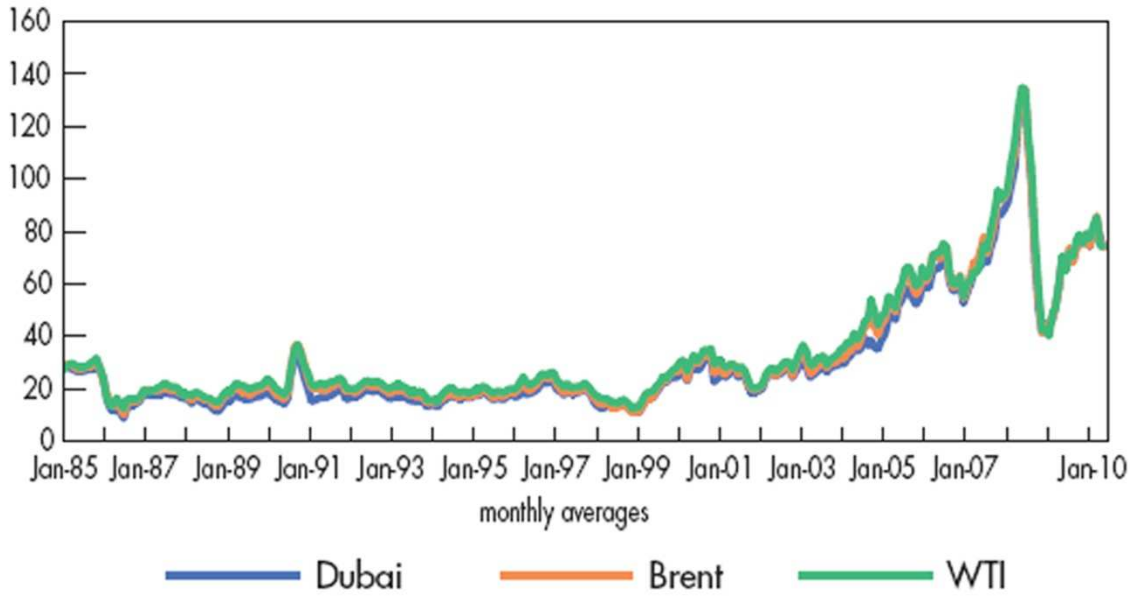


**Figure 1.1.** Key crude oil spot prices in USD/barrel (IEA).

There are many reasons to justify the use of renewable resources (wind, sun, water, biomass and internal earth heat) in order to shift the current oil based economy into the new biobased economy. Anticipated climate changes presumably caused by greenhouse gasses ($CO_2$ atmospheric accumulation) which in turn are caused by fossil fuels burning, security of energy supply, countries energy independence, high and fluctuating energy prices, development of the rural economy could be considered as the driving forces for finding alternative energy sources, renewable materials and ways to increase the energy efficiency of processes for the production of heat,

electricity, transportation fuels, and chemicals (Sanders et al. 2007; Percival Zhang 2008).

Countries across the globe have considered and directed state policies toward the increased and economic utilization of biomass for meeting their future energy demands in order to meet carbon dioxide reduction targets as specified in the Kyoto Protocol as well as to decrease reliance and dependence on the supply of fossil fuels (Sarkar et al. 2012). The European Union Directive 2003/30/EC (Biofuels Directive) adopted in 2003 targeted 2% of all petrol and diesel transport fuels to be biomass-derived by December 2005 and 5.75% by December 2010. This directive was motivated by concerns to ensure the security of the European energy supply, environmental sustainability, and achievement of Kyoto Protocol targets (Ragauskas et al. 2006). In addition, the European Union received 66.1% of its renewable energy from biomass, which thus surpassed the total combined contribution from hydropower, wind power, geothermal energy, and solar power. (Zakzeski et al. 2010). Whereas for energy production a variety of alternative resources (wind, sun, water, biomass, nuclear fission and fusion) can be established, industry based on conversion of sustainable material, for example the chemical industry, industrial biotechnology, and also the fuel generation, depends on biomass, in particular mainly on plant biomass (Kamm et al. 2006).

## 1.2 Biomass as new renewable feedstock

Several governments have recently passed legislation mandating increases in the gross domestic energy and chemical production from renewable resources, especially biomass. The U.S. Department of Agriculture and U.S. Department of Energy set ambitious goals to derive 20% of transportation fuels and 25% of U.S. chemical

commodities from biomass by 2030. As mentioned before, the European Union as a whole has set a mandatory target of 20% for renewable energy's share of energy consumption by 2020 and a mandatory minimum target of 10% for biofuels for all member states. These goals have contributed to the intensified interest in the development of technology and processes for biomass valorization in terms not only for energy production but also to yield biofuels and biomaterials (Figure 1.2) (Zakzeski et al. 2010). Biomass is produced via photosynthesis, which converts light energy to chemical energy, stores it in carbohydrates as "$6CO_2 + 6H_2O \rightarrow C_6H_{12}O_6 + 6O_2$", and fixes atmospheric carbon into biomass (Percival-Zhang 2008).

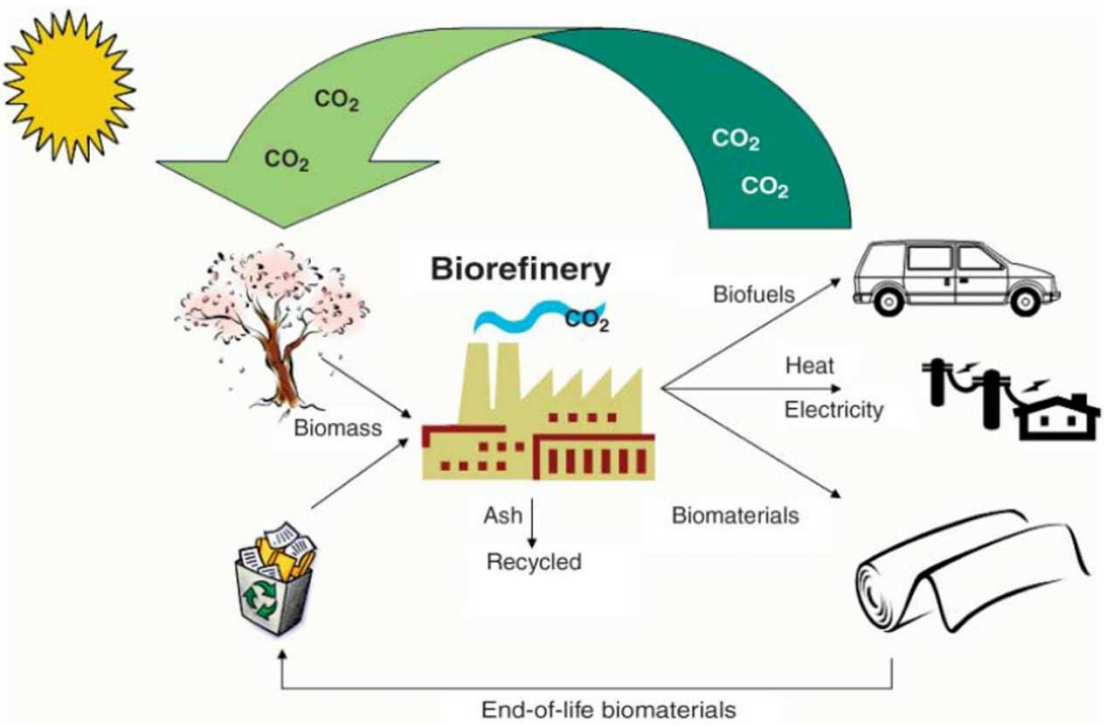


**Figure 1.2.** Biomass biorefiney scheme. Biorefinery inputs and outputs (Ragauskas et al. 2006).

Biomass is defined as the biodegradable fraction of products, waste and residues from biological origin from agriculture (including vegetal and animal substances), forestry and related industries including fisheries and aquaculture, as well as the biodegradable fraction of industrial and municipal waste (Directive 2009/28/EC).

Biomass is an important feedstock for the renewable production of fuels, chemicals, and energy. Biomass is also particularly attractive because it is the only current renewable source of liquid transportation fuel. This, of course, makes it an invaluable way to reduce oil imports. Biomass also has great potential to provide heat and power to industry and to provide feedstock to make a wide range of chemicals and materials or bioproducts (Figure 1.3).

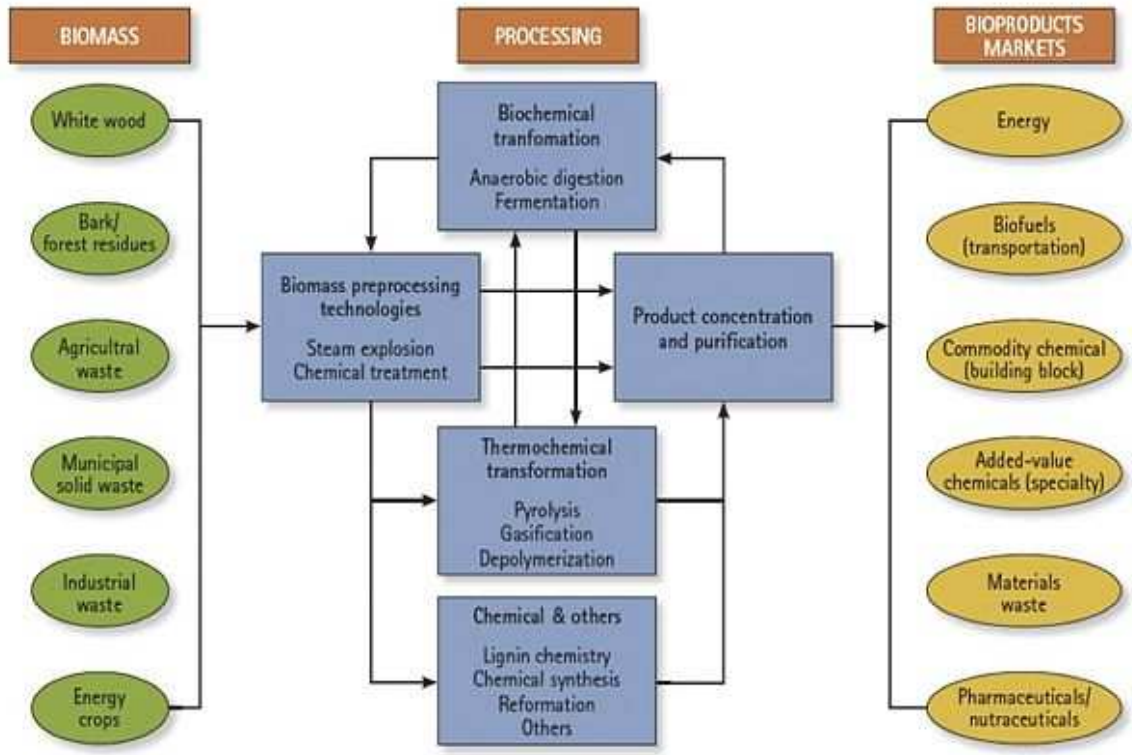


**Figure 1.3.** Biomass schematic utilization possibilities (www.extension.org).

Plant biomass always consists of the basic products carbohydrates, lignin, proteins, and fats, and a variety of substances such as vitamins, dyes, flavors, aromatic essences of very different chemical structure. Biomass, similar to petroleum, has a complex composition. Petrochemistry is based on the principle of generating simple to handle and well defined chemically pure products from hydrocarbons in refineries. In efficient product lines, a system based on family trees has been built, in which basic chemicals, intermediate products, and sophisticated products are produced.

This principle of petroleum refineries must be transferred to biorefineries. Biomass contains the synthesis performance of the nature and has different C:H:O:N ratio from petroleum (Kamm et al. 2006).

## 1.3 Lignocellulosic biomass

Lignocellulose is the most abundant biomass representing near of 70% of the total plant biomass with a yearly production of ~$200 \cdot 10^9$ tons (Percival Zhang 2008). Lignocellulosic feedstock can include straw, switch grass, hybrid poplar, corn stover, reed, wood, agricultural residues, forestry residues, paper and municipal wastes. The main advantages of its utilization are that the natural structures and structural elements are preserved, the raw materials are inexpensive, and large product varieties are possible and the fact that there is no concurrency with food industries. An important point for utilization of biomass as chemical raw material is the cost of raw material. For instance, crude oil price varying from $40 to $80 per barrel (i.e., $7.1–14.2/ GJ) is much higher than the price of lignocellulose ($0–3/ GJ) (Percival Zhang 2008) proving the cost-effective of this raw material.

Lignocellulose biomass contains microfibrils of cellulose, hemicelluloses, lignin and to a minor extent structural proteins, lipids and ash, which together form a complex and rigid structure (Figure 1.4) (Octave et al. 2009). The proportion of these compounds in the different lignocellulose materials depends essentially on the origin of the biomass (woody –hardwood or softwood-; grass and annual plants; energy crops; agricultural residues –straw, husk, bagasse-). These raw materials constitute what it is called second generation biomass and they replace other plant biomass raw materials that are also used for food proposes.

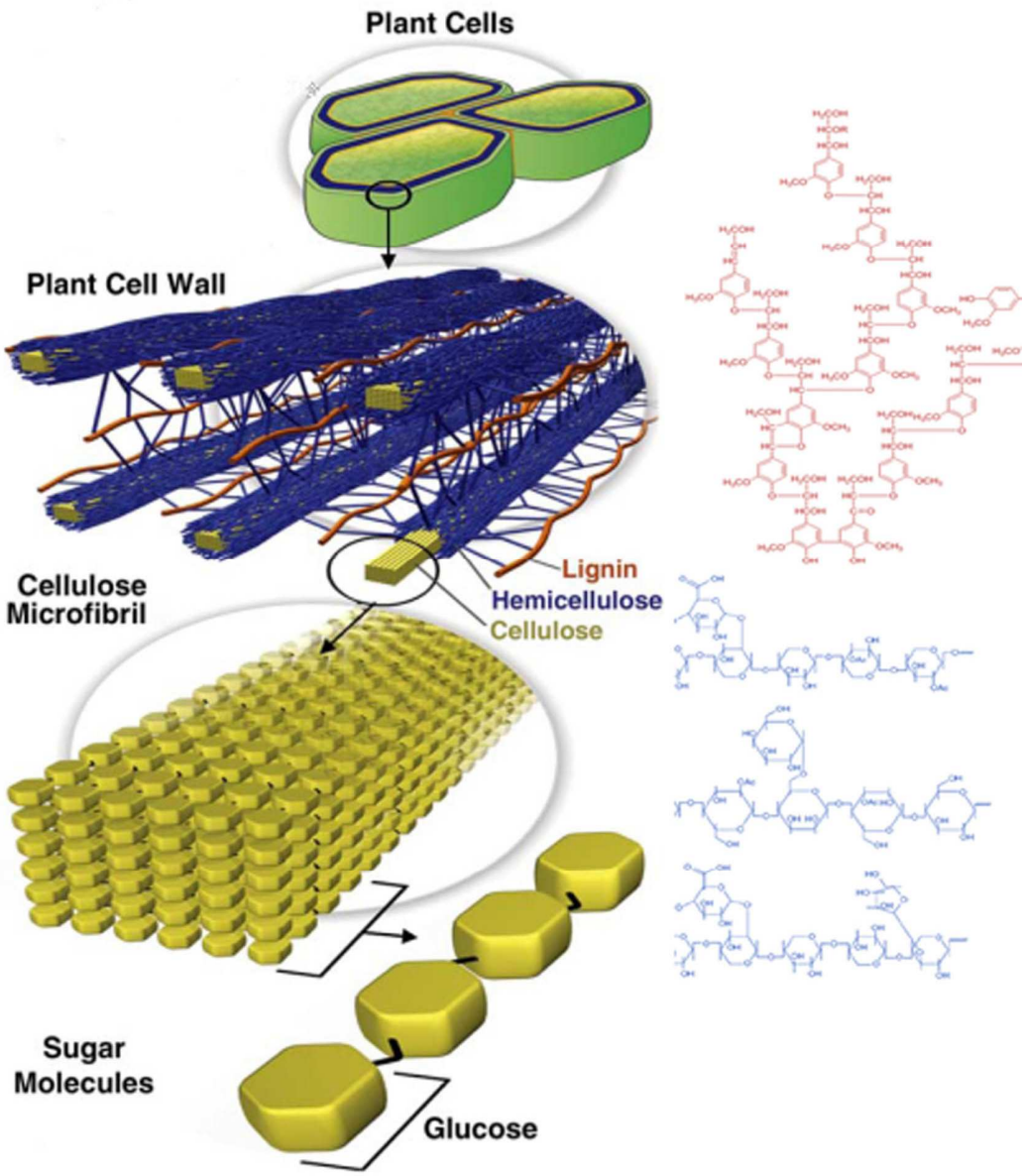


**Figure 1.4.** Schematic of plant cell wall utilization of lignin, hemicellulose and cellulose. Adapted from (Sannigrahi et al. 2010).

Classical uses of this raw material are for paper industries, building and textile that are using only 2% of this type of biomass (Pauly et al. 2008). The green technology biorefinery concept relies on economically feasible processing to achieve a complete utilization of most lignocellulosic biomass components, including lignin, using green technologies (LCF-Biorefinery). Among the potential large-scale industrial biorefineries the lignocellulose feedstock (LCF) biorefinery will most probably be

pushed through with the greatest success. However, an economic analysis report suggests that revenues from the multiple co-products, particularly the lignin, ethanol, and xylose fractions, ensure the economic viability of a small plant (approximately ~100 metric tons per day), which is one-fifteenth the size of a typical ethanol-only lignocellulose (Percival Zhang 2011). The second generation biofuel will be based on lignocellulose transformation triggering the development of biorefineries based on by-products valorization (Schubert 2006). A scheme of LignoCellulosic Feedstock Biorefinery is presented in Figure 1.5 taking into account multiproduct criteria.

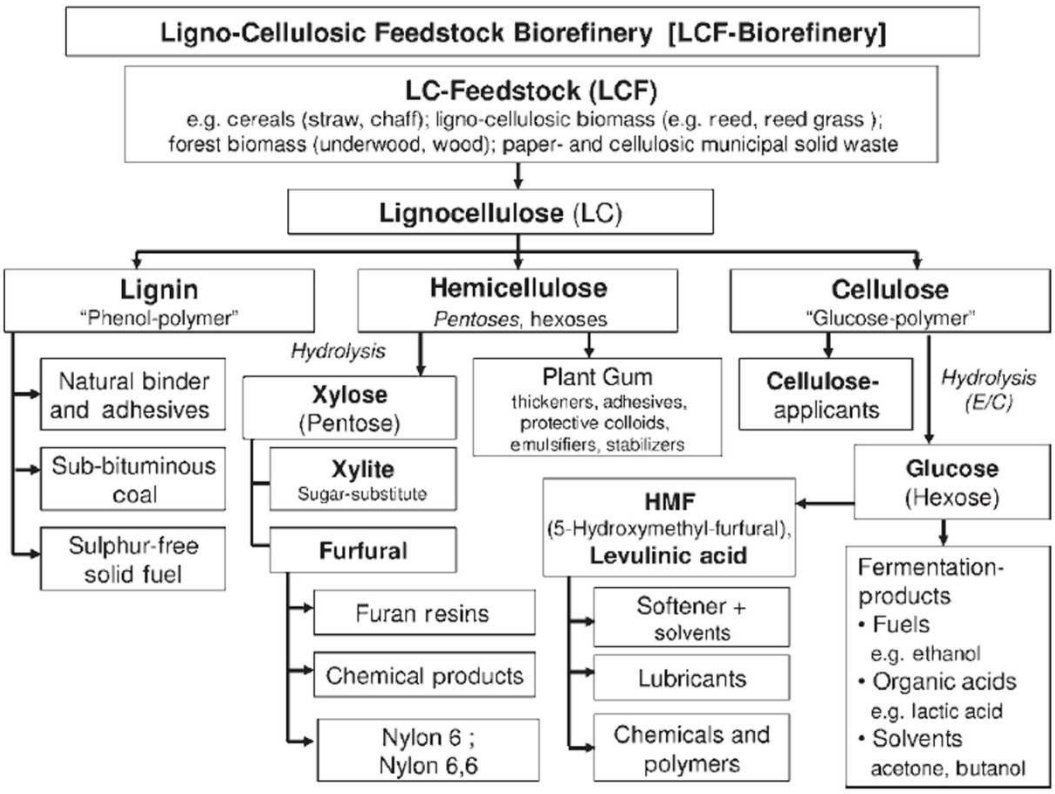


**Figure 1.5.** Example of LCF Biorefinery products scheme (Kamm et al. 2006).

### 1.3.1 Cellulose

Cellulose is the major component of the lignocellulosic materials, representing 40-60% of its total weight in wood (Kamide 2005). Cellulose is a linear biopolymer of

anhydroglucopyranose, connected by $\beta$-1,4-glycosidic bonds (Figure 1.6). Coupling of adjacent cellulose chains by orderly hydrogen bonds and Van der Waal's forces leads to a parallel alignment and a crystalline structure, resulting in low accessibility to enzymes (Percival Zhang 2008). The main function of the cellulose in the plant cell is as structural component. Cellulose in lignocellulosic biomass is usually organized into microfibrils, each measuring about 3 to 6 nm in diameter and containing up to 36 glucan chains having thousands of glucose residues. According to the degree of crystallinity, cellulose is classified into crystalline and paracrystalline (amorphous) cellulose (Zheng et al. 2009).

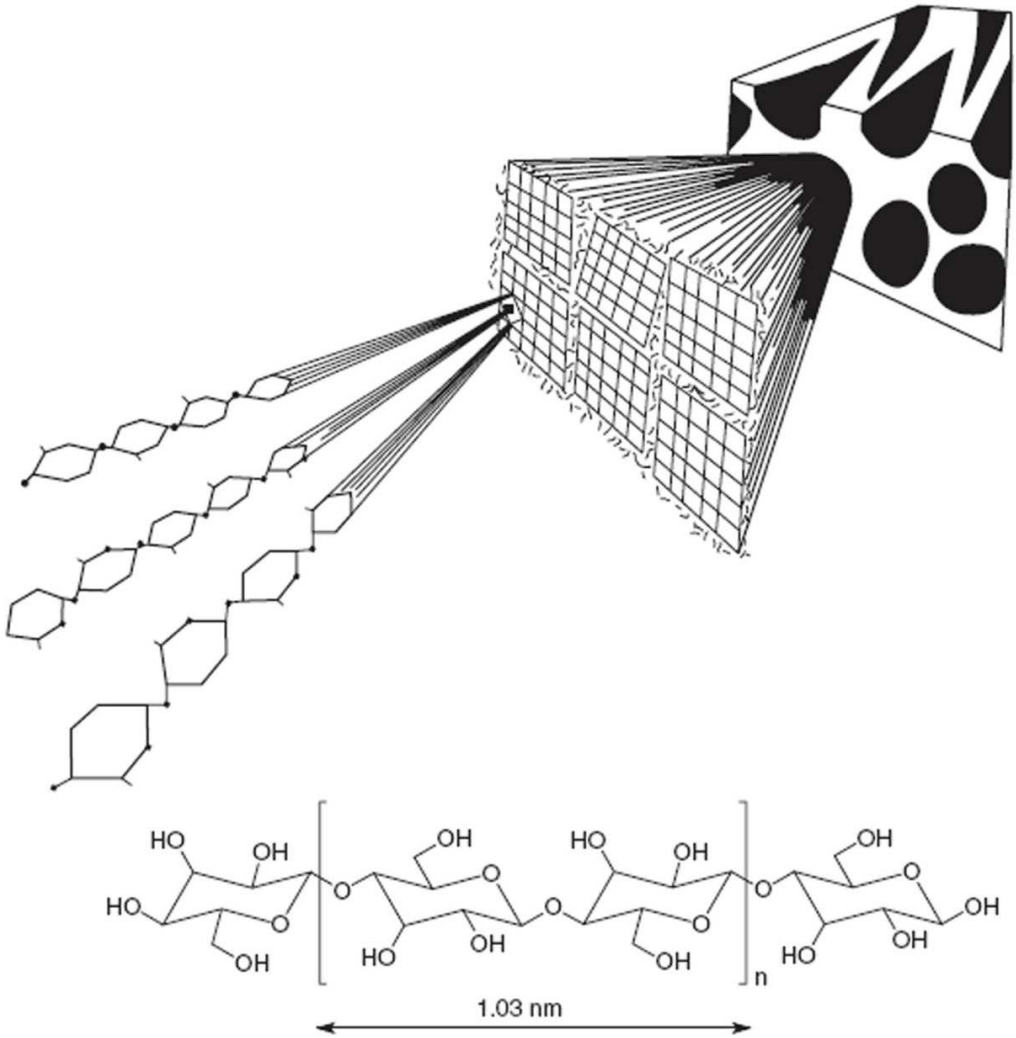


**Figure 1.6.** Schematic view of the components of cellulose fiber (Gandini 2008).

Cellulose is currently used mostly for paper manufacture and bioethanol production but is also used in the production of artificial fibers (cellulose acetate), plastics (cellulose nitrate), explosives (nitrocellulose), thickeners and gelling agents (cellulose ethers such as carboxymethylcellulose , hydroxyethylcellulose and hydroxypropylmethylcellulose) (Clasen et al. 2001).

### 1.3.2 Hemicelluloses

Hemicelluloses, on the other hand, are a large group of polysaccharides found in the primary and secondary cell walls constituting the second most abundant polysaccharide in nature. They are classically defined as alkali soluble material after removal of peptic substances, and have a much lower degree of polymerization (100–200 U) compared with that of cellulose (10,000–14,000). The principle sugar components are d-xylose, d-mannose, d-glucose, d-galactose, l-arabinose, d-glucuronic acid, 4-Omethyl- d-glucuronic acid (MeGlcA), d-galacturonic acid, and to a lesser extent, l-rhamnose, l-fucose, and various O-methylated sugars (Figure 1.7) (Xiao et al. 2001). Hemicelluoses could be classified into four groups (Spiridon 2008):

- Xylans (β-1,4-linked D-xylose units)
- Mannans (β-1,4-linked D-mannose units)
- Arabinans (α-1,5-linked L-arabinose units)
- Galactans (β-1,3-linked D-galactose units)

Xylans are the main hemicelluloses in hardwood and they also predominate in annual plants and cereals making up to 30 per cent of the cell wall material. Hardwood xylan (O-acetyl-4 methyl-glucuronoxylan) is substituted at irregular intervals with 4-O-

methyl-α-D-glucuronic acid groups joined to xylose by α-1,2-glycosidic linkages. On an average, every tenth xylose unit has an uronic acid group attached at C2 or C3 of the xylopyranose.

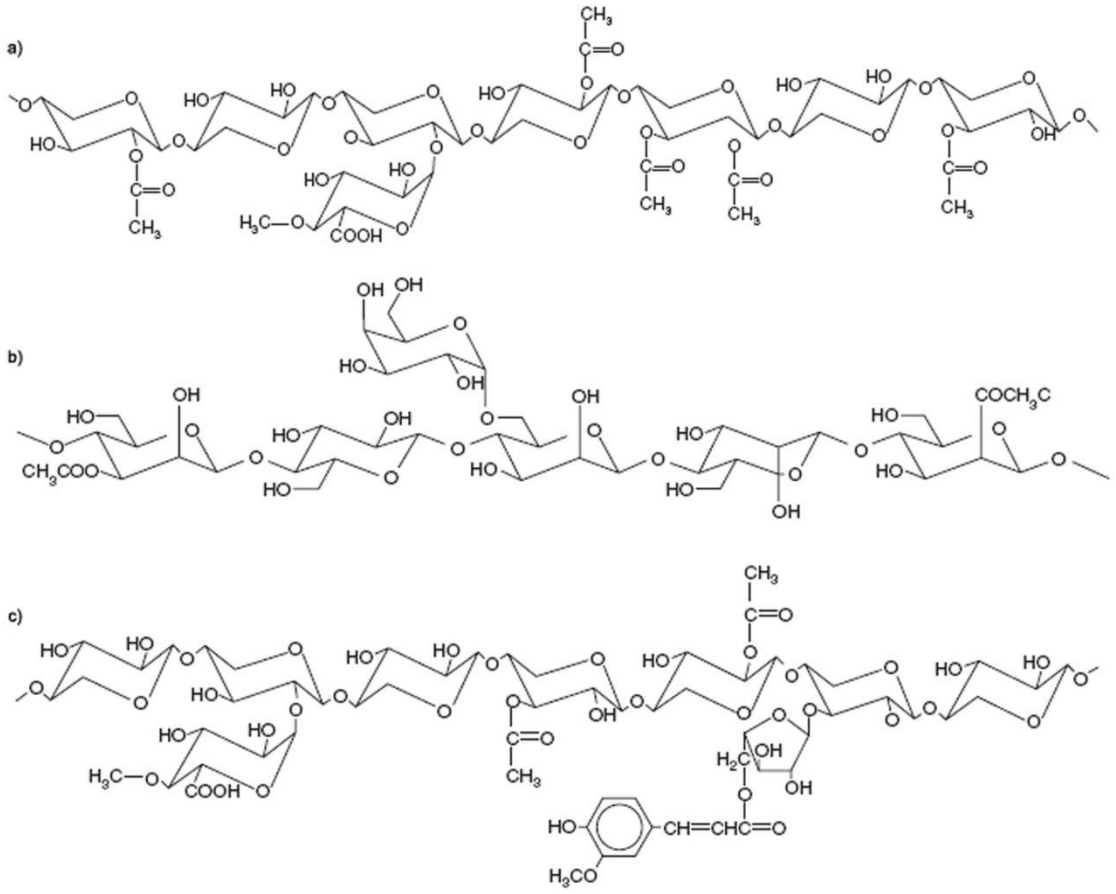


**Figure 1.7.** a) Structure of *O*-acetyl-(4-OMe-glucurono)xylan from hardwood. b) Structure of *O*-acetyl-galactoglucomannan. c) Structure of xylan from annual plants (Spiridon 2008).

## 1.4 Lignin

Lignin is a natural phenolic macromolecule present in the vegetal cell wall that is made up of three main phenylpropane units (monolignols), namely coniferyl alcohol (G), sinapyl alcohol (S) and *p*-coumaryl alcohol (H) (Figure 1.8). Lignin structure is

very complex and consists of a three dimensional randomized net linked to hemicelluloses (LCC). The main function of lignin in the plant is as biological barrier and as the glue that retains hemicelluloses and celluloses linked shaping the cell wall.

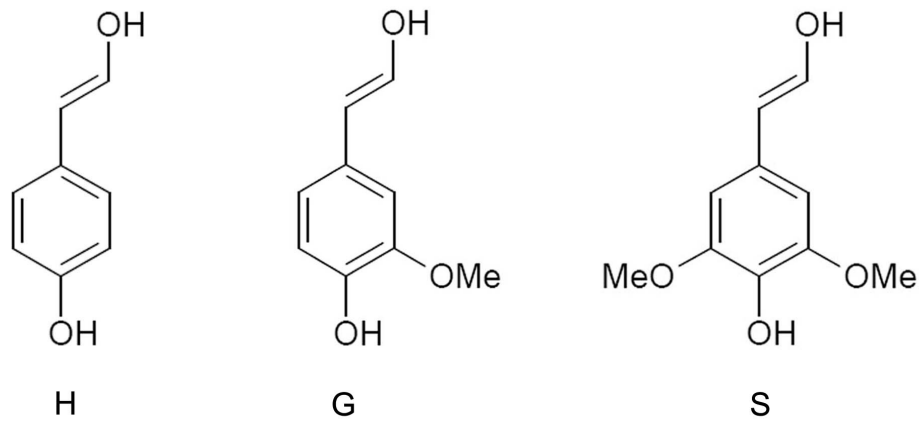


**Figure 1.8.** Most common monolignols in lignin. H: p-coumaryl alcohol. G: conyferil alcohol. S: sinapyl alcohol.

Depending on its origin lignin structure presents differences concerning its monolignol composition. In normal softwood lignin, usually referred to guaiacyl lignin, the structural elements are derived principally from coniferyl alcohol (G) and trace amounts of synapyl alcohol-derived units (S). On the other hand, normal hardwood lignin, termed guaiacyl-syringyl lignins, is comprised of coniferyl alcohol- and sinapyl alcohol-derived units in varying ratios. Grass lignins are also classified as guaiacyl-syringyl lignin. However, unlike hardwood lignins, grass lignins additionally contain small but significant amounts of structural elements derived fron p-coumaryl alcohol (H) (Dence 1992).

Monolignol polymerization is another important step during lignification which remains poorly understood and still needs to be explored further in the context of lignin engineering. In Figure 1.9 it can be observed the structure prosposal of spruce lignin by Adler (1977). The dehydrogenative polymerization of monolignols is thought

to be catalyzed by peroxidases and laccases (Weng et al. 2008). The most important reaction is cross-coupling to the growing polymer to extend the complex three-dimensional lignin network. Each extension of the polymer requires new radicals on each of the two coupling partners. Radicals on the growing lignin polymer are thought to be generated by radical transfer from monolignols or other intermediaries. Once polymerized, the lignin functional groups attached to the basic phenylpropanoid skeleton that provide greater impact on the reactivity of lignin include phenolic hydroxyl, benzylic hydroxyl and carbonyl groups (Dence 1992). The most common linkages formed during lignin biosynthesis are the β-O-4 ether linkages, followed by other types of ether and C–C linkages such as α-O-4, β–β, β-5, and 5-5 (Weng et al. 2008). In Table 1.1 the types and frequencies of the mentioned typical lignin bonds from different studies are presented.

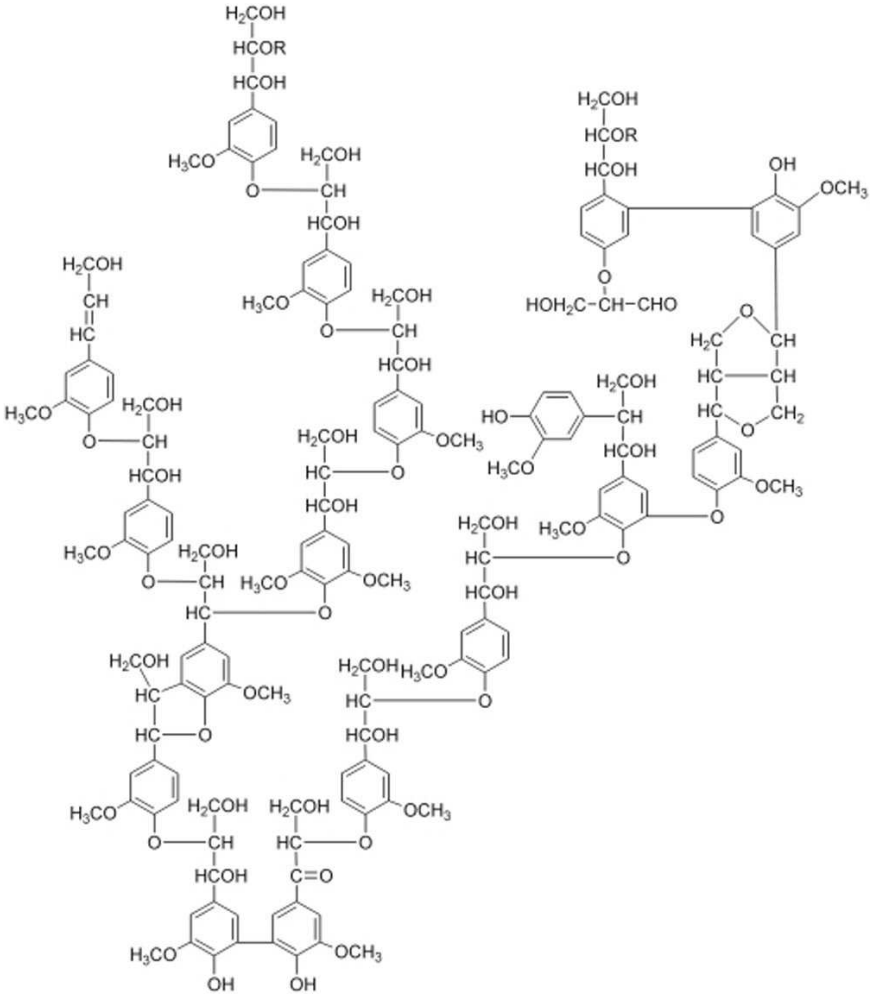

**Figure 1.9.** Structural model of spruce lignin proposed by Adler 1977.

| Linkage | Erikson et al. 1973 | Nimz 1974 | Adler 1977 | Glasser 1981 |
|---|---|---|---|---|
| β-O-4 | 49-51 | 65 | 48 | 55 |
| α-O-4 | 6-8 | | | |
| β-5 | 9-15 | 6 | 9-12 | 16 |
| β-1 | 2 | 15 | 7 | 9 |
| 5-5 | 9.5 | 2.3 | 9.5-11 | 9 |
| 4-O-5 | 3.5 | 1.5 | 3.5-4 | 3 |
| β-β | 2 | 5.5 | 2 | 2 |

**Table 1.1.** Types and frequencies of interunitary linkages by some authors.

### 1.4.1 Lignin applications

The second generation bioethanol plants will have to face not only ethanol production but also by-products valorization for the complete utilization of lignocellulosic raw materials (Octave et al. 2009). Tones of lignins are readily available from the pulp and paper industries and such quantities are expected to increase by the implementation of second generation bioethanol plants (Figure 1.10). The biorefinery concept relies on economically feasible processing to achieve a complete utilization of most lignocellulosic biomass components using as greener technologies as possible. Cost is an important factor for large scale expansion of lignocellusic bioethanol production. Indeed, alone-bioethanol production from lignocellulosic materials is discussed to be economically positive balance (Percival Zhang 2011). By-products (lignin) revalorization is a key economical factor that will ensure second generation bioethanol viability and the biorefineries implementation no matter the main product is paper or bioethanol. In this sense, lignin revalorization is nature's major source of aromatics; new ways are needed to produce small aromatic building blocks from lignin in order to satisfy the enormous and diverse industrial demand for aromatics (Clark et al. 2009).

Nowadays, lignin is available as lignosulfonates coming from pulp and paper industries. For instance, Lignoboost process produces sulfite lignin that can be used as a dispersant (Inventia) (www.inventia.com), Borregard (www.borregard.com) produces lignosulfonates and the also produces lignin derivates, such as vanillin. Many research works have been done to look for an application for lignin beside energy generation. The diversity of functional groups presented in lignin allows its use as dispersant in cement and gypsum blends (Yang et al. 2007; Matsushita et al. 2008), as emulsifier (Boeriu et al. 2004) or chelating agent for removing heavy metals from industrial effluents (Sena-Martins et al. 2008). Likewise, the high complexity of their structural ordering as well as its high porosity has been sources of diverse studies, suggesting lignin as an excellent adsorbent agent, even compared with the activated carbons (Mohan et al. 2006), product that is possible to obtain by means of carbonization treatments of the lignin and its subsequent activation by gasification (Rodriguez-Mirasol et al. 1993).

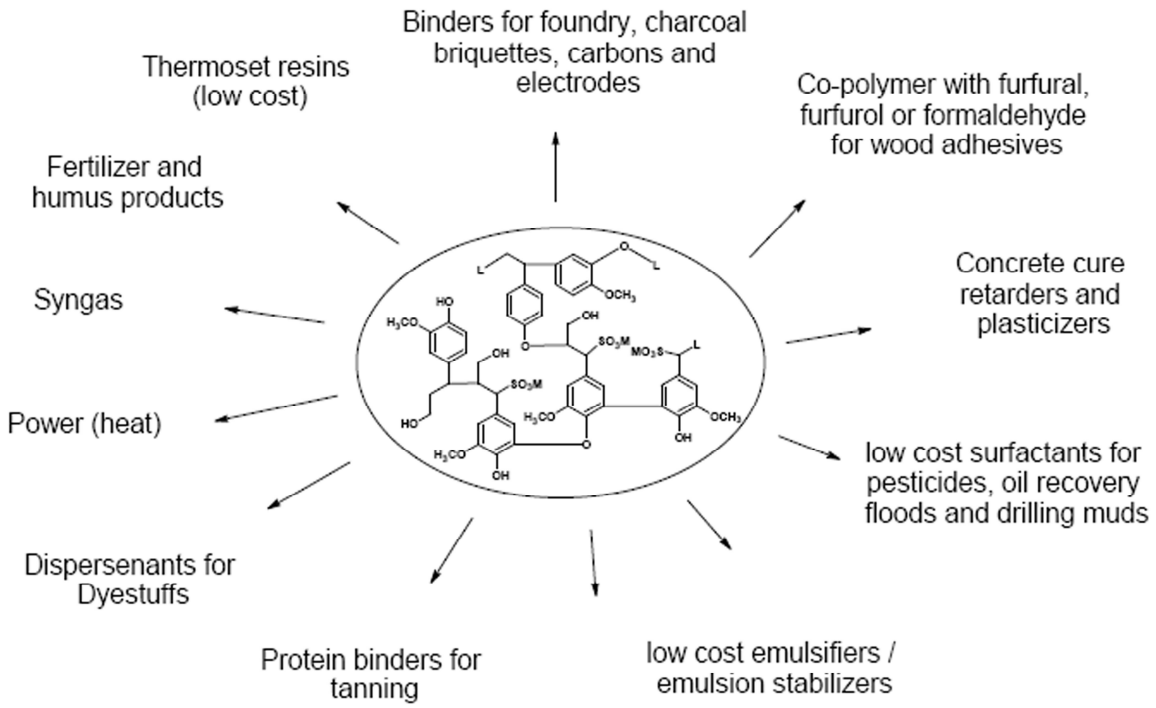


**Figure 1.10.** Current applications of lignosufonates (Bozel et al. 2007).

In addition, lignin is the most abundant source of aromatic compounds in nature and can generate a large amount of chemical reagents or adhesives to replace those derived from oil. This is the case of phenol-formaldehyde resins (El Mansouri et al. 2006; Tejado et al. 2007), in which part of phenol can be replaced by lignin that results more available, less toxic and less expensive than phenol.

Apart from the above applications, the high sulfur content (1–2% w/w) of kraft lignin is also a major reason why its main application has been in energy generation in pulp mills (Doherty et al. 2011). Moreover, lignosulfonates or technical lignins are said to not be suitable for further conversion to value-added chemicals productions because of the presence of sulfur substituent in lignin structure and salts (Percival Zhang 2011; Sannigrahi et al. 2010). In Figure 1.11 it can be observed the relationships between lignin potential markets, production and actual values that confirmed what Percival Zhang and Sannigrahi stated. Figure 1.12 and Figure 1.13 show future applications for sulfur-free lignins.

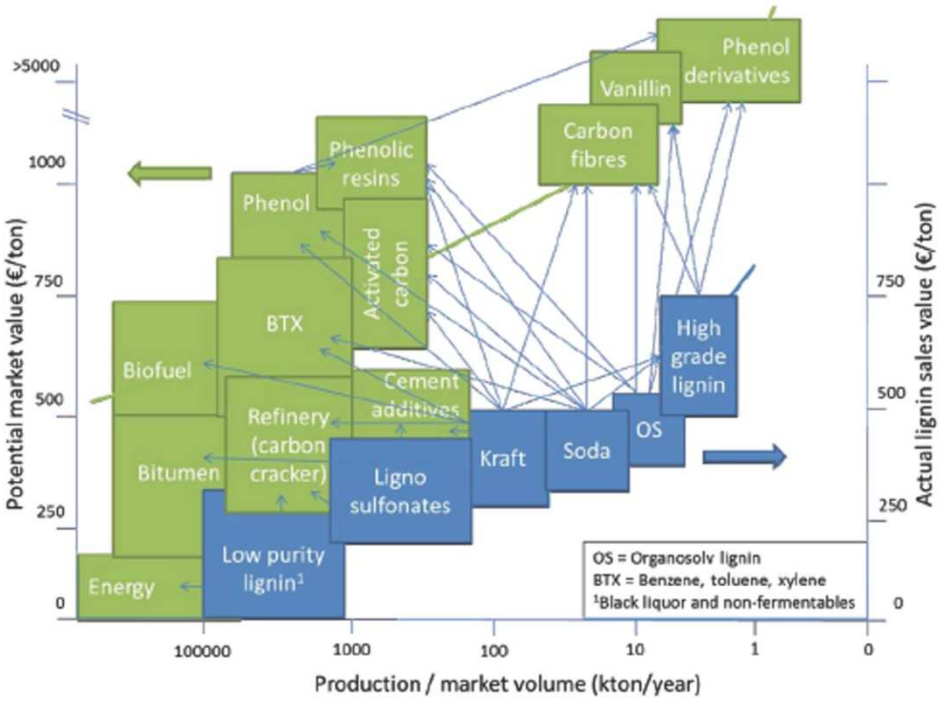


**Figure 1.11.** Lignin production and potential lignin derived product market and value (Gosselink 2011).

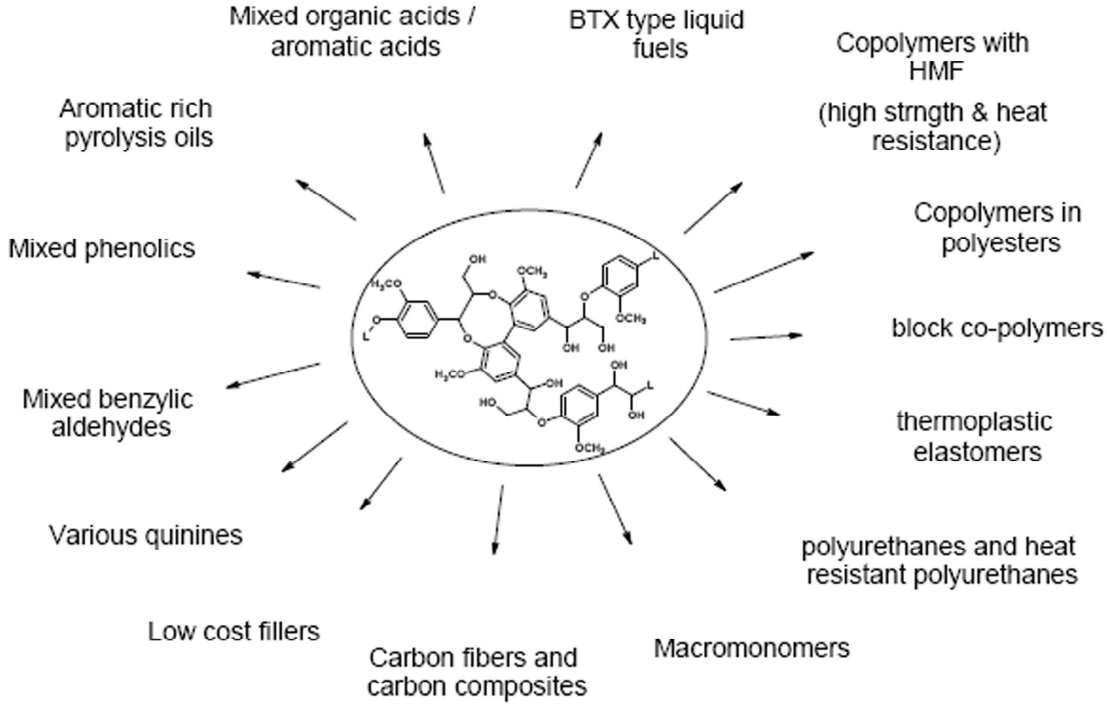


**Figure 1.12.** New product opportunities from lignin (Bozel et al. 2007).

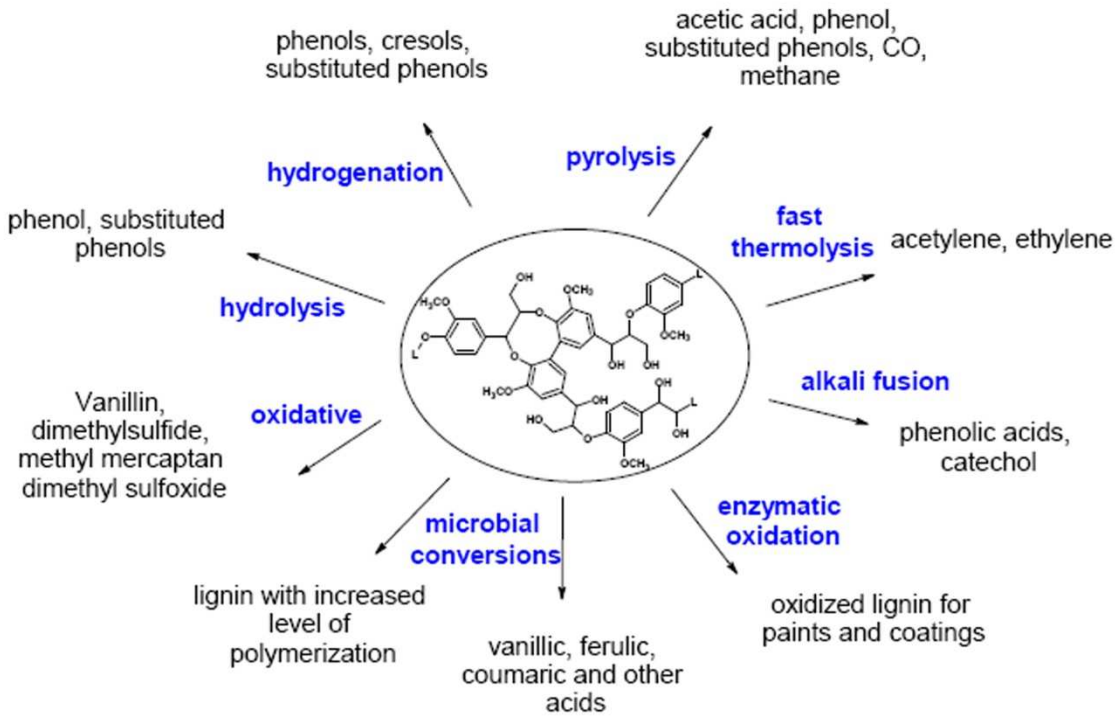


**Figure 1.13.** Summary of lignin catalytic transformations to high added value products (Bozel et al. 2007).

## 1.5 Olive tree pruning

Olive tree (*Olea europaea*) is an evergreen tree, long-lived, reaching 15 m tall, with broad crown and thick trunk, twisted and often very short. Bark is finely fissured, gray or silver. Leaves opposite, 2 to 8 cm long, lanceolate with the apex slightly pointed, entire, coriaceous, glabrous and green by the beam dark gray, paler and densely scaly beneath, more or less sessile or with a short stalk . The olive flowers are bisexual or polygamous, in axillary panicles multifloras, with white corolla. The fruit, the olive is a drupe succulent and very oily from 1 to 3.5 cm long, ovoid or somewhat globular, green at first, which requires a year to acquire black-purple color at full maturity. Flowering period in the northern hemisphere covers between July and August and its fruiting period comprises between September and October. (Enciclopedia Libre Universal en Español)

**Figure 1.14.** Olive tree cultivation field with olive tree pruning.

Olive tree cultivation is spread mainly through the Mediterranean countries being Spain the main producer all over the world. Olive tree pruning (Figure 1.14) is a periodical culture operation by means of which less productive branches are cut off and trees are rejuvenated. This action generates an annual volume of lignocellulosic residues estimated at 3000 kg/ha (Sánchez et al. 2002), thus constituting a widely available and renewable resource. Just in Spain, the main olive oil producer in the world, some $7 \cdot 10^6$ t/year of olive tree pruning biomass are available. A typical pruning lot includes leaves, thin branches and wood. To prevent propagation of vegetal diseases, these residues are commonly grinded and abandoned in the fields or burnt with associated costs, environmental concerns and, till date, no economical alternatives (Romero et al. 2010).

Many works have been published about the utilization of the olive tree pruning by applying different treatments such as hydrothermal conditions or ethanol pulping in order to make profit from the holocellulosic (cellulose + hemicelluloses) fraction to produce paper and bioethanol (Jimenez et al. 2001; Romero et al. 2007; Cara et al. 2008; Ballesteros et al. 2011) and as steam explosion to study the antioxidant capacity of the extractives of the olive tree pruning (Conde et al. 2009). However, none of these studies have been focused on the lignin fraction and its potential use even without thinking that dissolving as much lignin as possible in the liquid fraction favors the two main streams, the solid and the liquid, to be used in their most efficient way.

In this study olive tree pruning (variety Arróniz) was collected from the crop fields in Ayegui, Navarra. Olive tree pruning is composed of leaves, branches and wood. However, in this research leaves were dismissed and so, branches and wood were ground for its utilization.

## 1.6 Objectives

The research work has been focused on studying the lignocellulosic materials biorefinery processes for the production of chemicals and materials, to raise a chemical technology based on the use of biomass as an alternative to petrochemistry.

In these sense, the main objective was lignin revalorization in order to help to overcome the second generation bioethanol plants drawbacks as well as upgrading pulp and paper industries and ligoncellulosic processing industries. Lignin revalorization is a key economical process for these biofuel prodution processes to be cost-effective. The 3R's principles were taken into account for the whole process development: reduce –reducing contamination, reducing used solvents-, reuse –solvent reuse so as not to produce more wastes- and recycle –using agricultural residues as raw material-.

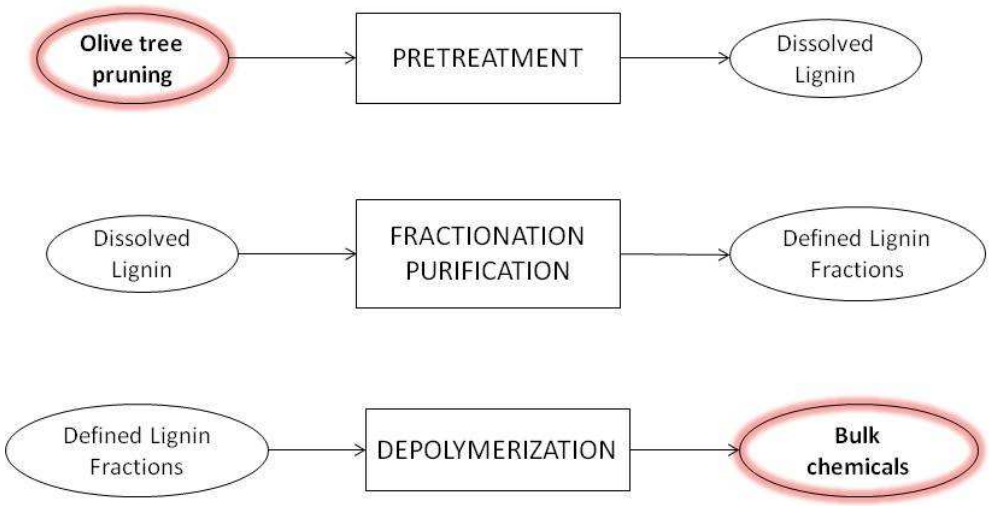


**Figure 1.15.** Scheme of the objectives of this thesis.

After a literature review of the current state of the art technology and new processes related to the use of lignocellulosic material, the experimental work was grouped into three major blocks (Figure 1.15):

- Pretreatment of the lignocellulosic biomass to extract lignin
- Lignin fractionation-purification to obtain specific defined lignin fractions
- Lignin depolymerization to produce high value added bulk chemicals

## 1.7 References

Adler, E. 1977. Lignin chemistry – past, present and future. Wood Sci Technol 11, 169-218.

Ballesteros, I.; Ballesteros, M.; Cara, C.; Sáez, F.; Castro, E.; Manzanares, P.; Negro, M.J.; Oliva, J.M. 2011. Effect of water extraction on sugars recovery from steam exploded olive tree pruning. Bioresour Technol 102, 6611-6616.

Boeriu, C.G.; Bravo, D.; Gosselink, R.J.A.; Van Dam J.E.G. 2004. Characterisation of structure-dependent functional properties of lignin with infrared spectroscopy. Ind Crops Prod 20, 205-218.

Bozel, J.J.; Holladay, J.E.; Johnson, D.; White, J.F. 2007. Top value-added chemicals from biomass. Volume II: results of screening for potential candidates from biorefinery lignin. PNNL and NREL.

Cara, C.; Ruiz, E.; Ballesteros, M.; Manzanares, P.; Negro, M. J.; Castro, E. 2008. Production of fuel ethanol from steam-explosion pretreated olive tree pruning. Fuel 87, 692–700.

Clark, J.H.; Deswarte, F.E.I.; Farmer, T.J. 2009. The integration of green chemistry into future biorefineries. Biofuels Bioprod Bioref 3, 72–90.

Clasen, C.; Kulicke, W.M. 2001. Determination of viscoelastic and rheooptical material functions of water-soluble cellulose derivative. Prog Polym Sci 26, 1839-1937.

Conde, E.; Cara, C.; Moure, A.; Ruiz, E.; Castro, E.; Dominguez, H. 2009. Antioxidant activity of the phenolic compounds released by hydrothermal treatments of olive tree pruning. Food Chem 114, 806–812.

Dence, C.W.; Lin, S.Y. 1992. Methods in lignin chemistry. Springer-Verlag Berlin Heidelberg.

Doherty, W.O.S.; Mousaviouna, P.; Fellows, C.M. 2011. Value-adding to cellulosic ethanol: Lignin polymers. Ind Crops Prod 33, 259–276.

El Mansouri, N.E.; Salvado, J. 2006. Structural characterization of technical lignins for the production of adhesives: application to lignosulfonate, kraft, sodaanthraquinone, organosolv and ethanol process lignins. Ind Crops Prod 24, 8-

16.

Enciclopedia Libre Universal en Español

Erickson, M.; Larsson, S.; Miksche, G.E. 1973. Gas-chromatographische Analyse von Ligninoxydationprodukten. VII. Zur Struktur des Lignins der Fichte. Acta Chem Scand 27, 903-904.

European Union Directive 2003/30/EC.

European Union Directive 2009/28/EC.

Glasser, W.G.; Glasser, H.R. 1981. The evaluation of lignin's chemical structure by experimental and computer simulation techniques. Paperi ja Puu 63(2), 71-83.

Gosselink, R.J.A. PhD Thesis. Wageningen University. 2011

Jimenez, L.; Perez, I.; García, J. C.; Rodríguez, A. 2001. Influence of process variables in the ethanol pulping of olive tree trimmings. Bioresour Technol 78, 63–69.

Kamide, K. 2005. Cellulose and cellulose derivaties: molecular characterization and its applications. Elsevier B.V.

Kamm, B.; Gruber, P.R.; Kamm, M. 2006. Biorefineries – Industrial Processes and Products: Status Quo and future. Wiley-VCH Verlag GmbH & Co. KGaA, Weinheim.

Matsushita, Y.; Imai, M.; Iwatsuki, A.; Fukushima, K. 2008. The relationship between surface tension and the industrial performance of water-soluble polymers prepared forma acid hydrolysis lignin, a saccharification by-product from woody materials. Bioresour Technol 99, 3024–3028.

Mohan, D.; Pittman, C.U.; Steele, P.H. 2006. Single, binary and multi-component adsorption of copper and cadmium from aqueous solutions on Kraft lignin –a biosorbent. J Colloid Interface Sci 297, 489-504.

Nimz, H.H. 1974. Beech lignin – proposal of a constitutional scheme. Angew Chem Int Ed 13, 313-321.

Octave, S.; Thomas, D. 2009. Biorefinery: Toward an industrial metabolism. Biochimie 91, 659–664.

Pauly, M.; Keegstra, K. 2008. Cell-wall carbohydrates and their modification as a resource for biofuels. The Plant Journal 54, 559–568.

Percival Zhang, Y.-H. 2008. Reviving the carbohydrate economy via multi-product lignocellulose biorefineries. J Ind Microbiol Biotechnol 35, 367–375.

Percival Zhang, Y.-H. 2011. What is vital (and not vital) to advance economically-competitive biofuels production. Process Biochem 46, 2091–2110.

Ragauskas, A.J.; Williams, C.K.; Davison, B.H.; Britovsek, G.; Cairney, J.; Eckert, C.A.; Frederick Jr., W.J.; Hallett, J.P.; Leak, D.J.; Liotta, C.L.; Mielenz, J.R.; Murphy, R.; Templer, R.; Tschaplinski, T. 2006. The path forward for biofuels and biomaterials. Science 311, 484-489.

Rodriguez-Mirasol, J.; Cordero, T.; Rodriguez, J.J. 1993. Preparation and characterization of activated carbons from eucalyptus kraft lignin. Carbon 31, 87-95.

Romero, I.; Moya, M.; Sánchez, S.; Ruiz, E.; Castro, E.; Bravo, V. 2007. Ethanolic fermentation of phosphoric acid hydrolysates from olive tree pruning. Ind Crops Prod 25, 160–168.

Romero, I.; Ruiz, E.; Castro, E.; Moya, M. 2010. Acid hydrolysis of olive tree biomass. Chem Eng Res Des 88, 633–64.

Sánchez, S.; Moya, A. J.; Moya, M.; Romero, I.; Torrero, R.; Bravo, V.; San Miguel, M. P. 2002. Aprovechamiento del residuo de poda del olivar. Ing Quim 34, 194–202.

Sanders, J.; Scott, E.; Weusthuis, R.; Mooibroek, H. 2007. Bio-Refinery as the bio-inspired process to bulk chemicals. Macromol Biosci 7, 105–117.

Sannigrahi, P.; Pu, Y.; Ragauskas, A. 2010. Cellulosic biorefineries—unleashing lignin opportunities. Current Opinion in Environmental Sustainability 2, 383–393.

Sarkar, N.; Ghosh, S.K.; Bannerjee, S.; Aikat, K. 2012. Bioethanol production from agricultural wastes: An overview. Renew Energ 37, 19-27.

Schubert, C. 2005. Can biofuels finally take center stage? Nature Biotechnol 24, 777–784.

Sena-Martins, G.; Almeida-Vara, E.; Duarte, J.C. 2008. Eco-friendly new products

form enzymatically modified industrial lignins. Ind Crops Prod 27, 189-195.

Spiridon, I.; Popa, V.I. 2008.Monomers, Polymers and Composites from Renewable Resources. Elsevier.

Tejado, A.; Peña, C.; Labidi, J.; Echeverria, J.M.; Mondragon, I. 2007. Physicochemical characterization of lignins from different sources for use in phenol-formaldehyde resin synthesis. Bioresour Technol 98, 1655-1663.

Weng, J.-K.; Li, X.; Bonawitz, N.D.; Chapple, C. 2008. Emerging strategies of lignin engineering and degradation for cellulosic biofuel production. Current Opinion in Biotechnology 19, 166–172.

www.extension.org

Xiao, B.; Sun, X.F.; Sun, R.C. 2001. Chemical, structural, and thermal characterizations of alkali-soluble lignins and hemicelluloses, and cellulose from maize stems, rye straw, and rice straw. Polym Degrad Stabil 74, 307–319.

Yang. D.; Qiu, X.; Zhou, M.; Lou, H. 2007. Properties of sodium lignosulfonate as dispersant of coal water slurry. Energ Convers Manage 48, 2433-2438.

Zakzeski, J.; Bruijnincx, P.C.A.; Jongerius, A.-L.; Weckhuysen, B.M. 2010. The Catalytic Valorization of Lignin for the Production of Renewable Chemicals. Chem Rev. 110 (6), 3552-99.

# 2. LIGNIN EXTRACTION STUDY

## 2.1 Introduction

Lignin is one of the main components of lignocellulosic biomass. The aim of the lignocellulosic fractionation process is to breakdown the cell wall structure in order to separate each component (cellulose, hemicelluloses and lignin).

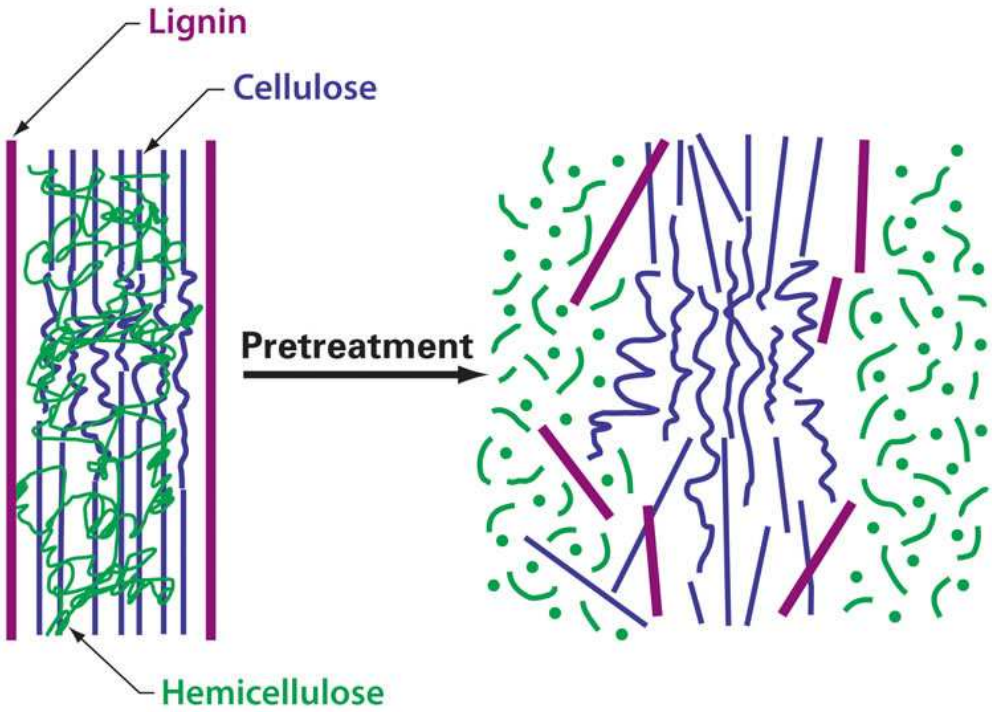


**Figure 2.1.** Schematic of goals of pretreatment on lignocellulosic material (Mosier et al. 2005).

The objective of pretreating lignocellulosics is to alter the structure of biomass and to make the cellulose and hemicelluloses more accessible/amenable to hydrolytic enzymes or more accessible for pulp or fibers production. Effective pretreatment technologies need to address several important criteria depending on the final utilization of each component, including (Sannigrahi et al. 2010, Fengel et al. 1984):

- Minimization of hemicelluloses degradation products
- Limiting the formation of by-products that inhibit ethanol fermentation
- Reducing energy/water use and lowering environmental impacts (air and water pollution)

- Capital and operating costs
- Reduction the amounts of chemicals required for the pretreatments
- Flexibility process for raw materials and products if possible

Pretreatment techniques have been developed in order to reach these requirements for various end uses of biomass feedstock. They can be classified into three groups: physical processes (mechanical pulping), chemical treatments and biological methods. In some cases, different treatments are combined to increase the final yields. Physical processes include stone grinding, refiner mechanical pulping… These are based on the defibration of the lignocellulosic material to single fibers and fiber bundles, and fibrillation involving the conversion of fibers to fibrillar elements (Fengel et al. 1984). The energy requirements for physical pretreatments are dependent on the final particle size and reduction in crystallinity of the lignocellulosic material and thus, generally physical processes are expensive and likely will not be used in a full-scale process (Brodeur et al. 2011). Biological pretreatments employ wood degrading microorganisms, including white-, brown-, soft-rot fungi, and bacteria to modify the chemical composition and/or structure of the lignocellulosic biomass so that the modified biomass is more amenable to enzyme digestion. However, its disadvantages are as apparent as its advantages since biological pretreatment is very slow and requires careful control of growth conditions and large amount of space to perform treatment. In addition, most lignolytic microorganisms solubilize/consume not only lignin but also hemicellulose and cellulose. Therefore, the biological pretreatment faces technoeconomic challenges and is less attractive commercially (Zheng et al. 2009). Among all chemical pretreatments that have been developed, in these studies, sulfur-free technologies were the only ones considered for lignin revalorization. In Table 2.1, a compendium of sulfur-free chemical pretreatments can be found. There, each pretreatment disadvantage and advantage derived from their used was also summarized.

| Pretratment | Advantages | Disadvantages |
|---|---|---|
| Alkali | • Efficient removal of lignin<br>• Low inhibitor formation | • High cost of alkaline catalyst<br>• Alteration of lignin structure |
| Acid | • High glucose yield<br>• Solubilizes hemicellulose | • High costs of acids and need for recovery<br>• High costs of corrosive resistant equipment<br>• Formation of inhibitors |
| Green solvents[1] | • Lignin and hemicellulose hydrolysis<br>• Ability to dissolve high loadings of different biomass types<br>• Mild processing conditions (low temperatures) | • High solvent costs<br>• Need for solvent recovery and recycle |
| Steam | • Cost effective<br>• Lignin transformation and hemicellulose solubilization<br>• High yield of glucose and hemicellulose in two-step process | • Partial hemicellulose degradation<br>• Acid catalyst needed to make process efficient with high lignin content material<br>• Toxic compound generation |
| LHW[2] | • Separation of nearly pure hemicellulose from rest of feedstock<br>• No need for catalyst<br>• Hydrolysis of hemicellulose | • High energy/water input<br>• Solid mass left over will need to be dealt with (cellulose/lignin) |

| Pretratment | Advantages | Disadvantages |
|---|---|---|
| AFEX[3] | • High effectiveness for herbaceous material and low lignin content biomass<br>• Cellulose becomes more accesible<br>• Causes inactivity between lignin and enzymes<br>• Low formation of inhibitors | • Recycling of ammonia is needed<br>• Less effective process with increasing lignin content<br>• Alters lignin structure<br>• High cost of ammonia |
| ARP[4] | • Removes majority of lignin<br>• High cellulose content after pretreatment<br>• Herbaceous materials are most affected | • High energy costs and liquid loading |
| Organosolv | • Enzime accesible cellulose<br>• Hemicelluloses solubilization<br>• Low molecular weight pure lignin | • High pressure reactor<br>• Solvents recover and recycle |
| Supercitrical fluid | • Low degradation of sugars<br>• Cost effective<br>• Increases cellulose accessible area | • High pressure requirements<br>• Lignin and hemicelluloses unaffected |

[1]Green solvents: ionic liquids
[2]LHW: liquid hot water
[3]AFEX: ammonia fiber explosion
[4]ARP: Ammonia Recycle Percolation

**Table 2.1.** Chemical (sulfur-free) lignocellulosic pretreatments. (Brodeur et al. 2011, Fengel et al. 1984)

### 2.1.1 Objective

The main purpose of this chapter was to fractionate the lignocellulosic biomass (olive tree pruning) taking into account obtained lignin structure. Since the aim of the thesis was lignin revalorization, a different outlook is proposed focusing the lignocellulosic fractionation process on lignin instead of cellulose.

First, a study was conducted on the influence that the applied chemical pretreatment provided to the final lignin structure and physicochemical properties. The objective of this study was to select the chemical pretreatment that produces the best quality lignin. Then, the selected chemical process was optimized for the olive tree pruning. The optimization was carried out applying a 23 experimental design. Finally, the optimum conditions were applied in order to produce high quality lignin that would be used in the following chapters.

## 2.2 Olive tree pruning lignin properties depending on the applied extraction process

The aim of this work was to characterize olive tree pruning lignin and to evaluate the effect of the applied extraction conditions on the final lignin structure and properties. With this purpose, olive tree pruning was subjected to three different treatments: alkali fractionation, autohydrolysis and organosolv process. Lignin applications depend primarily on the development of the production of sulfur-free high-quality lignin. Most technical lignins – Kraft sulfur-containing lignin and lignosulfonate – are not suitable for further conversion to value-added products (Percival Zhang 2011).

After isolating the obtained lignins, structural, composition and functional groups analyses were carried out in order to establish olive tree pruning lignin physicochemical properties.

### 2.2.1 Materials and methods

Olive tree pruning (Olea Europa, Arróniz variety) was kindly supply by the independent producer Luis Angel Toledano. It was locally collected and then dried at room temperature. The olive tree pruning (branches and wood) was ground in a Retsch 2000 hammer mill to produce 4-6 cm chips free of small stones, dust, and soil. Obtained wood chips were then characterized following TAPPI standards (Appendix I): ash content 3.1% ± 0.4, solubility in hot water 23.3% ± 1.3, solubility in 1% NaOH 34.4% ± 1.9, ethanol-toluene extractives 9.5% ± 0.4, acid-insoluble lignin 23.2% ± 0.7, and holocellulose 66.8% ± 1.2, α-cellulose 58.4% ± 0.5, and hemicelluloses 8.4% ± 0.3.

Olive tree pruning was subjected to different treatments in order to establish the delignification conditions influence on lignin structure. Three sulfur-free treatments were selected for lignocellulosic biomass fractionation: alkali, autohydrolysis and ethanol organosolv processes.

Alkali treatment was selected since pulp and paper industries use these conditions to produce paper obtaining black liquors rich in lignin as by-product. The olive tree pruning was treated with 7.5% (w/w) sodium hydroxide solution, solid:liquid ratio 1:6. The reaction was carried out in a 20 L glass reactor at 90 ºC for 90 minutes at atmospheric pressure. The liquid fraction, where the lignin was dissolved, was treated with sulfuric acid until reaching, approximately, pH 2. The precipitated alkali

lignin (AL) was isolated by centrifugation (4000 rpm, 15 minutes). Then, the isolated lignin was dried at 50 ºC.

Autohydrolysis process produces hemicellulosic sugars along with lignin. Olive tree pruning was charged in a 4 L pressure stainless steel batch reactor (EL0723 Iberfluid) controlled by Adkir software. The solid:liquid ratio was 1:6. The hydrolysis was carried out at 180 ºC for 30 minutes. Due to the low total dissolved solids content of the hydrolysis liquid fraction, this liquor was concentrated up to 50% of total dissolved solids before lignin precipitation. Two acidified water volumes (pH around 2) were added to the concentrated liquor to precipitate the lignin. The autohydrolysis lignin (HL) isolation was performed by centrifugation (4000 rpm, 20 minutes) and then, it was dried at 50 ºC.

Olive tree pruning was also subjected to ethanol organosolv treatment. Fractionation applied conditions consisted of a mixture of ethanol and water (60%, w/w), a solid:liquid ratio of 1:6 at 180 ºC for 90 minutes. The reaction was carried out in a 1500 mL pressure stainless steel reactor (Parr 4836) equipped with a heating mantle, mechanical stirrer, and a manometer. The liquid fraction was treated to precipitate the dissolved lignin. Two volumes of acidified water (pH around 2) were added to a known volume of liquid fraction in order to precipitate the lignin. The precipitated organosolv lignin (OL) was then separated by centrifugation (4000 rpm, 20 minutes) and dried at 50 ºC.

Alkali lignin (AL), autohydrolysis lignin (HL) and organosolv lignin (OL) were deeply characterized in order to determine their structure and composition. The analytical procedures for lignin characterization can be found in Appendix II. The analyses

comprise structural techniques such as attenuated-total reflection infrared spectroscopy (ATR-IR), nuclear magnetic resonance (NMR-HSQC), alkaline nitrobenzene oxidation, high performance size exclusion chromatography (HPSEC); composition analyses such as acid insoluble lignin (AIL), acid soluble lignin (ASL), sugars content, ash content and functional groups determination (carboxyl groups, carbonyl groups and total phenolic groups).

### 2.2.2 Liquid fractions characterization

Lignin was isolated from the different liquid fractions obtained by the applied pretreatments. Liquid fractions were physicochemically characterized following internal procedures (Appendix III) (Table 2.2). Lignin concentration in the liquid fractions was determined in order to evaluate which extraction process was more effective.

| | **Alkali** | **Autohydrolysis** | **Organosolv** |
|---|---|---|---|
| pH | 13.79 ± 0.01 | 3.52 ± 0.02 | 4.46 ± 0.02 |
| Density (g/mL) | 0.9986 ± 0.001 | 1.0847 ± 0.001 | 0.9021 ± 0.003 |
| Total dissolved solids (%) | 12.13 ± 0.09 | 4.74 ± 0.10 | 7.64 ± 0.04 |
| Inorganic matter (%) | 8.43 ± 0.12 | 0.11 ± 0.02 | 0.05 ± 0.00 |
| Organic matter (%) | 3.70 ± 0.03 | 4.63 ± 0.08 | 7.59 ± 0.03 |
| Lignin concentration (g/L) | 55.5 ± 0.07 | 0.59 ± 0.06 | 31.8 ± 0.03 |

**Table 2.2.** Physicochemical properties of the liquid fractions (dissolved lignin) obtained after applying different pretreatments to olive tree pruning.

Alkali treatment yielded the highest lignin concentrated liquid fraction (55.5 g/L) but, at the same time, alkali treatment presented the highest content of inorganic matter, being this value higher than its organic matter content. This observation could be

related to the high concentrated NaOH solution employed during the pretreatment to extract the lignin. Autohydrolysis pretreatment dissolves lignin but the real aim of this pretreatment is hemicelluloses solubilization. This is the reason why lignin concentration in autohydrolysis liquid fraction was so low. Liquid fractions from organosolv and autohydrolysis processes were mainly composed of organic compounds. The slightly low pH of the liquid fractions obtained by organosolv and autohydrolysis was caused by the fact that, during hemicelluloses degradation, some organic acids (acetic acid and formic acid) are formed.

### 2.2.3 Lignin characterization

The ATR-IR spectra of the different lignins are shown in Figure 2.2. Around 3345 $cm^{-1}$ it can be observed a wide vibration caused by the stretching of the O-H group, the intensity of this band varied between experiments proving that the different conditions used in the delignification process affected the extracted lignin structure. All spectra presented bands between 2930 and 2845 cm-1 that corresponded to the vibration of C-H bond in methyl and methylene groups. The asymmetric deformation of this bond also produced a band at around 1460 $cm^{-1}$. Three typical vibrations appeared in aromatic compounds such as lignin, these bands were exhibited around 1595, 1515 and 1425 $cm^{-1}$. Therefore, phenylpropane units (lignin skeleton) were identified in all extracted lignins. The vibration at around 1710 $cm^{-1}$ was associated to the C=O bond stretching in unconjugated ketones, carbonyl and ester groups while the vibration at around 1660 $cm^{-1}$ was related to the C=O bond stretching in conjugated p-substituted aryl ketones. The most significant bands in lignin spectra were those that corresponded to its main substructures (Figure 2.3) - guaiacylpropane (G), syringylpropane (S) and p-hydroxyphenylpropane (H) - such as the peak around 1330 $cm^{-1}$ that was related to the breathing of the syringyl ring with C-O stretching and the bands at around 1270 $cm^{-1}$ (shoulder) and 1220 $cm^{-1}$ that

were associated to the breathing of the guaiacyl ring with C-O stretching. Around 1150 $cm^{-1}$ a vibration can be distinguished that was caused by the deformation of the bond C-H in guaiacyl substructures while the same linkage but in syringyl substructures appeared at around 1120 $cm^{-1}$. The absence of some of these bands (1120 and 1330 $cm^{-1}$) in alkali lignin spectra suggested that the contamination of this sample was high enough to disguise these typical lignin subunit wavelengths.

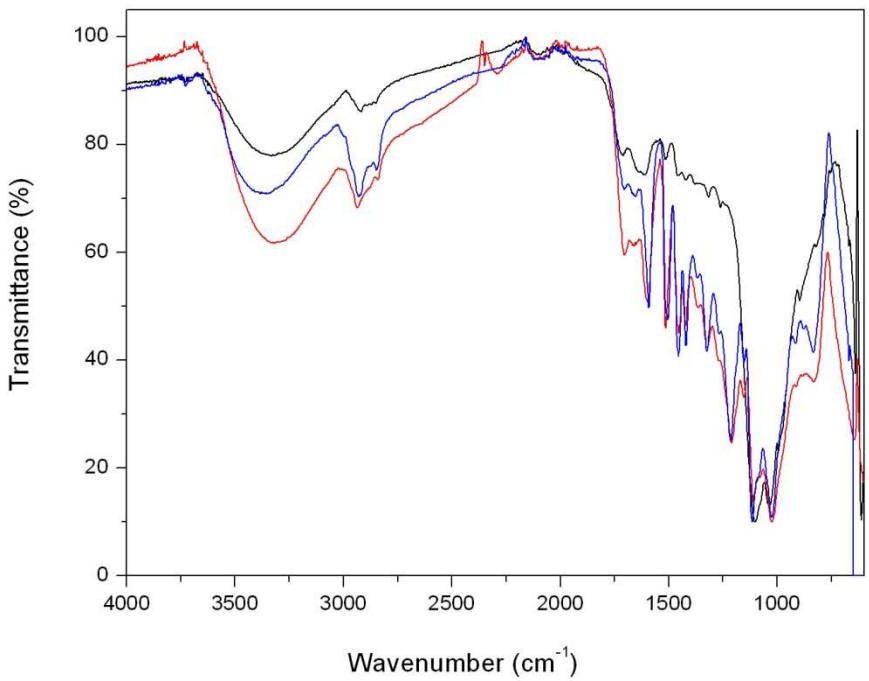


**Figure 2.2.** Olive tree pruning lignins ATR-IR spectra (4000-600 $cm^{-1}$). AL (black), HL (red) and OL (blue).

The vibration at around 1030 $cm^{-1}$ was due to the deformation or the aromatic C-H linkages in guaiacyl substructures and as well it can be related to the deformation of the bond C-O in primary alcohols. Finally, at around 835 $cm^{-1}$ there was a vibration caused by the linkage C-H in positions 2 and 6 in syringyl substructures and in all positions in H substructures. In the AL spectrum, at 1645 $cm^{-1}$ a band was observed that was associated with absorbed water. This band usually appeared in polysaccharides spectra. Bands between 1125 and 1000 $cm^{-1}$ are typical of xylans.

The prominent band at 1038 $cm^{-1}$ was due to the C–O, C–C stretching or C–OH bending in hemicelluloses. The sharp band at around 900 $cm^{-1}$ was related to β-linkage between the sugar units (Xiao et al. 2001). Some wavelengths could be associated to lignin structure as well as to polysaccharides. Further analyses would clarify their origin.

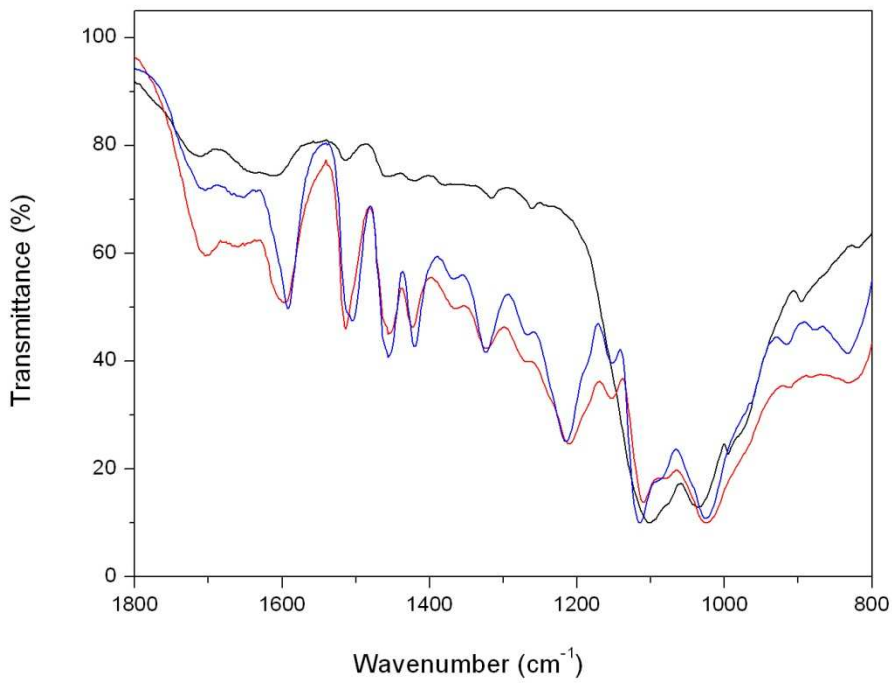


**Figure 2.3.** Olive tree pruning lignins magnified ATR-IR spectra (1800-800 $cm^{-1}$). AL (black), HL (red) and OL (blue).

Lignin typical bands could be appreciated in organosolv lignin, alkali lignin and hydrolysis lignin. However, the intensity of these bands varied strongly depending on the applied extraction process indicating that the prevalence of those groups was different since delignification chemistry is different for each extraction process. For instance, alkali lignin presented low intensity in those bands typically associated to lignin and high intensity of characteristic carbohydrates wavelengths. This observation could suggest that alkali lignin purity was really low indicating hemicellulosic contamination. Interestingly, organosolv and hydrolysis lignins showed

similar infrared profile with high intensity of typical lignin peaks and low presence of bands associated to hemicellulosic sugars.

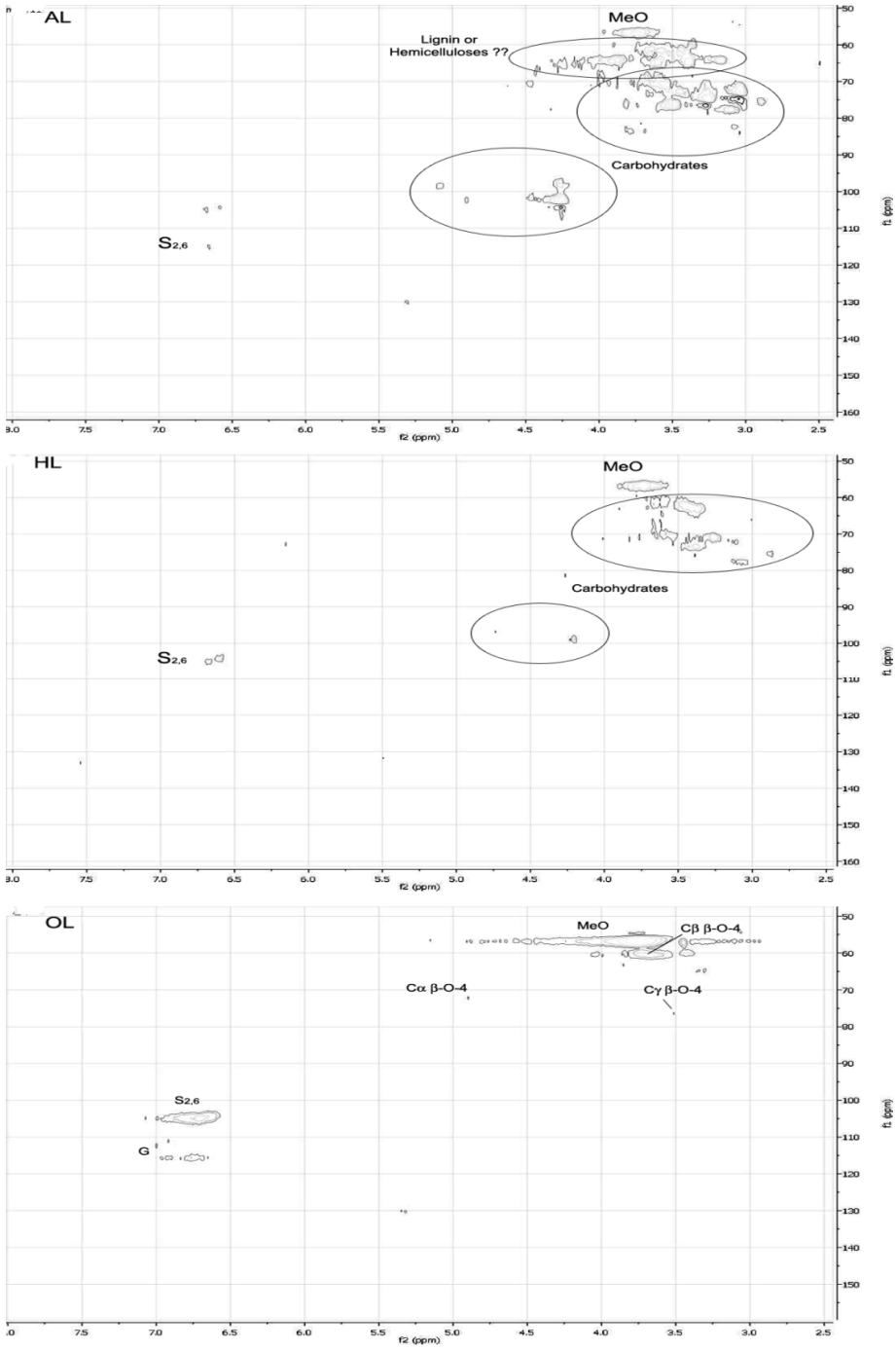


**Figure 2.4.** HSQC spectra of extracted lignins from olive tree pruning. AL (alkali lignin), HL (autohydrolysis lignin) and OL (organosolv lignin).

The HSQC-NMR data of the different extracted lignins are depicted in Figure 2.4, side chain region ($\delta_C/\delta_H$ 50–95/2.5–6.0 ppm) and the aromatic region ($\delta_C/\delta_H$ 95–160/5.5–8.0 ppm). NMR analyses were carried out to better elucidate lignin structure since 2D HSQC is a powerful tool for lignin structural characterization providing information of the structure of the inter-unit linkages present (Rencoret et al. 2009).

In the aromatic region, few signals were detected in AL and HL spectra. The most common aromatic structures in lignins are those with phenylpropane origin, namely guaiacol alcohol, syringol alcohol and p-hydroxyphenyl alcohol. Cross-signals from syringyl units were observed as a prominent signal for the $C_{2,6}$–$H_{2,6}$ correlation at around $\delta_C/\delta_H$ 105.0/6.7 ppm, while the guaiacyl units were only detected for OL and showed different correlations for $C_2$–$H_2$ ($\delta_C/\delta_H$ 112.5/7.00 ppm; 111.1/6.92), $C_5$–$H_5$ ($\delta_C/\delta_H$ 115.7/6.76; 114.0/6.65; 115.7/6.93). Interestingly, signals related to syringyl units were more intense than the ones associated to guaiacyl units suggesting higher abundance of S units in olive tree pruning lignin.

In the side-chain region, different signals could be observed in the olive tree pruning lignin spectra that corresponded to classical lignin substructures linkages such as β-O-4 which is the most common lignin interunits bond. Methoxyl cross-signals ($\delta_C/\delta_H$ 56.7/3.74) were the most predominant ones in the side-chain region of all olive tree pruning lignins spectra. In OL spectrum, the presence of the characteristic β-O-4 lignin linkage was pointed out by the cross-signals at $\delta_H/\delta_C$ 60.0/3.84 ppm (Cβ in β-O-4); $\delta_H/\delta_C$ 72.3/4.90 ppm (Cα in β-O-4) and $\delta_H/\delta_C$ 76.4/3.51 ppm (Cγ in β-O-4). However, these cross-signals were not clearly identified in AL and HL spectra due to the abundance of polysaccharide contamination cross-signals that were overlapped with the characteristic lignin cross-signals. These findings confirmed the obtained infrared data.

Hemicelluloses typical signals comprises the resonance of the (1→4)-β-d-Xylp at $\delta_C/\delta_H$ 73.2/3.22 (C2-H), 74.72/3.45 (C3-H), 76.04/3.69 (C4-H), 63.34/4.02 and 3.27 (C5-H) and the α-d-glucuronic acid residues at $\delta_C/\delta_H$ 71.72/3.56 (C2-H), 71.95/3.73 (C3-H), 82.57/3.15 (C4- H) and 72.25/4.25 (C5-H). In addition, cross-signals at $\delta_C/\delta_H$ 60.78/3.6–4.0 corresponded to C-6 of (1→4)-β-D-Man*p* and (1→4)-β-D-Glc*p*. (Samuel et al. 2011; Wen et al. 2011; Zhang et al., 2011). HL and AL spectra presented cross-signals in the area ($\delta_C/\delta_H$ 90–110/4.0-5.5) ppm that would reveal the presence of hemicellulosic sugars. Indeed, Zhang et al. (2011) reported that the anomeric carbons of β-D-Xyl*p*, β-D-Xyl*p*-2-O-Glc*p*A, β-D-Man*p*, β-d-Glc*p* and β-D-Glc*p*A were characterized by signals at $\delta_C/\delta_H$ 102.22/4.37, 100.75/4.57, 100.31/4.67, 103.43/4.43 and 97.56/5.21 in the HSQC NMR spectrum, respectively. These cross signals matched with the ones found in HL and AL spectra confirming that alkali and hydrolytic lignins were very contaminated.

The results of the alkali nitrobenzene oxidation of the olive tree pruning lignins extracted applying different treatments are shown in Table 2.3. The major products found in the oxidized mixture were vanillin and syringaldehyde that come from guaiacyl and syringyl lignin subunits, respectively. The presence of these main compounds together with the absence of products released from non-condensed p-hydroxyphenyl units (p-hydroxybenaldehyde and p-hydroxybenzoic acid) suggested that olive tree pruning lignin is GS type lignin, typical of hardwood. Ferulic acid was found to be one of the major components of the alkaline oxidized lignin mixture. Ferulic acid is laid down in ester linkages to primary cell wall polysaccharides and provides ether linkage initiation sites for lignin, while the p-coumaric acid does not become involved in this bridge, and it is more extensively esterified to lignin during the later wall development (Xiao et al. 2001). HL and OL presented similar S/G ratio with more proportion of phenolic acids or aldehydes released from non-condensed syringyl units than from guaiacyl units. Interestingly, AL showed totally different S/G

ratio as compared to HL and OL. AL S/G ratio was lower than one meaning that guaiacyl units' content was higher than syringyl units' contents. This fact was very confusing since the S/G ratio is associated to the wood specie and it cannot be affected by the employed extraction pretreatment.

| | **AL** | **HL** | **OL** |
|---|---|---|---|
| Vanillic acid | - | - | 0.30 |
| Syringic acid | 0.10 | 0.19 | 0.49 |
| 4-hydroxybenzaldehyde | - | - | - |
| Vanillin | 1.78 | 5.51 | 8.52 |
| Syringaldehyde | 1.81 | 14.41 | 27.52 |
| 4-hidroxybenzoic acid | - | - | - |
| Acetovanillone | 0.77 | 0.81 | 2.35 |
| Ferulic acid | 0.66 | 0.34 | 7.40 |
| Total | 5.12 | 21.26 | 46.58 |
| S/G ratio | 0.67 | 2.19 | 2.51 |

**Table 2.3.** Yields (%, w/w) of the detected phenolic acids and aldehydes compounds released from olive tree pruning lignins by alkaline nitrobenzene oxidation. S corresponded to the sum of syringic acid and syringaldehyde yields. G corresponded to the sum of vanillic acid, vanillin and acetovanillone yields.

The total phenolic acids and aldehydes yields were different depending on the applied conditions for lignin extraction. The degree of oxidation and, hence, the products yields have to deal with the structure of the obtained lignin. Higher condensation of the structure of extracted olive tree pruning lignin involved less oxidation products concentration since the capability of the nitrobenzene molecules to access the lignin structure is weak. This finding suggested that alkali treatment was able to produce lignins with more condense syringyl units that could not be attack during alkaline

nitrobenzene oxidation conditions. Although, AL data could be misleading given the fact that this sample presented high hemicellulosic contamination, proved by ATR-IR and HSQC.

Molecular weight distribution of the obtained olive tree pruning lignins and weight-average (Mw), number-average (Mn) molecular weight and polydispersity (Mw/Mn) of the different extracted lignins are shown in Figure 2.5 and Table 2.4. The obtained values are relative to polystyrene standards. Autohydrolysis lignin (HL) presented the lowest weight-average molecular weight compared to AL and OL.

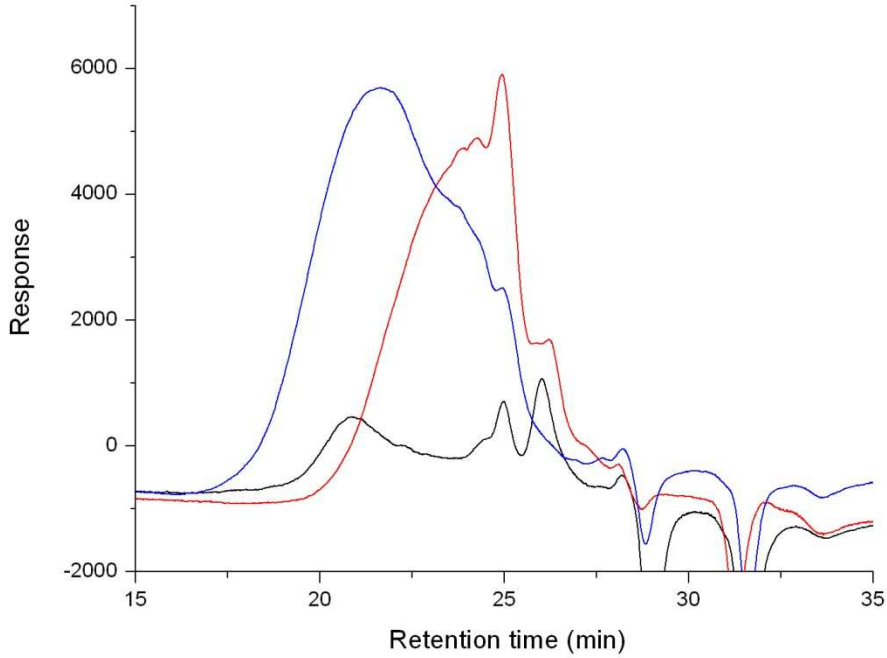


**Figure 2.5.** Molecular weight distributions (HPSEC) of extracted lignins. AL (black), HL (red) and OL (blue)

Organosolv treatments are said to produce low molecular weight lignins (Lora 2008) and, surprisingly, OL showed higher weight-average molecular weight than AL. However, this was explained given the fact that alkali lignin solubility in

dimethylformamide + 0.1% lithium bromide was poor, around 60% (w/w). Because the solubility of the alkaline lignins was very poor in DMF solution, the results of the molecular weight determination in this solvent were thought to reflect only the dissolved lignin part, which is likely to be only the low molecular weight fraction. In Figure 2.5, shoulders and peaks were identified at lower retention times than the main peak indicating the presence of low molecular weight (LMW) fraction in the extracted lignins.

| | **AL** | **HL** | **OL** |
|---|---|---|---|
| *Composition* | | | |
| AIL (%) | 4.55 ± 0.42 | 26.91 ± 0.93 | 65.77 ± 0.75 |
| ASL (%) | 2.59 ± 0.15 | 3.99 ± 0.52 | 1.93 ± 0.06 |
| Total sugars (%) | 23.10 ± 0.92 | 13.85 ± 0.37 | 8.33 ± 0.35 |
| Glucose (%) | 5.88 ± 0.58 | 7.15 ± 0.35 | 4.63 ± 0.70 |
| Xylose (%) | 15.88 ± 0.24 | 4.52 ± 0.23 | 3.56 ± 0.18 |
| Arabinose (%) | 1.33 ± 0.12 | 2.18 ± 0.20 | 0.14 ± 0.01 |
| Ash (%) | 43.63 ± 0.01 | 1.25 ± 0.06 | 0.12 ± 0.02 |
| *Molecular weight* | | | |
| Mw | 10875 | 3662 | 12919 |
| Mn | 4925 | 2120 | 2252 |
| Mw/Mn | 2.21 | 1.73 | 5.74 |

**Table 2.4.** Olive tree pruning lignins compositions extracted by different treatments. Weight-average (Mw), number-average (Mn) molecular weight and polydispersity (Mw/Mn) of the different lignins.

The number of C–C bonds between units is connected to the lignin molecular weight, mainly to the structures involving C5 in the aromatic ring. The most abundant aromatic rings in lignin are guaiacyl-type unit and syringyl-type unit. Guaiacyl-type units are able to form this kind of bonds, but this is not possible in syringyl-type units

as they have both C3 and C5 positions substituted by methoxy groups. Lignins mostly composed by guaiacyl units are expected to show higher MW than those presenting high contents of syringyl units (Glasser et al. 1993). These lignins with high fractions of low molecular weight molecules are more reactive than those with high molecular weight molecules (Pizzi 1994).

Wet chemical methods were employed to determined lignins composition (Table 2.4). These results were very enlightening and useful to confirm or explain the previously obtained results. It is readily apparent that the purity of the obtained lignin was totally different depending on the applied conditions to extract lignin. Since all the employed lignin isolation processes were based on lignin insolubility in acid media, it can be concluded that the measurement of the acid insoluble lignin (AIL) was related to the lignin purity for each process. In this sense, alkali treatment yielded lignin with very low purity (4.55%), autohydrolysis lignin presented better but still not very acceptable purity and organosolv lignin were likely to be the most pure lignin (65.77%). Acid soluble lignin (ASL) content remained low in all extracted lignins. Yasuda et al. (2001) suggested that ASL is probably composed of two components: lignin degradation products and secondarily formed hydrophilic materials such as lignin-carbohydrate. These findings could indicate that organosolv conditions were not hard enough to cleavage the suggested bonds.

Considering that polysaccharides entailed the most common contamination in lignin, total sugars content supported AIL results related to lignin purity. AL lignin presented the highest quantities of sugars, followed by HL and the less content was shown by OL. Among the sugars present in lignin, xylose was the major hemicellulosic sugar in AL lignin. Nevertheless, glucose represented the major sugar present in HL and OL lignins. Arabinose concentration in the isolated olive tree pruning lignins was very low

for all applied extraction conditions. The high sugars content, above all in AL and HL, confirmed 2D-NMR results where several cross-signals were identified and associated to hemicellulosic sugars presence. Lignin ash content was really influenced by the applied conditions to extract it. Organosolv and autohydrolysis conditions resulted in low ash content whereas the applied alkali conditions produced lignin with very high ash content (inorganic matter).

The analyses carried out to determine lignins composition were very helpful to understand the previous NMR, ATR-IR and HPSEC results. The low purity of alkali lignin and its high content in sugars were responsible of the ATR-IR profile more similar to hemicelluloses or cellulose than to the lignin typical spectrum. Moreover, as it was mentioned before, the high sugars content also disguised lignin 2D-NMR spectra. Alkali lignin composition, together with the solubility in DMF solution, could be also considered the reasons why the molecular weight was lower than expected. Also, it has to be noticed that the total yield of the oxidation products in the alkaline nitrobenzene oxidation is very similar to the results obtained when determining acid insoluble lignin. Thus, the obtained results were proved and confirmed. AL lignin composition should explain the weird alkaline nitrobenzene oxidation results. The low purity of this lignin could have modified the oxidation reaction yielding a totally different S/G ratio.

Lignin functionality is a key factor for further lignin applications. Keeping this in mind, carboxyl content, carbonyl content and phenolic content were measured in order to establish the relation between the lignin extraction process and lignin reactivity (Table 2.5). The chemistry of each applied treatment was different producing lignin with different functional groups depending on the oxidation reactions, coupling reactions… HL and OL lignins presented higher content of hydroxyl groups. AL

showed low hydroxyl groups content whereas the carboxyl content was high indicating that the applied alkali conditions promoted oxidation reactions. OL presented the lowest carboxyl content of the studied lignins. High carboxyl content has been related to more degradation in lignin structure (El Mansouri et al. 2007). Carbonyl content was low for all studied lignin extraction conditions.

| | **AL** | **HL** | **OL** |
|---|---|---|---|
| COOH (%) | 6.57 ± 0.07 | 7.15 ± 0.12 | 4.03 ± 0.08 |
| C=O (%) | 0.12 ± 0.01 | 0.53 ± 0.01 | 0.24 ± 0.01 |
| OH (%) | 2.62 ± 0.05 | 10.12 ± 0.18 | 9.81 ± 0.04 |

**Table 2.5.** Functional groups contents (%, w/w) of alkali lignin (AL), autohydrolysis lignin (HL) and organosolv lignin (OL).

### 2.2.4 Conclusions

Olive tree pruning was subjected to different pretreatments in order to extract lignin. Obtained lignins were extensively characterized in order to establish relationships between the extraction method and lignin structure and composition. Alkali treatment yielded very impure lignin with very low AIL content (4.55%) as it was confirmed by NMR and ATR-IR. The major contaminants present in alkali lignin were sugars, mainly xylose, and inorganic. Hydrolysis lignin turned out to be a medium quality lignin being its molecular weight its best quality. However, the hydrolysis extraction yield was extremely low. Moreover, the applied organosolv treatment conditions yielded the purest lignin with low content in sugars and almost no inorganic. In addition, organosolv extraction yield was high. Considering all obtained results, the highest quality lignin was obtained when ethanol organosolv conditions were applied to the olive tree pruning.

## 2.3 Experimental design for organosolv extraction process optimization

The data presented in section 2.2 allowed selecting ethanol organosolv pretreatment as the one that produced better quality lignin. Subsequently, an experimental design was considered as the best technique to optimize lignin production from olive tree pruning (only branches and wood). The idea was that dissolving as much lignin as possible in the liquid fraction also favors the other stream by yielding purest cellulosic solid fraction. Mathematical equations were employed to establish the relationships between the studied factors. High lignin concentrated liquid fractions were treated to precipitate the lignin. Obtained lignins were study to evaluate its quality. The objective was to achieve high lignin concentration liquors with good quality lignin.

The applied mathematical model uses a series of points (experiments) around a central one (central experiment) and several additional points (additional experiments) to estimate the first- and second-order interaction terms of a polynomial. This design meets the general requirement that every parameter in the mathematical model can be estimated from a fairly small number of experiments (Montgomery 1991). Experimental data were fitted to the following second-order polynomial:

$$Y = a_0 + \sum_{i=1}^{n} b_i x_{ni} + \sum_{i=1}^{n} c_i x_{ni}^2 + \sum_{i=1;j=1}^{n} d_{ij} x_{ni} x_{nj} \qquad (i<j) \qquad (1)$$

where,

$$x_n = 2\frac{X - \overline{X}}{X_{max} - X_{min}} \qquad (2)$$

Y denotes dependent variables (lignin content in solid fraction and lignin concentration in liquid fraction), n denotes the number of independent variables (3), $X_n$ independent variables (reaction time, reaction temperature and ethanol concentration) and ao, bi, ci and dij are constants.

The Xn were normalized from -1 to +1 using Eq. (2) in order to facilitate direct comparison of the coefficients and visualization of the effects of the individual independent variables on the response variable. This fact also results in more accurate estimates of the regression coefficients as it reduces interrelationships between linear and quadratic terms (Rowell 1993). In Eq. (2), Xn is the normalized value of temperature (XT), time (Xt) and ethanol concentration (XC); X is the experimental value of the variable concerned; $\overline{X}$ is the middle point of the variation range value for the variable in question; and Xmax and Xmin are the maximum and minimum values of such a variable.

### 2.3.1 Materials and methods

The raw material (olive tree pruning) was treated with an ethanol-water mixture using different ethanol concentrations, reaction times and temperature. The solid:liquid ratio used was 1:6 and held constant for all experiments. The reactions were carried out in a 1500 mL pressure stainless steel reactor (Parr 4836) equipped with a heating mantle, mechanical stirrer, and manometer. Temperature was controlled with the reactor controller and time with a chronometer. The time needed to reach the desired temperature was around 15 minutes for all experiments. When the reaction was stopped, the reactor was cooled to room temperature. The solid fraction was separated by gravity filtration from the liquid fraction. Three independent variables were varied during the delignification process: time (t) (60 -

120 minutes), temperature (T) (160 – 200 ºC) and ethanol concentration (C) (60 – 80%). The range used for each independent variable was established empirically on the basis of our own previous experience and taking into account those ranges studied by Jimenez et al (2001). The normalized values of independent variables, for the 27 experiments of the experimental design, are shown in Table 2.6.

| Experiment | $X_T$ | $X_t$ | $X_C$ | Experiment | $X_T$ | $X_t$ | $X_C$ |
|---|---|---|---|---|---|---|---|
| 1 | 180 | 90 | 70 | 15 | 200 | 120 | 60 |
| 2 | 160 | 90 | 70 | 16 | 180 | 120 | 80 |
| 3 | 180 | 60 | 70 | 17 | 200 | 90 | 80 |
| 4 | 180 | 90 | 60 | 18 | 200 | 120 | 70 |
| 5 | 160 | 60 | 60 | 19 | 200 | 90 | 60 |
| 6 | 200 | 60 | 60 | 20 | 180 | 60 | 80 |
| 7 | 160 | 120 | 60 | 21 | 160 | 120 | 70 |
| 8 | 160 | 60 | 80 | 22 | 180 | 90 | 80 |
| 9 | 180 | 60 | 60 | 23 | 180 | 120 | 70 |
| 10 | 160 | 90 | 60 | 24 | 200 | 90 | 70 |
| 11 | 160 | 60 | 70 | 25 | 160 | 90 | 80 |
| 12 | 200 | 120 | 80 | 26 | 180 | 120 | 60 |
| 13 | 160 | 120 | 80 | 27 | 200 | 60 | 70 |
| 14 | 200 | 60 | 80 | | | | |

**Table 2.6.** Experimental conditions applied to olive tree pruning. $X_T$ normalized temperature; $X_t$ normalized time; $X_C$ normalized ethanol concentration.

The effect of the considered factors variation (ethanol concentration, reaction time and reaction temperature) on the lignin content in pulp (LP) and on the lignin concentration in the liquid fraction (LL) was measured. The solid fraction was dried and then analyzed in order to determine the lignin content (Klason lignin) (%, w/w) following the TAPPI standard T-222. The liquid fraction was treated to precipitate the lignin present and its concentration was determined; two volumes of acidified water

(pH around 2) were added to a known volume of liquid fraction in order to precipitate the lignin. The precipitated lignin was then separated by centrifugation (4000 rpm, 20 minutes). The lignin concentration was determined gravimetrically (g/L).

Experimental results (LL and LP) were subjected to regression analysis using the STATGRAPHIC software (Montgomey 1991). Non-significant variables were eliminated one at a time using the stepwise method to discard those terms with a Snedecor's F-value smaller than four (Draper et al. 1981).

#### 2.3.1.1 Lignin characterization

The enhancement of lignin production also involves the production of good quality lignin. From the 27 experiments performed, those which yielded liquors with high lignin concentration were treated to precipitate the lignin in order to establish its physicochemical properties. Lignins were isolated by adding two volumes of acidified water (pH ≈ 2) to the liquid fraction. The precipitated lignin was then separated by centrifugation (4000 rpm, 20 minutes). Obtained lignins were characterized by fast techniques, namely attenuated-total reflection infrared spectroscopy (ATR-IR) and thermogravimetric analysis (TGA). ATR-IR spectroscopy was developed by direct transmittance in a single-reflection ATR System (ATR top plate fixed to an optical beam condensing unit with ZnSe lens) with an MKII Golden Gate SPECAC instrument. The region between 4000 and 600cm$^{-1}$ with a resolution of 4 cm$^{-1}$ and 20 scans were recorded. Lignin samples were dried before the analysis. TGA was carried out using a Mettler Toledo TGA/SDTA RSI analyzer. Samples of ~5mg were heated from 25 ºC up to 800 ºC at a rate of 10 ºC/min. A constant nitrogen flow was used, an inert atmosphere during the pyrolysis allowed the extraction of the gaseous and condensable products that could cause secondary interactions.

### 2.3.2 Experimental design results

As mentioned before, two dependent variables were measured to study the organosolv fractionation of olive tree pruning, namely, lignin content (%) in pulp (LP) and lignin concentration (g/L) in the liquid fraction (LL). The results of the 27 experiments carried out are shown in Table 2.7.

| Experiment | LP (%) | LL (g/L) | Experiment | LP (%) | LL (g/L) |
|---|---|---|---|---|---|
| 1 | 18.05 | 18.62 | 15 | 11.39 | 35.09 |
| 2 | 27.16 | 7.86 | 16 | 25.78 | 14.53 |
| 3 | 18.78 | 15.75 | 17 | 18.48 | 23.69 |
| 4 | 21.33 | 25.23 | 18 | 23.45 | 32.35 |
| 5 | 25.50 | 10.08 | 19 | 11.17 | 33.69 |
| 6 | 11.50 | 36.55 | 20 | 24.93 | 8.65 |
| 7 | 24.90 | 12.53 | 21 | 26.63 | 7.69 |
| 8 | 29.28 | 0.08 | 22 | 24.43 | 10.67 |
| 9 | 19.62 | 35.77 | 23 | 20.82 | 21.73 |
| 10 | 28.99 | 9.01 | 24 | 10.01 | 29.33 |
| 11 | 27.82 | 6.02 | 25 | 29.00 | 4.21 |
| 12 | 14.75 | 25.66 | 26 | 14.88 | 28.68 |
| 13 | 27.78 | 5.92 | 27 | 14.30 | 28.46 |
| 14 | 18.97 | 20.76 | | | |

**Table 2.7.** Lignin content in pulp (LP) and lignin concentration in liquid fraction (LL) of the experimental design runs.

Applying the statistical STATGRAPHICS Centurion XV software to the data in Table 2.7, the following equations (3) and (4) that predict the behavior of the dependant variables studied for the organosolv delignification process of olive tree pruning were obtained:

$$LP = 21.1 - 6.28*X_T + 2.45111*X_C \quad (3)$$

$$LL = 18.8374 + 11.2322*X_T - 6.24778*X_C + 1.89333*X_t*X_C \quad (4)$$

Table 2.8 shows the statistical values (Snedecor's F, R2 and R2-adjusted) for the different terms in the equations (3) and (4).From the statistical values obtained for both equations (3) and (4) it is found that the proposed model fitted the experimental values of lignin concentration in liquid fraction (LL) well since the calculated values for the dependent variable (LL) reproduces the experimental results with errors of 7%. However, for lignin content in pulp (LP) the model did not fit as wells as for LL. In this case, the calculated values for LP obtained from equation (3) reproduced the experiment results with errors higher than 15%. This is in accordance with other authors' works (Jiménez et al. 1999, 2001) where the error in lignin content measured as Klason lignin was around 15% and always higher than other parameters that can be measured in the solid fraction such as holocellulose or □-cellulose.

| Equation | | Snedecor's F | $R^2$ | $R^2$ - Adjusted |
|---|---|---|---|---|
| LP | | 54.75 | 0.82 | 0.80 |
| | $X_T$ | 75.01 | | |
| | $X_C$ | 11.43 | | |
| | | | | |
| LL | | 101.79 | 0.93 | 0.92 |
| | $X_T$ | 245.10 | | |
| | $X_C$ | 75.83 | | |
| | $X_t * X_C$ | 4.64 | | |

**Table 2.8.** Snedecor's F values for the terms in the obtained equations (3-4) for the lignin in liquor (LL) and lignin content in pulp (LP). $R^2$y adjusted-$R^2$ values obtained from the adjusted model equations (3) and (4).

From Figure 2.6, equation (4) and data in Table 2.6, it can be observed that the lignin concentration in the liquid fraction was highly influenced by the conditions used in the delignification process.

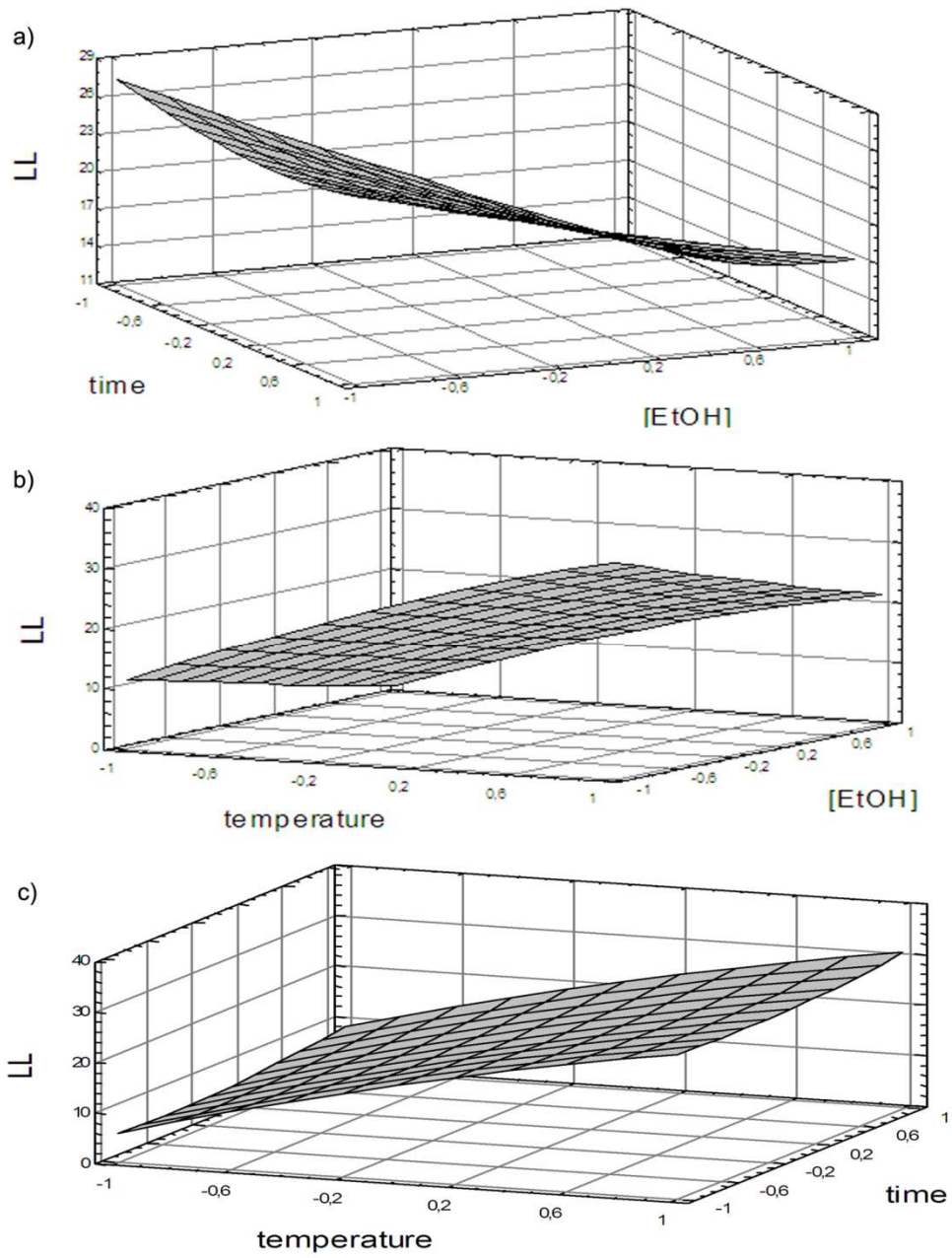


**Figure 2.6.** Variation of lignin concentration (g/L) in the liquid fraction (LL) a) with the reaction time (normalized) and the ethanol concentration (normalized) at the central temperature point; b) with the temperature (normalized) and the ethanol concentration (normalized) at the central time point; c) with the temperature (normalized) and the reaction time (normalized) at the central ethanol concentration point.

Experimentally, the highest lignin concentration in the liquid fraction (LL), 36.55 g/L, was obtained at the highest temperature (normalized value 1), the shortest reaction time (normalized value -1) and lowest ethanol concentration (normalized value -1). The experimental values for LL varied from nearly 0 g/L to 36.55 g/L with the temperature, being the most important factor that determined the yield of dissolved lignin in the liquid fraction. As the temperature used in the organosolv treatment raised, the lignin concentration in the liquid fraction increased while increasing the ethanol concentration resulted in the opposite behavior. The presence of water in the reaction mixture seemed to be important because the lower concentration of ethanol, the higher lignin concentration in the liquid fraction. The reaction time was not a variable that affected LL much; however, it had a synergetic effect with the ethanol concentration. To maximize dissolved lignin concentration in the liquid fraction, the organosolv conditions to be used are high temperature and low ethanol concentration.

For the present study, it was desirable to minimize lignin content in pulp (LP) what would mean that the lignin present in the raw material has been dissolved in the liquid fraction and so, it could be more easily isolated and utilized for further applications. The statistical program STATGRAPHICS Centurion gave the following optimized organosolv conditions to minimize the lignin content in pulp (LP): highest temperature (normalized value 1), lowest reaction time (normalized value -1) and lowest ethanol concentration (normalized value -1), i.e., these conditions would be, as expected, the same as with the other objective of this study: enhancement of lignin concentration in the liquid fraction. Nevertheless, the experimental data did not agree with the aforementioned conditions. The lowest LP data was 10.01% obtained at high temperature (normalized value 1), medium reaction time (normalized value 0) and medium ethanol concentration (normalized value 0). Such a variation could be explained by the error associated to the LP equation (3).

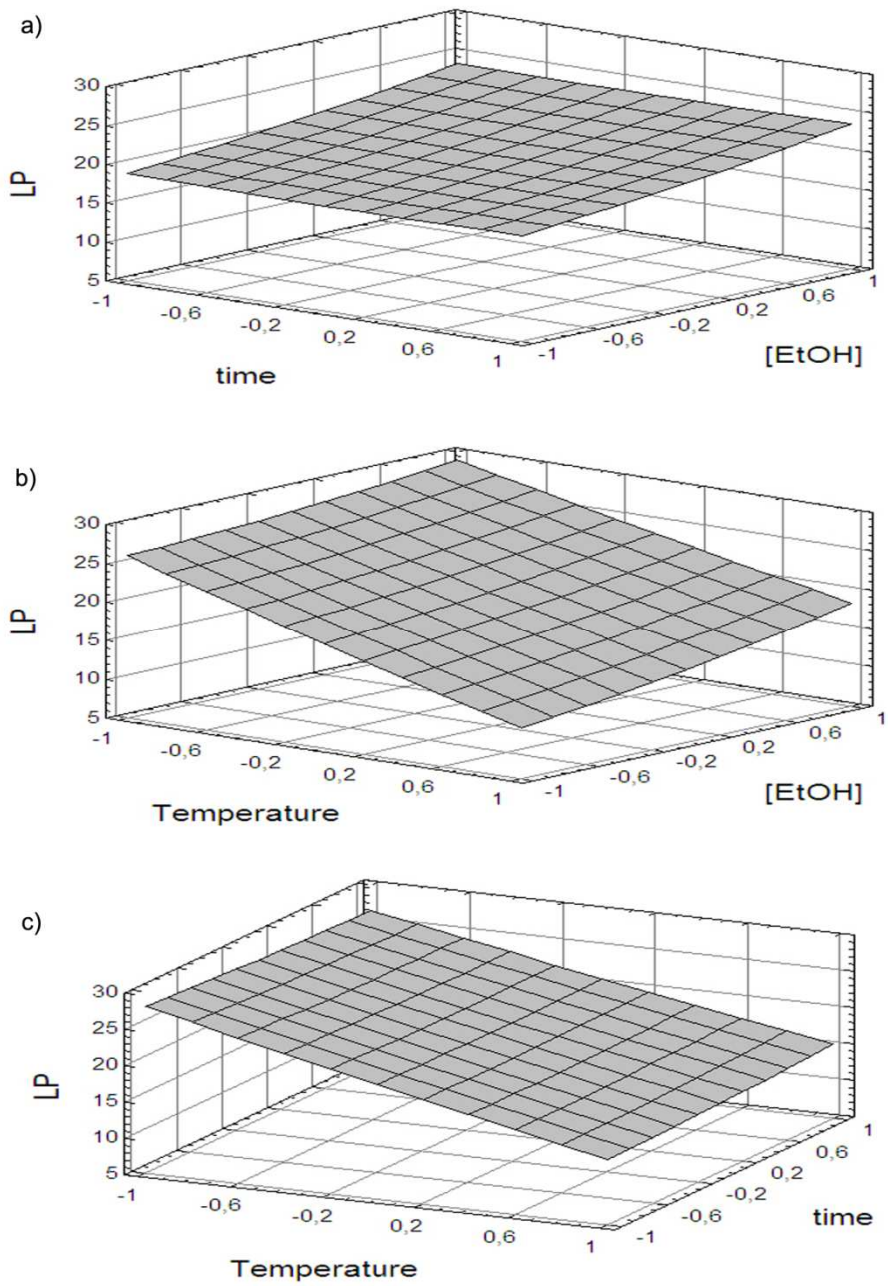


**Figure 2.7.** Variation of lignin content (%, w/w) in pulp (LP) a) with the reaction time (normalized) and the ethanol concentration (normalized) at the central temperature point; b) with the temperature (normalized) and the ethanol concentration (normalized) at the central time point; c) with the temperature (normalized) and the reaction time (normalized) at the central ethanol concentration point.

Others authors' studies presented similar error in their equations to predict the lignin content in pulp behavior (Jiménez et al. 1999, 2001; Mujté et al. 2005). The

obtained error could be comparable to the one obtained by these authors. In our opinion, the error could be justified due to the complex structure of the plant cell wall and its heterogeneity. These two factors affect the way the reaction mixture acts and make this variable (lignin content in pulp) difficult to be predicted with an error less than 10%. Also, re-polymerization and lignin redeposition on fiber surface (Xu et al. 2007) are others phenomena that could explain the obtained results.

From equation (3) and Figures 2.6 and 2.7, it is evident that the temperature used to extract lignin is the most important factor. The higher the temperature was, the less lignin content in pulp. As in the case of LL, employing low ethanol concentration led to low lignin content in pulp. The reaction time, as it can be noted in Figure 2.7, did not influence the percentage of lignin content in pulp since the surface of the graphics plot remains constant in the time axis.

### 2.3.3 Isolated lignins characterization

Since the quantity not was the only factor that mattered, the quality of some lignins was tested by means of the development of fast analyses. With this purpose, lignin concentration average of the 27 experiments was calculated and those experiments (experiment number: 4, 6, 9, 12, 14, 15, 17, 18, 19, 23, 24, 26 and 27) that produced liquid fraction with lignin concentration equal or higher than the average were considered for further characterization. Lignins were isolated, as explained before, and characterized, namely, by infrared spectroscopy (ATR-IR) and thermogravimetric analyses (TGA) and the results are presented below.

The ATR-IR spectra of the lignins isolated from most concentrated liquid fractions obtained after subjecting olive tree pruning to different organosolv extraction

conditions are shown in Figure 2.8. Around 3345 $cm^{-1}$ it can be observed a vibration caused by the stretching of the O-H group. All spectra present bands between 2950 and 2830 $cm^{-1}$ that corresponded to the vibration of C-H bond in methyl and methylene groups. The asymmetric deformation of this bond also produced a band at around 1460 $cm^{-1}$. The vibration at around 1710 $cm^{-1}$ was associated to the C=O bond stretching in unconjugated ketones, carbonyl and ester groups while the vibration at around 1660 $cm^{-1}$ was related to the C=O bond stretching in conjugated p-substituted aryl ketones. Three typical vibrations are present in aromatic compound such as lignin, these bands appeared around 1595, 1515 and 1425 $cm^{-1}$.

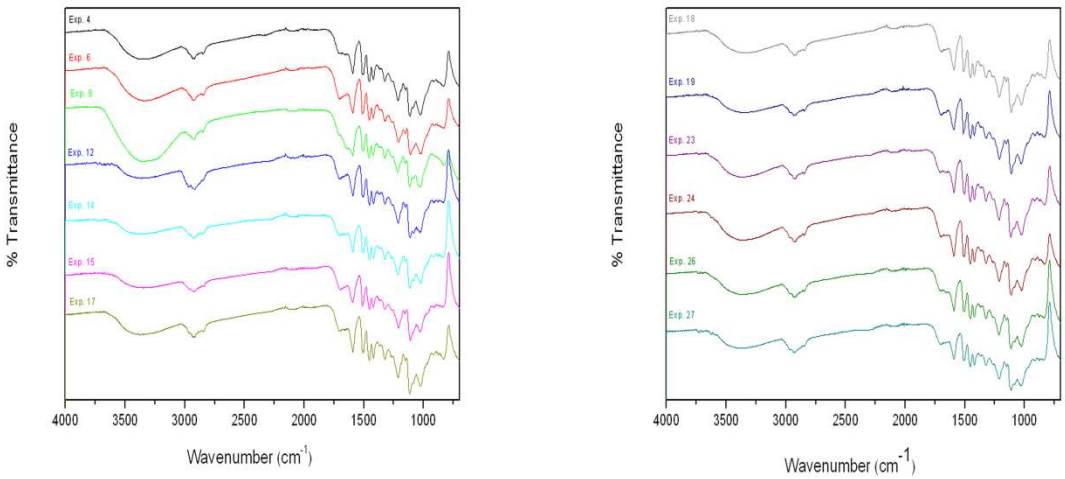


**Figure 2.8.** ATR-IR spectra of the analyzed lignins isolated from most concentrated liquid fractions.

The most significant bands in the lignin spectra are those that correspond to its main substructures - guaiacylpropane (G), syringylpropane (S) and 4-hydroxyphenylpropane (H) – such as at around 1330 $cm^{-1}$ related to the breathing of the syringyl ring with C-O stretching and at around 1270 $cm^{-1}$ (shoulder) and 1220 $cm^{-1}$ associated to the breathing of the guaiacyl ring with C-O stretching. Around 1150 $cm^{-1}$ it appeared a vibration that was caused by the deformation of the bond C-H in guaiacyl substructures while the same linkage, but in syringyl substructures

appeared at around 1120 $cm^{-1}$. The vibration at around 1030 $cm^{-1}$ was due to the deformation or the aromatic C-H linkages in guaiacyl substructures and can also be related to the deformation of the bond C-O in primary alcohols. Finally, at around 835 $cm^{-1}$ there was a vibration caused by the C-H linkage in positions 2 and 6 of the aromatic ring in syringyl substructures and in all positions of the aromatic ring in H substructures. This is in good agreement with previous studies (Faix 1991; Tejado et al. 2007) where different types of lignins were studied. Based on ATR-IR spectra, lignin is the major component of the precipitated obtained from the liquid fraction.

Selected samples of lignin were also subjected to thermogravimetric analysis in order to study their thermal behavior. The obtained results are summarized in Table 2.9. All samples showed a weight loss around 70 ºC that was associated to the moisture present in the lignin samples. Significant differences between lignins obtained from different experiments were observed regarding their degradation profile. Samples 4, 6, 12, 15, 18 and 19 presented weight losses below 185 ºC that can be attributed to hemicelluloses degradation products. The aggressive conditions used for the lignin extraction may affect hemicelluloses structure causing their degradation into small components such as acetic acid, furfural, hydroxymethylfurfural, ferulic acid. These components could be dissolved in the liquid fraction during the delignification process and in the lignin isolation stage they may be co-precipitated with the lignin. Between 185 and 260 ºC another weight loss was observed that can be related to the presence of hemicelluloses (Yang et al. 2007; Domínguez et al. 2008) signifying the contamination of lignin samples. The percentage of hemicelluloses contamination varies between the experiments because of the different conditions employed to extract the lignin from the raw material. Lignin degradation occurred slowly in a wide range of temperatures with maximal mass loss rate between 300 and 400 ºC, this fact being associated to the complex structure of lignin with phenolic hydroxyl, carbonyl groups and benzylic hydroxyl, which are connected by straight links

(Toledano et al. 2010). All lignin samples presented high percentage of final residue due to lignin aromatic polycondesations.

| Run | T (ºC) | WL (%) | R (%) |
|---|---|---|---|
| 4 | 75.1 | 6,0 | 39.6 |
| | 139.4 | 4.2 | |
| | 192.7 | 4.86 | |
| | 359.1 | 45.34 | |
| 6 | 70.4 | 4.4 | 40.8 |
| | 134.4 | 2.8 | |
| | 196.6 | 5.3 | |
| | 361.3 | 46.7 | |
| 9 | 61.8 | 1.9 | 40.4 |
| | 204.1 | 7.7 | |
| | 353.1 | 50.0 | |
| 12 | 73.8 | 3.2 | 39.1 |
| | 133.2 | 0.6 | |
| | 363.0 | 57.1 | |
| 14 | 70.0 | 3.8 | 40.0 |
| | 240.6 | 7.7 | |
| | 362.5 | 48.5 | |
| 15 | 73.9 | 3.3 | 40.9 |
| | 116.9 | 0.5 | |
| | 136.4 | 0.3 | |
| | 236.4 | 5.7 | |
| | 363.0 | 49.3 | |

| Run | T (ºC) | WL(%) | R (%) |
|---|---|---|---|
| 18 | 75.5 | 4.1 | 40.3 |
| | 150.22 | 0.8 | |
| | 244.9 | 6.7 | |
| | 364.1 | 48.1 | |
| 19 | 75.5 | 4.1 | 40.5 |
| | 146.2 | 1.1 | |
| | 231.4 | 8.3 | |
| | 314.3 | 9.4 | |
| | 364.1 | 36.6 | |
| 23 | 71.7 | 5.3 | 37.7 |
| | 188.2 | 7.8 | |
| | 363.0 | 49.2 | |
| 24 | 77.2 | 4.7 | 39.8 |
| | 210.6 | 5.5 | |
| | 364.6 | 50 | |
| 26 | 68.8 | 5.4 | 37.1 |
| | 222.6 | 11.8 | |
| | 359.1 | 45.7 | |
| 27 | 72.4 | 4.8 | 38.9 |
| | 225.3 | 7.7 | |
| | 364.1 | 48.6 | |

**Table 2.9.** Thermogravimetric analyses data of the analyzed lignins isolated from most concentrated liquid fractions. T (temperature, ºC); WL (weight loss, %); R (residue, %).

## 2.3.4 Conclusions

Optimization of lignin extraction from olive tree pruning ensures an almost lignin-free solid fraction rich in cellulose. The maximization of lignin concentration in the liquid fraction entailed using high temperatures and low ethanol concentration. These conditions also guarantee minimization of lignin content in the remaining pulp (solid fraction). Reaction time was of less importance for the delignification process in the

studied cases. The precipitated lignins from the highest concentrated liquid fractions were characterized in order to select a procedure to produce lignin in a large amount and good quality. Infrared spectroscopy showed, in most of the cases, typical lignin wavelengths. From the thermogravimetric analysis data the experimental conditions employed to extract lignin also extracted other components from the raw material such as hemicelluloses or other degradation products in different proportion depending on the severity of the treatment.

A compromise between the yield of lignin concentration in the liquid fraction and the composition of the lignin has to be achieved. Experiment 24 reached that compromise since the lignin was successfully extracted from the raw material and at the same time, lignin quality was adequate.

## 2.4 Lignin production from olive tree pruning

Once optimized the ethanol organosolv fractionation process, the objective was to produce lignin in such enough quantity so as to be able to continue studying lignin purification and depolymerization.

As lignin is deeply affected by the pretreatment and due to the heterogeneity of wood, the pretreatment is not totally reproducible or with low repeatability, the process of lignin production was performed by different batches whose liquid fractions (dissolved lignin) were reunited. The idea was to avoid structural differences (different molecular weight, different functionality…) in lignin structure. The total liquid fraction was divided in two, the major fraction was reserved for the

ultrafiltration process (Chapter 3) and the smallest part was used to recover lignin (rough lignin) by adding two volumes of acidified water. The scheme of the developed process is shown in Figure 2.9.

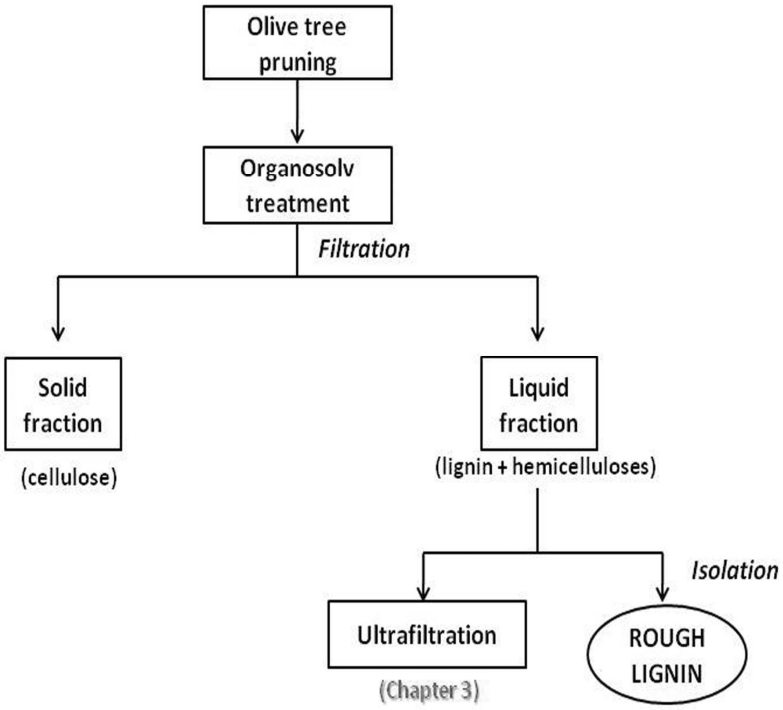


**Figure 2.9.** Scheme of the optimized lignin production process carried out.

### 2.4.1 Organosolv olive tree pruning lignin production

Olive tree pruning was subjected to selected organosolv pretreatment conditions (200 ºC, 70% (w/w), 90 minutes). The solid to liquid ratio was set at 1:6. Once the reaction had finished, the solid fraction was separated by filtration from the liquid fraction. The solid fraction was washed with an ethanol-water mixture (same reaction composition) in order to avoid lignin precipitation and redeposition on recovered fibers. The solid fraction was characterized following TAPPI analytical procedures (Appendix I). The washed liquids were joined together with the liquid fraction, from now on, liquid fraction. The liquid fraction was characterized following internal procedures (Appendix III).

Table 2.9 illustrates the chemical composition of the raw material and the solid fraction. The comparison of both compositions allowed confirming that organosolv delignification process was effective since the amount of lignin in the solid fraction decreased. As a result of this decrease, the holocellulose percentage (cellulose + hemicelluloses) increased. Therefore, chemical delignification can be effective means to overcome lignin recalcitrance to enzymes. Lignin protects cellulose from being accessible to cellulases, and the latter prevents the cellulases from accessing the cellulose for bioethanol production (Zhu et al. 2010). The extractives and ash content also decreased.

| | **Olive tree pruning** | **Solid fraction** |
|---|---|---|
| Ash (%) | 3.1 ± 0.4 | 2.5 ± 0.1 |
| Extractives (%) | 8.5 ± 0.4 | 6.6 ± 1.0 |
| Lignin (%) | 23.2 ± 0.7 | 11.4 ± 0.5 |
| Holocellulose (%) | 65.8 ± 1.2 | 78.7 ± 0.6 |
| α-cellulose (%) | 57.9 ± 0.5 | 63.5 ± 0.8 |
| Hemicelluloses (%) | 7.9 ± 0.3 | 15.1 ± 0.5 |

**Table 2.10.** Chemical composition of the raw material (olive tree pruning) and the solid fraction derived from optimized organosolv treatment.

Final liquid fraction was the result of the combination of the liquid fraction from the organosolv treatment and wash liquids to drag deposited lignin on fibers (solid fraction washes) or impregnated lignin in the solid fraction. Liquid fraction' physicochemical properties are presented in Table 2.10. Most of the total dissolved solids were organic compounds. pH was slightly acid since during organosolv treatment acids (formic acid and acetic acid) from the raw materials were released (Xu et al. 2006). Lignin concentration was half the obtained value in the experiment 24 (same reaction conditions) because this liquid fraction was diluted with the washes liquids.

| | **Liquid fraction** |
|---|---|
| pH | 4.58 |
| Density (g/mL) | 0.8703 ± 0.003 |
| Total dissolved solids (%) | 4.36 ± 0.03 |
| Inorganic matter (%) | 0.05 ± 0.02 |
| Organic matter (%) | 4.31 ± 0.03 |
| Lignin concentration (g/L) | 14.05 ± 0.05 |

**Table 2.11.** Physicochemical properties of the liquid fraction derived from the optimized organosolv treatment.

### 2.4.2 Organosolv olive tree pruning lignin characterization

As mentioned before, a portion of the liquid fraction was employed to precipitate the lignin which would constitute the rough lignin. Rough lignin was deeply characterized in order to determine its structure and composition. The analytical procedures can be found in Appendix II. The analyses comprise attenuated-total reflection infrared spectroscopy (ATR-IR), nuclear magnetic resonance NMR-HSQC, alkaline nitrobenzene oxidation, high Performance size exclusion chromatography (HPSEC), acid insoluble lignin (AIL), acid soluble lignin (ASL), sugars content, ash content, functional groups determination (carboxyl groups, carbonyl groups and total phenolic groups).

Figure 2.10 shows the ATR-IR spectrum of organosolv olive tree pruning lignin. The spectrum showed typical lignin skeleton peaks: 3345 $cm^{-1}$ (O-H group), 2950 and 2830 $cm^{-1}$ (C-H in methyl and methylene), 1710 $cm^{-1}$ (C=O in unconjugated ketones), 1660 $cm^{-1}$ (C=O in conjugated p-substituted aryl ketones) and 1595, 1515 and 1425 $cm^{-1}$ (aromatic ring). Lignin subunits (syringol (S), guaiacol (G) and p-

hydroxyphenol (H)) signals were found at 1330 $cm^{-1}$ (C-O in S), 1270 $cm^{-1}$ (shoulder) and 1220 $cm^{-1}$ (C-O in G), 1150 $cm^{-1}$ (aromatic C-H in G), 1120 $cm^{-1}$ (aromatic C-H in S), 1030 $cm^{-1}$ is (aromatic C-H linkages in G and C-O in primary alcohols) and 835 $cm^{-1}$ (C-H in S2,6 and C-H in all positions in H). The obtained spectrum corresponded to a high quality lignin.

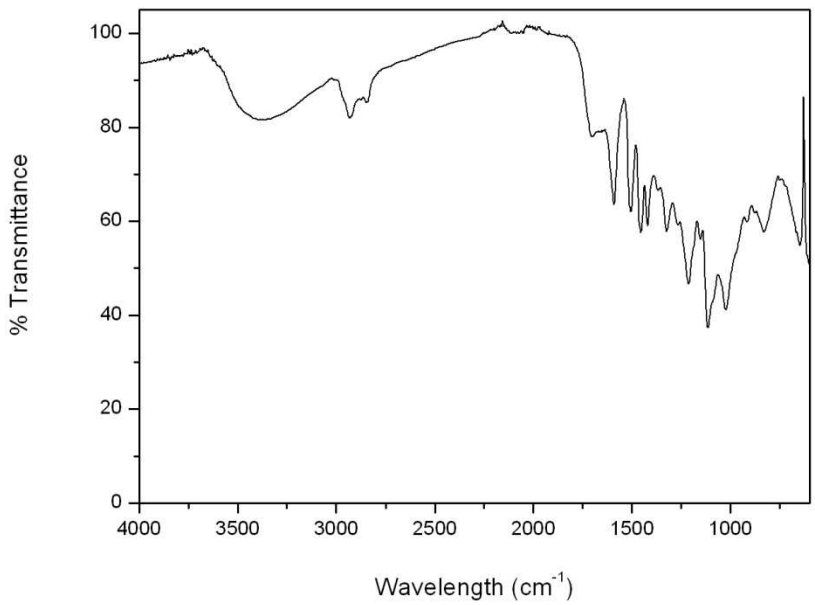


**Figure 2.10.** ATR-IR spectrum of the organosolv olive tree pruning lignin (200 ºC, 70% EtOH and 90 minutes)

HSQC experiment was developed in order to better elucidate lignin structure. As it can be observed in Figure 2.11, the main characteristic bonds in lignin structure were identified, including aromatic rings ($\delta_C/\delta_H$ 95–160/5.5–8.0 ppm) and cross-signals of the side-chain ($\delta_C/\delta_H$ 50–95/2.5–6.0 ppm). The assignments are plotted in the Figure 2.11 and explained in section 2.2. It has to be stressed that no hemicellulosic signals were found proving the high quality lignin obtained by the optimized organosolv conditions. Phenlypropanic signals were clearly detected confirming that the selected organosolv conditions produced high quality lignin.

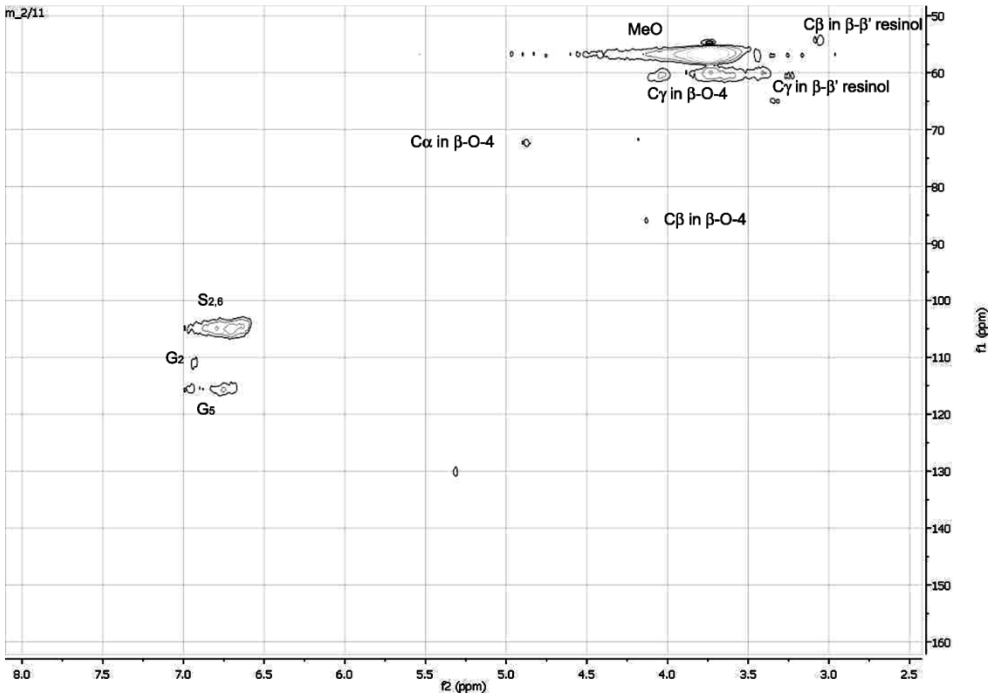


**Figure 2.11.** HSQC spectrum of the organosolv olive tree pruning lignin (200 ºC, 70% EtOH and 90 minutes)

The optimized organosolv conditions produced rough lignin with lower molecular weight with a narrower molecular weight distribution (polidispersity index, Mw/Mn). Nitrobenzene oxidation analyses confirmed that olive tree pruning lignin, as expected (hardwood), was GS type lignin. The presence of ferulic acid is related to the interlinkage that this compound establish to connect hemicelluloses with lignin (LCC complex). S/G ratio indicated that there were more S units in organosolv olive tree pruning lignin than G units. The composition obtained results verified that the selected organosolv conditions yielded very pure lignin. Acid insoluble lignin content was very high and the total sugars content decreased compared to non-optimized organosolv lignin. The main sugars found were glucose and xylose suggesting that they came from hemicelluloses degradation. Furthermore, the ash content was very small. The applied delignification conditions allowed obtaining a highly functionalized lignin.

| | Organosolv lignin | | Organosolv lignin |
|---|---|---|---|
| *Molecular weight* | | *Composition* | |
| Mw | 7232 | AIL[3] (%) | 71.90 ± 0.79 |
| Mn | 2125 | ASL[4] (%) | 1.63 ± 0.08 |
| Mw/Mn | 3.40 | Total sugars (%) | 2.94 ± 0.14 |
| | | Glucose (%) | 1.75 ± 0.12 |
| *Nitrobenzene oxidation* | | Xylose (%) | 1.10 ± 0.03 |
| Vanillin acid | 0.62 | Arabinose (%) | 0.09 ± 0.01 |
| Syringic acid | 7.48 | Ash (%) | 0.39 ± 0.01 |
| Vanillin | 16.80 | | |
| Syringaldehyde | 52.72 | *Functional groups* | |
| Acetovanillone | 5.06 | COOH (%) | 4.95 ± 0.23 |
| Ferulic acid | 15.31 | C=O (%) | 0.35 ± 0.00 |
| | | OH (%) | 11.08 ± 0.03 |
| S[1]/G[2] | 2.68 | | |

[1]S: syringic acid + syringaldehyde

[2]G: vanillic acid + vanillin + acetovanillone

[3]AIL: acid insoluble lignin

[4]ASL : acid soluble lignin

**Table 2.12.** Optimized organosolv lignin properties. Weight-average (Mw), number-average (Mn) molecular weight, polydispersity index (Mw/Mn), yields (%, w/w) of the detected phenolic acids and aldehydes compounds released from rough lignin alkaline nitrobenzene oxidation, rough lignin composition and functional groups contents (%, w/w).

## 2.5 Conclusions

Delignification technologies enable obtaining lignin-free cellulosic fraction that can be used in further applications and lignin rich liquid fraction. However, the applied conditions for lignin extraction affect its structure and hence, they determine lignin

final application. Considering the previous explanation, various studies were performed to select and optimize the lignin extraction method in order to produce high quality lignin.

It has been proved that the selected pretreatment to extract lignin influenced strongly the structure and physicochemical properties of lignin. The applied alkali conditions yielded very impure lignin (4.55% AIL) that was mainly contaminated by hemicelluloses and inorganics (sugars content 23.10% and ash 43.63%). Alkali lignin composition disguised structural and physicochemical analyses. Autohydrolysis lignin presented an interesting low molecular weight (3662) but its purity was not high enough (26.91%). Organosolv conditions produced the purest lignin (65.77%) with the lowest hemicellulosic and ash contamination, 8.33% and 0.12% respectively. This study also allows confirming that olive tree pruning lignin was GS type, typical from hardwood. Alkali nitrobenzene analysis revealed that olive tree pruning lignin presented an approximately 2.5 S/G ratio. The obtained results allowed selecting organosolv conditions as the most adequate pretreatment to produce high quality lignin. Moreover, organosolv pretreatment was proved to be an effective lignin extraction process as pointed out by the lignin concentration in the liquid fraction (31.76 g/L).

Then, an experimental design was carried out in order to optimize organosolv pretreatment for the raw material, olive tree pruning. The optimization was focus on the enhancement of lignin production from olive tree pruning. Lignin in pulp (LP) and lignin concentration in liquid fraction (LL) were mainly influenced by the same variables, reaction temperature and ethanol concentration. It was found that highest lignin concentration in the liquid fraction was obtained when using high temperatures and low ethanol concentration; conditions that also ensured the minimization of lignin

content in the remaining pulp (solid fraction). Reaction time resulted in a non-significant variable. High concentrated lignins were analyzed in order to evaluate which conditions produced also high quatity lignin. Hemicellulosic contamination was found in all cases but the extent depended on the applied conditions.

Experiment 24 conditions (200 ºC, 70% ethanol concentration and 90 minutes) were selected to produce high concentrated liquid fractions with high quality lignin. The obtained liquid fractions were divided in two portions, one to be used in the purification studies and the other fraction was treated in order to isolate the present lignin (rough lignin). The obtained results of rough lignin characterization allowed confirming that the developed experimental design led to an optimized delignification process. Obtained lignin presented typical GS lignin structure (ATR-IR and HSQC). The optimized organosolv conditions allowed producing higher quality lignin, high acid insoluble lignin content (71.90%) and low contamination (sugars 2.94% and ash 0.39%). Interestingly, optimized organosolv lignin presented a molecular weight of 7232. Obtained lignin seemed to be highly reactive due to its high functionality (11.08% COOH and 4.95% OH).

## 2.6 References

Brodeur, G.; Yau, E.; Badal, K.; Collier, J.; Ramachandran, K.B.; Ramakrishnan, S. 2011. Chemical and physicochemical pretreatment of lignocellulosic biomass: a review. Enzyme Research. doi:10.4061/2011/787532.

Dominguez, J.C.; Oliet, M.; Alonso, M.V.; Gilarranz, M.A.; Rodriguez, F. 2008. Thermal stability and pyrolysis kinetics of organosolv lignins obtained from *Eucalyptus Globulus*. Ind Crops Prod 27, 150–156.

Draper, N.; Smith, H. 1981. Applied Regression Analysis; Wiley: New York.

El Mansouri, N.-E.; Salvadó, J. 2007. Analytical methods for determining functional groups in various technical lignins. Ind Crop Prod 26, 116–124.

Faix, O. 1991. Classification of lignins from different botanical origins by FT-IR spectroscopy. Holzforschung 45, 21–27.

Fengel, D.; Wegener, G. 1984. Wood: Chemistry, Ultrastructure, Reactions. Verlag Kessel. ISBN: 3935638-39-6.

Glasser, W.G.; Dave, V.; Frazier, C.E. 1993. Molecular weight distribution of semi-commercial lignin derivatives. J Wood Chem Technol 13 (4), 545–559.

Jiménez, L.; de la Torre, M.J.; Ferrer, J.L.; García, J.C. 1999. Influence of process variables on the properties of pulp obtained by ethanol pulping of wheat straw. Process Biochem 35, 143–148.

Jimenez, L.; Perez, I.; García, J.C.; Rodríguez, A. 2001. Influence of process variables in the ethanol pulping of olive tree trimmings. Bioresour Technol 78, 63–69.

Lora, J. 2008. Industrial commercial lignins: Sources, properties and applications, in N.M. Belgacem, A. Gandini (eds.), Monomers, polymers and composites from renewable resources, Elsevier.

Montgomery, D.C. 1991. Diseño y Análisis de Experimentos; Grupo Ed. Iberoamericana: México.

Mosier, N.; Wyman, C.; Dale, B.; Elander, R.; Lee, Y.Y.; Holtzapple, M.; Ladisch, M. 2005. Features of promising technologies for pretreatment of lignocellulosic

biomass. Bioresour Technol 96, 673–686.

Mutjé, P.; Pélach, M.A.; Vilaseca, F.; García, J.C.; Jiménez, L. 2005. A comparative study of the effect of refining on organosolv pulp from olive trimmings and Kraft pulp from *Eucalyptus* wood. Bioresour Technol 96, 1125-1129.

Percival Zhang, Y.-H. 2011. What is vital (and not vital) to advance economically-competitive biofuels production. Process Biochem 46, 2091–2110.

Pizzi, A. 1994. in Advanced Wood Adhesives Technology, ed. Marcel Dekker, New York, 219-241.

Rencoret, J.; Marquesa, G.; Gutiérrez, A.; Nieto, L.; Jiménez-Barbero, J.; Martínez, A.T.; del Río, J.C. 2009. Isolation and structural characterization of the milled-wood lignin from *Paulownia fortunei* wood. Ind Crop Prod 30, 137–143.

Rowell, R. 1993. The Chemistry of solid wood. Advances in Chemistry Series; American Chemical Society: Washington (DC) 70-72.

Samuel, R.; Foston, M.; Jiang, N.; Allison, L.; Ragauskas, A.J. 2011. Structural changes in switchgrass lignin and hemicelluloses during pretreatments by NMR analysis. Pol Degrad Stabil 96, 2002-2009.

Sannigrahi, P.; Pu, Y.; Ragauskas, A. 2010. Cellulosic biorefineries—unleashing lignin opportunities. Current Opinion in Environmental Sustainability 2, 383–393.

Tejado, A.; Peña, C.; Labidi, J.; Echeverria, J.M.; Mondragon, I. 2007. Physicochemical characterization of lignins from different sources for use in phenol-formaldehyde resin synthesis. Bioresour Technol 98 (8), 1655–1663.

Toledano, A.; Garcia, A.; Mondragon, I.; Labidi, J. 2010. Lignin separation and fractionation by ultrafiltration. Sep Purif Technol 71, 38–43.

Wen, J.-L.; Xiao, L.-P.; Sun, Y.-C.: Sun, S.-N.; Xu, F.; Sun, R.-C.; Zhang, X.-L. 2011. Comparative study of alkali-soluble hemicelluloses isolated from bamboo (*Bambusa rigida*). Carbohyd Res 346, 111–120.

Xiao, B.; Sun, X.F.; Sun, R.C. 2001. Chemical, structural, and thermal characterizations of alkali-soluble lignins and hemicelluloses, and cellulose from maize stems, rye straw, and rice straw. Polym Degrad Stabil 74, 307–319.

Xu, F.; Sun, J.-X.; Sun, R.C.; Fowler, P.; Baird, M.S. 2006. Comparative study of organosolv lignins from wheat Straw. Ind Crop Prod 23, 180–193.

Xu, Y.; Li, K.; Zhang, M. 2007. Lignin precipitation on the pulp fibers in the ethanol-based organosolv pulping. Colloids Surf A 301, 255–263.

Yang, H.; Yan, R.; Chen, H.; Lee, D.H.; Zheng, C. 2007. Characteristics of hemicellulose, cellulose and lignin. Pyrolysis Fuel 86, 1781–1788.

Yasuda, S.; Fukushima, K.; Kakehi, A. 2001. Formation and chemical structures of acid-soluble lignin I: sulfuric acid treatment time and acid-soluble lignin content of hardwood. J Wood Sci 47, 69–72.

Zhang, X.-M.; Menga, L.-Y.; Xu, F.; Sun R.-C. 2011. Pretreatment of partially delignified hybrid poplar for biofuels production: Characterization of organosolv hemicelluloses. Ind Crop Prod 33, 310–316.

Zheng, Y.; Pan, Z.; Zhang, R. 2009. Overview of biomass pretreatment for cellulosic ethanol production. Int J Agric & Biol Eng 2 (3), 51-68.

Zhu, J.Y.; Pan, X.J. 2010. Woody biomass pretreatment for cellulosic ethanol production: Technology and energy consumption evaluation. Bioresour Technol 101, 4992–5002.

# 3. LIGNIN PURIFICATION STUDY

## 3.1 Background

Lignin presents a branched-randomized structure that varies depending on its origin, extraction method, plant age and harvesting. The high structural diversity of lignin and also its high and wide molecular weight distributions make its introduction in the industry a difficult task due to the non-homogeneity of the lignin fractions. Moreover, the size of the lignin molecules can vary between 1000 Da and 100,000 Da within a same sample, therefore, fractionation has become one of the best ways to obtain specific lignins. The aim of fractionation/purification is to obtain specific molecular weight fractions with different compositions and functionalities; so they can be then used as high added value products for specific applications.

Different methods have been proposed in the literature to fractionate-purify lignin:

- Solvent extraction (Mörck et al. 1986; Thring et al. 1996; Yuan et al. 2009)
- Differential precipitation (Sun et al. 1999; Mussatto et al. 2007)
- Membrane technology (Wallberg et al. 2003a, 2003b)

Previous works were developed in order to select the most adequate lignin fractionation-purification method. Solvent extraction was not considered so as to avoid the use of high solvent quantities, contamination problems and operational difficulties. The fractionation-purfication process selection was carried out taking into account differential precipitation (García et al. 2009) and membrane technology (ultrafiltration) (Toledano et al. 2010a) and in the end, comparing both techniques results (Toledano et al. 2010b). Although the treated liquid fractions were obtained by different pretreatment (alkali pretreatment) and from other raw material, the main and general conclusions regarding the effect of the fractionation-purification

process on lignin structure and its physicochemical properties could be assumed for applying it to other systems. Following, the main conclusions of the mentioned studies are commented.

Selective precipitation was achieved by decreasing the pH of the liquor at different values by acid addition and then, the obtained lignins were carefully characterized (GPC, NMR, ATR-IR, TGA and DSC). It was found that while decreasing pH from 12.64 to 0.72, the amount of precipitate increased and black liquor color attenuated, giving a maximum value of precipitate at pH 0.72. The lignin precipitated at pH 2.57 and 0.72 exhibited similar characteristics (IR spectra, thermograms, Mw and $^{1}H$ NMR) as commercial alkaline lignin. At other pH values, obtained lignin presented more impurities mainly due to the presence of hemicelluloses and silicates in the raw material. It was possible to conclude that there were clear differences between the precipitates obtained at different pH intervals, refereed to its composition and, especially, to the content and properties of obtained lignin.

Ultrafiltration was also investigated as a lignin fractionation-purification method. It was concluded that ultrafiltration process constituted a proper method to obtain different fractions of lignin with different and specific molecular weight as it was proved by size exclusion chromatography results. Lowest membrane cut-off yielded lignin fractions that presented high fractions of low molecular weight (LMW). By 2D NMR (HSQC) it was pointed out that the more than 15 kDa fraction (greater membrane cut-off of this study) was a highly contaminated fraction (very likely with LCC). Contrary to expectations, this study did not find a significant difference in different lignin fractions thermal behavior.

Both fractionation-purification methods were compared in order to establish which process provided best results. Primarily, it was found that both techniques yielded lignin fractions with different properties or composition. However, ultrafiltration

showed better results as the obtained lignin fractions were less contaminated with hemicelluloses as it was confirmed by thermal analysis. The thermogravimetric analysis is widely used to study how the organic polymers decompose. Results corresponding to the different fractions obtained by selective precipitation pointed out a weight loss around 90 ºC, which corresponded to the absorbed water evaporation. The second peak, which appeared at relative low temperatures (280-370 ºC), was, in most of the cases, a wide peak. These observations suggested the presence of hemicellulose–lignin complexes in the selective precipitated fractions. Decomposition temperature of these products was found to be intermediate between hemicelluloses one (around 230 ºC) and lignin, explaining the low DTG obtained value. On the other hand, ultrafiltered lignin fractions presented three clearly differenciated weight losses. First weight loss (DTGmax =75 ºC) was due to the moisture of the sample, subsequently the second peak (DTGmax = 235 ºC) could be ascribed to the degradation of polysaccharide (hemicelluloses) contamination due to the extraction process followed. The maximum DTG at 380 ºC belonged to lignin degradation. Ultrafiltered fractions presented lower contamination than differential precipitation samples since the hemicelluloses contamination were not deeply connected to the lignin structure.

Weight-average (Mw), number-average (Mn) and molecular weight and polydispersity (Mw/Mn) of the lignin fractions obtained by the studied fractionation-purification processes are presented in Table 3.1. For the ultrafiltered lignin fractions, there was a clear trend downwards of the weight-average molecular weight as the used cut-off to obtain the lignin fractions was smaller. As a consequence, the polydispersity also decreased with the pore size. By differential precipitation, all the obtained fractions presented low polydispersity. When the pH was strongly acidic the highest weight-average molecular weight was reached. Ultrafiltration yielded fractions with more differentiated weight-average molecular weight than selective precipitation. Both fractionating techniques produced fractions with low

polydispersity. Ultrafiltration allows selecting the right cut-off of the membrane; the weight-average molecular weight could be controlled.

| ULTRAFILTRATION | | | | SELECTIVE PRECIPITATION | | | |
|---|---|---|---|---|---|---|---|
| **Fraction** | **Mn** | **Mw** | **Mw/Mn** | **Fraction** | **Mn** | **Mw** | **Mw/Mn** |
| Rough | 1879 | 5654 | 3.01 | pH 0.72 | 3501 | 2908 | 1.20 |
| > 15 KDa | 2032 | 6300 | 3.10 | pH 2.57 | 2432 | 1311 | 1.86 |
| 15 KDa | 3091 | 3544 | 1.14 | pH 5.40 | 2120 | 1142 | 1.62 |
| 10 KDa | 946 | 2022 | 2.14 | pH 6.50 | 1990 | 1430 | 1.40 |
| 5 KDa | 940 | 1806 | 1.92 | pH 9.16 | 2160 | 1550 | 1.41 |

**Table 3.1.** Molecular weight of obtained lignin fractions by the studied fractionation processes.

Differential precipitation was an easier and simpler technique and less energy consuming than ultrafiltration, though lower lignin quality was produced since its weight-average molecular weight could not be controlled easily and because of the presence of lignin–carbohydrate complex (LCC) in lignin fractions was higher. Thermal analysis and IR spectra confirmed the contamination and LCC contamination was proved to affect degradation temperature. $^{1}H$ NMR spectra of the obtained fractions by the studied different fractionation processes supported also the findings that suggested that lignin fractions obtained by selective precipitation were more contaminated than the ultrafiltered lignin.

As the aim of this thesis was lignin depolymerization, ultrafiltration was selected as the most adequate fractionation-purification process. Subjecting ultrafiltered lignin fractions to different depolymerization conditions will allow the study of the influence of lignin molecular weight on its depolymerization behavior. At the same time, hemicellulosic contamination will be avoided by using ultafiltration as fractionation-purification process. Hemicellulosic contamination could decrease or mislead depolymerization results.

## 3.2 Membrane technology

Membrane separation processes have been studied extensively in recent years due to its implementation in the industry is of great interest in various sectors such as food, chemical and pharmaceutical industries (Mulder 1991; Baker 2000).

The membrane technology enables compliance with four goals:

- Separation
- Concentration
- Purification
- Fractionation

Membrane technology is a relatively new technology and because of its multidisciplinary character it can be used in a large number of separation processes. However, comparison between the different separation processes is difficult.

The benefits of membrane technology can be summarized as follows (Mulder 1991):

- Separation can be carried out continuously
- Energy consumption is generally low
- Membrane processes can easily be combined with other separation processes
- Separation can be carried out under mild conditions
- Up-scaling is easy
- Membrane properties are available and can be adjusted
- No additives are required

The following drawbacks should be mentioned:

- Concentration polarization/membrane fouling
- Low membrane lifetime
- Generally low selectivity

The low energy consumption, no need of reagents addition that can change the structure of the dissolved compounds and the easy scaling, makes membrane technology an optimal fractionation-purification method to be implemented in a biorefinery. The major drawbacks have to be taken into account but can be overcome as demonstrated by the existence today of facilities applying membrane technology in various fields (Baker 2000).

There are different types of membrane processes depending on the separation principle. The efficacy or efficiency of membrane technology based on molecular size separation depends strongly on the type of membrane used and the pore or particle size as to retain (Kovacs et al. 2009). The use of a pressure gradient as the driving force across the membrane allows the collection of permeate with a molecular size substances smaller than the pore size of the membrane, while those with greater size continue to be collected in the filtrate. Given the above, it can be distinguished four types of processes: microfiltration (MF), ultrafiltration (UF), nanofiltration (NF) and reverse osmosis (RO). These methods differ in the type of membrane and operating conditions required and, therefore, the field of application. Table 3.2 shows the data of each type of process depending on the pore size employed. The information contained in Table 3.2 allows selecting ultrafiltration as the most suitable pore size. Lignin is a macromolecule and that is why ultrafiltration has been selected in this study as the optimum membrane technology process for its fractionation and purification.

| Process | Membrane type and pore size | Membrane material | Driving force (bar) | Applications |
|---|---|---|---|---|
| MF | Symmetric microporous 0.1 - 10 μm | Ceramics, Metal oxides (Al-, Ti-, Zr-), Graphite, Polymers (Cellulose nitrate or acetate, PVDF, Polyamides, Polysulfone, PTFE,..) | 1-5 | Sterile filtration, Clarification |
| UF | Asymmetric microporous 1 - 10 nm | Ceramics, Polysulfone, Polypropylene, Nylon 6, PTFE, PVC, Acrylic Copolymer | 1-10 | Separation of macromolecular solutions |
| NF | Thin-film membranes | Cellulosic Acetate and Aromatic Polyamide | 1-10 | Removal of hardness and desalting |
| RO | Asymmetric skin-type 0.5 - 1.5 nm | Polymers, Cellulosic acetate, Aromatic Polyamide | up to 200 | Separation of salts and microsolutes from solutions |

**Table 3.2.** Common operating conditions and applications of different membrane separation processes (Mulder 1991).

### 3.2.1 Ultrafiltration

Many works related to the study of membrane processes for the concentration and the recovery of by-products from black liquors have been published (Tanistra et al. 1998; Dafinov et al. 2005; Žabková et al. 2007). For the recovery of waste products, various types of ultrafiltration (UF) membranes and effluent treatments have been considered (Bhattacharjee et al. 2005, 2006). UF has also been extensively studied to concentrate the black liquor resulting from the kraft pulp and paper process (Wallberg et al. 2003a,b; Jönsson et al. 2008, 2009). The main purpose of these researches lied on the application of ultrafiltration-nanofiltration (UF-NF) process for improvement of energy efficiency in the kraft process. These authors have considered various methods of filtration, operating parameters and costs associated with the application of membrane technology. The large amount of water used in this

industry, and the high cost of the recovery process derived from evaporating of the water contained in the black liquor before the reagent recovery, turn UF / NF into a promising alternative to the habitual methods of black liquor concentration. The combination of UF-NF process has also been studied for the separation of components different to lignin, e.g. the hemicelluloses present in black liquor (Schlesinger et al. 2006) or those obtained during the hydrolysis of lignocellulosic materials, confirming the effectiveness of this technology. More recently, Vegas et al. (2008) proved the efficiency of various membranes for the fractionation and purification of xylooligosaccharides from the hydrolysis of bran (shells) of rice.

Ultrafiltration membranes are rated on the basis of nominal molecular weight cut-off, but the shape of the molecule to be retained has a major effect on retentivity. Linear molecules pass through a membrane, whereas globular molecules of the same molecular weight may be retained (Figure 3.1) (Baker 2000). Bearing this in mind, lignin three dimensional randomized structure will behave more probably like globular molecules instead of linear molecules. This fact may be the reason why the lignin fraction molecular weight may not be correlated to the pore size.

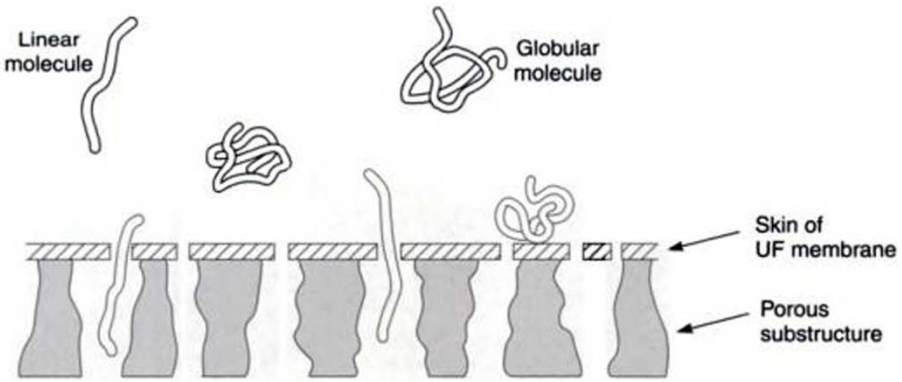


**Figure 3.1**. Schematic operation of ultrafiltration membranes (Baker 2000).

## 3.3 Materials and methods

The organosolv liquid fraction obtained by the optimized pretreatment conditions (Chapter 2) was subjected to ultrafiltration fractionation process. The ultrafiltration continuous system was built in our laboratory in order to be able to filter big amounts of liquids (Figure 3.2). The UF module used in the present work was supplied by IBMEM – Industrial Biotech Membranes (Frankfurt, Germany) and the membranes were supplied by TAMI Industries.

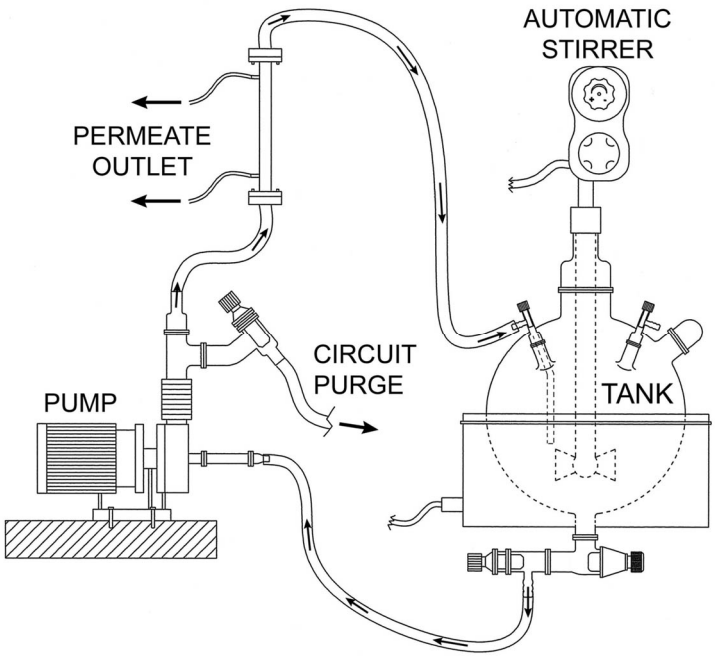


**Figure 3.2.** Scheme of the used ultrafitration system.

The membranes were made of ceramic material and were tubular and multichannel type, with an external and hydraulic diameter of 10 and 2 mm respectively, and a surface of 110 $cm^2$ (Figure 3.3). Liquid fraction solution was filtered successively decreasing the different membrane cut-offs (300, 150, 50, 15 and 5 kDa).

**Figure 3.3.** Detail of the tubular ceramic ultrafiltration membrane section used in this work.

The liquid fraction passed through the membrane where the dissolved molecules with a molecular weight lower than the cut-off or a shape that fitted the cut-off came out to be collected (permeate). The remaining liquid fraction was back recirculated to the tank (retentate). The temperature used for this process was 60 °C, provided by the pumping system. Liquid fraction was recirculated until no permeate was generated. Then, the resulting retentates (Table 3.2) were characterized following the analytical procedures in Appendix III.

| **Retentates** | **Fraction** |
|---|---|
| > 300 kDa | F1 |
| < 300 kDa > 150 kDa | F2 |
| < 150 kDa > 50 kDa | F3 |
| < 50 kDa > 15 kDa | F4 |
| < 15 kDa > 5 kDa | F5 |
| < 5 kDa | F6 |

**Table 3.3.** Lignin ultrafiltered fractions after using different membrane cut-offs.

Once the retentates were characterized, they were treated with two volumes of acidified water (adding $H_2SO_4$ -95-98 % purity, Panreac- until pH around 2) to

precipitate the dissolved lignin. Afterwards, the suspensions were centrifugated at 4000 rpm for 20 minutes to recover the lignin. Lignin was then dried at 50 ºC. Lignin fractions were characterized to determine their composition, sturucture, molecular weight distributions and physicochemical properties following the procedures described in Appendix II.

## 3.4 Ultrafiltration results

The resulted retentates were collected and characterized in order to evaluate their physicochemical properties (Table 3.4). Retentate pHs were slightly acidic in all cases due to organosolv pretreatment. The applied organosolv conditions did not involved acid addition but acetic acid was generated from hydrolysis of acetyl groups associated with the hemicelluloses acidifying the liquid fraction (Xu et. al 2006; El Hage et al. 2010).

| | **F1** | **F2** | **F3** | **F4** | **F5** | **F6** |
|---|---|---|---|---|---|---|
| pH | 4.34 | 5.65 | 4.42 | 3.90 | 4.33 | 4.45 |
| Density[1] | 0.9389 | 0.9068 | 0.8987 | 0.9289 | 0.9283 | 0.9076 |
| TDS | 16.14 ± 0.15 | 7.01 ± 0.10 | 6.14 ± 0.02 | 9.78 ± 0.01 | 7.24 ± 0.06 | 5.29 ± 0.02 |
| OM | 16.00 ± 0.19 | 6.96 ± 0.08 | 6.08 ± 0.02 | 9.67 ± 0.01 | 7.13 ± 0.08 | 5.22 ± 0.02 |
| IM | 0.11 ± 0.00 | 0.05 ± 1.00 | 0.06 ± 0.05 | 0.11 ± 0.01 | 0.11 ± 0.02 | 0.07 ± 0.00 |
| Lignin | 89.91 ± 0.12 | 33.05 ± 0.07 | 27.39 ± 0.11 | 45.92 ± 0.17 | 25.55 ± 0.05 | 16.28 ± 0.21 |

[1]Density standard deviation ≤0.01

**Table 3.4.** Physicochemical properties of obtained retentates by ultrafiltration. Density (g/L); TDS: total dissolved solids (%); OM: organic matter (%); IM: inorganic matter (%) and lignin concentration (g/L).

Totat dissolved solids (TDS) content was higher for the retentate resulted after using the greater membrane cut-off (300 kDa), as expected, F1 was made up of the biggest and complex structures. The lowest TDS value was obtained when the lowest membrane cut-off (5 kDa) was applied. Unexpectedly, TDS clear trend was not observed. Taking into account organic and inorganic matter (OM and IM), it can be stated that mostly all compounds present in the filtrates presented organic origin. Lignin concentration in the different obtained rententates presented different values and no trend was found. This fact could be explained given the fact that during organosolv pretreatment lignin was extracted from the raw material yielding different size and shape lignin fragments. Also, it has to be taken into consideration that ultrafitration process achieved not only products separation but also products concentration. In general, retentates presented high lignin concentration.

### 3.4.1 Ultrafiltered lignin fractions characterization

The ATR-IR spectra of the obtained ultrafiltered lignin fractions are shown in Figure 3.4. Around 3380 $cm^{-1}$, a vibration could be observed caused by the stretching of the hydroxyl group. Some differences in the intensity of this peak between ultrafiltered lignin fractions were observed. All spectra presented bands between 2937 and 2840 $cm^{-1}$ that corresponded to the vibration of C-H bond in methyl and methylene groups ($CH_3$ and $–CH_2$-). The asymmetric deformation of this bond also produced a band at around 1456 $cm^{-1}$. The vibration at around 1705 $cm^{-1}$ was associated to the C-O bond stretching in unconjugated ketones, carbonyl, and ester groups. The vibration around 1661 $cm^{-1}$ was related to C-O bond stretching in conjugated p-substituted aryl ketones. Three typical aromatic ring vibrations were identified around 1425, 1515 and 1595 $cm^{-1}$.Typical lignin wavelengths were found at around 1323 $cm^{-1}$ related to the breathing of the syringyl ring with C-O stretching and at around 1269

$cm^{-1}$ (shoulder) and 1212 $cm^{-1}$ associated to the breathing of the guaiacyl ring with C-O stretching. Around 1116 $cm^{-1}$, a vibration that was caused by the deformation of the C-H linkage in syringyl substructures was observed. The vibration at around 1025 $cm^{-1}$ was due to the deformation or the aromatic C-H linkages in guaiacyl substructures but this vibration could also be associated to the deformation of the bond C-O in primary alcohols. Finally, at around 834 $cm^{-1}$, there was a vibration caused by the C-H linkage in positions 2 and 6 of the aromatic ring in syringyl substructures. These findings suggested that in general lignin was the main component of the obtained ultrafiltered organosolv olive tree prugnin ligin according to other authors (Faix et al. 1991; Tejado et al. 2007).

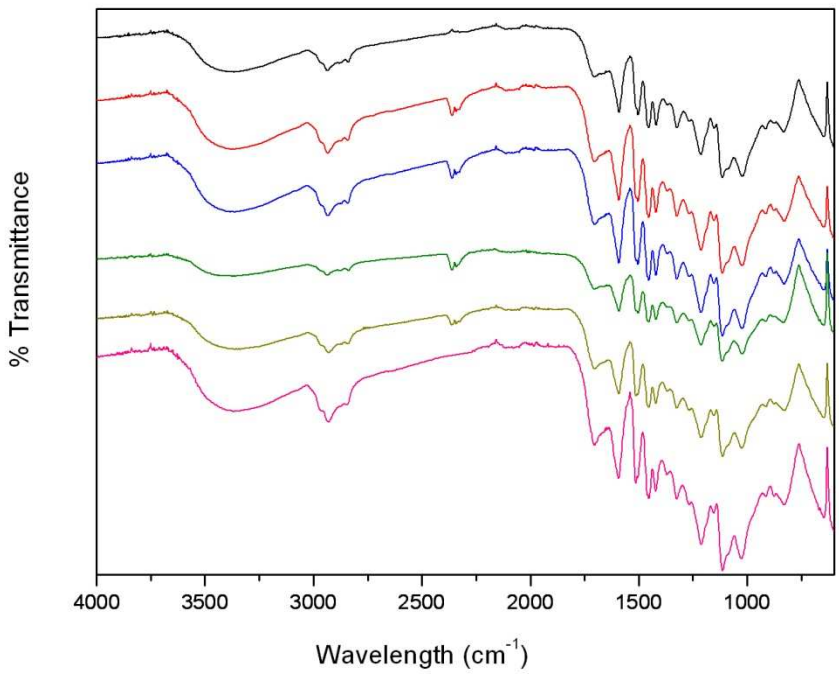


**Figure 3.4.** ATR-IR spectra of the obtained ultrafiltered organosolv olive tree pruning lignin. Black (F1), red (F2), blue (F3), green (F4), dark yellow (F5) and pink (F6).

Then lignins were subjected to different analytical procedures with the aim of determining their composition. In Table 3.5 the results of the compositions of ultrafiltered lignin fractions are shown. Lignin compositions were evaluated in terms

of acid insoluble lignin (AIL), acid soluble lignin (ASL), total sugars (glucose, xylose and arabinose) and ash content. Acid insoluble lignin content increased as the used cut off was smaller reaching a maximum of 83%. Moreover, AIL percentage could be considered as a measurement of lignin purity since lignin isolation from the liquid fraction was based on its insolubility in acidic media. Comparatively, sugar content presented the opposite behaviour, with decreasing total sugar contents along with decreasing membrane cut-off. Total sugars were determined after strong acidic hydrolysis. This process achieved the breakdown of sugars chains. Such chains probably presented higher sizes than the cut-off and that was why when using low cut-off, the total sugars in isolated lignins decreased. These facts confirmed that ultrafiltration is not only a fractionation process but also a purification process. Organosolv treatment allows the obtaining of high quality lignin and sulfur-free lignin but the implementation of an ultrafiltration system makes possible lignin purification, achieving highly pure lignin.

| | **F1** | **F2** | **F3** | **F4** | **F5** | **F6** |
|---|---|---|---|---|---|---|
| AIL | 72.90 ± 0.67 | 80.43 ± 0.85 | 81.30 ± 0.29 | 81.47 ± 0.63 | 81.33 ± 0.27 | 82.97 ± 0.91 |
| ASL | 2.48 ± 0.02 | 1.92 ± 0.08 | 1.67 ± 0.07 | 1.84 ± 0.13 | 2.24 ± 0.12 | 2.28 ± 0.07 |
| Sugars | 3.26 ± 0.15 | 1.36 ± 0.06 | 1.01 ± 0.06 | 1.21 ± 0.14 | 0.74 ± 0.08 | 0.57 ± 0.04 |
| Glucose | 0.91 ± 0.03 | 0.38 ± 0.01 | 0.30 ± 0.01 | 0.38 ± 0.02 | 0.35 ± 0.03 | 0.28 ± 0.02 |
| Xilose | 2.25 ± 0.12 | 0.91 ± 0.05 | 0.64 ± 0.05 | 0.75 ± 0.13 | 0.32 ± 0.05 | 0.24 ± 0.03 |
| Arabinose | 0.10 ± 0.00 | 0.07 ± 0.02 | 0.06 ± 0.01 | 0.08 ± 0.00 | 0.06 ± 0.00 | 0.07 ± 0.02 |
| Ash | 0.15 | 0.52 | 0.44 | 0.56 | 0.20 | 0.20 |

AIL: acid insoluble lignin ; ASL: acid soluble lignin.

**Table 3.5.** Ultrafiltered lignin fractions composition. Composition (%, w/w).

Acid soluble lignin content remained low for all ultrafiltered fractions but it could not be observed any clear trend. Yasuda et al. (2001) suggested that ASL is probably

composed of two components: lignin degradation products and secondarily formed hydrophilic materials such as lignin-carbohydrate. As mentioned before, total sugars content decreased along with the size of the used cut-off. Among sugars content, glucose, xylose and arabinose content was analyzed resulting in different monomer content behavior. Glucose content was reduced as the applied membrane cut off was smaller. Xylose decreased dramatically when filtrating through 300 kDa membrane and then, xylose continued diminishing at decreasing cut-offs (reaching a minimum of 0.24%). Xylose constituted the main hemicellulosic sugar in all obtained lignin fractions and its content decrease proved that ultrafiltration process allowed lignin purification. All ultrafiltered fractions presented low ash content.

The objective of the ultrafiltration process was to obtain specific molecular weight lignin fractions and it was clearly reached as it is shown in Table 3.6, (number-average (Mn), weight-average (Mw) molecular weight and polydispersity (Mw/Mn)). The obtained values are relative to the employed polystyrene standards. As expected, all the aforementioned lignin properties decreased with decreasing the membrane cut-off sizes. The molecular weight distributions were narrower as the membrane cut off was lower confirming the drop in the polydispersity and proving that purification occurred by applying ultrafiltration to the lignin rich liquid fraction. The relatively low polydispersity found indicated the high fractions of low molecular weight (LMW) present in lignin samples.

| | **F1** | **F2** | **F3** | **F4** | **F5** | **F6** |
|---|---|---|---|---|---|---|
| Mw | 12798 | 9302 | 7882 | 6555 | 5184 | 4527 |
| Mn | 3060 | 2489 | 2183 | 2165 | 1686 | 1567 |
| Mw/Mn | 4.18 | 3.74 | 3.61 | 3.03 | 3.07 | 2.89 |

**Table 3.6.** Weight-average (Mw), number-average (Mn) molecular weight and polydispersity (Mw/Mn) of the obtained ultrafiltered lignin fraction.

As explained before, the number of C–C bonds between units is connected to the lignin molecular weight, mainly to the structures involving C5 in the aromatic ring. The most abundant aromatic rings in lignin are guaiacyl-type unit and syringyl-type unit. Guaiacyl-type units are able to form this kind of bonds, but this is not possible in syringyl-type units as they have both C3 and C5 positions substituted by methoxy groups. 4-O-5 and β-5 structures also present C5 position free and therefore, are susceptible of forming this C-C linkage. Lignins mostly composed by guaiacyl units are expected to show higher MW than those presenting high contents of syringyl units (Glasser et al. 1993). Such lignins with high fractions of low molecular weight molecules are more reactive than those with high molecular weight molecules (Pizzi 1994).

Functional lignin groups were also studied in order to determine if the ultrafiltration process affected also lignin reactivity. With this purpose, carboxyl groups, carbonyl groups and total phenolic content were analyzed. The results summarized in Table 3.7 suggested that ultrafiltered lignin fractions are highly reactive since the amounts of functional groups were high.

| | **F1** | **F2** | **F3** | **F4** | **F5** | **F6** |
|---|---|---|---|---|---|---|
| COOH | 4.72 ± 0.08 | 4.83 ± 0.17 | 5.52 ± 0.09 | 5.98 ± 0.25 | 5.77 ± 0.17 | 5.77 ± 0.09 |
| C=O | 0.38 ± 0.01 | 0.40 ± 0.00 | 0.41 ± 0.01 | 0.43 ± 0.01 | 0.48 ± 0.01 | 0.49 ± 0.01 |
| OH | 9.53 ± 0.04 | 10.79 ± 0.05 | 10.73 ± 0.02 | 9.47 ± 0.16 | 12.61 ± 0.09 | 12.73 ± 0.05 |

**Table 3.7.** Functional groups (%, w/w) of the ultrafiltered lignin fractions.

During organosolv delignification, lignin is dissolved essentially by acid-catalyzed (acids generated from lignin) cleavage of such bonds as β-aryl ether and arylglycerol-β-aryl ether in the lignin macromolecule. However, the cleavage of β-aryl ether bonds

occurs at lower extent. The cleavage of ether bonds gives rise to new phenolic hydroxyl groups in lignin, which affect some industrial uses of lignins and lignocellulosic materials, since they increase lignin solubility (favoring its alkaline extraction during paper or pulp manufacture), and modifies the reactivity of technical lignins to be used as raw material for manufacture of lignin-based adhesives and other applications (Sarkanen, 1990; Goyal et al., 1992; Camarero et al. 1999; Xu et al. 2006).

It could be clearly observed in Figure 3.5 that there was a direct relation between the obtained ultrafiltered lignin fraction and its functionality. All analyzed functional groups (carboxyl, carbonyl and total phenolic) enlarged as the membrane cut-off used to obtain the lignin fraction was smaller, ie, increased as the lignin molecular weight was lower. Nevertheless, slightly behavioral differences between the analyzed functional groups could be noticed.

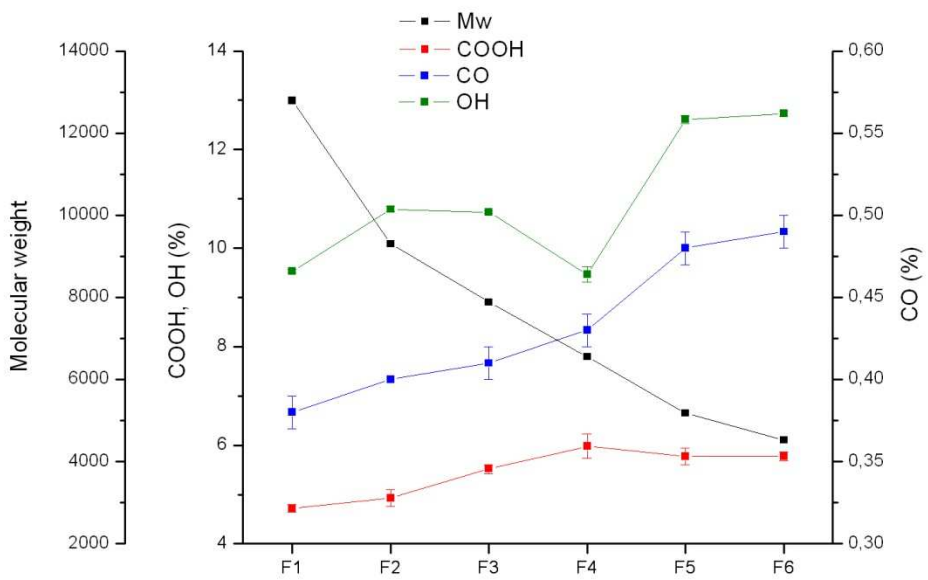


**Figure 3.5.** Influence of molecular weight on lignin functionality.

For instance, carboxyl groups presented an increasing tendency when decreasing the molecular weight until the lower molecular weight lignin fractions where plateau was reached. Furthermore, carbonyl content also presented a growing tendency while decreasing the lignin molecular lignin but it should be stressed that the increase was really slight. The total phenolic content, besides being the most abundant functional group analyzed in ultrafiltered lignin fractions, showed the higher growing trend. Surprisingly, F4 was found to be out of this growing tendency as its carboxyl content was similar to the F1's one. High functionality implies high reactivity of obtained ultrafiltered organosolv olive tree pruning lignin fractions.

## 3.5 Conclusions

Liquid fraction resulted from the organosolv pretreatment was subjected to ultrafiltration using different membranes cut-off (300, 150, 50, 15 and 5 kDa). As a result, six different retentes were obtained and treated to isolate the present lignin. Ultrafiltered lignin fractions were deeply characterized in order to determine their composition and physicochemical properties.

Ultrafiltered lignin fractions were proved to present different molecular weight related to the membrane cut-off used to obtain them. This fact has confirmed that ultrafiltration is a good fractionation process. In addition, the second major finding was that the AIL content increased as the use membrane cut-off was smaller yielding purer ultrafiltered lignin fractions. Besides fractionation, ultrafiltration has been proved to be an effective process to purificate lignin. Functional groups content in lignin fractions have been confirmed to be associated to the lignin fraction molecular

weight. The most obvious finding to emerge from this study is that controlling the membrane cut-off used allows producing the desire lignin physicochemical properties or composition.

## 3.6 References

Baker, R.W. 2000. Membrane technology and applications. Wiley. ISBN 0-07-135440-9.

Bhattacharjee, P.K.; Todi, R.K.; Tiwari, M.; Bhattacharjee, C.; Bhattacharjee, S.; Datta, S. 2005. Studies on ultrafiltration of spent sulphite liquor using various membranes for the recovery of lignosulphonates. Desalination 174, 287-297.

Bhattacharjee, S.; Datta, S.; Bhattacharjee, C. 2006. Performance study during ultrafiltration of Kraft black liquor using rotating disk membrane module. J Clean Prod 14, 297-504.

Camarero, S.; Bocchini, P.; Galletti, G.C.; Martinez, A.T. 1999. Pyrolysis–gas chromatography/mass spectrometry analysis of phenolic and etherified units in natural and industrial lignins. Rapid Commun Mass Spectrom 13, 630–636.

Dafinov, A.; Font, J.; García-Valls, R. 2005. Processing of black liquors by UF/NF ceramic membranes. Desalination 173, 83- 90.

El Hage, R.; Chrusciel, L.; Desharnais, L.; Brosse, N. 2010. Effect of autohydrolysis of Miscanthus x giganteus on lignin structure and organosolv delignification. Bioresour Technol 101, 9321–9329.

Faix, O. 1991. Classification of lignins from differente botanical origins by FT-IR spectroscopy. Holzforschung 45, 21-27.

García, A.; Toledano, A.; Serrano, L.; Egüés, I.; González, M.; Marín, F.; Labidi, J. 2009. Characterization of lignins obtained by selective precipitation. Sep Purif Technol 68, 193–198.

Glasser, W.G.; Dave, V.; Frazier, C.E. 1993. Molecular weight distribution of (semi-commercial lignin derivatives. J Wood Chem Technol 13 (4), 545–559.

Goyal, G.C.; Lora, J.H.; Pye, K.E. 1992. Autocatalyzed organosolv pulping of hardwoods: effect of pulping conditions on pulp properties and characteristics of soluble and residual lignin. Tappi J 75, 110–116.

Jönsson, A.-S.; Nordin, A.K.; Wallberg, O. 2008. Concentration and purification of lignin in hardwood kraft pulping liquor by ultrafiltration and nanofiltration. Chem Eng Res Des 86 (11), 1271-1280.

Jönsson, A.-S.; Wallberg, O. 2009. Cost estimates of kraft lignin recovery by ultrafiltration. Desalination 237, 254- 267.

Kovacs, Z.; Discacciati, M.; Samhaber, W. 2009. Modelling of batch and semi-batch membrane filtration processes. J Membrane Sci 327, 164–173.

Mörck, R.; Yoshida, H.; Kringstad, K.P. 1986. Fractionation of kraft lignin by successive extraction with organic solvents: functional groups, $^{13}C$ NMR spectra and molecular weight distributions. Holzforschung 40, 51.

Mulder, M. 1991. Basic principles of membrane technology. Kluwer Academic Publishers. ISBN 0-7923-4247-X (HB), ISBN 0-7923-4248-8 (PB).

Mussatto, S.I.; Fernandes, M.; Roberto, I.C. 2007. Lignin recovery from brewer' s spent grain black liquor. Carbohydr Polym 70, 218–223.

Pizzi, A. 1994. in Advanced Wood Adhesives Technology, ed. Marcel Dekker, New York, 219-241.

Sarkanen, K.V. 1990. Chemistry of solvent pulping. Tappi J 73, 215–219.

Schlesinger, R.; Götzinger, G.; Sixta, H.; Friedl, A.; Harasek, M. 2006. Evaluation of alkali resistant nanofiltration membranes for the separation of hemicellulose from concentrated alkaline process liquors. Desalination 192, 303- 314.

Sun, R.-C.; Tomkinson, J.; Bolton, J. 1999. Effects of precipitation pH on the physicochemical properties of the lignins isolated from the black liquor of oil palm empty fruit bunch fibre pulping. Polym Degrad Stab. 63 (2), 195–200.

Tanistra, I.; Bodzek, M. 1998. Preparation of high-purity sulphate lignin from spent black liquor using Ultrafiltration and diafiltration, Desalination 115,) 111- 120.

Tejado, A.; Peña, C.; Labidi, J.; Echeverria, J.M.; Mondragon, I. 2007. Physicochemical characterization of lignins from different sources for use in phenol-formaldehyde resin synthesis. Bioresour Technol 98 (8), 1655–1663.

Thring, R.W.; Vanderlaan, M.N.; Griffin, S.L. 1996. Fractionation of Alcell lignin by sequential solvent extraction. J Wood Chem Technol 16 (2), 139–154.

Toledano, A.; García, A.; Mondragon, I.; Labidi, J. 2010a. Lignin separation and fractionation by ultrafiltration. Sep Purif Technol 71, 38–43.

Toledano, A.; Serrano, L.; Garcia, A.; Mondragon, I.; Labidi, J. 2010b. Comparative study of lignin fractionation by ultrafiltration and selective precipitation. Chem Eng

J 157, 93–99.

Vegas, R.; Moure, A.; Domínguez, H.; Parajó, J.C.; Álvarez, J.R.; Luque, S. 2008. Evaluation of ultra- and nanofiltration for refining soluble products from rice husk xylan. Bioresour Technol 99, 5341-5351.

Wallberg, O.; Jönsson, A.-S.; Wimmerstedt, R. 2003a. Ultrafiltration of kraft black liquor with a ceramic membrane. Desalination 156, 145–153.

Wallberg, O.; Jönsson, A.S. 2003b. Influence of the membrane cut-off during ultrafiltration of kraft black liquor with ceramic membranes. Trans IChemE 81, 1379–1384.

Xu, F.; Sun, J.-X.; Sun, R.C.; Fowler, P.; Baird, M.S. 2006. Comparative study of organosolv lignins from wheat Straw. Ind Crop Prod 23, 180–193.

Yasuda, S.; Fukushima, K.; Kakehi, A. 2001. Formation and chemical structures of acid-soluble lignin I: sulfuric acid treatment time and acid-soluble lignin content of hardwood. J Wood Sci 47, 69–72.

Yuan, T.-Q.; He, J.; Xu, F.; Sun, R.-C. 2009. Fractionation and physico-chemical analysis of degraded lignins from the black liquor of Eucalyptus pellita KP-AQ pulping. Polym Degrad Stab 94, 1142–1150.

Žabková, M.; Borges da Silva, E.A.; Rodrigues, A.E. 2007. Recovery of vanillin from lignin/vanillin mixture by using tubular ceramic ultrafiltration membranes. J Membrane Sci 301, 221-237.

# 4. LIGNIN DEPOLYMERIZATION BY HYDROLYSIS

## 4.1 Introduction

In the past and until now, the most common lignin application in the pulp and paper industry has been energy generation through its combustion. However, lignin structure is unique in nature and supposes an exceptional source of aromatic compounds. Taking into account this uniqueness, lignin revalorization in high added value platform chemicals could provide a qualitative leap to the exploitation of this side stream in pulp and paper industries and in the future second generation bioethanol plants.

Lignin conversion into simple aromatic products is a difficult task due to lignin recalcitrant structure. Thus, catalysis is regarded as a key enabling technology for biomass conversion in general and for fulfilling the promise of lignin valorization in particular (Zakzeski et al. 2010). Lignin depolymerization can be achieved by different strategies -oxidation, hydrolysis, hydrogenation, pyrolysis, enzymatic reactions… Although lignin catalytic depolymerization is a hot topic, there is still much to do in order to improve yields and to workup products separation procedures.

Early studies concerning the obtaining of simple monomers from lignin were performed by Freudenberg et al. (1936, 1937, 1938, 1939a, 1939b, 1940). The developed works were aimed to find evidence for the aromatic nature of lignin. The most famous developed method, alkaline nitrobenzene oxidation, is currently used as analytical method for determining lignin subunits. By the action of an alkaline solution together with the presence of nitrobenzene, lignin oxidation is achieved by producing, mainly, vanillin, syringaldehyde and p-hydroxybenzaldehyde, in addition to their respective acids. The concentration of these released compounds allows

establishing the relationship between units S, G and H, and the lignin origin (hardwood, softwood or grass and annual plants). Subsequently, studies were conducted to determine the reaction mechanism of alkaline nitrobenzene oxidation (Leopold et al. 1951a, 1951b, 1952a, 1952b, Pew 1955). In these, it was observed that the phenolic aldehydes are derived from oxidative degradation of the corresponding p-hydroxyphenylpropane units and their ether, in particular the corresponding 4-O-alkylated and α-O-4 and β-O-4 lignin substructures. Gierer et al. (1985, 1986) proved that phenolic hydroxyl groups play a prominent role by virtue of its ability to promote the base-catalyzed cleavage of interunitary ether linkages and the oxidative degradation of lignin. Although the ability of these hydrolytic alkaline treatments to produce simple phenolic compounds has been demonstrated, the toxicity of nitrobenzene makes unviable scaling this process.

Since then, many studies have been performed to optimize the production of chemicals with high added value from lignin by hydrolysis. Thring (1994) studied the alkaline degradation of ALCELLL® lignin by means of the combined effect of time and temperature reaction. The highest concentration of the monomers identified was obtained when using 0.5% (w/w) sodium hydroxide. The identifiable monomeric products decreased with increasing severity of treatment, indicative of the increasing importance of pyrolytic and recondensation reactions occurring in lignin structure under these conditions. Moreover, char formation was minimized with increasing alkali concentration, demonstrating that condensation reactions between the lignin fragments are greatly reduced by small concentrations of alkali in solution. Thring concluded that a compromise between the yield of methylene chloride solubles and char formation had to be found. Miller et al. (2002a, 2002b) developed two studies on the depolymerization by alkali hydrolysis of lignin in two solvents, water and alcohols. The study using low molecular weight alcohols as solvents allowed observing that the first reaction taking place in lignin models during depolymerization

reaction was the solvolysis of ether linkages that subsequently continued reacting. Acetic acid formation (that neutralized the added base) was observed during lignin model compounds depolymerization coming from ethanol. Miller et al. (2002a) performed the same experiments but using water as solvent. In this study, they observed that the base concentration was one of the most important factors governing lignin depolymerization. They found that molar excess of a strong base (NaOH) gave better results but also that a little amount of a strong base together with a larger amount of a less expensive base (CaO) produced good results. Karagöz et al. (2004) attempted to obtain simple phenolic compounds by lignin depolymerization. To this end, biomass was directly subjected to alkaline hydrolysis conditions using rubidium and cesium carbonate as catalyst. With the conditions applied, solids dramatically decreased after the reaction and consequently, the yield of phenolic oil and gaseous products increased. However, the all together treatment without previous extractions or treatments produced a wide product mixture in the isolated oil making more difficult its later refining step for further applications. More recently, Roberts et al. (2011) studied the alkaline depolymerization of lignin and lignin model compounds. The results obtained enabled them to conclude that the formation of monomers is directly proportional to the concentration of sodium hydroxide in the aqueous medium. They also proposed a mechanism for the NaOH-catalyzed breakdown of the ether bonds of lignin explaining the preferential formation of derivatives of syringol, based on the stabilizing effect that the methoxy groups provides to the transition states of the carbenium ions. They also concluded that the production of monomers is limited by the oligomerization and polymerization reactions of the products formed.

Most of the studies presented are based on the depolymerization of lignin by hydrolysis but using basic inorganic compounds as catalysts. There are also several studies in the literature (Saisu et al. 2003; Okuda et al. 2004, 2008; Wahyudinono et

al. 2008,2009) which have developed their experiments with lignin or lignin model compounds only in water, without catalysts, applying in most cases water supercritical conditions. The general conclusion of all the articles is that the increase in the density of water (supercritical conditions) favored the conversion into compounds of both high and low molecular weight. Water aids in the depolymerization of lignin (or models), but at the same time causes reactions between activated functional groups and other fragments or lignin itself by producing lignin repolymerization in the original lignin or high molecular weight products, char.

### 4.1.1 Objective

The main objective of this chapter was to study lignin depolymerization by hydrolysis in order to produce high added value products, such as simple monomeric phenolic compounds, that could be introduced in existing industrial processes. The addition of a basic catalyst to the reaction mixture was determined in order to avoid, as far as possible, the oligomerization or polymerization reactions.

The objectives were focus on improving the knowledge and yields of lignin hydrothermal depolymerization. Best performance base catalyst was investigated by studying the addition of different bases to the reaction mixture. Then, depolymerization reaction was evaluated by means of reaction conditions. The aim was to determine the optimal reaction conditions that provided best oil yield and phenolic monomers composition. These optimization conditions (catalyst and reaction conditions) were applied to ultrafiltered lignin fractions (obtained in Chapter 3). Finally, the maximization of the oil yield by the addition of a capping agent was studied. The capping agent is supposed to avoid oligomerization reactions and hence, its addition favors phenolic monomers production.

## 4.2 Materials and methods

Depolymerization reactions were conducted in a pressure batch reactor -5500 Parr reactor- equipped with a 4848 reactor controller. Lignin:solvent (water) ratio was 1:20 and this ratio remained constant for all the experiments. Catalyst concentrations selected for all reactions was 4% (w/w) referred to lignin weight. Catalyst concentration was chosen taking into consideration the results obtained by other authors (Thring 1994; Miller et al. 2002a, 2002b; Roberts et al. 2011).

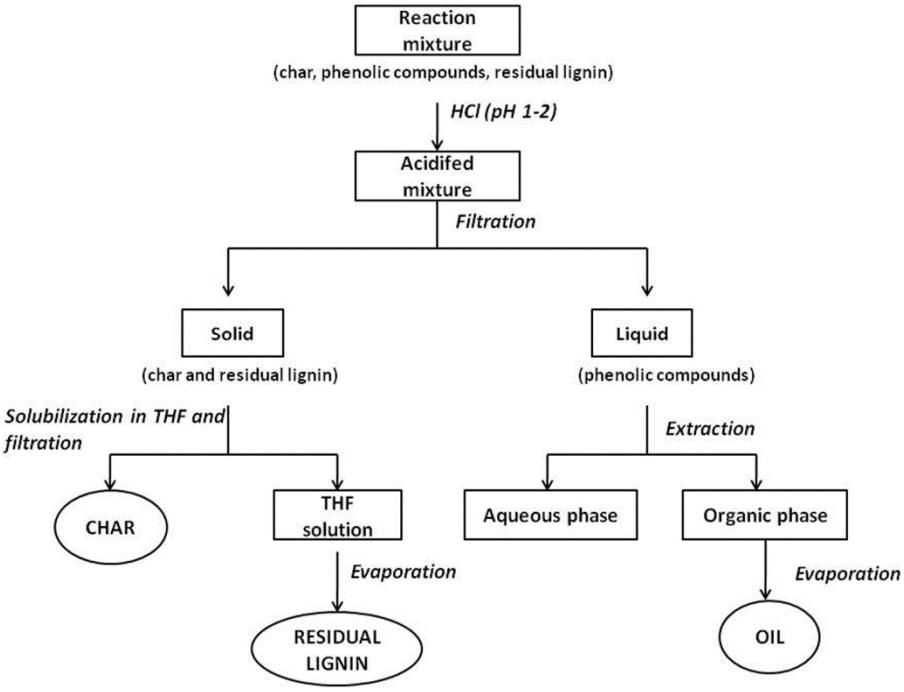


**Figure 4.1.** Scheme of the products separation procedure carried out in lignin depolymerization by hydrolysis.

Once the reaction of lignin depolymerization had finished, reaction mixture was subjected to different treatments in order to separate the products generated during the reaction, namely phenolic oil, char and residual lignin. The separation procedure scheme is depicted in Figure 4.1. The separation procedure consisted of transferring,

once cool, the mixture to a beaker and adding hydrochloric acid (37%) until reaching a pH of approximately 1. Acidification caused the appearance of a solid (solid 1) which was separated by filtration (filter Mn 640W). The filtrate was extracted with ethyl acetate to separate the phenolic compounds produced during lignin depolymerization. All extracts were joined and the solvent was evaporated under vacuum to obtain the phenolic oil. Solid 1 was composed of char and residual lignin. To separate these two products, the solid was solubilized in tetrahydrofuran (THF) and then gravity filtered (filter Mn 640W). The char was retained in the filter and the residual lignin is soluble in THF. Dissolved lignin was recovered by THF evaporation under vacuum. The yield of the three products, oil, char and residual lignin was determined gravimetrically, referred to the initial lignin weight.

### 4.2.1 Products characterization

Phenolic products resulting from lignin depolymerization were isolated as oil. This oil was characterized by gas chromatography with mass selective detector (GC-MS) and matrix assisted laser desorption/ionization time-of-flight mass spectrometry (MALDI-TOF).

GC-MS analysis was performed to identify and to quantify the monomers present in the oil. Thus, the oil was dissolved in ethyl acetate (HPLC grade). The solution was injected in a GC (7890A)-MS (5975C inert MSD with Triple-Axis Detector) Agilent equipped with a capillary column HP-5MS ((5%-Phenyl)-methylpolysiloxane, 60 m x 0.32 mm). The temperature program started at 50 ºC then, the temperature is raised to 120 ºC at 10 ºC/min, held 5 minutes, raised to 280 ºC at 10 ºC/min, held 8 minutes, raised to 300 ºC at 10 ºC/min and held 2 minutes. Helium was used as carrier gas. Calibration curves were done using pure compounds (Sigma-Aldrich) –

phenol, o-cresol, m-cresol, p-cresol, guaiacol, catechol, 4-methylcatechol, syringol, acetovanillone, syringaldehyde, acetosyringone and 4-hydroxy-3-methoxyphenylacetone-.

Oil was also analyzed by MALDI-TOF in order to evaluate the molecular weight distribution of the products present in the oil. The use of this technique allowed us to estimate the lignin depolymerization degree reached in each experiment. Matrix assisted Laser desorption/ionization time-of-flight mass spectrometry (MALDI-TOF) analyses were carried out in a Voyager-DE™ STR Biospectrometry™ Workstation of Applied Biosystems. A 15 g/L solution of DABP (3,4-diaminobenzophenone) in a methanol-water mixture (8:2) was used as matrix. The analyses were developed in negative mode.

Residual lignins were recovered and their molecular weight was evaluate as it was an important measurement to check the extent in which lignin has released molecules from its structure.

With this purpose, residual lignins were subjected to High Performance Size Exclusion Chromatography (HPSEC) to evaluate lignin molecular weight (Mw) and molecular weight distribution (MWD). The analyses were developed using a JASCO instrument equipped with an interface (LC-NetII/ADC) and a refractive index detector (RI-2031Plus). Two PolarGel-M columns (300 x 7.5 mm) and PolarGel-M guard (50 x 7.5 mm) were employed. Dimethylformamide + 0.1% lithium bromide solution was used as eluent. The flow rate was 0.7 mL/min and the analyses were carried out at 40 ºC. 0.5% (w/w) solutions were prepared to measure samples molecular weight. Calibration curve was developed using polystyrene standards (Sigma-Aldrich) ranging

from 266 to 70000 g/mol. Therefore, the obtained values are relative to the employed polystyrene standards.

## 4.3 Effect of base nature on lignin hydrothermal depolymerization

This study was conducted in order to optimize and to improve reaction conditions for lignin depolymerization by hydrolysis. As explained above, it was decided to add a base catalyst to promote the production of phenolic monomers. Therefore, a base catalyst screening was carried out in order to find out the effect of the nature and the strength of the employed base on the phenolic monomeric yield and composition, coke yield and residual lignin.

To determine the most suitable catalyst, rough organosolv olive tree pruning lignin was used as raw material with the purpose of maintaining lignin properties constant. The reactions were performed at 300 °C for 40 minutes reaching pressures of approximately 90 bars. The studied catalysts were medium and strong bases, namely sodium hydroxide (NaOH), potassium hydroxide (KOH), lithium hydroxide (LiOH), calcium hydroxide ($Ca(OH)_2$) and potassium carbonate ($K_2CO_3$). In the reaction mixture all the added substances (lignin and catalyst) were dissolved (homogeneous catalysis) and the initial pH of all experiments was 14. Catalyst concentration was 4% (wt.) to maximize the effect of the added base. An experiment was also performed without catalyst as blank. Other aspects of the reaction conditions, product separation procedure and products analyses have been previously described in section 4.2.

### 4.3.1 Effect on the oil yield and composition

Oil yields obtained in each experiment are shown in Figure 4.2. The highest yield (19.7%, w/w) was obtained with sodium hydroxide and the lowest (6.9%, w/w) when no catalyst was added to the reaction mixture (blank). Oil yield was also high for the experiment where potassium carbonate (16.8%) was the base that catalyzed the oxidation. Considering the experiments where a catalyst was added to the reaction mixture, calcium hydroxide catalyst gave the lowest oil yield (10.2%). It was observed that the action of a base as a catalyst improved in all cases the oil yield gave by the no-catalyst experiment suggesting that high hydroxyl ion and carbonate concentration favored lignin hydrothermal depolymerization. The results entailed that, as described in the literature (Miller et al. 2002a, 2002b; Thring 1994), the presence of a base improved the yield of the phenolic products generated by hydrothermal lignin depolymerization. High hydroxyl ion or carbonate ion concentration favored lignin hydrothermal depolymerization.

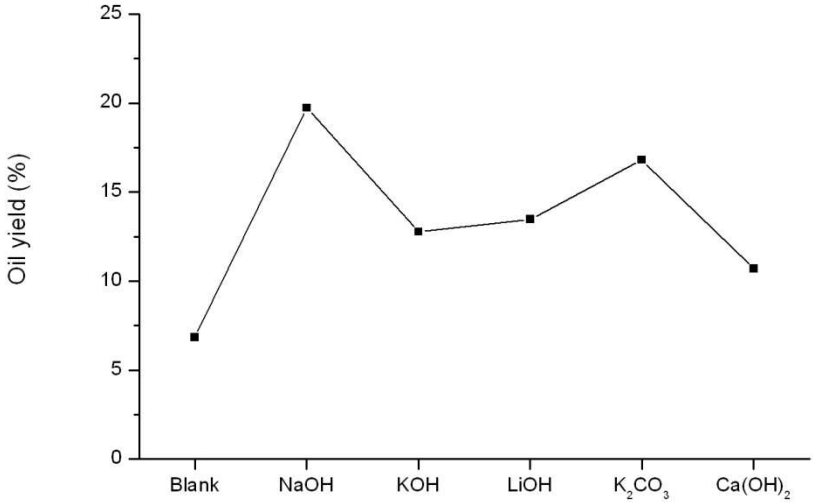


**Figure 4.2.** Obtained oil yield by processing lignin with different bases that act as catalyst. Oil yields (%, w/w) referred to initial lignin weight.

As described above, the phenolic oil was analyzed by GC-MS to identify and to quantify the simple monomers present therein. The obtained data are summarized in Table 4.1. When no catalyst was added (blank), a variety of products were obtained. Among them, it has to be stressed the high guaiacol and syringol content and the absence of cresols. Potassium carbonate experiment yielded the widest monomeric compounds diversity. Catechol was the main product and cresols obtaining was not favored. Hydroxide catalysts yielded as main compounds: phenol, cresols, guaiacol, catechol and 4-methylcatecol. This was not the case of calcium hydroxide. Calcium hydroxide was not strong enough to enhance phenol, cresol and catechol production.

| **Compounds** | **Blank** | **NaOH** | **KOH** | **LiOH** | **$K_2CO_3$** | **$Ca(OH)_2$** |
|---|---|---|---|---|---|---|
| Phenol | 0.37 | 1.01 | 1.07 | 0.91 | 0.49 | 0.27 |
| o-Cresol | - | 0.16 | 0.15 | 0.14 | - | - |
| p-Cresol | - | 0.23 | 0.22 | 0.23 | 0.08 | - |
| m-Cresol | - | 0.25 | 0.24 | 0.25 | - | - |
| Guaiacol | 13.86 | 1.24 | 1.58 | 0.45 | 2.14 | 5.15 |
| Catechol | 0.76 | 10.22 | 15.13 | 7.86 | 13.58 | 0.65 |
| 4-Methylcatechol | - | 5.16 | 3.11 | 7.00 | 5.56 | 0.48 |
| Syringol | 20.40 | - | - | - | 0.14 | 0.27 |
| Acetovanillone | 0.17 | - | - | - | 0.08 | - |
| Syringaldehyde | - | - | - | - | 0.07 | - |
| Acetosyringone | 0.24 | - | - | - | 0.05 | - |
| 4-Hydroxy-3-methoxi-phenilacetone | 0.36 | - | - | - | - | - |

**Table 4.1.** Oil phenolic compounds obtained by processing lignin with different base catalysts. Compounds yields (%, w/w) referred to oil weight.

These results suggested that the reaction took place via different mechanisms for the hydroxide catalysts, in the case of the calcium hydroxide seemed to be more similar to the hydrolysis experiment (blank) where no cresols where obtained and syringol

was produced. In addition, four different behaviors were identified suggesting that the base nature and strength was deeply connected to the depolymerization reaction mechanism.

Between the different linkages present in lignin structure, β-O-4 is said to be the first to be cleaved during hydrothermal degradation of lignin (Li et al. 2007). Roberts et al. (2011) stated that the cleavage of the β-O-4 ether bond takes place heterolytically via the formation of a sodium phenolate derivative and a carbenium ion like transition state, which is instantly neutralized by a hydroxide ion. The sodium cations catalyze the reaction by forming cation adducts with lignin and, thus, polarizing the ether bond. These findings suggest that the polarization of the base is a key step that will govern the kinetic and the mechanism follow in the depolymerization reaction. This is in agreement with the obtained results since the absence of a base yielded different proportion of the phenolic monomeric compounds and when a base was used, its nature also affected strongly the nature and the abundance of phenolic monomeric compounds present in oil.

Concerning the obtained phenolic compounds, it seemed that guaiacol and syringol were produced easily when no catalyst was added to the reaction mixture but the yields of both products decreased as the employed base was stronger, above all, syringol content that disappeared for sodium, potassium and lithium hydroxides experiments. As explained before, the reaction takes place via carbenium ions meaning that syringylic carbenium is more stable than guaiacylic carbenium since it has more methoxy substituent to disperse the positive charge. Then, syringylic products are produced easier as the reaction intermediate is more stable. Miller et al. (2002a) conducted an experiment with syringol in aqueous NaOH and they observed the formation of guaiacol, catechol and other phenolic compounds. They also

reported that dealkylation, demethylation and demethoxylation reactions occurred in base catalyzed depolymerization of lignin model compounds. These results are in accordance with the obtained results since for NaOH, KOH, LiOH and $K_2CO_3$ experiments, 4-methylcatechol and catechol were produced, being the last one the main product. Demethoxylation reactions of guaiacol and syringol took place to produce cresols, these reactions only occurred when the strongest bases were added to the reaction mixture. As mentioned before, calcium hydroxide did not present the same variety of products than the other hydroxides. The reason for that behavior could be that the dissociation of the base was not very clear and so, the phenolate derivative and the carbenium ion could not be formed avoiding product formation. Calcium hydroxide is a medium strength base and as the air was not purge from the reactor, calcium hydroxide could be transformed into calcium carbonate. These two facts could have decreased the oil yield and also affected the depolymerization mechanism.

MALDI-TOF analyses were performed to evaluate the molecular weight distribution of the compounds present in the phenolic oil (Figure 4.3). Considering that a prototype lignin subunit for instance, phenylpronane syringol has a molecular weight of 197 g/mol and a phenylpropane guaiacol is about 166 g/mol, it could be observed in Figure 4.3 that most of the obtained products were mainly monomers and also dimmers. It could be observed that the oil molecular weight distribution pattern was very different depending on the used catalyst, indicating that the base nature is one of the main factors to be considered in the base catalyzed lignin hydrothermal depolymerization. Sodium hydroxide experiment yielded more monomeric and dimeric compounds than the others. Despite the fact that all experiments presented signals in the range around 500-700 g/mol that corresponded to trimers, it has to be stressed that for the experiment where potassium carbonate was the catalyst it could be observed in a remarkable way a small peak in that range indicating the increase

of trimers presence. Calcium hydroxide experiment yielded less quantity of monomers and dimmers than the others catalysts. The results obtained by MALDI-TOF confirm the poor results obtained in the experiment carried out with $Ca(OH)_2$ as the signal strength of the products is much less than with other catalysts.

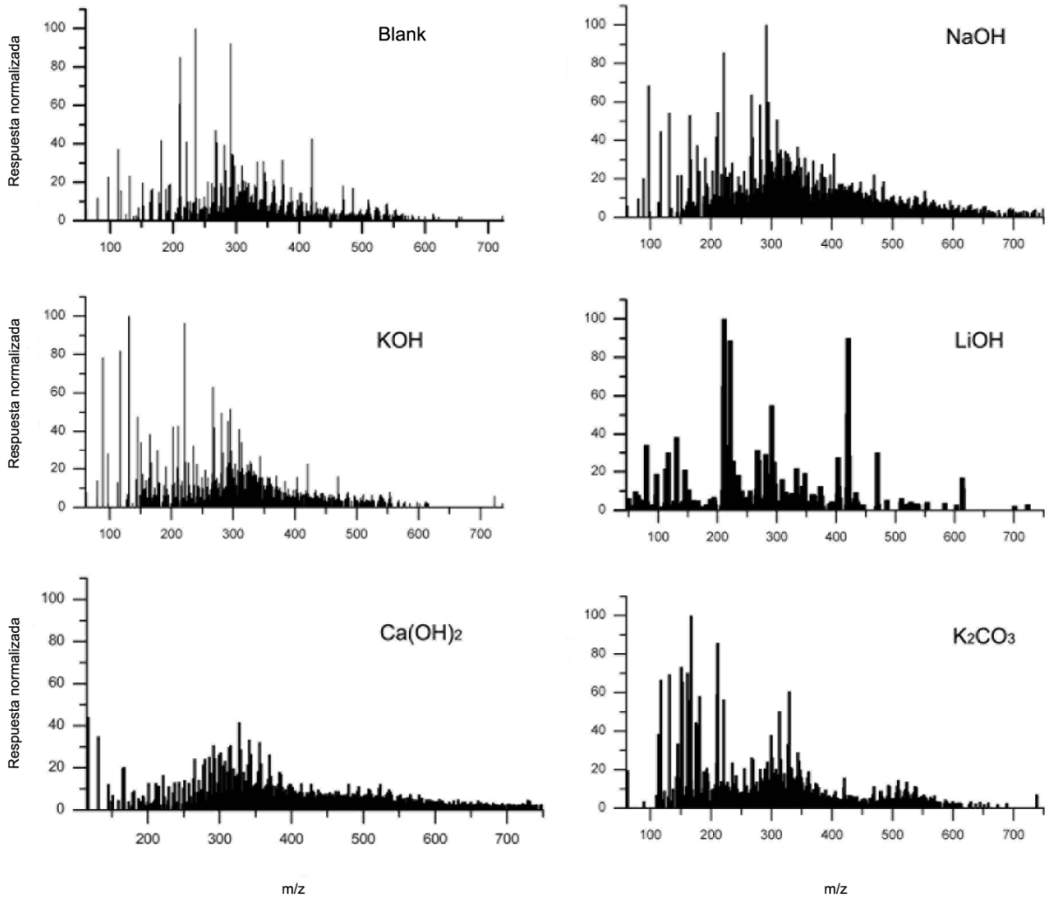


**Figure 4.3.** MALDI-TOF analyses of the oil obtained by processing lignin with different bases that act as catalyst.

## 4.3.2 Effect on char formation

Lignin depolymerization reactions produced also an undesired product, char. The obtained char yields with the different catalysts are shown in Figure 4.4. Clearly it can be observed that char formation was favored by hydrolysis. The results shown in

the figure suggested that the addition of a base –no matter the nature- to the reaction mixture prevented char formation. It seemed that the presence of a base changed the reaction mechanism, favoring the production of monomers and dimers. Taking into account just the experiments carried out with a base catalyst, lithium hydroxide presented the maximum char yield (13.61%). As well, calcium hydroxide and potassium carbonate produced char yields around 10%. Sodium and potassium hydroxide experiments yielded the lowest char content. Char could not be recovered for further analyses since the amounts in most of the cases were negligible.

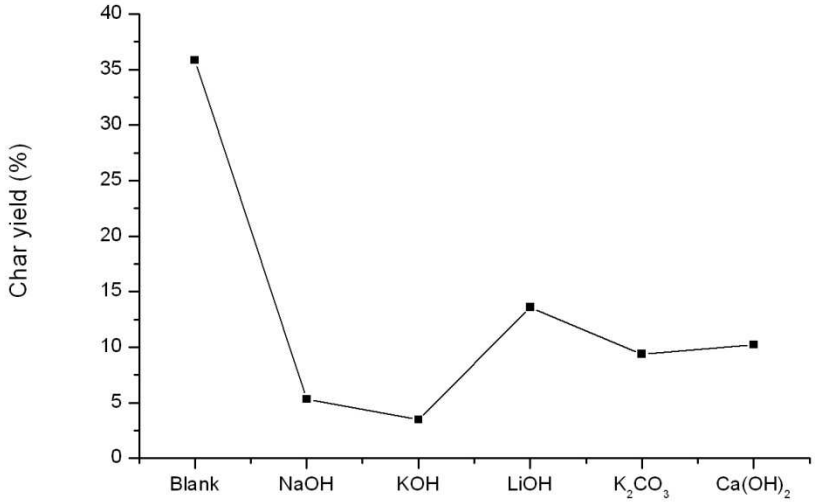


**Figure 4.4.** Obtained char yields by processing lignin with different bases that act as catalyst. Char yields (%, w/w) referred to initial lignin weight.

### 4.3.3 Effect on residual lignin

Residual lignins recovered from the experiments are shown in Figure 4.5. Residual lignin results seemed to be confusing. For instance, the blank presented the lowest residual lignin content, suggesting the best conversion but it should be noticed that its char yield is much higher than its oil yield. In conclusion, low residual lignin

content did not involve high oil yield. These two concepts are not directly related. Except for the blank, the residual lignin content was high for all the experiments. The highest values were obtained when sodium, potassium and lithium hydroxides were used as catalyst. The lowest value was obtained for the carbonate experiment. These data suggested that lignin alkali depolymerization could be improved.

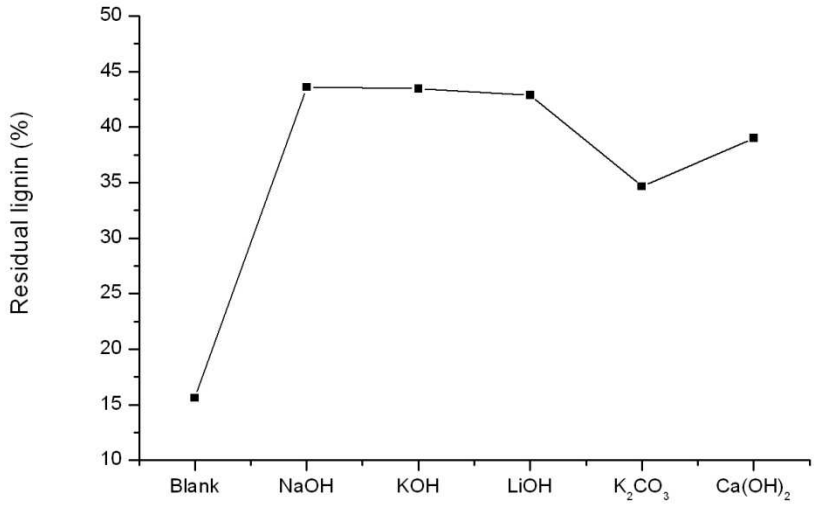


**Figure 4.5.** Recovered residual lignin after processing lignin with different bases that act as catalyst. Residual lignin (%, w/w) referred to initial lignin weight.

Isolated residual lignins were analyzed by HPSEC for evaluating the molecular weight distributions. Rough lignin was also analyzed and was plotted as reference. HPSEC results were very enlightening to explain yield results. As it can be observed in Figure 4.6, all residual lignins molecular weight distributions presented two peaks, one related to the unconverted lignin and the other one to a lower molecular weight lignin as a result of the depolymerization. The first peak of the experiments where a base was added to the reaction mixture appeared earlier than for the rough lignin meaning higher molecular weight lignin (Tabla 4.2). The reason for this behavior was the occurrence of repolymerization reactions that have been reported by other authors (Miller et al. 2002b; Yuan et al. 2010). Repolymerization reactions consisted in the

reactions between instable lignin fragments and original lignin producing unconverted lignin with higher molecular weight than the initial lignin. As it can be noticed, repolymerization degree depended on the employed base. On the other hand, the experiment developed without catalyst (blank) did not follow that behavior. The first peak appeared at the same retention time that the rough lignin indicating that no repolymerization reaction took place.

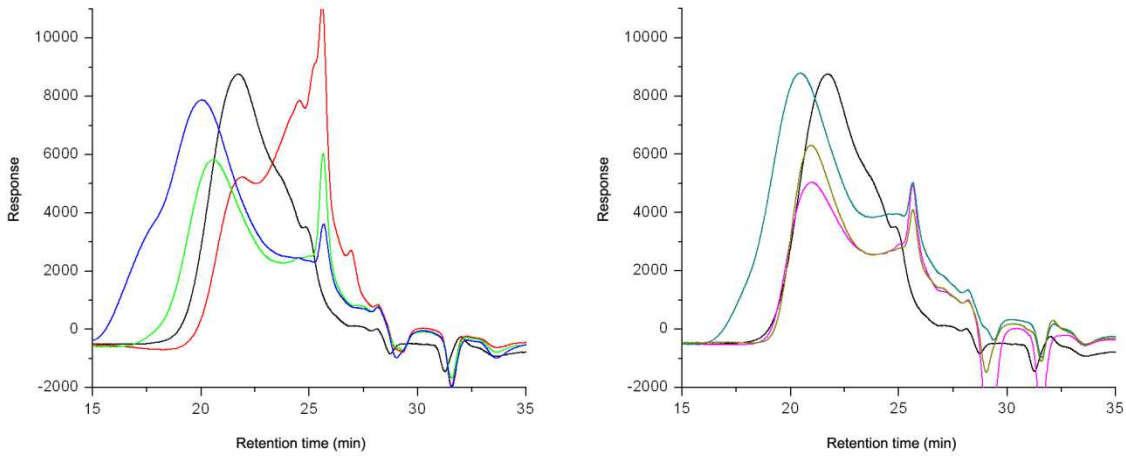


**Figure 4.6.** Molecular weight distributions of residual lignins recovered after processing lignin with different bases that act as catalyst (HPSEC). Left graphic: black (rough lignin), red (blank, $H_2O$), green (NaOH) and blue (KOH). Right graphic: black (rough lignin), purple (LiOH), dark yellow ($Ca(OH)_2$) y light blue ($K_2CO_3$).

In Figure 4.6, it could be observed that all residual lignin molecular weight distributions presented peaks at higher retention time than the rough lignin that were associated to low molecular weight lignin fractions. These peaks emerged in all samples with different intensities and shapes proving that depolymerization reaction had occurred. This low molecular weight lignin fraction could be originated due to depolymerization reactions but also could be related to the presence of oligomerization products with lower molecular weights than the rough lignin. Probably, these oligomers were dragged when precipitating the residual lignin and coke at the first step of the separation procedure.

Many authors have reported repolymerization reactions or condensation reactions that occurred during lignin hydrothermal depolymerization (Miller et al. 2002b; Roberts et al. 2011; Yuan et al. 2010; Fang et al. 2008; Wahyudiono et al. 2008). Li et al. (2007) claimed that polymerization takes place simultaneously with acidolysis and that both reaction pathways have the same intermediate state, namely, a carbenium ion, generated at the $\alpha$-carbon atom. The ether bond in the intermediate can then be cleaved (depolymerized) or attacked by an adjacent aromatic ring forming stable carbon–carbon bond (polymerized). Since base catalyzed lignin hydrothermal depolymerization, as discussed earlier, takes place also via carbenium ions, Li et al (2007) affirmations could be assumed. The results suggested that repolymerization reactions were an important matter since all catalyst generated residual lignins that presented a peak at lower retention times than rough lignin meaning higher molecular weights and in the end, this phenomenon decreased depolymerization extent. Wahyudiono et al. (2008) stated that re-polymerization of low molecular weight compounds occurred as seen by the formation of char through condensation reaction. However, repolymerization and oligomerization products were isolated as residual lignin since char yields did not increase with any catalysts but residual lignin content did enlarge.

| | **Mw** | **Mn** | **Mw/Mn** |
|---|---|---|---|
| Rough | 7232 | 2125 | 3.40 |
| Blank | 8080 | 5096 | 1.59 |
| NaOH | 19957 | 4768 | 4.19 |
| KOH | 47316 | 3136 | 15.09 |
| LiOH | 10272 | 3371 | 3.05 |
| $Ca(OH)_2$ | 9701 | 3689 | 2.63 |
| $K_2CO_3$ | 27558 | 5646 | 4.88 |

**Table 4.2.** HPSEC results of the first peak of the recovered residual lignins related to repolymerization phenomena.

As shown in Table 4.2, the experiments carried out with potassium catalysts (KOH and $K_2CO_3$) showed the highest degree of repolymerization, which implies that the reaction intermediates of potassium tended to attack the original lignin rather than other cationic reaction intermediates. The experiment without catalyst (blank) presented the lowest degree of repolymerization. Polymer degradation was revealed by the lowering of the polydispersity index. This trend was observed in almost all cases, except, especially, in those in which the catalyst was made up by potassium.

Considering the phenolic oil composition, the concentration of guaiacol and syringol was high in the blank experiment and very low in the experiments with catalysts. As explained in section 4.3.1, guaiacol and syringol were easily released but these compounds tended to undergo subsequently dealkylation, demethoxylation and demethylation reactions, generating reaction intermediates that could be responsible of repolymerization reactions. Blank oil composition presented very low concentration or even absence of phenol, cresols, catechol and 4-methylcatechol because of the lack of demethoxylation, demethylation and dealkylation reactions. Indeed, the absence of such reactions prevented the formation of the reaction intermediates responsible of repolymerization phenomena. Table 4.2 data proved that in blank experiment, repolymerization reactions did not take place. Nevertheless, these phenolic compounds (phenol, cresol, catechol ...) were released in the experiments carried out with basic catalyst and the recovered residual lignin showed repolymerization phenomena proving that the subsequent reactions were involved in residual lignin repolymerization.

Figure 4.7 shows the obtained solids from the first stage of separation procedure. This first solid was composed of char and residual lignin. Visual inspection of this solid was very useful to notice how lignin depolymerization had worked. The picture corresponding to blank ($H_2O$) solid showed very different appearance compared to

the solid of the other experiments. The blank solid was black, shiny and granulated which confirmed that depolymerization reactions had occurred in a different way, as it has been demonstrated by the oil, char and residual lignin results. In the case of calcium hydroxide catalyst, remarkable differences were also observed. In this case, the $Ca(OH)_2$ solid presented lignin appearance suggesting that original lignin had not suffered any change. The aforementioned obtained results confirmed the hypothesis arose from solid observation.

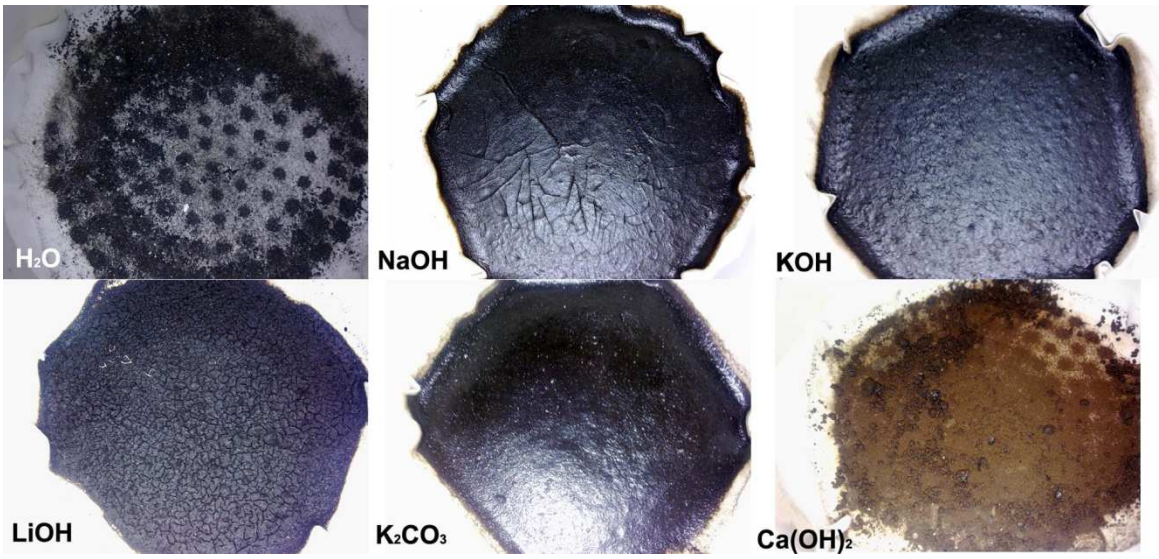


**Figure 4.7.** Solids recovered in the first step of the separation procedure, composed by residual lignin and char.

### 4.3.4 Conclusions

The aim of this study was to investigate the influence of the catalyst nature on the lignin hydrothermal depolymerization. As discussed throughout this point, the nature of the employed base affected decisively the nature of the obtained simple phenolic compounds. Repolymerization phenomena were observed in all cases in which a base was added to the reaction mixture in order to catalyze lignin hydrothermal depolymerization. As in the case of the obtained phenolic compounds, the base nature influenced the residual lignin degree of repolymerization.

Considering all the obtained results -oil yield and composition, depolymerization degree, char yield, residual lignin yield and residual lignin repolymerization reactions-, the best results were achieved when sodium hydroxide was used as catalyst, especially, considering the simple phenolic monomers concentration and the almost absence of char.

## 4.4 Effect of reaction conditions on lignin hydrothermal depolymerization

For the optimization of the base-catalyzed lignin hydrothermal depolymerization, the severity factor was employed in order to simplify the study. Overend et al. (1992) developed a mathematical equation (treatment severity parameter) for modeling lignocellulosic fractionation assuming that homogeneous models and laws could be used to model lignocellulosic hydrolysis, that each lignocellulosic component (cellulose, hemicelluloses and lignin) do not interact during hydrolysis and that each one of these components is predominantly characterized by a distinct chemical linkage which is typically an ether bond. They also studied the application of the model to the case study of hemicelluloses solubilization via aqueous/steam treatments concluding that kinetic formalism for a complex reacting system can be developed based on a limited number of parameters grouped within a single severity factor. The severity factor $R_o$ is defined as follows:

$$R_o = \int_0^t exp\left(\frac{T_{exp}-T_b}{14.75}\right) dt \quad (1)$$

$$\log R_o = \log\left(t \cdot \left(\frac{T_{exp}-T_b}{14.75}\right)\right) \quad (2)$$

where $T_{exp}$ is the experimental temperature in ºC, $T_b$ the boiling water temperature (100 ºC), and t is the reaction time (minutes) (Kadam et al. 2009) .

Since then, many researchers have used this treatment severity factor to study the behaviors of lignocellulosic fractionation processes. Garrote et al. (2008) performed non-isothermal treatments of barley husks in aqueous media under a variety of operational conditions using the severity parameter to study the hydrolytic degradation of hemicelluloses. Autohydrolysis processes have been examined using the mathematical severity factor model such as the generation of xylooligomers and monosaccharides (Saska et al. 1995), the production of furfural (Rubio et al. 1998). Thring (1994) studied alkaline lignin degradation using the severity factor since alkaline lignin degradation takes place hydrolytically.

| **Temperature (ºC)** | **Time (min)** | **Log $R_o$** |
|---|---|---|
| 250 | 90 | 6.4 |
| 270 | 75 | 6.9 |
| 290 | 50 | 7.3 |
| 300 | 40 | 7.5 |
| 310 | 30 | 7.7 |

**Table 4.3.** Studied conditions in the base catalyzed lignin depolymerization.

Concerning this study, the pH effect was not considered since the same base catalyst concentration was used for all experiments (4% NaOH). Five reaction time and reaction temperature combinations were applied to the reaction mixtures (Table 4.3). Reaction time and temperature limits were established according to literature (Miller et al. 2002a, 2002b; Roberts et al. 2011; Yuan et al. 2008) and taking into account reactor limitations. The reactions reached pressures from 40 to 105 bars depending on the applied conditions. Other aspects of the reaction conditions, product

separation procedure and products analyses have been already described in section 4.2. The results are presented below.

### 4.4.1 Effect on the oil yield and composition

The obtained oil yields for each severity factor referred to initial lignin weight are shown in Figure 4.8. As it can be observed, the oil yield clearly increased as the severity factor was higher. Therefore, the highest oil yield (22.5%) was obtained when the highest severity factor ($LogR_o$ 7.7) was applied to the reaction mixture. Surprisingly, the oil yield obtained in the experiment with severity factor 7.5 was lower than the one obtained for the experiment with severity factor 7.3 and this one, lower than the 6.9 experiment. Interestingly, only the hardest conditions involved great oil yield increase. The oil yield tendency was not very clear and it seemed that not much improvement was achieved increasing the severity parameter until the hardest conditions were applied.

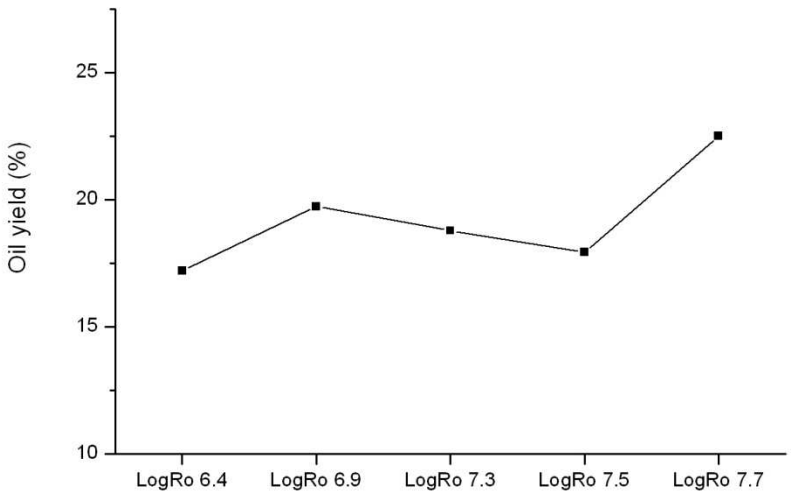


**Figure 4.8.** Obtained oil yield by applying different severity factors. Oil yield (%, w/w) referred to initial lignin weight.

These data suggest that the severity factor slightly affected the oil obtaining. As the reaction conditions did not affect the base-catalyzed lignin depolymerization, it seemed that there was a limit in oil obtaining. Several authors (Saisu et al. 2003; Vigneault et al. 2006) have reported the existence of limitations in the oil production by base catalyzed lignin hydrothermal depolymerization associated with repolymerization and/or condensation reactions occurring during the reaction time that blocked the production of simple phenolic compounds.

The determination of the phenolic compounds present in the oil was performed by GC-MS and the results are summarized in Table 4.4. In this table, large differences in the oils composition depending on the applied severity factor can be noticed.

| Compounds | LogRo 6.4 | LogRo 6.9 | LogRo 7.3 | LogRo 7.5 | LogRo 7.7 |
|---|---|---|---|---|---|
| Phenol | 0.17 | 0.49 | 0.76 | 1.01 | 3.32 |
| o-Cresol | - | - | 0.12 | 0.16 | 0.73 |
| p-Cresol | - | 0.08 | 0.18 | 0.23 | 1.22 |
| m-Cresol | - | - | 0.19 | 0.25 | 1.30 |
| Guaiacol | 5.31 | 5.52 | 1.82 | 1.24 | 1.21 |
| Catechol | - | 5.92 | 16.85 | 10.22 | 42.58 |
| 4-Methylcatechol | - | 1.41 | 8.24 | 5.16 | 35.29 |
| Syringol | 3.83 | 0.85 | - | - | - |
| Acetovanillone | 0.17 | 0.08 | - | - | - |
| Acetosyringone | 0.26 | - | - | - | - |

**Table 4.4.** Phenolic compounds obtained by applying different severity factors. Compound yields (%, w/w) referred to oil weight.

The experiment at the weakest conditions ($LogR_o$ 6.4) yielded a broad variety of phenolic compounds, being guaiacol and syringol the main products. It should be stressed that no cresols nor catechol or catechol derivates were obtained. The

following experiment (LogRo 6.9) yielded the widest phenolic compounds variety. In this experiment, cresols started to appear and guaiacol and catechol were the main products. Syringol content decreased significantly compared to the experiment with $LogR_o$ 6.4. However, the disparity of the obtained phenolic compounds was concluded when applying higher severity factor (LogRo 7.3, LogRo 7.5 and LogRo 7.7) to the reaction mixture since in these experiments similar phenolic compounds profile was found. These runs yielded more defined products such as phenols, cresols, guaiacol, catechol and 4-methylcatechol. The absence of syringol was remarkable and it suggested that syringol needed weaker conditions to be produced and when stronger conditions were used, syringol undergoes oligomerization or degradation reactions. Guaiacol concentration decreased as the conditions were harder but phenols and cresols presented the opposite behavior. It should be stressed that the experiment carried out at the strongest conditions, severity factor LogRo7.7, showed the highest monomeric yields.

Taking into account the obtained oil yields and their compositions, the main difference in applying different severity factors lay on the nature of the phenolic monomeric products present in the isolated oil. From the experiment carried out at $LogR_o$ 7.3 and on, only certain phenolic compounds (phenol, cresols, catechol and 4-methylcatechol) were produced which implied that the reaction mechanism did not vary. These findings suggested that the activation energy needed for these products to be generated was achieved, at least, from severity factor $LogR_o$ 7.3. However, below this severity factor, the nature of the phenolic compounds changed indicating that the reaction mechanism was different. The experiment conducted at the lowest severity factor ($LogR_o$ 6.4) produced primarily guaiacol and siringol but also more complex structures such as acetovanillone and acetosyringone. Comparatively, the experiment at $LogR_o$ 6.9 produced mainly guaiacol and catechol suggesting that the mechanism changed as the applied conditions were more severe.

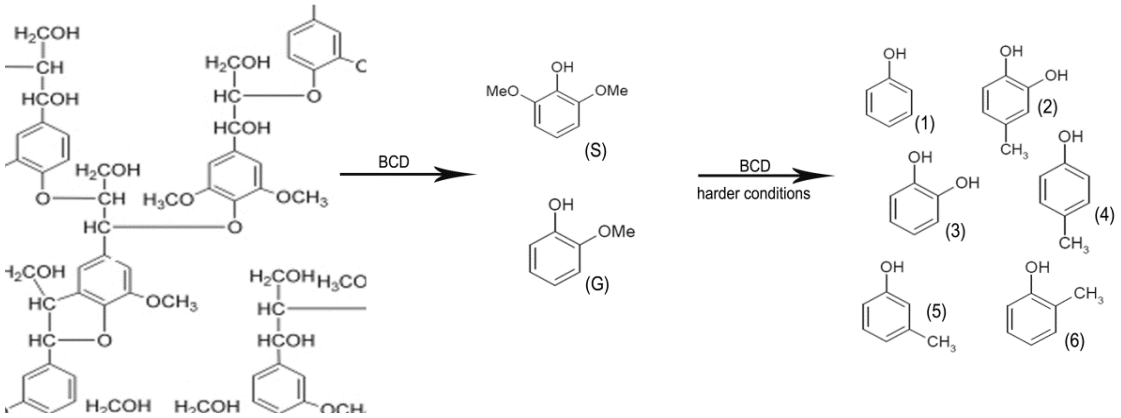


**Figure 4.9.** Proposed sequential reactions in base-catalyzed lignin depolymerization. (S) Syringol, (G) Guaiacol, (1) Phenol, (2) 4-Methylcatechol, (3) Catechol, (4) p-Cresol, (5) m-Cresol y (6) o-Cresol.

Phenol and cresols increased their yields as the reaction conditions were stronger indicating that the activation energy that the reaction intermediates had to exceed was high. Catechol and 4-methylcatechol were the main products for most of the experiments carried out and their obtaining was favored as the applied severity parameter was higher, reaching a maximum yield of 42.58% and 35.29% (LogRo7.7), respectively. On the other hand, as mentioned before, guaiacol and syringol presented the opposite behavior. These compounds yields decreased dramatically (syringol even disappeared) as the applied reactions conditions were stronger. The disappearance of guaiacol and syringol and the appearance of other phenolic compounds (aforementioned) suggested that the formers were involved in the second ones production (Figure 4.9).

Miller et al. (2002a) conducted an experiment with syringol in aqueous NaOH and the formation of guaiacol, catechol and other phenolic compounds was observed. They reported that dealkylation, demethylation and demethoxylation reactions were involved in the formation of these compounds. These findings are in agreement with the obtained results. As shown in Table 4.4, the formation of final products (phenol,

cresols and catechols) by sequential reactions suggested in Figure 4.8, strongly depended on the reaction conditions applied for the lignin depolymerization indicating that the activation energy of reaction intermediates play an important role in the oil final composition, as expected. LogRo 7.3 seemed to provide the lowest but enough energy activation so as these final products (phenol, cresols and catechols) could be generated. Roberts et al. (2011) stated that the cleavage of the β-O-4 ether bond (main bond involved in base catalyzed lignin depolymerization) takes place heterolytically via the formation of a sodium phenolate derivative and a carbenium ion like transition state, which is instantly neutralized by a hydroxide ion. In this study, it has been proved that as the reactions conditions were stronger the final products formation was favored.

The fact that guaiacol was still present in oil even at the hardest conditions ($LogR_o$7.7) could be explained given the fact that the reaction takes place via carbenium ions meaning that syringylic carbenium is more stable than guaiacylic carbenium since it has more methoxy substituent to disperse the positive charge. Then, syringylic products are produced easier as the reaction intermediate is more stable. Moreover, Miller et al. (2002b) and Asmadi et al. (2011) reported that starting from syringol; guaiacol was produced by syringol demethoxylation. Dealkylation, demethylation and demethoxylation reactions have been reported to occur in lignin depolymerization (Miller et al. 2002a; Roberts et al. 2011; Asmadi et al. 2011) of lignin model compounds and it has been confirmed by the presence in oil of phenol, cresols, catechol and 4-methylcatecol that using lignin the same reactions took place.

The monomers analyzed by GC-MS were not the only components of the oil. With the purpose of determining the molecular weight distribution of the compounds present

in the oil, MALDI-TOF analyses were performed whose results are shown in Figure 4.10. The lignin structure is made up of, as mentioned above, three types of structures: p-hydrophenyl , guaiacyl and syringyl propane. Given that the molecular weight of a guaiacyl subunit is around 166 g/mol and a siringyl subunit is 197 g/mol, it could be observed Figure 4.10, the majority of the compounds present in the obtained oils by base-catalyzed lignin hydrothermal depolymerization were monomers and dimers.

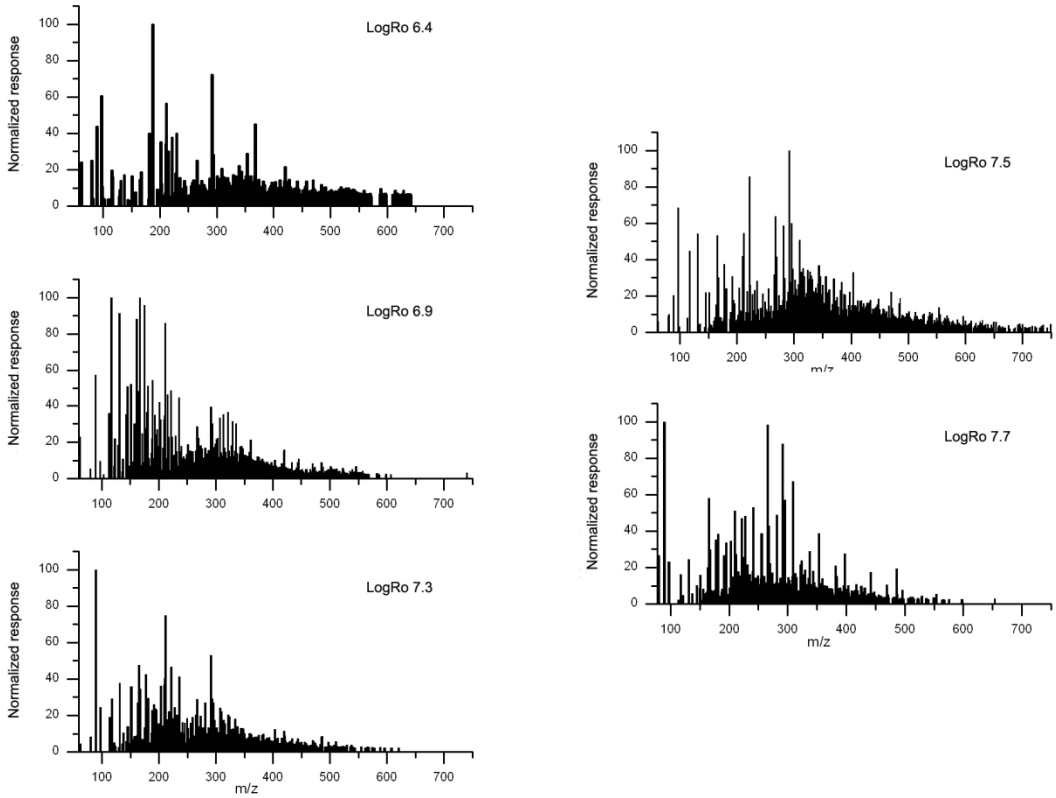


**Figure 4.10.** MALDI-TOF analyses of the obtained oil by applying different severity factors.

Surprisingly, LogRo 6.9 experiment yielded more quantity of monomers since the signals around 200 g/mol were more intense than the ones of the other experiments. However, the large amount of monomers suggests by MALDI-TOF analyses was not appreciated when the simplest monomers were identified and quantified by GC-MS. GC-MS technique could only detect compounds with relative low boiling temperature.

The signals in the range of 500 to 700 g / mol were associated with the presence of trimers in the oil. These signals were present in almost all experiments. Nevertheless, it should be noticed that LogRo 6.4 experiment yielded more compounds in the range of 200-700 g/mol indicating the prevalence of complex dimeric and trimeric compounds. A high trimers presence also suggested low lignin depolymerization degree, confirming the results obtained by GC-MS. The experiment $LogR_o$ 7.7 did not present almost no signal in the range corresponding to the trimers proving the stronger conditions cause greater lignin depolymerization.

### 4.4.2 Effect on char formation

Char constitutes the other product of the base-catalyzed lignin hydrothermal depolymerization, but its yield was intended to be minimum or nonexistent since it was considered as undesired product.

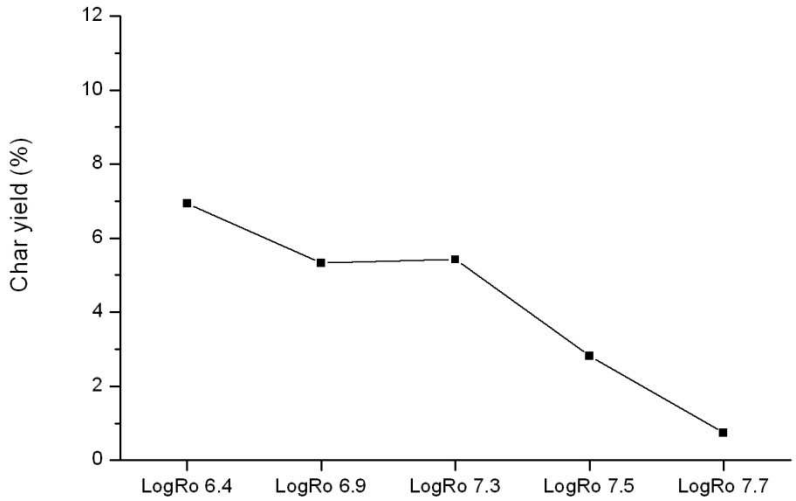


**Figure 4.11.** Obtained char yields by applying different severity factors. Char yields (%, w/w) referred to initial lignin weight.

Char yields obtained by applying different severity factors are displayed in Figure 4.11. Char yields were very low in all studied cases and decreased as the applied severity factor was increased to almost disappear (LogRo 7.7, 0.74%). The addition of a base to lignin hydrothermal depolymerization was claimed to decrease the possibility of char formation (Karagöz et al. 2004; Yuan et al. 2008). Char could not be recovered for further analyses since the amounts in most of the cases were negligible.

### 4.4.3 Effect on residual lignin

The yields of residual lignin recovered from the lignin depolymerization process applying different severity factors are shown in Figure 4.12. Residual lignin content increased dramatically as the depolymerization conditions were harder, reaching a maximum of approximately 60% for severity factor of LogRo 7.7.

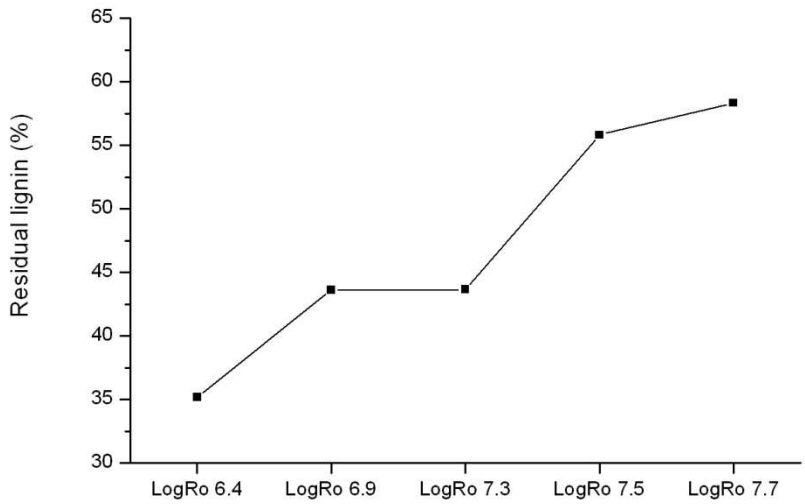


**Figure 4.12.** Recovered residual lignin after applying different severity factors. Residual lignin (%, w/w) referred to initial lignin weight.

It should be noticed that experiments with severity factor of LogRo 6.9 and LogRo 7.3 presented similar results, not much improvement was achieved with that increase in the severity factor. As it was mentioned in 4.3.3 section, residual lignin should not be directly related to conversion since that relationship could be misleading given the fact that lignin depolymerization leads to oil but also to coke, undesirable product. Therefore, low residual lignin content did not involve high oil content.

Residual lignins were analyzed by HPSEC in order to determine the molecular weight distributions (Figure 4.13) and averages molecular weights (Table 4.5). Rough lignin was also analyzed as reference. In all cases, residual lignins distribution showed two peaks, one related to the unconverted lignin and the other one to a lower molecular weight lignin as a result of the depolymerization.

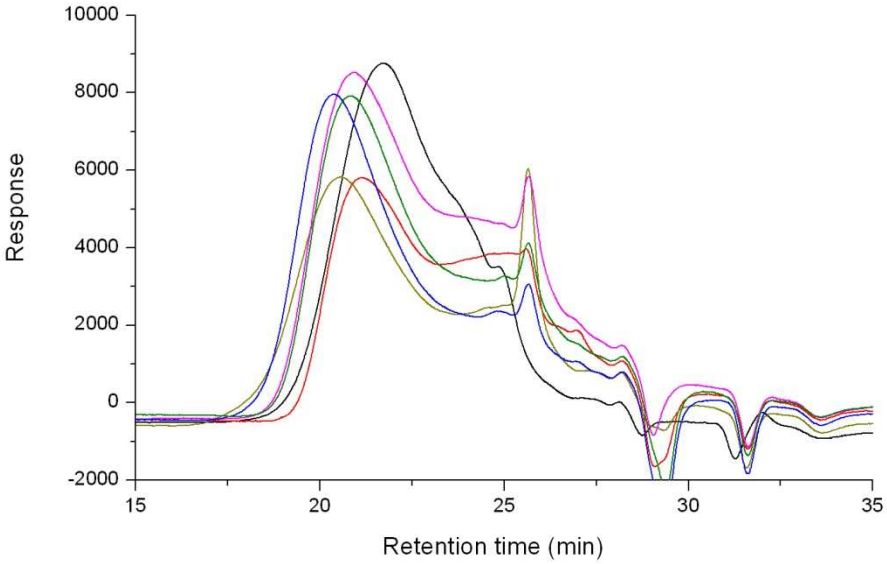


**Figure 4.13.** Molecular weight distributions of residual lignins recovered after applying different severity factors. Black (Rough lignin), red ($LogR_o$ 6.4), blue ($LogR_o$ 6.9), green ($LogR_o$ 7.3), dark yellow ($LogR_o$ 7.5) and magenta ($LogR_o$ 7.7).

The first peak of the experiments appeared earlier than the rough lignin main peak meaning higher molecular weight lignin (Table 4.5). The reason for that behavior was the repolymerization reactions that have been reported by other authors (Miller et al. 2002a; Yuan et al. 2008) and consisted in the reaction between instable lignin fragments and original lignin producing unconverted lignin with higher molecular weight than the initial lignin. Repolymerization phenomena affected all samples regardless of the applied severity parameter. Residual lignins from experiments LogRo 6.9 and LogRo 7.5 presented the highest molecular weight repolymerized fractions. Additionally, peaks at higher retention time than the rough lignin could be observed and they were associated to low molecular weight lignin fractions. These peaks emerged in all samples with different intensities and shapes proving that depolymerization reaction had occurred.

| | **Mw** | **Mn** | **Mw/Mn** |
|---|---|---|---|
| Rough | 7232 | 2125 | 3.40 |
| $LogR_o$ 6.4 | 9207 | 4321 | 2.13 |
| $LogR_o$ 6.9 | 17577 | 4118 | 4.27 |
| $LogR_o$ 7.3 | 11181 | 2995 | 3.73 |
| $LogR_o$ 7.5 | 19957 | 4768 | 4.19 |
| $LogR_o$ 7.7 | 9663 | 1742 | 5.55 |

**Table 4.5.** HPSEC results of the first peak of the recovered residual lignins related to repolymerization phenomena for each severity factor.

The recovered residual lignin amount increased as the applied severity factor was greater. This increase could be associated with the repolymerization phenomenon. Li et al. (2007) claimed that polymerization takes place simultaneously with acidolysis and that both reaction pathways have the same intermediate state, namely, a carbenium ion, generated at the $\alpha$-carbon atom. The ether bond in the intermediate

can then be cleaved (depolymerized) or attacked by an adjacent aromatic ring forming stable carbon–carbon bond (polymerized). In this sense, as the reaction conditions were getting harder more syringol and guaiacol could be produced but these products could instantly transformed whether into phenolic compound or into fragments that react with lignin (repolymerization). The data in Table 4.5 suggested that syringol and guaiacol should be the products involved in this phenomenon since the other phenolic products yield increased at hard conditions. Wahyudiono et al. (2008) stated that repolymerization of low molecular weight compounds occurred as seen by the formation of char through condensation reaction. However, HPSEC results (Figure 4.13) suggested that repolymerization affected residual lignin content and did not affect coke yield.

Based on the obtained experimental results, the applied reaction temperature was not high enough to produce char, the applied conditions favored lignin repolymerization recovered as residual lignin. The molecular weight distribution showed a peak at lower retention times than rough lignin indicating that the residual lignin molecular weight was higher that organosolv olive tree pruning lignin. Nevertheless, reaction conditions, despite the fact of being a key factor for products formation, seemed not to completely govern repolymerization phenomena since not a clear tendency of growing residual lignin molecular weight was observed.

### 4.4.4 Conclusions

The aim of this section was to study the reaction conditions of the base-catalyzed lignin hydrothermal depolymerization. It has been proved that the nature of phenolic compounds was influenced decisively by the reaction conditions applied. The study has confirmed the reaction mechanism that was involved in the formation of some of

the phenolic compounds formed, such as phenol, cresol, catechol ... The highest phenolic compounds concentration was achieved by applying the reaction conditions more severe. The char yield remained low in all studied cases. Recovered residual lignin increased as the employed conditions in the lignin depolymerization were harder. Residual lignin was found to suffer repolymerization reactions.

## 4.5 Process proposal for lignin revalorization by hydrothermal depolymerization

Lignin fractions obtained by ultrafiltration (Chapter 3) were subjected to hydrothermal depolymerization conditions for the production of high added value simple phenolic compounds. From the results obtained in section 4.3 where the positive action of a base on lignin hydrothermal depolymerization was studied, sodium hydroxide was chosen to catalyze lignin hydrothermal depolymerization. The reaction conditions consisted of performing the reaction at 310 °C for 30 minutes ($LogR_o$ 7.7) reaching pressures of 105 Bars (best results of section 4.4 regarding phenolic monomeric yields and char yield). Other aspects of the reaction conditions, product separation and products analysis have been already discussed in section 4.2. The results are presented below.

### 4.5.1 Effect on the oil yield and composition

The yield of recovered oil from the lignin ultrafiltrated fractions depolymerization are shown in Figure 4.14. The highest value was obtained for the lignin fraction 4

(19.5%) and the lowest oil yield (15.7%) for lignin fraction 5. The oil yield tendency was not very clear suggesting that the oil obtaining was not directly related to lignin properties such as molecular weight distribution or composition. Many authors (Saisu et al. 2003; Vigneault et al. 2006) have concluded that base catalyzed lignin depolymerization present an important technique limit referred to oil yield obtaining meaning that no matter to which conditions lignin is exposed, if workup procedures are comparable, each approach to depolymerize its structure does not exceed yields of approximately 20–23% (w/w) of product oil. This limitation in lignin conversion can be attributed to polymerization of the highly reactive lignin cleavage products to form higher molecular weight compounds, char, and a lignin-like material (Roberts et al. 2011.).

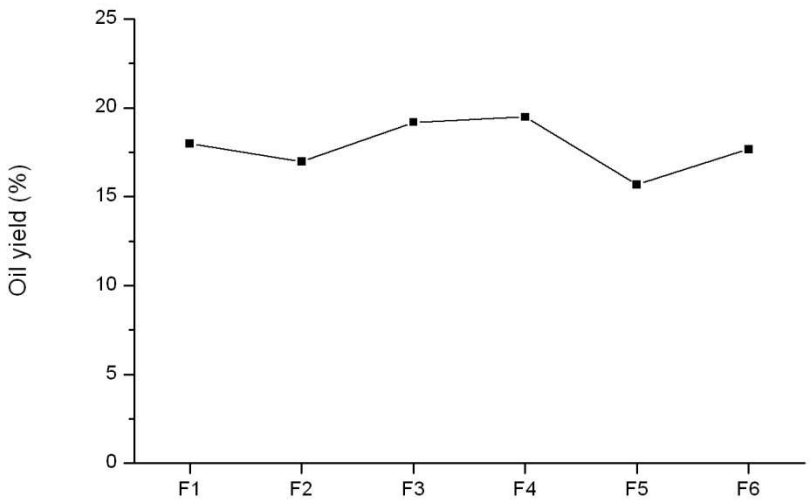


**Figure 4.14.** Obtained oil yield of ultrafiltered lignin fractions. Oil yields (%, w/w) referred to initial lignin weight.

The compositions of phenolic compounds determined by GC-MS of the recovered oils from the depolymerization of lignin ultrafiltered fractions are detailed in Table 4.6. Five compounds were mainly found in all experiments: phenol, cresols, guaiacol, catechol and 4-methylcatechol. Phenol, catechol and 4-methylcatechol yields

increased greatly as the lignin fraction molecular weight was lower (F6). Cresols concentration slightly rose as the lignin fraction molecular weight decreased whereas guaiacol concentration remained practically constant.

| Compounds | F1 | F2 | F3 | F4 | F5 | F6 |
|---|---|---|---|---|---|---|
| Phenol | 2.71 | 3.03 | 6.09 | 3.22 | 4.18 | 7.35 |
| Cresols | 1.21 | 1.62 | 2.81 | 1.37 | 1.59 | 2.79 |
| Guaiacol | 0.42 | 0.44 | 0.52 | 0.43 | 0.53 | 0.56 |
| Catechol | 8.08 | 8.36 | 11.44 | 13.25 | 19.11 | 22.82 |
| 4-Methylcatechol | 3.73 | 3.97 | 4.45 | 4.26 | 6.56 | 8.20 |
| Total monomers | 16.15 | 17.42 | 25.31 | 22.53 | 31.97 | 41.72 |

**Table 4.6**. Phenolic compounds obtained from ultrafiltered lignin fractions. Compounds yields (%, w/w) referred to oil weight.

Concerning oil total phenolic monomeric concentration, it has to be mentioned that the total monomers yield increased spectacularly as the molecular weight of lignin ultrafiltered fractions decreased. This fact suggested that lignin molecular weight was involved as one of the main factors that governed base catalyzed lignin depolymerization confirming what it was explained before, low polydispersity lignins presented higher reactivity. The lignin composition may also be implicated in the hydrothermal depolymerization since the purest ultrafiltered fraction (fraction 6) was the one that produced higher proportion of phenolic compounds. The trend in the composition is the same positive trend observed in the production of phenolic compounds.

Between the different linkages present in lignin structure, β-O-4 is said to be the first to be cleaved during hydrothermal degradation of lignin (Li et al. 2007). Roberts et

al. (2011) stated that the cleavage of the β-O-4 ether bond takes place heterolytically via the formation of a sodium phenolate derivative and a carbenium ion like transition state, which is instantly neutralised by a hydroxide ion. The sodium cations catalyze the reaction by forming cation adducts with lignin and, thus, polarizing the ether bond. The reaction takes place via carbenium ions meaning that syringylic carbenium is more stable than guaiacylic carbenium since it has more methoxy substituent to disperse the positive charge. Then, syringylic products are produced easier as the reaction intermediate is more stable. Miller et al. (2002a) conducted an experiment with syringol in aqueous NaOH and they observed the formation of guaiacol, catechol and other phenolic compounds. They also reported that dealkylation, demethylation and demethoxylation reactions occurred in base catalysed depolymerization of lignin model compounds. These findings would explain the absence of syringol in the phenolic oil and the high catechol concentration.

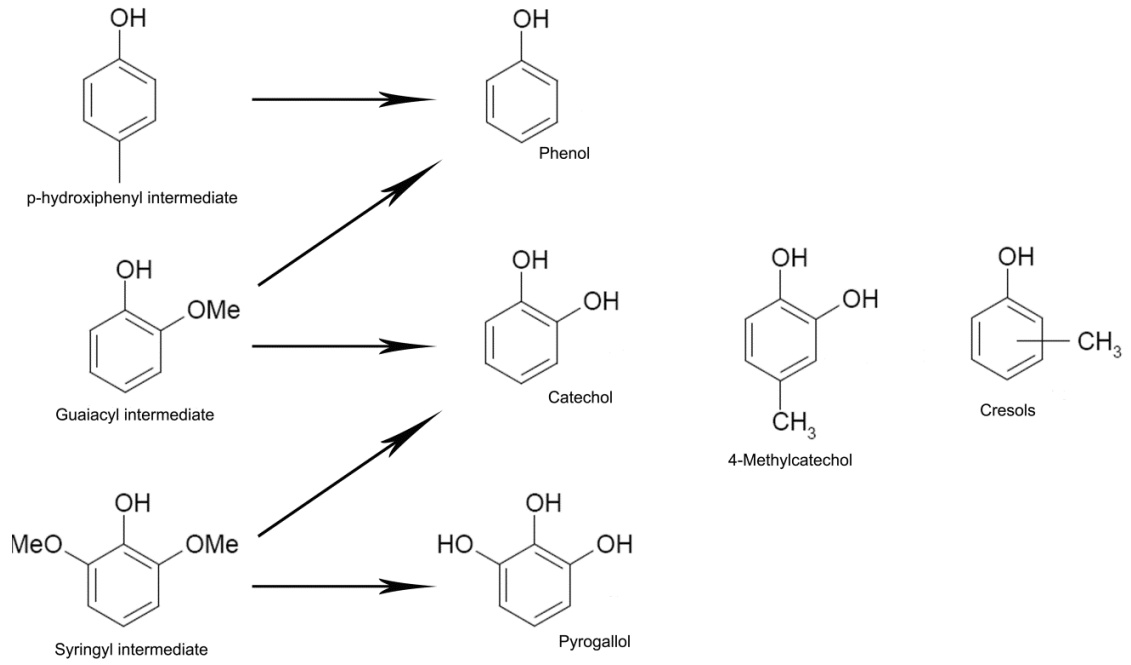


**Figure 4.15.** Suggested lignin intermediates mechanism during base catalyzed depolymerization.

Guaiacyl intermediates were less stable and that is why it could be found guaiacol in oil but not syringol. However, the high amount of catechol and 4-methylcatechol indicated that syringol was rapidly released from lignin structure but then syringylic intermediates underwent demethoxylation reaction to produce catechol type products instead of forming pyrogallol (Figure 4.15). Demethoxylation reactions of guaiacyl and syringyl, besides p-hydroxybenzyl intermediates, intermediates could also be the origin of the phenol found in the oil.

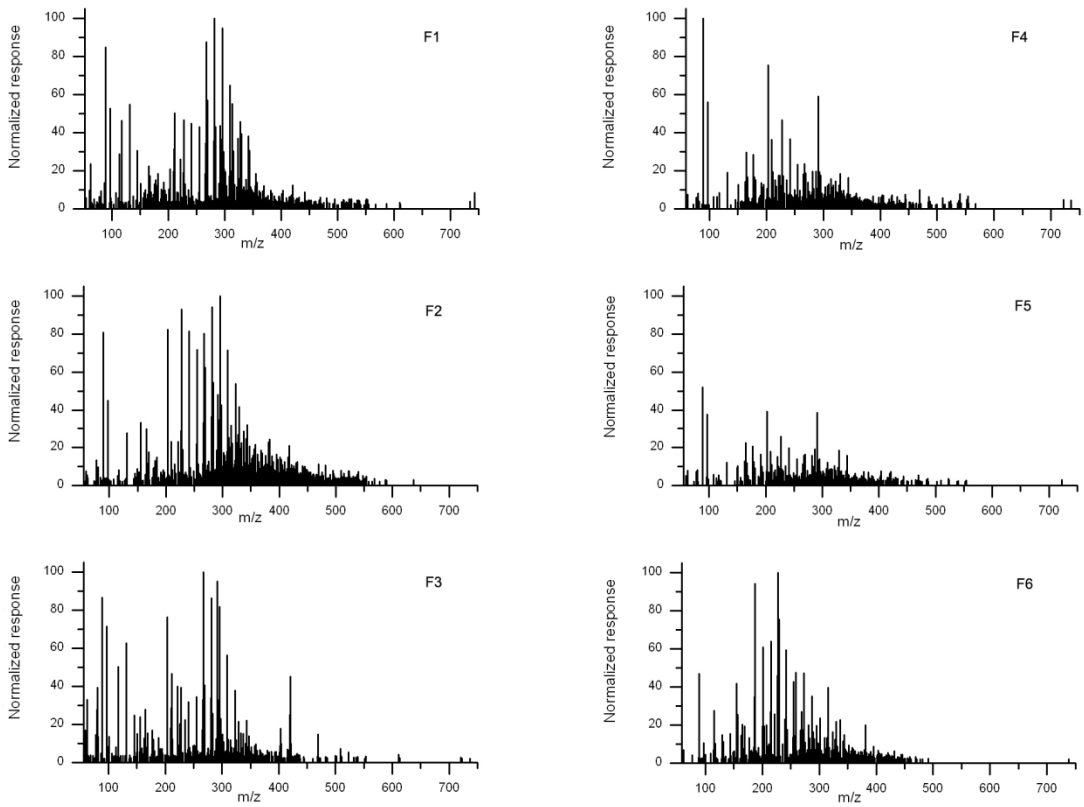


**Figure 4.16.** MALDI-TOF oil analyses of each ultrafiltered lignin fractions.

The total monomers percentage suggested that there were more products in oil that could not be detected by GC-MS, technique that can only detect compounds with low boiling temperature. In order to find out more about oil composition, MALDI-TOF analyses were carried out (Figure 4.16). Since no signals were detected after 700

m/z, Figure 4 showed only expanded plot range between 0 and 700 m/z. Considering that a prototype lignin subunit for instance, phenylpronane syringol has a molecular weight of 197 g/mol and a phenylpropane guaiacol is about 166 g/mol, it could be observed in Figure 4.16 that most of the obtained products were mainly monomers and also dimers. It could be observed that the oil molecular weight distribution pattern was very different depending on the ultrafiltrated lignin fraction. Despite the fact that most of the experiments presented signals in the range around 500-700 g/mol that corresponded to trimers, these signals were more abundant as the membrane cut off used was greater when the resulting lignin fraction presented higher molecular weights. In Figure 4.16, fraction 6 did not show signal in that range meaning that the production of complex dimers or trimers was not favored. In most of the ultrafiltered fractions, the most abundant signals were in the range of 300-400 g / mol which would correspond to the presence of dimers or monomers with complex structures which could not be detected or separated mediating the conditions used in the GC-MS due to its high boiling temperature

### 4.5.2 Effect on char formation

Char yields are shown in Figure 4.17. Coke was considered as an undesirable product since the objective of this study was to transform ultrafiltered lignin fractions into platform chemicals (higher value added products than char). In general, it could be said that all ultrafiltrated lignin fractions yielded low coke percentage (below 8%). In section 4.3, it was proved that the addition of a catalyst decreased char formation. Although not much char was obtained, the experiments with lower molecular weight lignin (F4, F5 and F6) presented slight higher char formation. This fact could be related to the demethoxylation, dealkylation, demethylation reaction intermediates, reactions which are more favored by lower molecular weight lignin fractions.

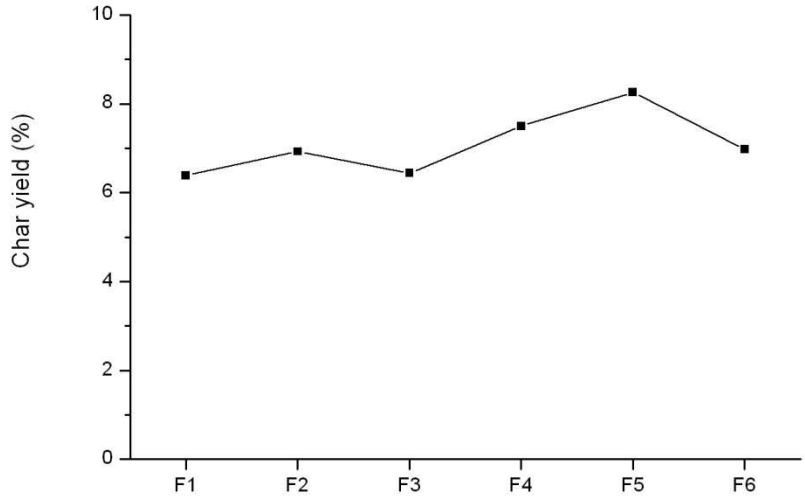


**Figure 4.17.** Obtained char yields of ultrafiltered lignin fractions. Char yields (%, w/w) referred to initial lignin weight.

### 4.5.3 Effect on residual lignin

Figure 4.18 shows residual lignin recovered in the screening experiments carried out. The main target of lignin base catalyzed depolymerization process was to decrease residual lignin percentage and, at the same time, to increase oil yield and oil monomeric composition. All experiments yielded high residual lignin content but unfortunately although no trend was observed along with the molecular weight of the ultrafiltered lignin fractions. The high residual lignin content was associated to repolymerization phenomenon. Repolymerization phenomenon has been reported by other authors (Li et al. 2006; Yuan et al. 2008) and consisted of the reactions that occur between instable lignin fragments and original lignin producing unconverted lignin with higher molecular weight than the initial lignin. Again, it should be noticed that residual lignin concept is not directly related with conversion concept since it cannot be assumed that all lignin was transformed into monomeric products, there was also an undesirable product, char.

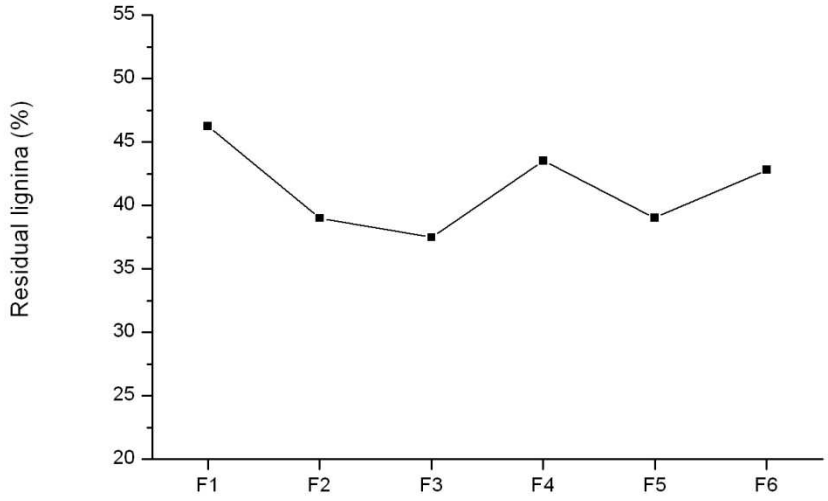


**Figure 4.18.** Recovered residual lignin of ultrafiltered lignin fractions. Residual lignin (%, w/w) referred to initial lignin weight.

In Table 4.7 are shown the number-average (Mn), weight-average (Mw) molecular weight and polydispersity (Mw/Mn) of the residual lignin obtained after base catalyzed ultrafiltrated lignin depolymerization (relative to polystyrene standards).

| | **Ultrafiltered lignin** | | | **Residual lignin** | | |
|---|---|---|---|---|---|---|
| | **Mw** | **Mn** | **Mw/Mn** | **Mw** | **Mn** | **Mw/Mn** |
| **F1** | 12798 | 3060 | 4.18 | 14733 | 5392 | 2.73 |
| **F2** | 9302 | 2489 | 3.74 | 9687 | 4198 | 2.31 |
| **F3** | 7882 | 2183 | 3.61 | 14674 | 4245 | 3.46 |
| **F4** | 6555 | 2165 | 3.03 | 8609 | 3587 | 2.40 |
| **F5** | 5184 | 1686 | 3.07 | 13724 | 4320 | 3.18 |
| **F6** | 4527 | 1567 | 2.89 | 8900 | 3756 | 2.37 |

**Table 4.7.** HPSEC results of the first peak of the recovered residual lignins related to repolymerization phenomena for each ultrafiltered lignin fraction and their corresponding rough lignin.

HPSEC results were very enlightening. Residual lignin molecular weight increased in all cases compared to the rough corresponding ultrafiltrated lignin proving that repolymerization phenomenon occurred. However, all experiments presented different repolymerization extent meaning that instable fragments reactions did not follow any trend. Some authors (Wahyudiono et al. 2008; Roberts et al. 2011) have tried to explained repolymerization reactions mechanisms concluding that the main occurrence is carbon to carbon bond formation between monomers intermediates and original lignin. In the other hand, residual lignin polydispersity of all experiments carried out was lower than the rough ultrafiltrated lignin which is the normal trend for polymer degradation.

### 4.5.4 Ultrafiltration and hydrolysis as the pathway to revalorize lignin

This study suggests a lignin revalorization pathway to produce high value added product as platform chemicals. This process involves different stages such as ultrafiltration, lignin depolymerization and recovery processes (Figure 4.19).

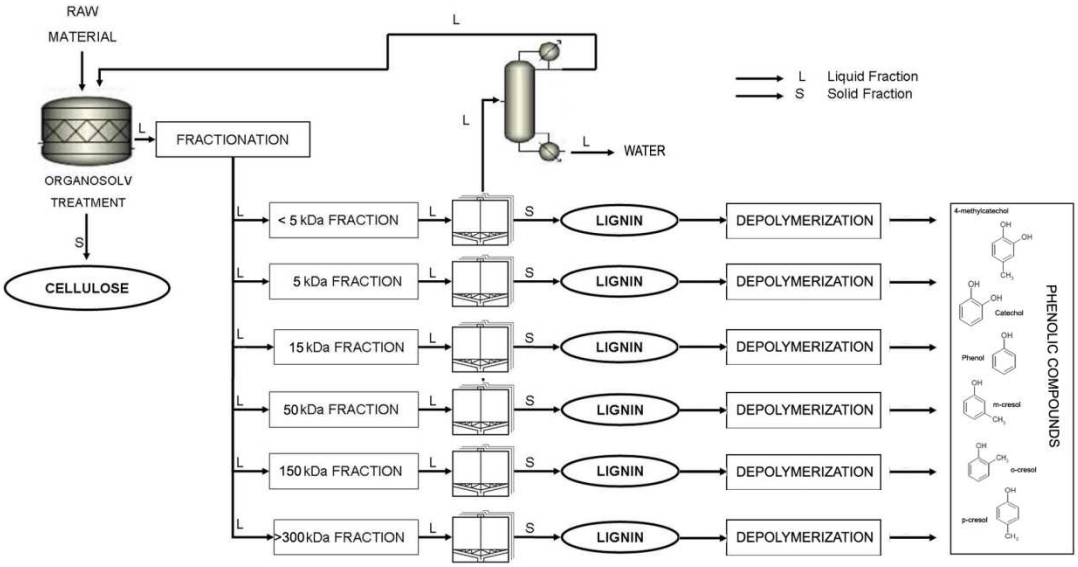


**Figure 4.19.** Lignin revalorization by hydrothermal depolymerization process scheme.

The aim of the first step –fractionanation + ultrafiltration- was to obtain specific molecular weight lignin fractions. Starting from agricultural residues (olive tree pruning), organosolv treatment was used as fractionation process. Applied organosolv treatment (Chapter 2) seemed to be a viable future fractionation alternative because of the relatively low capital investment required for a new mill, the absence of pollution problems (Sánchez et al. 2011), and the advantage of obtaining polyoses (Fengel et al. 1998) and lignin easily and largely unchanged for further high value utilization. Organosolv technology enabled the fractionation of the raw material into different products (cellulose, hemicellulose-derived sugars, and lignin) allowing the subsequent recovery of the solvents by distillation with high yields and low energy consumption (González Alriols et al. 2010) converting organosolv treatment into a green technology.

The obtained liquid fraction was subjected to ultrafiltration in order to obtained specific molecular weight lignin fractions. Ultrafiltration (Chapter 3) allowed producing not only molecular weight defined lignin fraction but also purified lignin fractions by removing sugar content. The economical viability of this first stage (fractionation and ultrafiltration) was studied by Gonzalez Alriols et al. (2010). They concluded that a distillation unit allowed the recovery of significant amounts of ethanol that could be sent back to the digester unit and also the recovery of water to be used in the pulp washing stage and the lignin precipitation unit. A cost estimation of the obtained lignin fractions by ultrafiltration process resulted in 52 €/tone of lignin, which was found higher than reported costs of kraft lignin (33 €/tone) but the high quality of the product related with its high purity and specific molecular weight convert it in a potential high added value product.

The conversion of organosolv ultrafiltrated lignin into high added value compounds could improve the economical profitability of the whole process. With this aim, base

catalyzed lignin hydrothermal depolymerization was added as a new stage to accomplish the platform chemicals obtaining. The obtained results were very promising since interesting monomeric phenolic compounds were obtained. Along this section, it has been showed that catechol and catechol derivatives were the main monomeric products. Catechols are the precursors of synthetic vanillin and ethyl vanillin that are used in flavors and fragrance industries. Rhodia, the production leader, produces vanillin based on a technology involving the catechol / guaiacol process route. Rhodia's cash cost of production of catechol has been estimated to range between $ 2.73/kg and $ 3.11/kg for input prices of phenol ranging between $ 0.60/kg and $ 1.00/kg (www.nedlac.org.za/home.aspx; www.rhodia.com). Catechol is also used in the manufacture of the insecticides carbofuran and propoxur. The pharmaceuticals drug used in the treatment of Parkinson's disease and hypertension, L-dopa and methyl L-dopa, are manufactured from catechol (Karakhanov et al. 2010). Other obtained phenolic monomeric compounds were phenol or cresols that have a wide market in polymers formulations, pharmaceutical industry...

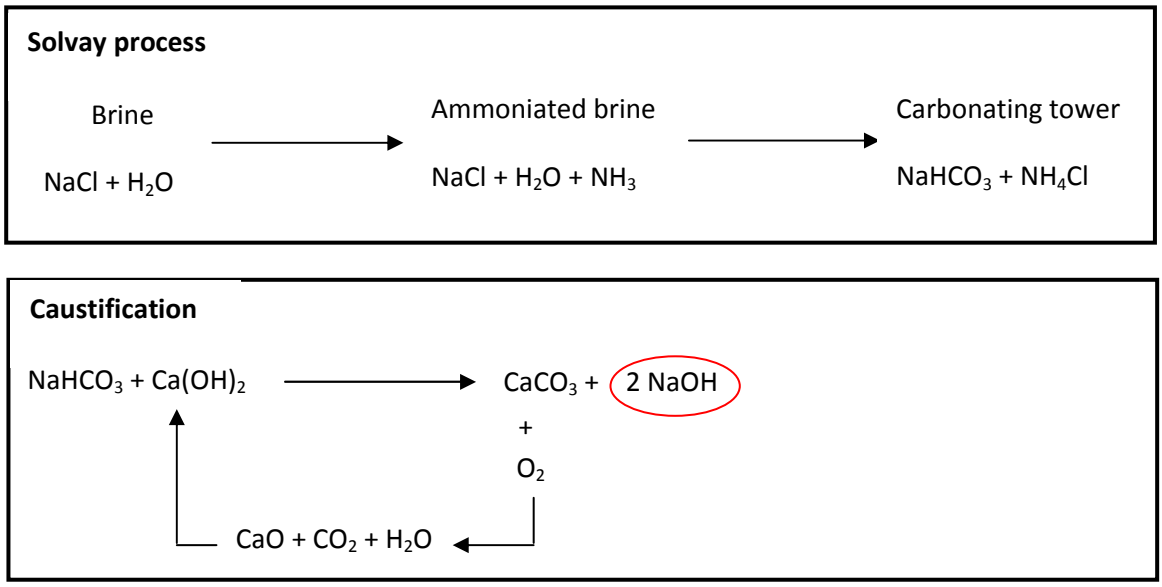


**Figure 4.20.** Chemicals recovery scheme from BCD separation procedure.

Base Catalysed lignin Depolymerization process could also recover most of the chemicals used in the separation procedure by a two steps process, first the well-known acid/base recovery process of NaCl (Solvay process) and then $NaHCO_3$ caustification to produce NaOH (Figure 4.20) (Geankoplis; Vian Ortuño 1998). These high value added applications would increase depolymerize bio-oil market price and compensate the high ultrafiltration costs.

### 4.5.5 Conclusions

A lignin revalorization process was suggested to overcome cost-effective second generation bioethanol plants. Ultrafiltration process has been proved to be an effective fractionation and purification process. Subsequently, ultrafiltrated lignin fractions were subjected to base catalyzed depolymerization. Base catalyzed depolymerization has been confirmed to produce phenolic compounds from lignin. Catechol and 4-methylcatechol were the main products in all cases. The phenolic monomer content increased as the ultrafiltrated lignin fraction presented lower molecular weight relating depolymerization with lignin molecular weight. In addition, it should be noticed that lower molecular weight fractions were also less contaminated lignin fractions and this fact could have allowed the base to better interact with lignin molecules. However, repolymerization phenomenon was observed. These reactions decreased oil yield given the fact that instable fragments reacted with original lignin instead of forming phenolic monomeric compounds. A whole process was suggested including chemicals recovery from the first stage (fractionation and ultrafiltration) and from the second stage (base-catalyzed lignin hydrothermal depolymerization). Base catalysed depolymerization produced very interesting compounds that could be introduced in existing industrial processes but the yield should be improved. Moreover, repolymerization phenomena should be avoided.

## 4.6 Improvement of lignin hydrothermal depolymerization

The results previously obtained showed that hydrothermal lignin depolymerization constitutes a promising process to revalorize lignin since simple and interesting phenolic compounds were obtained. Other benefits from hydrothermal depolymerization are the homogeneous phase that facilitates reaction engineering and the cheap chemicals needed not only for the reaction itself but also for the separation procedure. However, as it was mentioned in all studies carried out, the main problem of hydrothermal lignin depolymerization is repolymerization phenomenon decreasing and limiting oil obtaining.

In order to solve repolymerization problems Roberts et al. (2011) studied the use of boric acid to protect the phenolic OH groups and suppress repolymerization. In addition to blocking reactions of phenols, boric acid can also act as catalyst for the acidic ether hydrolysis. They found that the presence of boric acid increased the oil yields considerably (15%, w/w) compared to the uncatalyzed system (6%, w/w). They proved that a combination of the BCD process and use of boric acid also affected product composition of the obtained oil. In general, with an increasing amount of NaOH, the molecular weight distribution was shifted towards lower molecular weight products, with increased monomer fraction of the oil. Okuda et al. (2004) claimed that the reaction in the water–phenol mixture effectively decomposed lignin without producing the cross-linked higher molecular weight compounds. Their results showed that the water– phenol mixtures are excellent solvents for depolymerization of lignin. Okuda et al. (2008) also reported good results of lignin depolymerization in water-p-cresol mixtures.

A capping agent is a chemical compound that is added to the reaction medium in order to avoid polymerization reactions. Two capping agents were studied and

compared, namely boric acid and phenol, to determine their effect on base catalyzed lignin depolymerization. Different lignin to capping agent ratios were evaluated in order to establish their influence in oil yield and composition. The reaction temperature was set at 300 ºC during 40 minutes reaching pressures around 90 bars. An experiment was carried out without capping agent as reference (blank). The resulting pH of each experiment is presented in Table 4.8. Other aspects of the reaction conditions, product separation and products analysis have been already discussed in section 4.2. The results are presented below.

| Lignin | $H_3BO_3$ | Phenol | pH |
|---|---|---|---|
| 1 | 0.75 | - | 12.7 |
| 1 | 1 | - | 12.6 |
| 1 | 2 | - | 10.0 |
| 1 | - | 0.75 | 12.7 |
| 1 | - | 1 | 12.7 |
| 1 | - | 2 | 11.4 |

**Table 4.8.** Initial pH of the resulting reaction mixtures composition (w/w). All experiments were carried out adding 4% (w/w) of sodium hydroxide as catalyst.

### 4.6.1 Effect on oil yield and composition

Low molecular weight compounds from olive tree pruning lignin depolymerization were isolated as oil. Oil yields (%, w/w) are presented in Figure 4.21. As it was mentioned before, an experiment without capping agent was carried out in order to determine how the capping agent acted during depolymerization reaction (blank experiment). The highest yields were obtained when phenol was acting as capping agent. The hightest yield (151 %) was obtained when the ratio lignin:phenol was 1:2 since the phenol excess that was not involved in avoiding repolymerization phenomenon remained in the organic phase and it was isolated in the oil. It has to be

pointed out that the experiments where phenol was the capping agent showed oil yield values even higher than 100 % given the fact that the majority of the added phenol remained in the reaction mixture and it was extracted at the same time than the low molecular weight phenolic compounds. As expected, the increase of the lignin:phenol ratio rose in line with the obtained oil yield for those experiments. In the other case, when boric acid was used as capping agent, the same behavior was observed. However, the increased of the oil yield could not be noticed until the lignin:boric acid ratio was 1:2 meaning that a boric acid excess was needed to enhance oil obtaining. The other ratios (1:0.75 and 1:1) did not improve the oil yield of the experiment carried out without capping agent, even it could be observed a slightly decrease in the oil yield.

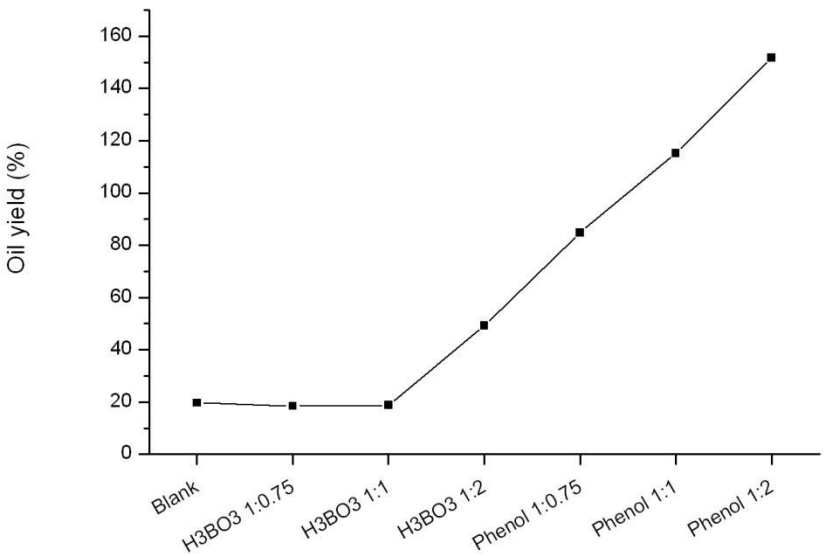


**Figure 4.21.** Obtained oil yields after adding different capping agents. Oil yields (%, w/w) referred to initial lignin weight.

Obtained oils were analyzed by GC-MS in order to determine the simple phenolic compounds. Table 4.9 shows oil composition, the compounds percentages are referred to oil weight. When no capping agent was added (blank), the main products were catechol and 4-methylcatechol. Moreover, phenol and cresols were obtained.

Capping agents were added with the purpose of avoiding repolymerization but in the end, they interfered in the products obtaining by trapping reaction intermediates. The results clearly showed different reaction behavior or mechanism depending on the used capping agent (different pKa constant).

| Compound | Blank | $H_3BO_3$ 1:0.75 | $H_3BO_3$ 1:1 | $H_3BO_3$ 1:2 | Phenol 1:0.75 | Phenol 1:1 | Phenol 1:2 |
|---|---|---|---|---|---|---|---|
| Phenol | 1.01 | 1.56 | 0.53 | 0.19 | 94.34 | 213.22 | 86.23 |
| Cresols | 0.65 | 0.37 | - | - | 5.85 | 23.34 | 7.4 |
| Guaiacol | 1.24 | 1.26 | 1.19 | 0.55 | 0.11 | 0.46 | 0.06 |
| Catechol | 10.22 | 4.49 | 0.18 | - | 4.10 | 18.57 | 3.13 |
| 4-methylcatechol | 5.16 | - | - | - | 1.92 | 8.82 | 1.01 |
| Syringol | - | 0.22 | 0.40 | 0.14 | - | 0.10 | 0.03 |
| 4-hydroxybenzaldehyde | - | - | - | - | 0.13 | 0.88 | 0.07 |
| Acetovanillone | - | - | 0.09 | - | - | 0.03 | - |
| 4-hydroxybenzoic acid | - | - | - | - | 0.09 | 1.37 | 0.08 |
| 4-hidroxy-3-methoxy-phenylacetone | - | - | - | - | - | 0.05 | - |
| Ferulic acid | - | - | - | - | - | 7.16 | 5.39 |

**Table 4.9.** Phenolic compounds obtained after adding different capping agents. Compounds yields (%, w/w) referred to oil weight.

When using boric acid as capping agent, not many products were obtained. As the lignin to boric acid ratio increased, the phenolic compounds yield was lower suggesting that the excess of this capping agent was toxic for the monomers reaction mechanism. Bearing in mind oil yield results, this finding was unexpected since the highest oil yield was obtained at the highest ratio. This unexpected result may be explained given the fact that the excess of boric acid (ratio 1:2, pH 10.0) decreased the reaction mixture pH and boric acid capping agent capability strongly depended on pH. At pH values in the range of 4–12, polyborates existed predominantly in solution, and were less prone to react with phenolic and catecholic compounds (Roberts et al. 2011). The initial pH values of the experiments decreased along with the time

reaction because the formation of some products such as formaldehyde, acetic acid… The decreased in the pH affected borates structure and so, its capability to trap reaction intermediates. As this reaction intermediates underwent condensation reactions, phenol, cresols and catechol products were not identified in the oil obtained at the highest lignin to boric acid ratio. It was clearly observed that all depolymerization products concentration decreased as the boric acid concentration in the reaction mixture was higher.

Base Catalyzed Lignin Depolymerization (BCLD) reaction takes place via carbenium ions meaning that syringylic carbenium is more stable than guaiacylic carbenium since it has more methoxy substituent to disperse the positive charge. Then, syringylic products are produced easier as the reaction intermediate is more stable. However, syringylic intermediates can undergo demethoxylation, dealkylation, demethylation reactions yielding simpler phenolic compounds such as guaiacol, phenol, cresols, catechols… as it was reported by Miller et al. (2002a). These findings would explain that syringol concentration was lower at all studied ratios compared to guaiacol concentration. At the lowest boric acid concentration, it was found that intermediates could end up easily in simple monomeric compounds due to these reactions. The pH of this solution (ratio 1:0.75) was adequate for the boric acid to act as capping agent. However, the increase of the boric acid concentration affected the pH and so, its structure. The consequence of these changes was that syringol intermediates could not undergo dealkylation reactions to produce catechols, cresols and phenol because boric acid capping agent activity decreased. Comparing boric acid results with blank compounds results, any improvement in the oil phenolic composition was observed; even a yield worsening was detected.

Concerning the obtained results when phenol was used as capping agent in lignin BCD, it has to be pointed out that high phenol yield was due to the separation procedure. The phenol molecules that remained in the reaction mixture (not involved

in repolymerization avoiding) remains in the reaction mixture and were extracted with the lignin depolymerization products. Moreover, phenol was produced from lignin as it was confirmed by the blank experiment. This latter fact made it impossible to calculate a phenol mass balance (phenol in oil –generated and added- and phenol in residual lignin) since the generated phenol and the distribution coefficient were unknown. Unfortunately, blank phenol data (no capping agent experiment) could not have been considered as the presence of phenol in the reaction mixture favored the monomers production as it can be observed in the Table 4.9 data.

Phenol capping agent allowed a wide variety of phenolic compounds production. The increase in the lignin to phenol ratio did not present a clear trend suggesting that it was not a matter of excess; the capping agent addition should be stoichiometric being the lignin to phenol 1:1 ratio experiment the one that gave the best results. Omitting phenol as a product, it could be observed that the addition of phenol to the reaction mixture had an extremely positive effect in the monomeric phenolic compounds production. Cross-linking reactions were depressed due to entrapment of active fragments (formaldehyde, etc.) and capping of active sites by excess phenol they are formed in rapid decomposition of lignin by hydrolysis and dealkylation (Okuda et al. 2004). Cresols yield at least increased in nine times the blank result constituting the main products for all the conducted experiments. Catechol and 4-methylcatechol presented the same behavior, they both increased at the 1:1 ratio but decreased at the 1:0.75 and 1:2 ratios comparing to blank results. Moreover, it could be observed that guaiacol and syringol yields dramatically decreased, even disappeared, at all studied ratios suggesting that their demethoxylation reaction (to produce phenol, catechol and cresols) were favored. Guaiacol derived structures such as acetovanillone and 4-hydroxy-3-methoxyphenylacetone were detected mainly in the experiment carried out at the lignin to phenol ratio of 1:1. The presence of phenol allowed the stability of bigger structures which in further reactions would be

transformed into simpler monomeric phenolic compounds. In addition, phenolic compounds derived from lignin p-hydroxyphenyl subunits such as 4-hydroxybenzaldehyde and 4-hydroxybenzoic acid were obtained. The highest concentration of this p-hydroxyphenyl derivates was produced at the lignin to phenol ratio of 1:1. Ferulic acid was also found in the obtained oils when using phenol as capping agent. Ferulic acid is laid down in ester linkages to primary cell wall polysaccharides and provides ether linkage initiation sites for lignin, while the p-coumaric acid does not become involved in this bridge, and it is more extensively esterified to lignin during the later wall development (Xiao et al. 2001).

In the chromatograms, it could also be detected simple dimmers (low boiling temperature compounds) in the experiments carried out using phenol as a capping agent (Figure 4.22). These dimeric compounds were identified (NIST library) as *o*-(*o*-hydroxybenzyl)phenol, *o*-(*p*-hydroxybenzyl)phenol, 4,4'-ethylidenediphenol, *p*-(*p*-hydroxybenzyl)phenol and 2,2'-ethylidenediphenol.

| Compound | Phenol 1:0.75 | Phenol 1:1 | Phenol 1:2 |
|---|---|---|---|
| o-(o-hydroxybenzyl)phenol | 0.97 | 5.93 | 1.80 |
| o-(p-hydroxybenzyl)phenol | 0.72 | 2.80 | 0.85 |
| 4-4'-Ethylidenediphenol | 0.24 | 1.31 | 0.39 |
| p-(p-hydroxybenzyl)phenol | 0.49 | 1.82 | 0.54 |
| 2-2'-Ethylidenediphenol | 0.27 | 1.47 | 0.41 |

**Table 4.10.** Dimers present in the obtained oil using phenol as capping agent. Compounds yields (%) referred to oil weight (w/w).

In Table 4.10 are shown their relative concentrations. Dimers relative concentration was calculated relating phenol area and concentration (calculated by a calibration curve) with dimers area. *o*-(*o*-hydroxybenzyl)phenol, *o*-(*p*-hydroxybenzyl)phenol and

*p*-(*p*-hydroxybenzyl)phenol were produced by dimerization of cresols coming from depolymerization reactions, for instance: two *o*-cresol molecules yielded *o*-(*o*-hydroxybenzyl)phenol, the reaction between *o*-cresol and p-cresol yielded *o*-(*p*-hydroxybenzyl)phenol and finally, the reaction between two *p*-cresol molecules yielded *p*-(*p*-hydroxybenzyl)phenol). *o*-(*o*-hydroxybenzyl)phenol was the main dimer product for all the studied ratios suggesting that o-cresols intermediates were more stable.

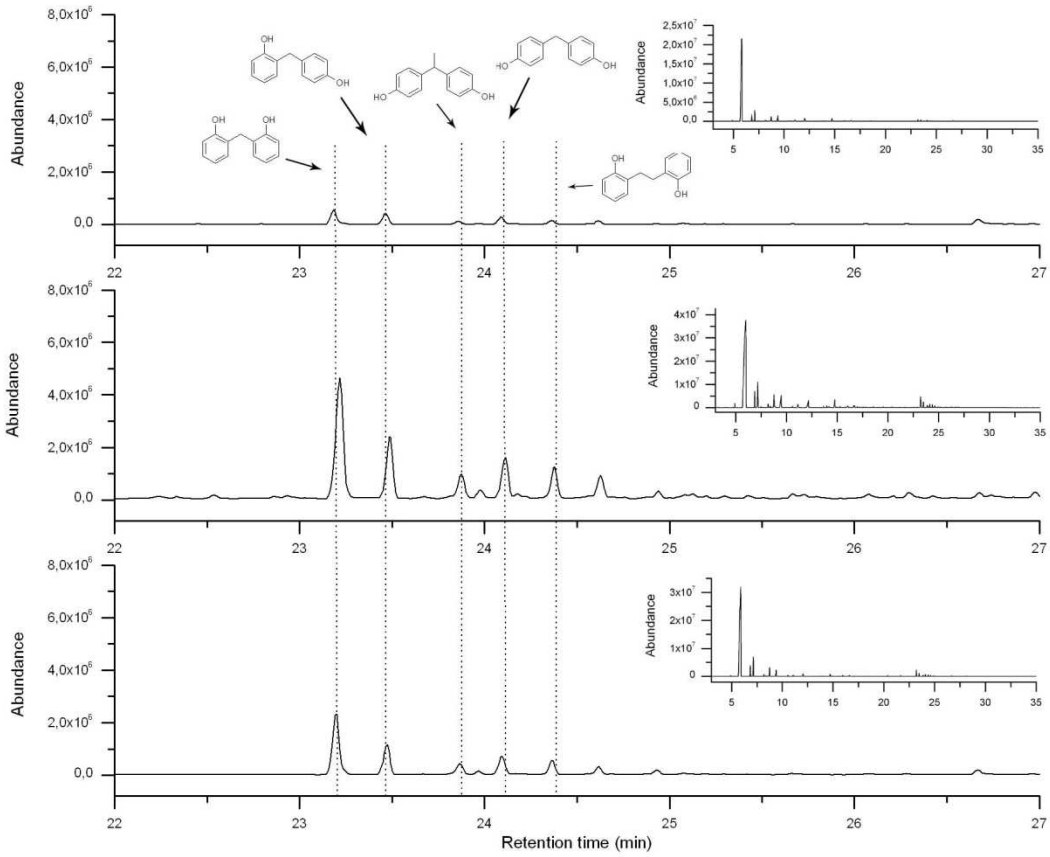


**Figure 4.22.** Chromatograms of experiments carried out using phenol as capping agent. Above (phenol 1:0.75), middle (phenol 1:1) and bottom (phenol 1:2).

Moreover, the other dimer where o-cresol was involved was the second most abundant confirming that o-intermediates were more stable. The origin of 4,4'-ethylidenediphenol and 2,2'-ethylidenediphenol products should be associated to guaiacol intermediates, cresols (*o*-cresol, *p*-cresol or *m*-cresol) intermediates,

phenol, formaldehyde or phenylpropane intermediates that could be involved in these products formation reactions. These reactions could occur at the sites in lignin (ether, hydroxyl group, etc.) by the attack of carbanions forming this kind of dimers. The abundance of these dimers did not follow any trend. The lignin to phenol ratio of 1:1 gave the highest presence of these compounds and the lowest concentration was found for 1:0.75 ratio suggesting that the blocking capacity of phenol is a key factor for dimers formation.

MALDI-TOF oil analyses are shown in Figure 4.23. These analyses were carried out with the purpose of determining the compounds molecular weight present in the oil since GC-MS technique could only detect low molecular weight compounds with low boiling temperature. As explained before, considering that a prototype lignin subunit for instance, phenylpronane syringol has a molecular weight of 197 g/mol and a phenylpropane guaiacol is about 166 g/mol, it could be observed in Figure 4.23 that most of the obtained products were mainly monomers and also dimers. It could be observed that the oil molecular weight distribution pattern was very different depending on the used capping agent. The blank experiment gave a wide distribution of molecular weights.

In general, the experiments carried out using boric acid as capping agent did not produce trimers, though in the experiment at 1:2 ratio it could be faintly detected some trimers. The absence of trimers could be related to char formation or residual lignin repolymerization phenomenon. As the lignin to boric acid ratio increased, the intensity of peaks at higher molecular weights also rose reaching the most intensive signal when the used lignin to boric acid ratio was 1:2. This finding was in accordance with the fact that the initial pH of the reaction mixture (10.0) caused polyborates to exist predominantly in solution and were not able to react with

phenolic and catecholic compounds producing products with higher molecular weight. Comparing boric acid ratios results, it seemed that the MALDI-TOF analyses were in conflict with oil composition results since for instance, oil composition at 1:2 ratio slightly contained monomers. The experiment carried out at 1:2 lignin to boric acid ratio, the oil yield increased up to nearly 50%. This percentage should be composed mainly by complex dimers with high boiling temperatures that cannot be detected by GCMS since in Table 2 the total monomers concentration was really low. The intense molecular weight products distribution made us suspect that the main depolymerization products formed at these conditions (1:2) should be complex phenolic dimers.

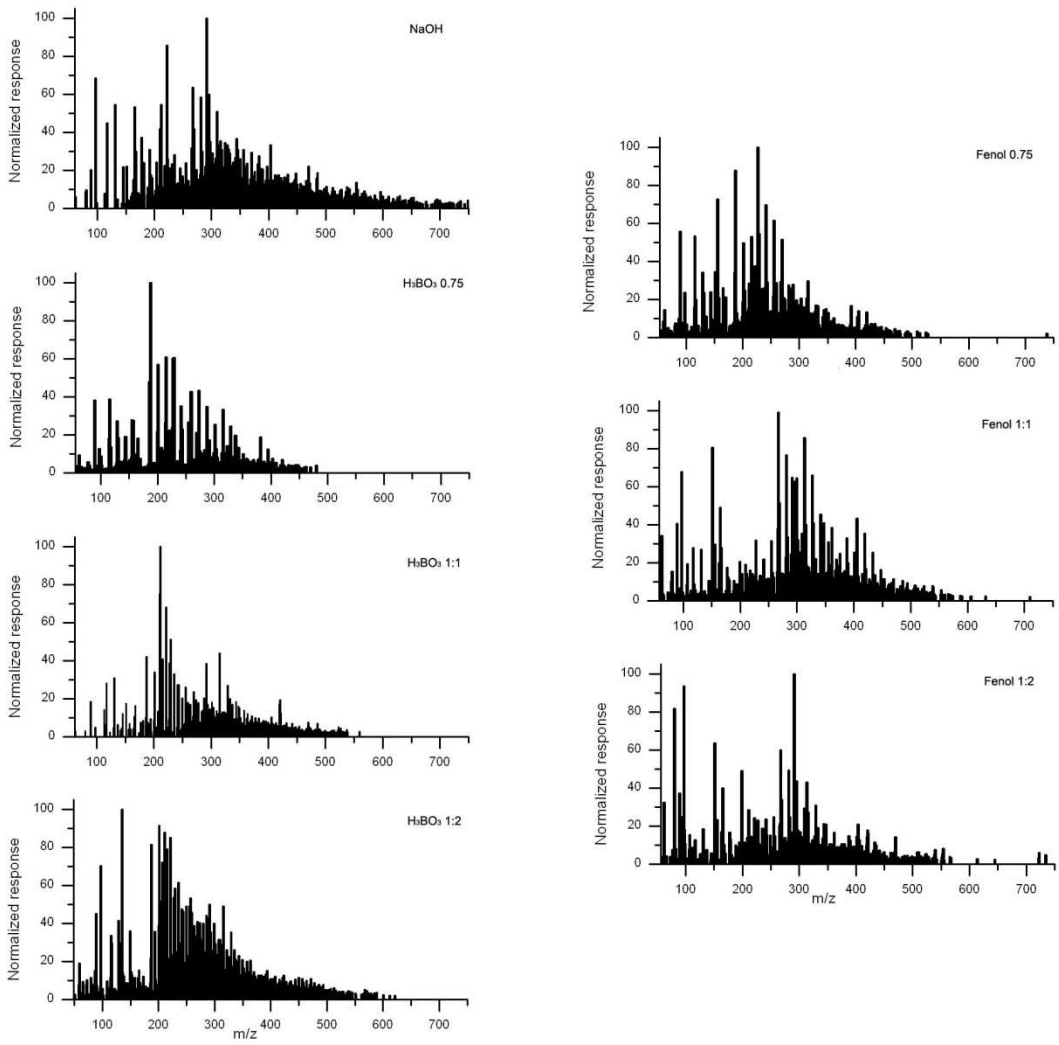


**Figure 4.23.** MALDI-TOF oil analyses of each capping agent experiment.

When using phenol as a capping agent, some trimers were detected for 1:1 and 1:2 ratios suggesting that the excess of phenol allowed trimers formation. MALDI-TOF analyses of phenol samples presented especially intense signals in the range from 0-500 g/mol. Despite the fact that most of the experiments presented signals in the range around 500-700 g/mol that corresponded to trimers, it has to be stressed that the blank experiment was the one that showed more intense signals proving that the action of a capping agent prevented oligomerization reactions. Comparing both capping agents, phenol seemed to reach higher lignin depolymerization degree.

### 4.6.2 Effect on char formation

Char yields are shown in Figure 4.24. The idea when adding a capping agent was not to vary the reaction mechanism in such a way that the char yield would remain similar to the one of the blank that was already low as show in previous sections.

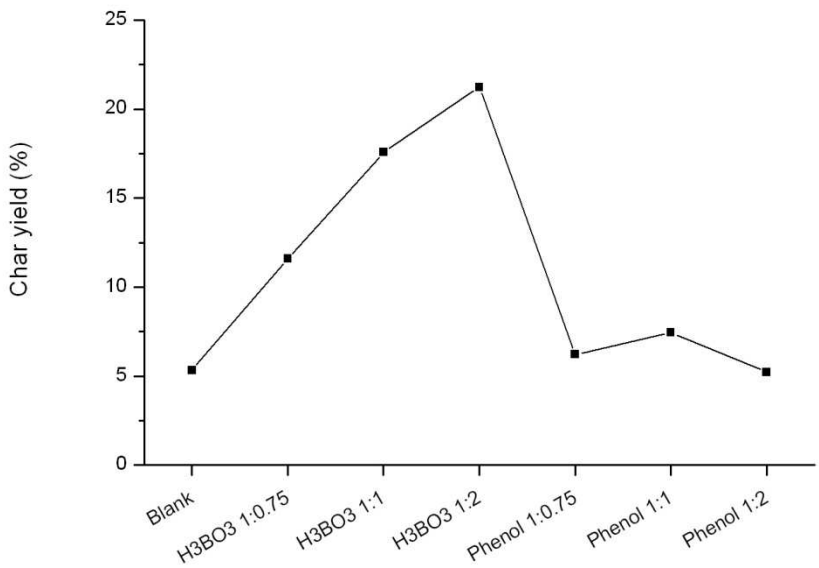


**Figure 4.24.** Obtained char yields after adding different capping agents. Char yields (%, w/w) referred to initial lignin weight.

Boric acid did not reach that purpose as it can be observed in Figure 4.24. Boric acid coke yields dramatically increased when the lignin to boric acid ratio was enlarged reaching a maximum value of 21.24% at 1:2 ratio. This fact suggested that boric acid was involved, indeed favored, in the char formation mechanism producing lignin cleavage fragments that would take part in char formation. When using phenol as a capping agent, char yields were similar to blank char yield indicating that phenol did not play any role in the char formation mechanism. Unlike boric acid capping agent, the increase in the lignin to phenol ratio did not follow any consistent behavior. Char could not be recovered for further analyses since the amounts in most of the cases were negligible.

### 4.6.3 Effect of capping agent on residual lignin

Figure 4.25 shows residual lignin content of the capping agents experiments carried out. The main target of this study was to improve base catalyzed lignin hydrothermal depolymerization by decreasing residual lignin percentage and, at the same time, increasing oil yield and oil monomeric composition. When no capping agent was added to the reaction mixture, the recovered residual lignin was approximately 45% referred to initial lignin.

Focusing in boric acid capping agent, residual lignin percentage spectacularly decreased down to 25% when increasing the lignin to boric acid ratio. These results could be confusing since low residual lignin content did not involve best conversions because it should be noticed that their char yields were really high. In conclusion, low residual lignin content did not imply high monomeric oil yield. Boric acid prevented repolymerization reactions in the lignin structure but did not avoid oligomerization reactions yielding char instead of monomeric phenolic compounds.

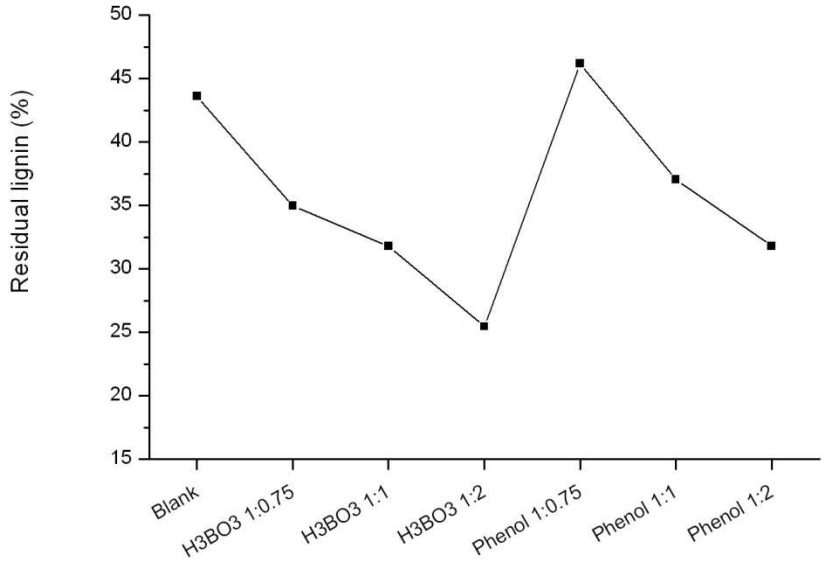


**Figure 4.25.** Recovered residual lignin after adding different capping agents. Residual lignin (%, w/w) referred to initial lignin weight.

Phenol capping agent produced less residual lignin as the lignin to phenol ratio was increased. However, residual lignin reduction was not as good as in the case of boric acid but it decreased down to 32% for the highest lignin to phenol ratio. In Figure 4.25, it could be observed that low lignin to capping agent ratios did not improve base catalyzed lignin depolymerization and a capping agent excess was needed to avoid lignin repolymerization. It is truly difficult to compare both capping agents' results in view of the fact that the whole depolymerization mechanism seemed to be completely different. However, taking into account the char formation and residual lignin results, phenol capping agent seemed to give better results.

Figure 4.26 shows molecular weight distributions of residual lignin and in Table 4.11 are summarized the number-average (Mn), weight-average (Mw) molecular weight and polydispersity (Mw/Mn) of the analyzed samples. Rough lignin was also analyzed and was plotted as a starting point and also the blank was analyzed and plotted as

the highest repolymerization limit that should be improved. HPSEC results were very enlightening. In all cases in Figure 4.26, two peaks were observed in all molecular weight distributions, one related to the unconverted lignin and the other one to a lower molecular weight lignin fraction (lower molecular weight than 800 Da) as a result of the lignin depolymerization process or oligomerization reactions. Probably, these oligomers were dragged when precipitating the residual lignin and coke at the first step of the separation procedure.

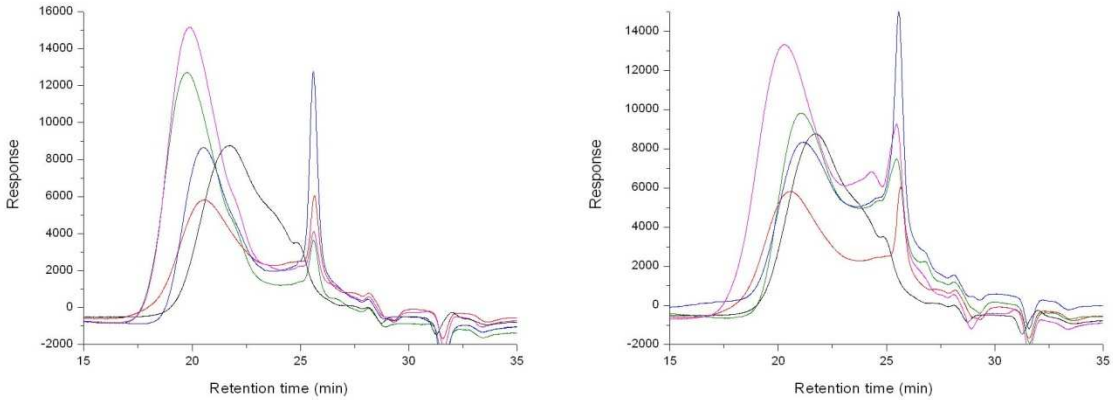


**Figure 4.26.** Molecular weight distributions of residual lignins recovered after adding different capping agents. Left graphic: black (rough lignin), red (blank), blue ($H_3BO_3$ 1:0.75), green ($H_3BO_3$ 1:1) and magenta ($H_3BO_3$ 1:2). Right graphic: black (rough lignin), red (blank), blue (phenol 1:0.75), green (phenol 1:1) and magenta (phenol 1:2).

In Table 4.11, molecular weights of the first peak (shorter retention times) are shown. That peak is the one involved in repolymerization phenomenon. Repolymerization phenomenon has been reported by other authors (Li et al. 2006; Yuan et al. 2008) and as explained before, consisted in the reactions between instable lignin fragments and original lignin producing unconverted lignin with higher molecular weight than the initial lignin. Unfortunately, the studied capping agents did not completely avoid lignin repolymerization. In the case of boric acid capping agent, only the lowest ratio (1:0.75) avoided in some extend repolymerization reactions comparing to the blank experiment. As the lignin to boric acid ratio increased, the

repolymerization reactions were more important and could not be avoided by boric acid and that is why the molecular weight increased. Polydispersity of boric acid samples increased along with the ratio suggesting that repolymerization reactions occurred at random and lignin instable fragments could react with the original lignin randomly. These findings would suggest that boric acid interfered in the BCD mechanism by favoring oligomerization reactions instead of forming monomeric compounds. The observed decrease in the residual lignin was due to the fact that intermediates yielded oligomers.

| | **Mw** | **Mn** | **Mw/Mn** |
|---|---|---|---|
| Rough lignin | 7232 | 2125 | 3.40 |
| Blank | 19957 | 4768 | 4.19 |
| $H_3BO_3$ 1:0.75 | 15448 | 5366 | 2.88 |
| $H_3BO_3$ 1:1 | 31305 | 10023 | 3.12 |
| $H_3BO_3$ 1:2 | 27515 | 6711 | 4.10 |
| Phenol 1:0.75 | 10296 | 3637 | 2.83 |
| Phenol 1:1 | 10267 | 3797 | 2.70 |
| Phenol 1:2 | 25594 | 7833 | 3.27 |

**Table 4.11.** HPSEC results of the first peak of the recovered residual lignins related to repolymerization phenomena for each capping agent ratio.

Even that the absence of repolymerization reaction was not achieved, phenol capping agent showed the best results since at 1:0.75 and 1:1 ratios the molecular weight of the recovered residual lignins were lower than in the case of the blank experiment and closer to rough lignin molecular weight. However, the phenol excess (1:2 ratio) seemed to enhance repolymerization reactions. It could be assumed that the excess of phenol along with instable fragments and reaction intermediates reacted with the original lignin structure. Phenol excess would favor this type of undesirable reactions.

In general, residual lignin polydispersity of most of the experiment (except the highest ratio for boric acid) was lower than the rough lignin which is the normal trend for polymer degradation.

### 4.6.4 Conclusions

Boric acid and phenol were studied as capping agents in order to improve base catalyzed lignin hydrothermal depolymerization. Concerning oil composition, capping agents showed totally different behavior. Phenol experiments yielded high quantities of monomeric phenolic compounds (cresols, catechols, ferulic acid...) that could be considered for further applications in material science or pharmaceutical industries. Boric acid prevented in some extent repolymerization phenomenon by increasing char formation. Boric acid oil composition was confirmed by MALDI-TOF analyses to be formed mainly by complex dimers. Phenol capping agent yielded low char content and its residual lignin decreased slightly down to 25%. The main action of phenol capping agent was to prevent oligomerization reaction by not avoiding demethoxylation, dealkylation... reactions and that is why monomeric compounds in oil rose dramatically comparing to the blank experiment. Repolymerization phenomenon was avoided in some extent at low capping agents' concentrations.

Taking into account all the obtained results, the capping agent that provided a real improvement of the process was phenol. The inclusion of phenol in the process outlined in section 4.5 would mean the addition of a recovery stage to save fresh phenol input. Phenol recovery could be achieved by distillation since its boiling point (181 ºC) is the lowest of the phenolic compounds mixture in the isolated oil. So then, the final obtained products would be cresols, catechol and 4-methylcatechol. The economy of this step should be considered.

## 4.7 Hydrothermal lignin depolymerization conclusions

Among all lignin application possibilities, bulk chemicals production seems to be one of the most hopeful pathways to add high value to lignin products. This chapter attempted to present a thorough study of lignin hydrothermal depolymerization as one of the most promising routes for lignin upgrading. To this end, several studies were conducted in order to optimize as well as a deeper understanding of the reaction mechanism of lignin hydrothermal depolymerization.

Base catalysts screening was performed. The results confirmed that the nature and thus the strength of the employed base as catalyst influenced decisively the phenolic products. The base determined the reaction mechanism since the cations catalyze the reaction by forming cation adducts with lignin and, thus, polarizing the ether bond. Depending on the base strength, different products profile was observed. Weak bases ($Ca(OH)_2$ and $K_2CO_3$) yielded mainly guaiacol, syringol and more complex monomers. Interestingly, strong bases such as NaOH, KOH and LiOH produced phenol, cresols and catechol. Repolymerization reactions were found to occur, especially when using potassium catalysts. Sodium hydroxide was considered as the best option to catalyze lignin hydrothermal depolymerization.

The reaction conditions optimization was studied by the use of a term (severity factor) which allowed simplifying the study. As expected, the nature of phenolic compounds was influenced decisively by the reaction conditions applied. The increment in the applied severity factor allowed the better understanding of the mechanism of reaction that follows the hydrothermal depolymerization of lignin. First obtained compounds were guaiacol and syringol even at the weakest conditions.

These products were found to undergo demethylation, demethoxylation, dealkylation reactions to yield phenol, cresols and catechol. However, the activation energy needed for these further transformations was pointed to only occur when applying high severity factors. Moreover, it was confirmed oil obtaining limitation due to repolymerization reactions. The best results were obtained when the highest severity factor ($LogR_o$ 7.7) was applied.

The optimized hydrothermal lignin depolymerization conditions (base + severity factor) were applied to the obtained ultrafiltered lignin fractions (Chapter 3). Thus, a scheme for lignin revalorization process has been considered. This study revealed the influence of the properties of lignin in its base-catalyzed hydrothermal depolymerization. As the lignin molecular weight was lower and as the purity of lignin was higher, the production of simple phenolic compounds was enhanced. The main obtained compounds were catechol and 4-methylcatechol. However, recovered residual lignin was high due to unconverted lignin and repolymerization phenomenon.

In these previous studies, it was found that the major drawback for the implementation of base-catalyzed lignin hydrothermal depolymerization was the high residual lignin content caused mainly by repolymerization phenomenon that constrained the production of phenolic compounds. Two capping agents (boric acid and phenol) were tested to overcome this limitation. Boric acid avoided repolymerization just at low ratios but at the same time, phenolic compound production was suppressed (mainly only guaiacol and syringol were produced). Boric acid interfered in the depolymerization mechanism avoiding repolymerization but favoring char formation. Furthermore, the capping agent performance of boric acid was found to be highly influenced by the reaction mixture pH. Interestingly, phenol capping agent presented different behavior. Low lignin to phenol ratios resulted in a

dramatic increase in the yield and distribution of phenolic compounds while largely avoided the repolymerization phenomenon. Repolymerization reactions were depressed due to entrapment of active fragments (formaldehyde, etc.) and capping of active sites by phenol. Phenol was concluded to be the best studied capping agent.

## 4.8 References

Asmadi, M.; Kawamoto, H.; Saka, S. 2011. Thermal reactions of guaiacol and syringol as lignin model aromatic nuclei. J Anal Appl Pyrol 92, 88–98.

Fang, Z.; Sato, T.; Smith Jr., R.L.; Inomata, H.; Arai, K.; Kozinski, J.A. 2008. Reaction chemistry and phase behavior of lignin in high-temperature and supercritical water. Bioresour Technol 99, 3424–3430.

Fengel, D.; Wegener, G. 1989. Eds. Wood: Chemistry, Ultrastructure, Reactions; Walter de Gruyter: Berlin and New York.

Freudenberg, K.; Janson, A.; Knopf, E.; Haag, A. 1936. Zur Kenntnis des Lignins. Ber Dtsch Chem Ges 69, 1415-1425.

Freudenberg, K.; Meister, M.; Flickinger E. 1937. Fichtenlignin (XVI.Mitteil. Über lignin). Ber Dtsch Chem Ges 70, 500-514.

Freudenberg, K.; Müller, H. 1938. Zur Kenntnis des Buchenlignins (XVI.Mitteil. Über lignin). Ber Dtsch Chem Ges 71, 1821-1825

Freudenberg K. 1939a. Über lignin. Angew Chem 52, 362-363.

Freudenberg, K.; Lautsch, W. 1939b. Zur Konstitution des Fichtenlignins. Naturwissenschaften 27, 227-228.

Freudenberg, K.; Lautsch, W.; Engler, K. 1940. Die Bildung von Vanillin aus Fichtenlignin. Ber Dtsch Chem Ges 73, 167-171.

Garrote, G.; Cruz, J.M.; Domínguez, H.; Parajó, J.C. 2008. Non-isothermal autohydrolysis of barley husks: Product distribution and antioxidant activity of ethyl acetate soluble fractions. J Food Eng 84, 544–552.

Geankoplis, C.J. Procesos de transporte y operaciones unitarias (3ª Edición) Compañía Editorial Continental. ISBN: 9682613167.

Gierer, J. 1985. Chemistry of deligninfication. Part 1. General concept and reactions

during pulping. Wood Sci Technol 19, 289-312.

Gierer, J. 1986. Chemistry of delignification. Part 2. Reactions of lignins during bleaching. Wood Sci Technol 20, 1-33.

González Alriols, M.; García, A.; Llano-ponte, R.; Labidi, J. 2010. Combined organosolv and ultrafiltration lignocellulosic biorefinery process. Chem Eng J 157, 113–120.

Kadam, K.L.; Chin, C.Y.; Brown, L.W. 2009. Continuous biomass fractionation process for producing ethanol and low-molecular-weight lignin. Environ Prog Sus Energ 28 (1), 89-99.

Karagöz, S.; Bhaskar, T.; Muto, A.; Sakata Y. 2004. Effect of Rb and Cs carbonates for production of phenols from liquefaction of wood biomass .Fuel 83 (17–18), 2293-2299.

Karakhanov, E.A.; Maximov, A.L.; Kardasheva, Y.S.; Skorkin, V.A.; Kardashev, S.V.; Ivanfova, E.A.; Lurie-Luke, E.; Seeley, J.A.; Cron, S.L. 2010. Hydroxylation of phenol by hydrogen peroxide catalyzed by copper(II) and iron(III) complexes: The structure of the ligand and the selectivity of ortho-hydroxylation. Ind Eng Chem Res 49, 4607–4613.

Leopold, B.; Malmström, I.L. 1951a. Nitrobenzene oxidation of compounds of the lignin type. Acta Chem Scand 5, 936-940

Leopold, B. 1951b. Nitrobenzene oxidation of the products formed by the condensation of resorcinol with lignin models. Acta Chem Scand 5, 1393-1421.

Leopold, B. 1952a. Studies on lignin. III. Oxidation of wood from Picea abies (L.) Karst. (Norway spruce) with nitrobenzene and alkali. Acta Chem Scand 6, 38-39.

Leopold, B. 1952b. Studies on lignin. VI. Nitrobenzene oxidation of lignin sulfonic acids. Acta Chem Scand 6, 55-63.

Li, J.; Henriksson, G.; Gellerstedt, G. 2007. Lignin depolymerization/repolymerization and its critical role for delignification of aspen wood by steam explosion. Bioresour Technol 98, 3061–3068.

Miller, J.E.; Evans, L.R.; Mudd, J.E.; Brown, K.A. 2002a. Sandia National Laboratories Report SAND2002-1318, USA.

Miller, J.E.; Evans, L.R.; Littlewolf, A.E.; Trudell, D.E. 2002b. Sandia National Laboratories Report SAND2002-1317, USA.

Okuda, K.; Umetsu, M.; Takami, S.; Adschiri, T. 2004. Disassembly of lignin and chemical recovery—rapid depolymerization of lignin without char formation in water–phenol mixtures. Fuel Process Technol 85, 803– 813.

Okuda, K.; Ohara, S.; Umetsu, M.; Takami, S.; Adschiri, T. 2008. Disassembly of lignin and chemical recovery in supercritical water and p-cresol mixture: Studies on lignin model compounds. Bioresour Technol 99 (6), 1846-1852.

Overend, R.P.; Abatzoglou, N.; Chornett, E.; Belkacemi, K. 1992. Phenomenological kinetics of complex systems: the development of a generalized severity parameter and its application to lignocellulosics fractionation. Chem Eng Sci 47 (5), 1109-1122.

Roberts, V.M.; Stein, V.; Reiner, T.; Lemonidou, A.; Li, X.; Lercher, J.A. 2011. Towards quantitative catalytic lignin depolymerization Chem-Eur J 17, 5939–5948.

Rubio, M.; Tortosa, J.F.; Quesada, J.; Gómez, D. 1998. Fractionation of lignocellulosics. Solubilization of corn stalk hemicelluloses by autohydrolysis in aqueous medium. Biomass Bioenerg 15, 483–491.

Saisu, M.; Sato, T.; Watanabe, M.; Adschiri, T.; Arai, K. 2003. Conversion of lignin with supercritical water-phenol mixtures. Energy Fuels 17, 922-928.

Sánchez, R.; Rodríguez, A.; García, J.C.; Rosal, A.; Jiménez, L. 2011. Exploitation of hemicellulose, cellulose and lignin from Hesperaloe Funifera. Bioresour Technol 102, 1308–1315.

Saska, M.; Ozer, E. 1995. Aqueous extraction of sugarcane bagasse hemicellulose and production of xylose syrup. Biotechnol Bioeng 45, 517–523.

Thring, R.W. 1994. Alkaline degradation of ALCELL® lignin. Biomass Bioenerg 7, 125-130.

Vian Ortuño, A. 1998. Introducción a la química industrial. Editorial Reverté, Barcelona.

Vigneault, A.J.D.; Chornett E. 2006. Advance in the termal depolymerization of lignin via base-catalysis, in Science in Thermal and Chemical Biomass Conversion. CPL Press.

Wahyudiono, Sasaki, M.; Goto, M. 2008. Recovery of phenolic compounds through the decomposition of lignin in near and supercritical water. Chem Eng Process 47, 1609–1619.

Wahyudiono, Sasaki, M.; Goto, M. 2009. Conversion of biomass model compound under hydrothermal conditions using batch reactor. Fuel 88 (9), 1656-1664.

www.nedlac.org.za/home.aspx

www.rhodia.com

Xiao, B.; Sun, X.F.; Sun, R.C. 2001. Chemical, structural, and thermal characterizations of alkali-soluble lignins and hemicelluloses, and cellulose from maize stems, rye straw, and rice straw. Polym Degrad Stabil 74 (2), 307–319.

Yuan, Z.; Cheng, S.; Leitch, M.; Xu, C. 2010 Hydrolytic degradation of alkaline lignin in hot-compressed water and etanol. Bioresour Technol 101, 9308–9313.

Zakzeski, J.; Bruijnincx, P.C.A.; Jongerius, A.-L.; Weckhuysen, B.M. 2010. The Catalytic Valorization of Lignin for the Production of Renewable Chemicals. Chem Rev 110 (6), 3552-99.

# 5. LIGNIN DEPOLYMERIZATION BY HYDROGENOLYSIS

## 5.1 Introduction

It is important to note that the economic necessity for a lignocellulosic biorefinery to produce chemicals in addition to biofuels has been advocated (Percival Zhang 2008). Indeed, the production of both fuels and products is necessary to justify construction of the biorefinery in order to achieve a high energy impact and proper return on investment (Zakzesky et al. 2011). Lignin valorization to produce high added value products is a major goal for Biorefinery processes to be cost-effective.

Pyrolysis (thermolysis), gasification, hydrogenolysis, chemical oxidation, and hydrolysis under supercritical conditions are the major thermochemical methods studied concerning lignin depolymerization (Pandey et al. 2011). The replacement of petrochemical- based routes for the production of bulk aromatic compounds, such as benzene, toluene, and xylene (B, T, X), as well as phenol, by renewable routes has nonetheless received relatively little attention (van Haveren et al. 2008). With regard to reductive lignin depolymerization, the emphasis of the reported studies is mainly on the production and upgrading of bio-oils and fuels, although the production of phenols as a chemical commodity is also considered (Zakzesky et al. 2011).

Hydrogenolysis is defined as the process in which cleavage of a carbon-carbon or carbon-hetero atom single bond is accomplished by reaction with hydrogen. Thermal treatment in a hydrogen environment seems very promising for converting lignin to liquid fuel and chemicals like phenols (Pandey et al. 2011) For lignin reductions, typical reactions involve the removal of the extensive functionality of the lignin subunits to form simpler monomeric compounds such as phenols, benzene, toluene, or xylene (Zakzesky et al. 2011). Unlike lignin oxidation (BCD), which are generally

carried out at high temperatures and strong conditions, hydrogenolysis can be accomplished at lower temperatures and, hence, favors higher yields of liquid including monomeric phenols.

The selective catalytic hydrogenation of lignin and its model compounds has been studied for many years and is the subject of several publications (Zakzesky et al. 2011). The first isolation of degradation products which contained the complete C6-C3 skeleton was reported by Harris and Adkins (1938). These authors obtained fair yields of propylcyclohexane derivatives when they subjected a methanol lignin from aspen to catalytic hydrogenation under vigorous conditions. Guaiacylpropane and syringylpropane derivatives were later obtained by Hibbert, Pepper, Schuerch and other workers whose results were summarized by Hrutfiord (1971) in a very complete review on lignin reduction and hydrogenolysis using a variety of conditions. Indeed, catalytic hydrogenolysis was said to be one of the most effective methods of obtaining valuable information about the chemical structure of lignin since high yields of mono-, di-, tri-, and oligolignols are formed without the occurrence of secondary or polymerization reactions (Sakakibara 1992).

Hydrogneolysis product yields and distribution depend on the severity of the reaction conditions and type of catalyst used. Previous work and results in this field (Pepper et al. 1963, 1969) point to a general consensus in catalytic hydrogenolysis methodologies as a valuable approach to unravel structural features of lignin through the production of significant lignin degradation products. Meier et al. (1992) studied lignin hydrogenation focusing on excluding any influence of a solvent system on the catalytic hydrogenation of lignin. Therefore, they applied hydropyrolysis in a process where lignin reacted directly with hydrogen in a gas-solid reaction. Besides phenol, the main components were cresols, dimethylphenols, ethyl- and propylphenol. Thring

et. al (1996) conducted different studies about lignin hydrogenlolytic depolymerization at high temperatures. The main obtained monomeric compounds were phenols, guaiacols, syringols, catechols and aldehyde. More recently, Torr et al. (2011) carried out lignin hydrogenolysis experiments with molecular hydrogen. The major components of the hydrogenolysis oils from *P. radiata* lignins were guaiacol derivate compounds and they studied the presence of dimeric structures mainly linked with β-5, 5-5, 4-O-5 and β-1 linkages in the isolated oils.

Comparing to traditional hydrogenations; the transfer hydrogenations are considered as generally simpler and environmentally friendly processes as the use of molecular hydrogen is avoided (thus minimizing risks of explosions, leaks and related hazards), high-pressurized devices are also avoided and mild reaction conditions are favored that normally lead to improved selectivities (Su et al. 2008). The use of microwave-assisted protocols has been recently reported (Baruwati et al. 2009) to be agreeable because of providing efficient hydrogen transfer systems in very short times of reaction. Yoshida et al. (2010) studied an efficient hydrogenation of carbonyl compounds using low-loaded supported copper nanoparticles under microwave irradiation. This study confirmed the positive effect of microwave in transfer hydrogenation reactions employing similar reaction systems as the ones that are going to be described in this chapter.

### 5.1.1 Objective

The major aim of this chapter was to study lignin hydrogenolytic depolymerization using heterogeneous catalysts to produce phenolic monomeric compounds. This study was developed in collaboration with Dr. Rafa Luque from the Organic Department of the University of Córdoba (Spain).

First, different supported metal catalysts were tested in order to study their influence on the oil yield and on the nature of the obtained simple phenolic compounds. Subsequently, the reaction media was varied by employing different hydrogen-donor solvents (hydrogen source) with the purpose of finding the best reaction conditions that yielded the highest quantity of phenolic oil and the most interesting phenolic compounds. The optimized conditions (best catalyst and best hydrogen-donor solvent) were applied to lignin ultrafiltered fractions (obtained in Chapter 3). The final objective is the proposal of an entire lignin valorization process.

## 5.2 Materials and methods

Hydrogenolysis reactions were carried out in a microwave reaction system Milestone ETHOS 1. The reactor was filled employing a lignin:catalyst ratio of 1:1 and a solid:liquid ratio of 1:12.5. Since these studies were the first time that these kinds of reactions were carried out in a microwave system, no references for reactions conditions were found. The applied power in all cases was determined taking into account the microwave temperature limit (200 ºC). Given the fact that microwave chemistry is claimed to need shorter times than conventional reactions, hydrogenolysis reactions were carried out during 30 minutes. The yield of every product was calculated gravimetrically referring to the initial lignin weight.

### 5.2.1 Catalysts preparation and characterization

The bifunctional catalysts were rationally designed from a fundamental understanding point of view to maximize lignin depolymerization under the

investigated conditions. These include 1) the maximization of the accessibility and activity of the metal sites (supported metal nanoparticles synthesized by ball milling have been proved to predominantly deposit in the external surface of a support being highly active and accessible even at very low loadings (Pineda et al. 2011) as well as 2) the minimization of repolymerization and related side reactions (by using a mild hydrogenolytic approach under reducing conditions that can in principle quench radicals and unstable intermediates formed during depolymerization) which avoids, at the same time, the addition of hydrogen in the systems. Al-SBA-15 was chosen as support due to its good (hydro)thermal stability, large surface area (useful for the deposition of nanoparticles) and most importantly combination of Brönsted and Lewis moderate acidity which is a pre-requisite to promote dealkylations, deacylations and related chemistries involved in lignin valorization practices (Binder et al 2009).

The studied catalysts were prepared following a previously reported novel dry mechanochemical approach (Pineda et al. 2011). In a typical synthesis, 0.2 g Al-SBA-15 was grinded with the needed quantity of metal precursor (to reach a theoretical 2% (w/w) metal) in a Retsch PM-100 planetary ball mill using a 125 mL reaction chamber and 10 mm stainless steel balls. Milling conditions were 10 minutes at 350 rpm (optimized conditions). Upon milling as-synthesized materials were washed to remove the excess of unreacted and/or physisorbed precursor and directly calcined at 400 ºC under air atmosphere for 4 h. Prior to the reaction, the catalysts were activated and reduced in a flow of hydrogen/helium for 1 hour.

#### 5.2.1.1 Catalyst characterization

Catalysts were characterized in order to determine their physicochemical properties and composition to better explain the obtained results. The prepared catalysts were

subsequently characterized by a number of techniques including X-Ray Diffraction (XRD), $N_2$ physisorption, Transmission electron microscopy (TEM), Energy-dispersive X-ray spectroscopy (EDX) and Inductively Coupled Plasma (ICP, for metal determination) and X-Ray Photoelectron Spectroscopy (XPS).

XRD patterns were collected on a Siemens D-5000 diffractometer (40 kV, 30 mA) equipped with a Ni filter and a graphite monochromator, using Cu $K_\alpha$ radiation ($\lambda$ = 1,54 Å). Scans were performed from 10 to 80º range at a step time of 0,040 at 1º/min.

Nitrogen adsorption measurements were carried out at 77 K using an ASAP 2010 volumetric adsorption analyzer from Micromeritics. The samples were outgassed for 2 hour at 100 $^{o}$C under vacuum (pressure < $10^{-2}$ Pa) and subsequently analyzed. The linear part of the BET equation (relative pressure between 0.05 and 0.22) was used for the determination of the specific surface area.

TEM (Transmission electron microscopy) micrographs were recorded on a FEI Tecnai G2 fitted with a CCD camera for ease and speed of use. The resolution is around 0.4 nm. Samples were suspended in ethanol and deposited straight away on a copper grid prior to analysis.

XPS (X-ray photoelectron spectroscopy) (aka ESCA) measurements were performed in a ultra high vacuum (UHV) multipurpose surface analysis system (Specs$^{TM}$ model, Germany) operating at pressures <$10^{-10}$ mbar using a conventional X-ray source (XR-50, Specs, Mg-Kα, 1253.6 eV) in a "stop-and-go" mode to reduce potential

damage due to sample irradiation. The survey and detailed Fe and Cu high-resolution spectra (pass energy 25 and 10 eV, step size 1 and 0.1 eV, respectively) were recorded at room temperature with a Phoibos 150-MCD energy analyser. Powdered samples were deposited on a sample holder using double-sided adhesive tape and subsequently evacuated under vacuum ($<10^{-6}$ Torr) overnight. Eventually, the sample holder containing the degassed sample was transferred to the analysis chamber for XPS studies. Binding energies were referenced to the 1s line at 284.6 eV from adventitious carbon. The curve deconvolution of the obtained XPS spectra was obtained using the Casa XPS program.

The metal content in the materials was determined using Inductively Coupled Plasma (ICP) in a Philips PU 70000 sequential spectrometer equipped with an Echelle monochromator (0.0075 nm resolution). Samples were digested in $HNO_3$ and subsequently analyzed by ICP at the SCAI (Universidad de Cordoba).

### 5.2.2 Products characterization

Phenolic products resulting from lignin depolymerization were isolated as oil. This oil was characterized by gas chromatography with mass selective detector (GC-MS) and matrix assisted laser desorption/ionization time-of-flight mass spectrometry (MALDI-TOF).

The GC-MS analyses were performed to identify and quantify the monomers present in the oil. Thus, the oil was dissolved in ethyl acetate (HPLC grade) in a metric flask. The solution was injected in a GC (7890A)-MS (5975C inert MSD with Triple-Axis Detector) Agilent equipped with a capillary column HP-5MS ((5%-Phenyl)-

methylpolysiloxane, 60 m x 0.32 mm). The temperature program started at 50 ºC then, the temperature is raised to 120 ºC at 10 ºC/min, held 5 minutes, raised to 280 ºC at 10 ºC/min, held 8 minutes, raised to 300 ºC at 10 ºC/min and held 2 minutes. Helium was used as carrier gas. Compounds were identified by employing NIST Agilent library and quantification was determined using phenol as internal standard.

The oil was also analyzed by MALDI-TOF in order to establish the molecular weight distribution of the products present in the isolated oil. The use of this technique allowed us to evaluate the depolymerization degree that had occurred in the sample. Matrix assisted Laser desorption/ionization time-of-flight mass spectrometry (MALDI-TOF) analyses were carried out in a Voyager-DE™ STR Biospectrometry™ Workstation of Applied Biosystems. A 15 g/L solution of DABP (3,4-diaminobenzophenone) in a methanol-water mixture (8:2) was used as matrix. The analyses were developed in negative mode.

Residual lignins were subjected to High Performance Size Exclusion Chromatography (HPSEC) to evaluate lignin weight-average molecular weight (Mw), number-average molecular weight (Mn), polydispersity (Mw/Mn) and molecular weight distribution (MWD) using a JASCO instrument equipped with an interface (LC-NetII/ADC) and a refractive index detector (RI-2031Plus). Two PolarGel-M columns (300 x 7.5 mm) and PolarGel-M guard (50 x 7.5 mm) were employed. Dimethylformamide + 0.1% lithium bromide solution was used as eluent. The flow rate was 0.7 mL/min and the analyses were carried out at 40 ºC. 0.5% (w/w) solutions of residual lignins were prepared to measure samples molecular weight. Calibration was made using polystyrene standards (Sigma-Aldrich) ranging from 266 to 70000 g/mol. Therefore, the obtained values are relative to the employed polystyrene standards.

## 5.3 Effect of the nature of the catalyst on lignin hydrogenolytic depolymerization

A series of considerations for the rational design of heterogeneous catalysts for lignin depolymerization practices using heterogeneous catalysts can be drawn to start with. The hydrogenation catalyst is typically composed of cobalt, tungsten, palladium, or nickel, and the cracking component typically consists of zeolites or amorphous silica-alumina with various compositions (Thring et al. 1996). More recently, Zakzesky et al. (2011) accomplished a very complete review on lignin and mainly, on lignin model compounds hydrogenolytic depolymerization. In this review, it can be observed that many different catalyst preparation attempts have been developed with the objective of giving insights on lignin depolymerization. These catalysts preparations corresponded to many different metals (Cu, Rh, Fe, Mo, Pd, Ni, Ru, Pt, V…), metals combinations (Rh-Co, Ni-Cu, Co-Mo, Ni-Mo) and supports (carbon, $Al_2O_3$, $SiO_2$-$Al_2O_3$, zeolite and activated charcoal).

Contrary to most reports to date in which Rh, Pt and Pd-based catalysts were the most widely employed in the transformations of lignin model compounds (Yan et al. 2008; Binder et al. 2009; Liguori et al. 2011; Li et al. 2012) the promising potential of Ni catalysts in C-O bond cleavage combined with a suitable acidic support for C-C bond cleavage has been highlighted in recent works (Sergeev et al. 2011; Li et al. 2012; Horacek et al. 2012). Li et al. (2012) recently reported the use of a carbon supported Ni-$W_2C$ catalyst for the direct catalytic conversion of raw woody biomass (e.g. birch, poplar, pine and related feedstocks) into monophenols up to 46.5% yield (based on lignin) without any pretreatment step. These authors showed this type of catalyst exhibited a comparable activity to that of noble metals, paving the way to a further development of Ni-based materials for lignin depolymerization.

### 5.3.1 Materials and methods

Tetralin was used as hydrogen-donor solvent (four hydrogen atoms released from each tetralin molecule) since it leads to a stable product (naphthalene) that does not interfere in lignin hydrogenolysis. Connors et al. (1980) established the hydrogen-donating effect of tetralin upon the hydrocracking of kraft lignin. The advantages of tetralin as a hydrogen-donor solvent include its high boiling point as well as its ready release of hydrogen atoms under hydrocracking conditions, leading to the formation of naphthalene, a relatively stable compound (Thring et al. 1996).

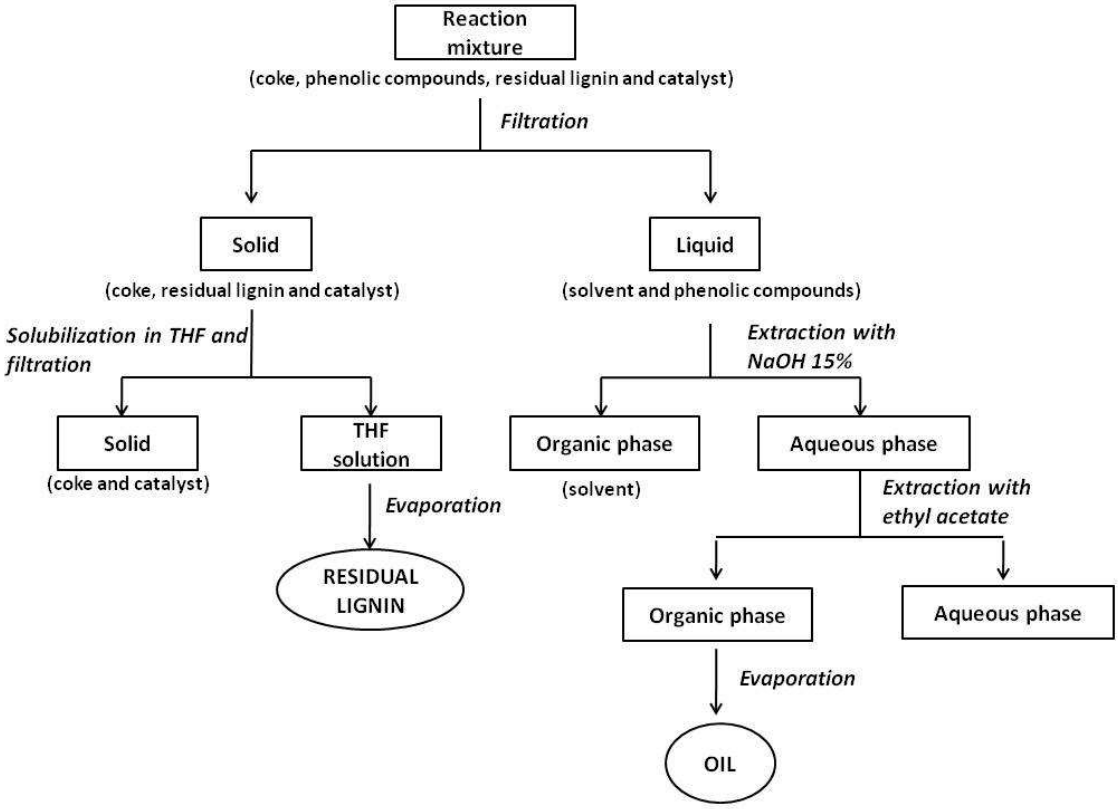


**Figure 5.1.** Scheme of products separation in hydrogenolysis screening experiments.

The studied catalysts consisted of metals supported (Ni, Pd, Pt and Ru) on aluminosilicates (Al-SBA-15), namely Ni 2% SBA15, Ni 5% SBA15, Ni 10% SBA15, Pd 2% SBA15, Pt 2% SBA15 and Ru 2% SBA15. An experiment without catalyst was

carried out as blank. Microwave power was set constant at 400 W for all experiments in order to evaluate the microwave effect on oil yield and composition, reaching an average temperature of 150 ºC. The applied power was determined taking into account the microwave temperature limit (200 ºC). A scheme of the product separation is provided in Figure 5.1.

### 5.3.2 Catalysts properties and characteristics

Table 5.1 summarizes the properties of the investigated catalysts. All materials maintained high surface areas, pore volumes and pore diameters from the parent aluminosilicate, with reduced values due to the partial deposition of metal nanoparticles (NP) on the support.

| Catalyst | Textural properties | | | Metal content[d] | | | NP size (nm)[e] | |
|---|---|---|---|---|---|---|---|---|
| | $S_{BET}$[a] | Pore Volume[b] | Pore diameter[c] | ICP (%) | EDX (%) | XPS (%) | TEM[f] | XRD[g] |
| Al-SBA-15 | 804 | 1.03 | 8.2 | - | - | - | - | - |
| Ni2%AlSBA | 614 | 1.01 | 7.5 | 1.84 | 1.63 | 1.79 | 32 | 42 |
| Ni5%AlSBA | 642 | 0.96 | 7.7 | 4.72 | 3.01 | 3.45 | 20 | 25 |
| Ni10%AlSBA | 642 | 1.00 | 7.4 | 9.32 | 4.57 | 5.05 | 29 | 40 |
| Pd2%AlSBA | 617 | 0.91 | 7.6 | 1.75 | 2.97 | 1.64 | 5 | 8 |
| Pt2%AlSBA | 600 | 0.98 | 7.3 | 1.76 | 1.20 | 1.35 | -[g] | 37 |
| Ru2%AlSBA | 520 | 0.71 | 6.7 | -[b] | 1.26 | 1.67 | -[g] | 17 |

[a]($m^2 \cdot g^{-1}$); [b]($mL \cdot g^{-1}$); [c](nm); [d](w/w); [e]Average nanoparticle size from TEM (averaging >50 NPs); [e]Averaged NPs size counting 50 nanoparticles from TEM images (excluding large aggregates); [f]Calculated using the Scherrer ecuation; [g]Not measured

**Table 5.1.** Textural properties, metal content and nanoparticle sizes of the various investigated supported metal nanoparticles in the depolymerization of rough lignin.

The deposition of nanoparticles was predominantly found to take place on the external surface of the support and not within the porous network as indicated by ICP and XPS results, in accordance to the little reduction of pore diameters and pore volumes observed even at large metal loadings (e.g. Ni10%AlSBA). These results were in good agreement with previous reports (Pineda et al. 2011, 2012). In any case, at larger metal loadings (5%, w/w, and above) a significant proportion of metal sites are believed to be embedded within the porous network as suggested by the remarkable differences in metal content detected by EDX and XPS (surface techniques) as compared by ICP (digestion of the actual catalyst). NPs sizes were worked out from TEM micrographs only for Ni catalysts and showed the expected trend of larger nanoparticles at higher metal loadings (Table 5.1). These results corroborated the findings of previous works (Pineda et al. 2011, 2012). NPs sizes were worked out from TEM micrographs as well as for XRD patterns (using the Scherrer equation) and showed, in general, a relative agreement between TEM and XRD data.

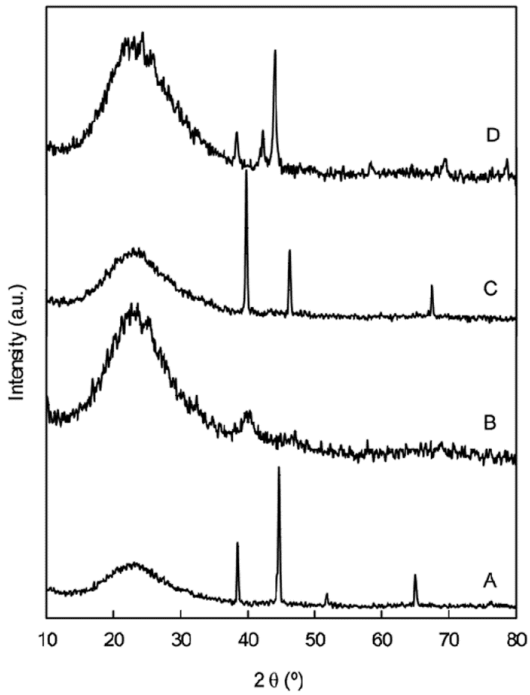


**Figure 5.2.** XRD patterns of 2% (w/w) materials; from bottom to top A) Ni2%AlSBA; B) Pd2%AlSBA; C) Pt2%AlSBA; D) Ru2%AlSBA.

Also some large aggregates could be observed in most materials, particularly those obtained for larger loadings (Ni10% AlSBA), indicating that these may be correlated to the existing differences of averaged NP sizes in TEM (for which aggregates were not accounted) and XRD patterns (which show average NP sizes of in principle all particles). All catalysts were found to contain metals in their reduced metal state as clearly shown in XRD patterns (Figure 5.2) and XPS data (Table 5.2) (Couto et al. 2007; Fang et al. 2011).

| **Catalyst** | **XPS main lines (eV)** **Metal** |
|---|---|
| Ni2%AlSBA | $Ni2p_{3/2}$ (853.6 eV)-$Ni^0$ |
| Ni5%AlSBA | $Ni2p_{3/2}$ (854.2 eV) -$Ni^0$ |
| Ni10%AlSBA | $Ni2p_{3/2}$ (854.0 eV) -$Ni^0$ |
| Pd2%AlSBA | $Pd3d_{3/2}$ (338.9 eV)-$Pd^0$ |
| Pt2%AlSBA | $Pt4f_{5/2}$ (74.8 eV)-$Pt^0$ |
| Ru2%AlSBA | $Ru3d_{3/2}$ (278.7 eV)-$Ru^0$ |

**Table 5.2.** XPS data of the prepared catalysts including the main lines for the different metal nanoparticles.

The supported metal nanoparticles were homogeneously dispersed and clearly visible as depicted in TEM micrographs in Figure 5.3 (A, B and C), although these were not very visible at low metal loadings (2%, w/w, Figure 5.3A). This even distribution was also maintained at higher metal loadings (Figure 5.3B for Ni10%AlSBA), although for these materials some larger aggregates (<100 nm) could be observed in some areas as shown in Figure 5.3C. In the case of Ni10%AlSBA, interesting cubical nanoparticle shapes were also found, which are yet to be investigated if these shapes and/or large particle sizes can influence the activity of the materials in lignin hydrogenolytic depolymerization. The mesoporous hexagonal channels of the parent Al-SBA-15

support were preserved in all cases regardless of the quantity and type of metal in the systems.

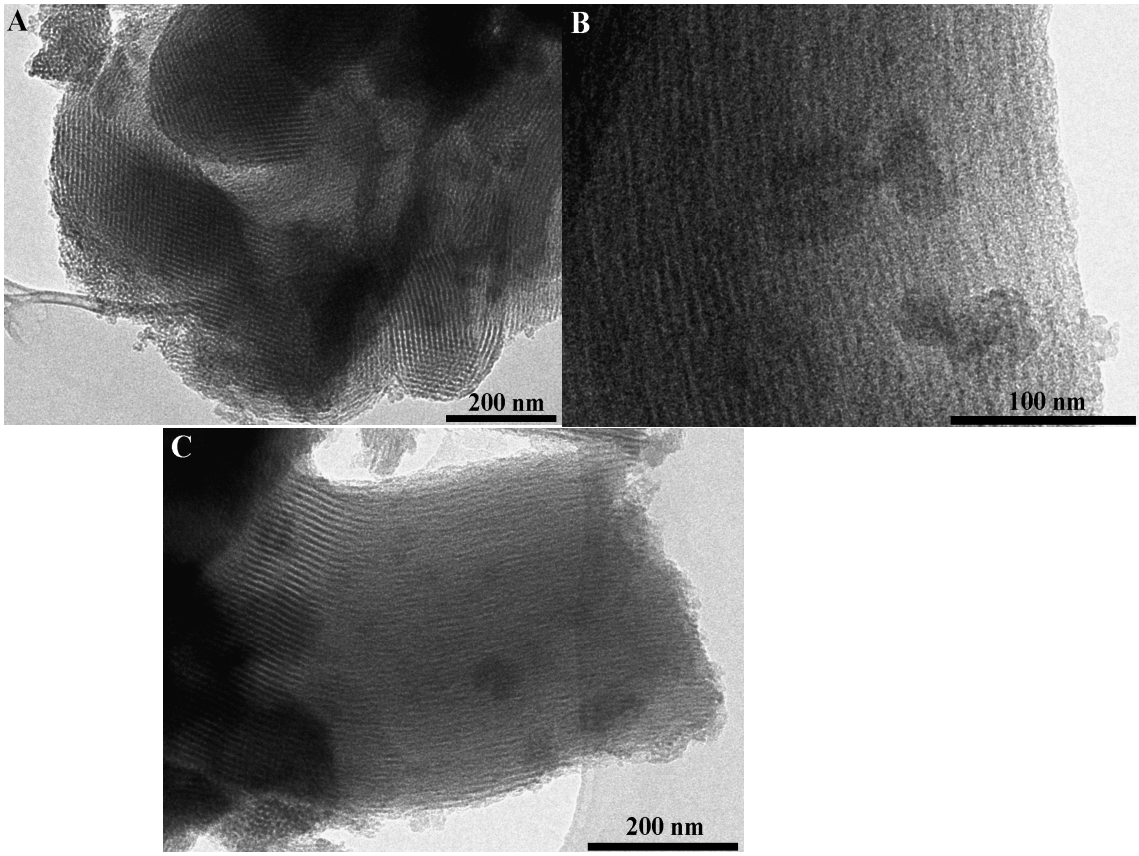


**Figure 5.3.** TEM micrographs of A) Ni2%AlSBA; B) Ni10%AlSBA (Ni nanoparticles can be spotted as little black dots) and C) Ni10%AlSBA showing some NP aggregates.

A catalyst screening of the supported metal nanoparticles catalysts was then carried out in the depolymerization of rough lignin from olive tree pruning. Three main fractions, apart from gaseous products that were not quantified in the systems, were obtained: oil enriched in phenolics, char and residual lignin. The obtained products (oil) and by-products (char and residual lignin) were analyzed in order to determine their composition and to find out the effect of the nature of the reduced metal catalysts employed on the phenolic monomeric and char yields as well as reaction conversion.

### 5.3.3 Effect on oil yield and composition

Phenolic compounds were recovered and isolated as oil in order to study the influence of the catalyst on their yield and composition. Figure 5.4 shows the oil yield referred to the initial lignin weight (%, (w/w)). All catalysts were found to provide improved results as compared to blank run oil, indicating the positive effect of the catalyst on lignin hydrogenolysis.

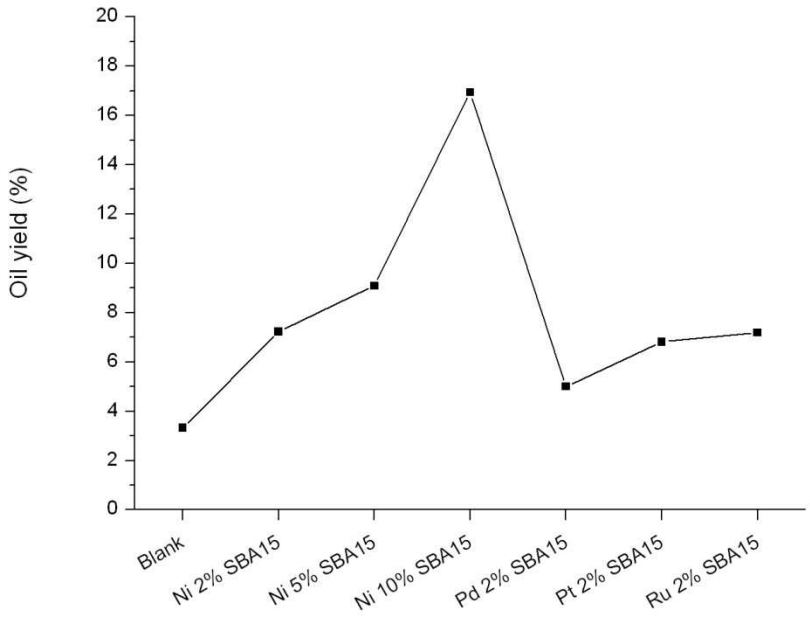


**Figure 5.4.** Obtained oil yields (%, w/w) referred to initial lignin weight for each catalyst.

However, interesting differences were observed depending on the supported metal. Nickel catalysts gave better yields as compared to the other metals results, in good agreement with recent reports (Sergeev et al. 2011; Li et al. 2012). The highest oil yield (17%) was obtained when Ni10%AlSBA was utilized as catalyst in lignin hydrogenolysis, its activity being remarkably higher than that of the other studied catalysts. Unexpectedly, palladium-based catalyst exhibited the lowest oil yield (5%, w/w) in spite of the remarkably smaller nanoparticle sizes (5-6 nm) obtained for this

material and its excellent hydrogenation properties. However, given the large differences observed in NP sizes as compared to other catalysts investigated in the reaction (5-6 vs. 35-40 nm), it can be hypothesized the presence of these larger NP sizes may be convenient for an improved interaction metal-lignin due to the bulky structure of lignin (with the possibility of the metal nanoparticles to target various hydrogenolytic neighboring sites of the complex lignin molecule). This multiple interaction will not be possible in catalysts containing small NPs sizes, thus leading to lower bio-oil production. Furthermore, the presence of such small Pd NPs within the pores of the aluminosilicate support (as opposed to those larger nanocrystallites which are undoubtedly deposited on the external surface of the catalyst) which could in principle make them less accessible to lignin (and thus giving low or no activity) cannot be ruled out. More evidences have to be found to prove the aforementioned hypothesis.

The oil was subsequently analyzed by GC-MS to determine the nature and concentration of the isolated simple phenolic monomers (Table 5.3, Figure 5.5). Apart from tetralin (1) as reaction solvent, diethyl phthalate (8) and butyl-octyl phthalate (10) ester were also found in the bio-oil. These products could have been formed from tetralin due to the reaction conditions used in this research (microwave assisted) as it was confirmed by the increase of diethyl phthalate concentration at low metal concentrations (2 wt. %, Table 5.3). However, the origin of phthalates was not clear since diethyl phthalate has also been previously reported to be obtained under biodegradation of lignin under anaerobic and sulfate reducing conditions (Ko et al. 2009). Deeper investigations about the origin of these products should be developed in order to clarify their origin. Taking into account only the phenolic products with lignin origin, the main simple monomeric products were mesitol in tetralin experiments including blank runs. Vanillin (7) origin could be associated to the release of guaiacyl intermediates. On the other hand, mesitol (2), 2,3.6-

trimethylphenol (3), 6-ethyl-o-cresol (4) and syringaldehyde (9) had their origin in the release of lignin syringyl units. Interestingly, the presence of 4-ethyl-m-cresol (5) and 3,4-dimethoxyphenol (6) could not be clearly understood. The absence of substituents in carbons adjacent to hydroxyl phenolic groups would suggest p-hydroxylbenzyl origin but the presence of a substituent in meta- position with respect to hydroxyl phenolic groups could not be totally explained.

| | **Blank** | **Ni 2% AlSBA** | **Ni 5% AlSBA** | **Ni 10% AlSBA** | **Pd 2% AlSBA** | **Pt 2% AlSBA** | **Ru 2% AlSBA** |
|---|---|---|---|---|---|---|---|
| Mesitol (2) | 0.56 | 2.26 | 1.19 | 1.13 | 0.49 | 1.67 | 1.40 |
| 2,3,6-trimethylphenol (3) | 0.19 | 0.76 | 0.22 | 0.28 | 0.18 | 0.17 | 0.45 |
| 6-ethyl-o-cresol (4) | 0.13 | 0.14 | 0.04 | - | - | 0.32 | 0.19 |
| 4-ehtyl-m-cresol (5) | - | 0.11 | 0.04 | - | - | 0.08 | - |
| 3,4-dimethoxyphenol (6) | 0.05 | 0.12 | 0.05 | 0.15 | 0.24 | 0.09 | 0.09 |
| Vanillin (7) | 0.20 | 0.20 | 0.19 | 0.20 | - | 0.13 | 0.11 |
| Diethylphthalate (8) | 2.34 | 10.10 | 1.67 | 1.69 | 10.93 | 10.66 | 7.44 |
| Syringaldehyde (9) | 0.47 | 0.68 | 0.57 | 0.56 | 0.15 | 0.43 | 0.43 |
| Butyl Octyl Ester phthalic acid (10) | 0.21 | 0.36 | 0.30 | 0.19 | 0.34 | 0.36 | 0.37 |

**Table 5.3.** Compounds present in the obtained oil in catalyst screening study. Compounds yields concentration in mg of each compound per gram of lignin.

The difference in quantities of products derived from guaiacyl units, syringyl units or p-hydroxyphenol units may be indicative of the proportions of each type of structure in the parent lignin (olive tree pruning origin). It may also evidence differences in the way in which these types of units are hydrogenolysed under the selected conditions. Pepper et al. (1969) stated that the higher prevalence of products with guaiacyl origin could be correlated to syringyl units undergoing demethoxylation reactions to form guaiacyl derivatives. Cresols derivates were present in low yields for all the studied catalysts, even disappearing for Ni10%AlSBA and Pd2%AlSBA. The largest

quantities obtained of diethyl phthalate were favoured at low metal concentrations (2% (w/w), Table 5.3). Syringaldehyde yield increased when using supported nickel NPs as catalyst, while Pd NPs gave the worst results in the hydrogenolysis (still improving the yields of the blank run). The principal reaction in the hydrogenolysis of lignins is the cleavage of ether linkages connecting the α–, β- and γ-carbon atoms of a side chain and the 4-position of a phenolic ring in an adjacent unit. Depending on the reaction conditions, carbon-carbon linkages may also be ruptured during hydrogenolysis especially at sites α-β and β-γ (Sakakibara 1992).

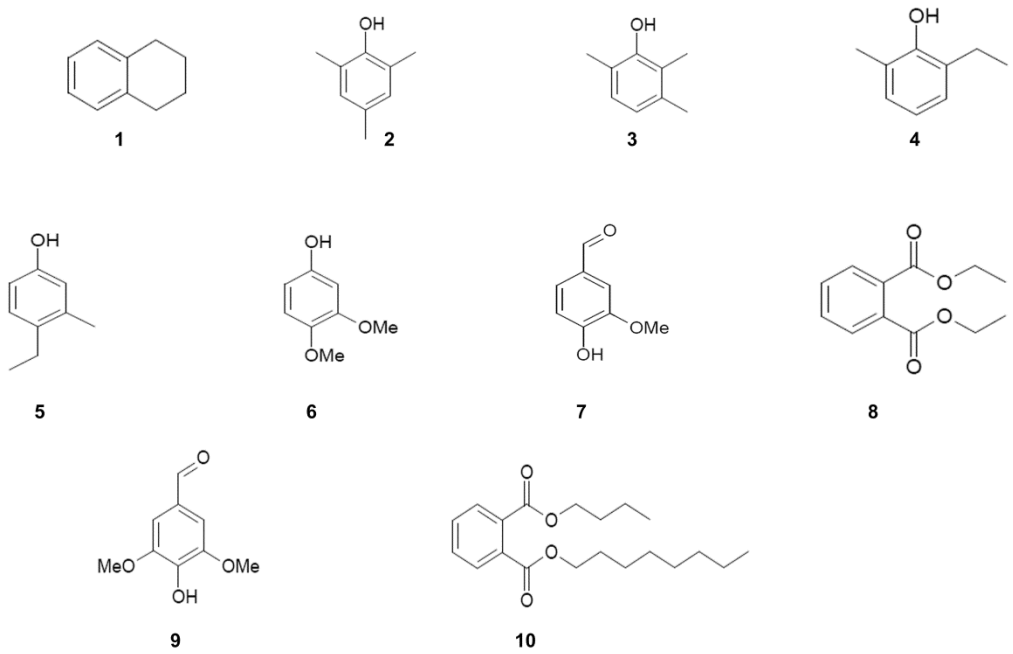


**Figure 5.5.** Compounds found in isolated oils. (1) Tetralin (solvent) (2) Mesitol (3) 2,3,6-trimethylphenol (4) 6-ethyl-o-cresol (5) 4-ethyl-m-cresol (6) 3,4-dimethoxyphenol (7) Vanillin (8) Diethyl phthalate (9) Syringaldehyde (10) Butyl Octyl Ester Phthalate.

Compounds 2, 5, 6, 7 and 9 are likely to arise from such carbon-carbon cleavage reactions (dealkylation and/or deacylation-related reactions) which take place preferentially on the acid sites of the aluminosilicate material (Binder et al. 2009; Roberts et al. 2010a, 2010b, 2011). Comparatively, the structure of compounds 3 and 4 suggested that these underwent further demethoxylation reactions (where the

carbon-carbon cleavage of 4 ring position and α-alkyl chain may occur). Hydrogenation reactions in the metal sites can be in principle responsible for the lost of methoxy groups (above all in positions 2 and 6 of the aromatic phenolic ring) and the presence of methyl groups in the structures. Structures 2, 3, 4 and 5 did not possess methoxy groups but methyl groups, this transformation could be due to radical reactions.

Most importantly, the profile of monomeric products was found to be different from other studies results (Meier et al. 1992; Thring et. al 1996; Torr et al. 2011), and only relatively similar to those recently reported by Li et al. (2012). The difference may be associated to the use of rapid and homogeneous heating achieved under microwave irradiation, which is able to accelerate and favor the rates of reaction and influence selectivity to products in reactions catalyzed by supported metal nanoparticles as it has been previously demonstrated (Balu et al. 2012). NPs sizes might also influence yields to simple aromatics as well as oil yields by means of an improved interaction metal-lignin for highly accessible and relatively large (30-40 nm) metal nanoparticles obtained under mechanochemical ball milling conditions on the external surface of the aluminosilicate supports (Pineda et al. 2011; 2012).

MALDI-TOF oil analyses to determine the molecular weight of the compounds present in the oil were carried out as GC-MS could only detect low molecular weight and relatively low boiling point compounds. Results are depicted in Figure 5.6. Considering that a prototype lignin subunit e.g. phenylpropane syringol has a molecular weight of 197 g/mol and a phenylpropane guaiacol unit is about 166 g/mol, results from Figure 5.6 clearly demonstrate that most of the obtained products were primarily dimers and also monomers. In addition, these analyses provided insights into the degree of lignin depolymerization.

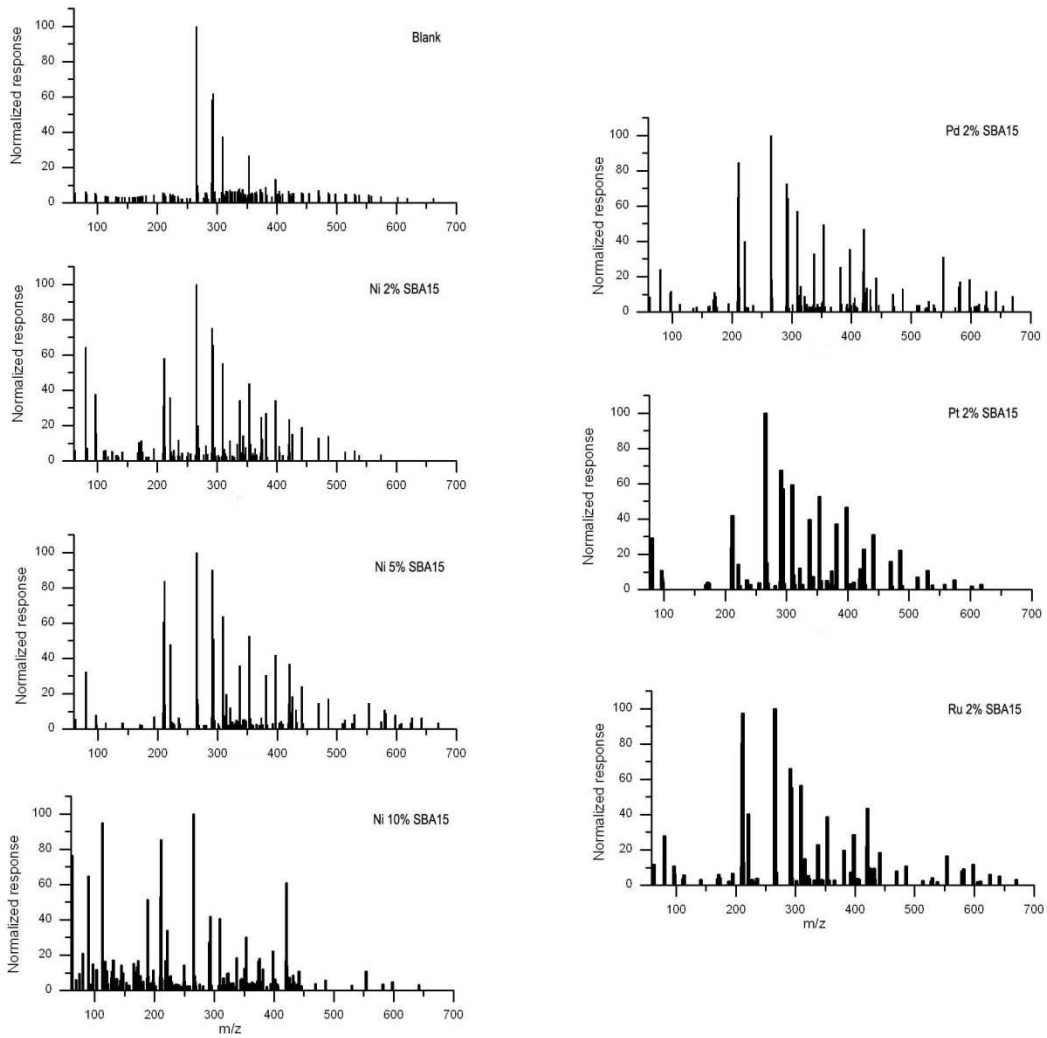


**Figure 5.6.** MALDI-TOF oil analyses of all catalysts in the depolymerization of lignin.

The blank profile was remarkably different from the catalysts samples. Weak signals were mostly observed for the blank run (reference) indicating a low extent of lignin depolymerization. As expected, all catalysts exhibited more intense signals to those of the blank which confirmed that the addition of a metal supported catalyst enhanced lignin depolymerization by hydrogenolysis under the investigated mild reaction conditions. Interestingly, significant differences between catalysts can also be clearly noticed. Except for Ni10%AlSBA, MALDI-TOF analyses revealed that the abundance of monomers was generally very low, dimers were more abundant in all cases and trimers could also be detected. In the case of Ni5%AlSBA, Pd2%AlSBA and

Ru2%AlSBA, the presence of trimers was more significant in the obtained oil. Ni10%AlSBA exhibited the most desirable MALDI-TOF profile as signals that corresponded to monomeric compounds were more intense and abundant compared to those of other investigated catalysts.

### 5.3.4 Effect on char formation

Char yields have been depicted in Figure 5.7. In general, the addition of catalysts in the systems did not significantly reduce char quantities produced.

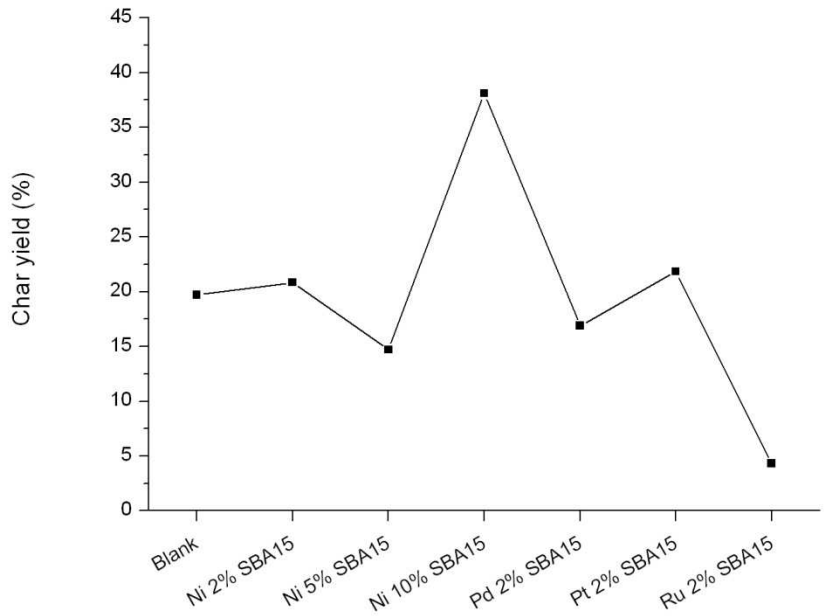


**Figure 5.7.** Obtained char yields (%, w/w) referred to initial lignin weight for each catalyst.

Such yields were high for all studied catalysts, reaching the maximum char production for Ni10%AlSBA (38% (w/w)), which is likely due to its high metal content. Supported ruthenium gave the minimum char yield (4% (w/w)). Char formation from lignin under mild reaction conditions is a consequence of the cleavage of labile lignin bonds such as alkyl-aryl ether linkages and the resulting formation of

more resistant condensed structures (Domburg et al. 1982). Microwave irradiation may have generated unstable fragments and/or radicals that could not be quenched in the hydrogen transfer reaction by tetralin, reacting between each other and forming complex structures, which generate high quantities of char for catalysts with high metal loadings (with the exception of Ni5%AlSBA). Char was not recovered for further analyses.

### 5.3.5 Effect on residual lignin

In Figure 5.8, the results of residual lignin yields in the microwave-assisted hydrogenolysis reactions are shown. It is readily apparent that the content of residual lignin was high for all employed catalysts. However, the addition of supported metal nanoparticles as catalyst had a positive effect on lignin hydrogenolytic depolymerization. Ruthenium catalyst residual lignin content was the highest, taking into account only the experiments where a catalyst was added to the reaction. The best residual lignin content was obtained for Ni10%AlSBA, at the expense of its very high char production. It is worth noting that the concept of residual lignin does not relate to conversion concept, which in turn means that a low residual lignin is not necessary associated with a high concentration of phenolic monomers since in the depolymerization reaction another product (undesirable) was also produced, char. Residual lignin decreased along with the increase of char for most of the runs. At this point, it was clear that the mass balance was not completed. The difference to 100 observed taking into account Figure 5.4, 5.7 and 5.8 corresponded to gaseous products (Meier et al. 1992). The yield of gases produced from the thermolysis of a kraft lignin in tetralin at hydrocracking temperatures has been reported by Connors et al. (1980) to depend strongly on the treatment severity. The gaseous products generated in this work were not recovered for further identification or quantification.

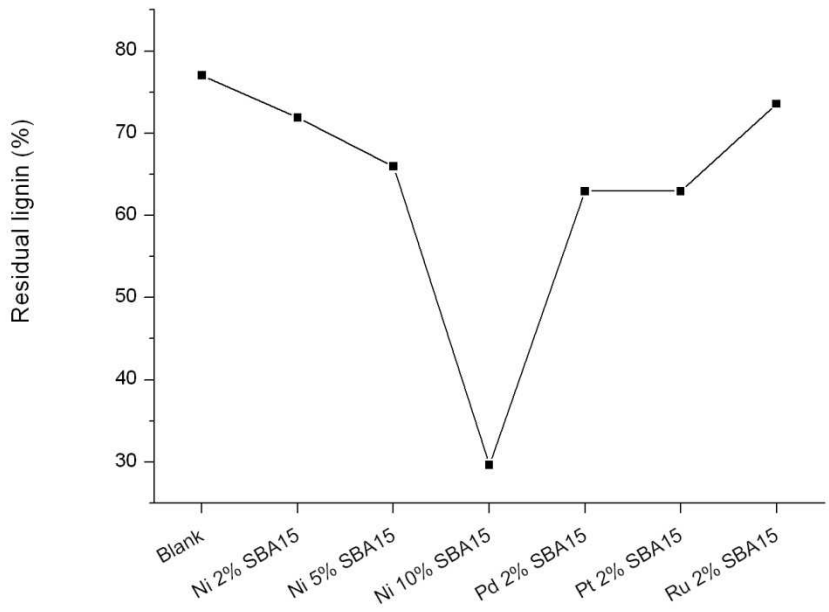


**Figure 5.8.** Residual lignin (%, w/w) referred to initial lignin weight for each catalyst.

Residual lignins were subjected to high performance size exclusion chromatography in order to evaluate lignin behavior during depolymerization (Figure 5.9 and Table 5.4). In all cases, two peaks were observed, a peak related to the unconverted lignin and another peak (and a shoulder) corresponding to lower molecular weight lignins as a result of depolymerization. The right graphic (Figure 5.9), representing palladium, platinum and ruthenium catalysts, showed the peak corresponding to unconverted lignin appeared at shorter times to that of rough lignin, suggesting that repolymerization had taken place. As in the char case, microwave irradiation could have originated high radicals or unstable fragments (that could not be quenched under the reaction conditions) which reacted with the parent lignin structure. In fact, other authors have proposed the use of additional capping agents (e.g. boric acid) to minimize condensation of initially formed products under base-catalyzed lignin processing (Roberts et al. 2010a). The blank experiment confirmed the repolymerization trend that lignin shows when trying to depolymerize it and in Table 5.4, it could be observed that the nature of the supported metal affected strongly the

occurrence of this phenomena. Nickel catalysts comparably seemed to minimize repolymerization phenomena as indicated by the presence of the unconverted lignin peak in the residual lignins at the same retention time to that of rough lignin. In particular, the peak corresponding to unconverted lignin from Ni10%AlSBA appeared at longer retention times, which points to a suppression of repolymerization reactions together with the large extension of degree of depolymerization obtained in this case. The nature and strength of the acid sites in the Al-SBA-15 support (required for dealkylation and/or deacylation-related reactions in lignin depolymerization) were also carefully controlled to avoid secondary lignin self-condensation undesirable reactions (Binder et al. 2009; Roberts et al. 2011).

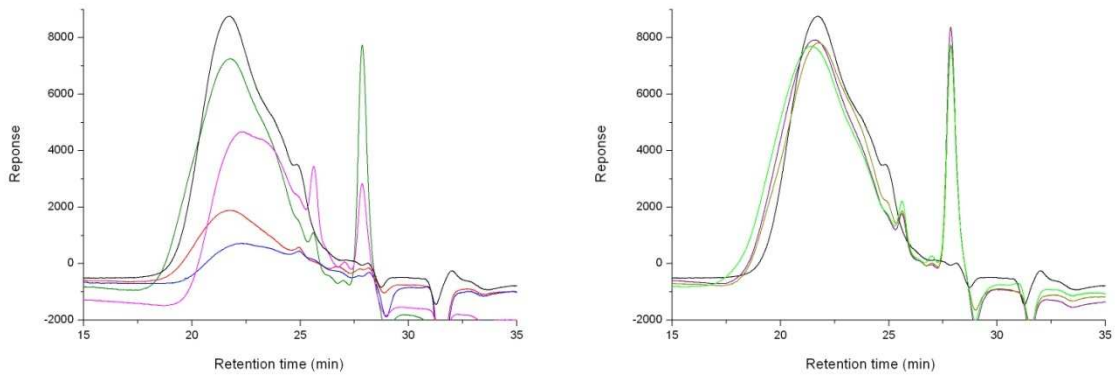


**Figure 5.9.** Residual lignin HPSEC results for each catalyst. Left graphic: black (rough lignin), red (blank), blue (Ni2% SBA15), olive green (Ni5%AlSBA) and magenta (Ni10% AlSBA). Right graphic: black (rough lignin), purple (Pd2%AlSBA), dark yellow (Pt2%AlSBA) and light green (Ru2%AlSBA).

Average-weight molecular weights of nickel 2% and 10% were the only ones that decreased compared to crude lignin molecular weight. This fact suggested a high depolymerization degree for these two catalysts. In these experiments, polydispersity index (Mw/Mn) also decreased referred to crude lignin, which is the normal trend in polymer degradation.

| | Mw | Mn | Mw/Mn |
|---|---|---|---|
| Rough lignin | 7232 | 2125 | 3.40 |
| Blank | 8549 | 2227 | 3.84 |
| Ni 2% AlSBA | 5043 | 1828 | 2.76 |
| Ni 5% AlSBA | 9663 | 1871 | 5.16 |
| Ni 10% AlSBA | 3984 | 1231 | 3.24 |
| Pd 2% AlSBA | 10674 | 2002 | 5.33 |
| Pt 2% AlSBA | 9806 | 1811 | 5.42 |
| Ru 2% AlSBA | 14396 | 2178 | 6.61 |

**Table 5.4.** Residual lignins number-average (Mn), weight-average (Mw) molecular weight and polydispersity (Mw/Mn) of residual lignin of screening catalyst study. Rough lignin was also characterized for comparative purposes

These findings were in good agreement with MALDI-TOF analyses as well as with our hypotheses of the improved interaction metal-lignin as Ni2% and Ni10%AlSBA materials exhibited in principle the largest NPs sizes (together with Pt). Comparatively, Pd, Pt and Ru favored repolymerization phenomena yielding residual lignins with higher molecular weights to those of the parent crude lignin. Their polydispersity index increased (rather than decreasing), proving the poor effect on lignin depolymerization by hydrogenolysis using such novel metal as catalysts. Last and most importantly, our results also correlate well with those recently reported by Li et al. (2012) which pointed out the outperforming hydrogenolytic properties of Ni as compared to noble metal catalysts in lignocellulosic valorization.

The elemental analyses of the residual lignins were carried out in order to establish a carbon balance between rough lignin and residual lignins. The objective was to evaluate changes in carbon content. (Figure 5.10). The percentages of carbon in residual lignin of experiments with Ni5%AlSBA, Pd2%AlSBA, Pt2%AlSBA and Ru2%AlSBA increased as compared to the blank run without catalyst, indicating low

lignin degradation. In addition, this growth will also confirm the repolymerization phenomena that occurred during lignin hydrogenolysis.

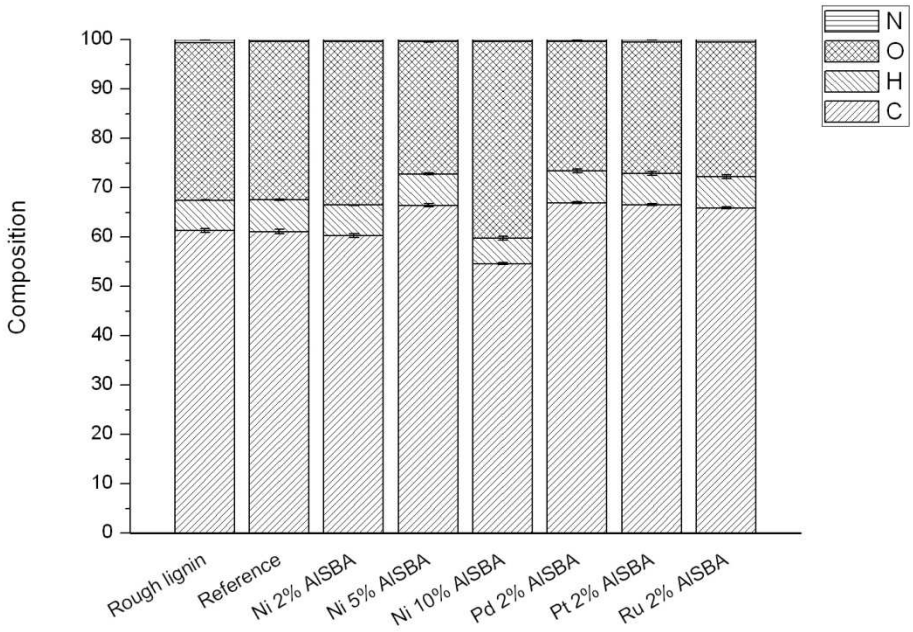


**Figure 5.10.** Elemental analyses of recovered residual lignins for each catalyst.

The elemental analysis of the residual lignin obtained in the reaction using Ni10%AlSBA revealed that this experiment reached the highest depolymerization degree, indicated by the decrease in carbon percentage and the increase in the oxygen percentage. These findings were also in good agreement with HPSEC and MALDI-TOF analyses which pointed out Ni10%AlSBA as optimum depolymerization catalyst.

### 5.3.6 Conclusions

Rough organosolv olive tree pruning lignin was subjected to a heterogeneously catalyzed mild hydrogenolytic depolymerization approach assisted by microwave irradiation. A range of designer bifunctional catalysts featuring a combination of

metal nanoparticles (Ni, Ru, Pd and Pt) supported on an acidic aluminosilicate (Al-SBA-15) were proved to provide access to simple phenolic products including diethyl phthalate, mesitol and syringaldehyde. The nature and composition of the phenolic compounds was found to be influenced by the microwave irradiation which changed the profile of expected obtained compounds. Ni10%AlSBA provided the optimum degree of lignin depolymerization among all catalysts, which in general possess high char yields and residual lignin contents. Repolymerization phenomena took place in most cases except for Ni-based catalysts, decreasing the production of phenolic monomer compounds.

These results suggested that the proposed mild lignin hydrogenolysis approach could be improved. In any case, the reported protocol is remarkably simple and environmentally sound as compared to most lignin valorization approaches to date as it avoids the use of molecular hydrogen (thus minimizing risks of explosions, leaks and related hazards), high-pressure devices and was carried out at mild reaction conditions (temperatures and times of reaction) that normally lead to improve selectivity to target compounds.

## 5.4 Effect of hydrogen-donor solvent on lignin hydrogenolytic depolymerization

Both the process and the type of catalysts utilized for lignin hydrogenolysis are generally not well approached from a rational viewpoint based on fundamental understanding. All reported protocols to date have an appalling hydrogen economy (high pressures and large quantities of molecular hydrogen as well as high

temperatures) and poorly understood catalytic systems which eventually lead to poorly controllable methodologies that provide large quantities of fully hydrogenated rings of low industrial value. Molecular hydrogen has also high diffusivity (being highly flammable) and entails considerable hazards when employed at a large scale. Catalytic transfer hydrogenation processes, in which hydrogen is transferred from a hydrogen donor molecule to an acceptor, is a comparably interesting alternative to hydrogenate organic compounds, with substantial advantages compared to processes employing molecular hydrogen (Gandarias et al. 2011). Upon dehydrogenation/decomposition, hydrogen-donating solvents readily generate in-situ hydrogen atoms which can subsequently promote hydrogenation reactions.

This approach, based on fundamental understanding of the systems, entailed the design of highly accessible and sufficiently large supported nanoparticle systems (able to provide several interaction points with the bulky lignin structure) as part of a microwave-asissted mild hydrogenolitic hydrogen-free protocol which takes advantage of the hydrogen-donating properties of certain solvents for an in-situ efficient hydrogen generation under very mild conditions. The hydrogen-donating effect of organic compounds (i.e. tetralin) in the hydrocracking of kraft lignin was described by Connors et al. (1980). Many attempts have also been conducted using formic acid in different lignin systems (Kleinert et al. 2009; Pandey et al. 2011; Liguori et al. 2011). Recently, a novel solvolysis method has been proposed involving thermal treatment of lignin in a high pressure reactor with formic acid as active hydrogen donor and ethanol as solvent (Kleinert et al. 2008). Upon heating, formic acid decomposed completely into $CO_2$ and active hydrogen, which combined with oxygen from the methoxy groups of lignin to form water. Since both depolymerization and hydrodeoxygenation occur simultaneously, such a solvolysis reaction can result in monomers with low oxygen contents in a single step (Pandey et al. 2011). Other authors have also successfully utilized glycerol as green solvent and

hydrogen donor in catalytic transfer hydrogenation-dehydrogenation reactions (Wolfson et al. 2009). Glycerol-derived hydrogen to hydrogenate various unsaturated organic compounds under mild reaction conditions allowed a facile separation of products and catalyst recycling. Isopropanol has also been widely utilized in hydrogenation reactions as hydrogen-donor solvent as originally highlighted by Johnstone et al. (1985) as well as by recent reports (Gracia et al. 2009).

### 5.4.1 Materials and methods

In order to find the best reaction system for lignin hydronolytic depolymerization, different hydrogen-donor solvents were studied, namely, tetralin, isopropanol, glycerol and formic acid. Blank experiments (without catalysts) were carried out for each solvent. The microwave method was generally temperature controlled, where certain microwave power was applied in order to heat the reaction mixture to a set average temperature of 150 ºC. The applied power was determined taking into account the microwave temperature limit (200 ºC) and the solvent loss tangent (tan θ) of each hydrogen-donor solvent. The final reaction mixture was subsequently filtered to separate solids. Afterwards, solids were solubilized in tetrahydrofuran (THF) and then filtered. The non-soluble solids were found to be char and the catalyst, while the residual lignin was soluble in THF. The liquid was extracted with sodium hydroxide, and then subsequently acidified. The acidic solution was extracted with ethyl acetate in order to isolate the phenolic compounds produced during lignin depolymerization. Ethyl acetate was evaporated to obtain the phenolic oil. The separation procedure of the final reaction mixture was adapted for each solvent based on the same principles. The yield of every product was calculated gravimetrically referring to the initial lignin. Other aspects of the reaction conditions, catalyst preparation, products separation procedure and products analyses have been already described in section 5.2. The results are presented below.

### 5.4.2 Effect on oil yield and composition

Phenolic compounds were recovered and isolated as oil in order to study the influence of the employed hydrogen source. Figure 5.11 shows oil yields referred to initial lignin weight (%, wt). As it can be observed, most catalyst experiments provided improved results to those of their respective blank runs in terms of oil yield, which indicated a positive catalyst action on lignin hydrogenolysis. Interestingly, this was not the case for the use of isopropanol as hydrogen-donating solvent in the systems. The blank isopropanol run gave a significantly larger oil yield as compared to the experiment in the presence of Ni10%AlSBA15. These unexpected findings may be related to the dehydrogenation of isopropanol to acetone, which can compete with the active sites (e.g. acid sites of the support) of the Ni10%AlSBA15 catalyst, thus reducing its effectiveness in hydrogenolysis.

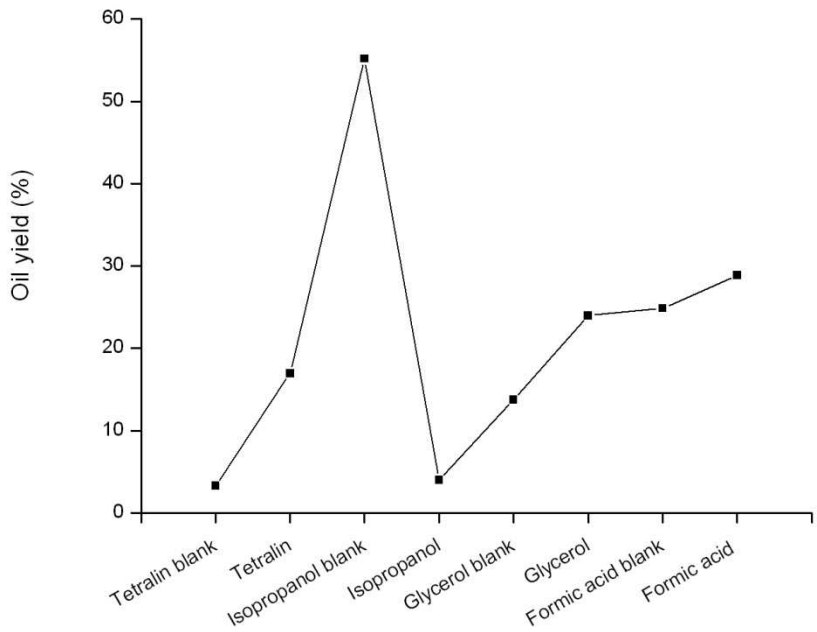


**Figure 5.11.** Obtained oil yields (%, w/w) referred to lignin weight for each hydrogen-donor solvent.

A minimum char production was observed for the isopropanol blank run, which is also worth noting. In any case, a comparison of hydrogen-donating solvents, clearly leaves formic acid as best solvent which produces high oil yields together with a negligible char production (as it decomposes into $CO_2$ and $H_2$), followed by glycerol and tetralin.

The oil was subsequently analyzed by GC-MS in order to determine the nature and concentration of the isolated phenolic monomeric compounds (Table 5.5, Figure 5.12). It was readily apparent that the nature of phenolic products remarkably changed depending on the solvent used in the lignin hydrogenolytic reaction systems. Among all the obtained simple phenolic compounds in each system, only three compounds (syringol, vanillin and syringaldehyde) were produced in all experiments so they can be compared in order to establish relationships and behaviors associated to the different hydrogen sources employed. Syringol was readily obtained when formic acid was used as solvent, with the lowest production obtained for isopropanol. Vanillin was found in similar concentrations regardless of the utilized solvent. Syringaldehyde showed a comparable trend to syringol, increasing its yield in the case of using formic acid as solvent. It should be noticed that vanillin, which presented different trend than syringol and syringaldehyde, comes from the cleavage and transformation of a guaiacyl lignin subunit whereas, obviously, syringaldehyde and syringol derived from syringyl lignin subunit. The compounds origin is going to be discussed later on.

With regards to the range of products depending on solvents, the use of tetralin gave phthalates and mesitol as main products (Figure 5.12, compounds 2 and 8) as compared to desaspidinol and aspidinol obtained when using formic acid (Figure 5.12, compounds 12, 13).

| Compound | $R_t$ (min) | TL blank | TL | IP blank | IP | GLY blank | GLY | FA blank | FA |
|---|---|---|---|---|---|---|---|---|---|
| Guaiacol (1) | 7.44 | - | - | - | - | - | - | 0.27 | 0.31 |
| Mesitol (2) | 9.68 | 0.56 | 1.12 | - | - | - | - | - | - |
| 2,3,6-trimethoxyphenol (3) | 10.43 | 0.19 | 0.28 | - | - | - | - | - | - |
| Syringol (4) | 14.01 | 0.05 | 0.15 | 0.05 | - | 0.08 | 0.11 | 0.50 | 1.02 |
| Vanillin (5) | 15.18 | 0.20 | 0.20 | 0.17 | 0.15 | 0.24 | 0.27 | 0.24 | 0.22 |
| Guaiacylacetone (6) | 17.70 | - | - | - | - | - | - | 0.14 | 0.31 |
| 4-hydroxyacetyl-2-methoxyphenol (7) | 18.60 | - | - | - | - | - | - | 0.38 | 0.07 |
| Diethylphthalate (8) | 18.67 | 2.34 | 1.69 | - | - | - | - | - | - |
| Methoxyeugenol (9) | 18.79 | - | - | - | 0.13 | - | - | - | - |
| Syringaldehyde (10) | 19.60 | 0.47 | 0.55 | 0.36 | 0.55 | 0.42 | 0.48 | 1.35 | 0.93 |
| Acetosyringone (11) | 20.54 | - | | - | - | - | 0.03 | 0.08 | 0.11 |
| Desaspidinol (12) | 21.00 | - | - | - | - | - | - | 1.77 | 2.94 |
| Aspidinol (13) | 21.66 | - | - | - | - | - | - | 1.23 | 0.27 |
| Butyl Octyl Ester phthalic acid (14) | 22.07 | 0.21 | 0.19 | - | - | - | - | - | - |
| G derivatives (1, 5, 6, 7, 8, 14) | | 0.20 | 0.20 | 0.17 | 0.15 | 0.24 | 0.27 | 1.03 | 0.91 |
| S derivatives (2, 4, 9, 10, 11, 12, 13) | | 1.08 | 1.82 | 0.41 | 0.68 | 0.50 | 0.63 | 4.93 | 5.00 |

**Table 5.5.** Compounds present in the obtained oil for each hydrogen-donor solvent. Compounds yields concentration in mg of each compound per gram of lignin. TL (tetralin), IP (isopropanol), GLY (glycerol) and FA (formic acid)

Unfortunately, the main products of tetralin were phthalates (8, 14) that came from subsequent reaction of tetralin under the applied conditions and not from lignin. This fact strongly affected the monomeric compounds concentration derived from lignin since tetralin instead of helping hydrogenolytic lignin depolymerization, suffered degradation reactions losing its hydrogen transfer properties. The use of formic acid as solvent not only provided the optimum oil yields (with the exception of the blank isopropanol run) but also yielded the widest variety of phenolic monomeric products.

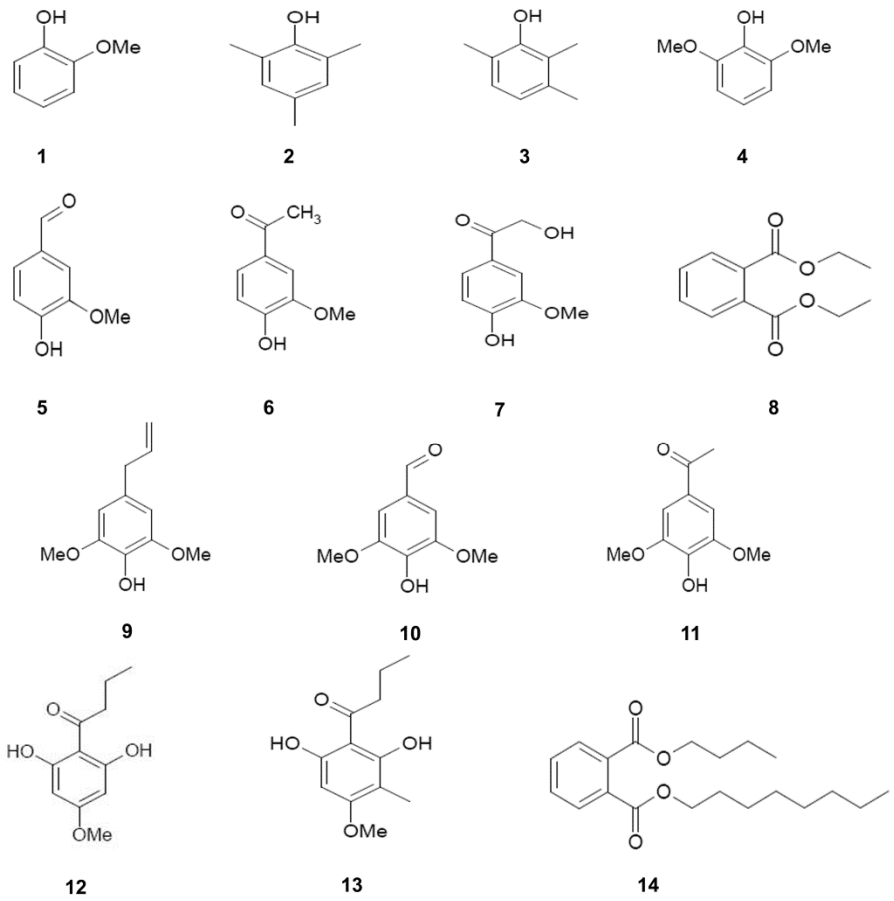


**Figure 5.12.** Compounds found in isolated oils. (1) Guaiacol (2) Mesitol (3) 2,3,6-trimethylphenol (4) Syringol (5) Vanillin (6) Guaiacylacetone (7) 2,4'-dihydroxy-3'-methoxyacetophenone (8) Diethylphthalate (9) Methoxyeugenol (10) Syringaldehyde (11) Acetosyringone (12) Desaspidinol (13) Aspidinol (14) Butyl Octyl Ester Phthalate.

Comparably, isopropanol and glycerol solvents produced low phenolic compounds variety. The differences in nature of the phenolic compounds between solvents is likely to be associated to the quantities and way of in-situ hydrogen released in each system (e.g. dehydrogenation, decomposition, etc.) under the investigated mild conditions as well as to the interaction of the respective products (upon solvent dehydrogenation) in the lignin depolymerization mechanism. In particular, the plausible formation of acetone upon isopropanol dehydrogenation can interfere in the hydrogenolytic process (especially interacting with the acid sites of the support which could lead to side reactions) as compared to a more efficient decomposition of formic

acid into $CO_2$ and $H_2$. In fact, tetralin dehydrogenation to naphthalene (4) and glycerol to dihydroxyacetone (8) seemed to have particularly remarkable different synergetic/interference effects on lignin depolymerization and char production as discussed in subsequent sections.

As mentioned before, the principal reaction in the hydrogenolysis of lignin is the cleavage of ether linkages connecting α, β and γ carbon atoms of a side chain and the 4-position of a phenolic ring in an adjacent unit. Depending on reaction conditions, carbon-carbon linkages may also be disrupted during hydrogenolysis especially at α-β and β-γ sites (Sakakibara 1992). Compounds 1, 2, 3 and 4 seemed to have been generated from such ether linkage bond cleavage, followed by carbon-carbon breakdown reactions (carbon-carbon cleavage of 4 ring position and α-alkyl chain may occur). Hydrogenation reactions can be accounted to be responsible for the disappearance of methoxy groups in compounds 2 and 3 (particularly in positions 2 and 6 of the aromatic phenolic ring) which lead to methyl groups. These transformations could also be due to radical reactions caused by microwave irradiation. Compounds 5, 6, 7, 10, 11 and 12 exhibited a carbonyl group in α-position (ketone or aldehyde) that could have its origin in further reactions of the intermediates formed during the ether linkage cleavage between an aliphatic carbon and the oxygen from the ether bond (generally in 4-position). Demethoxylation reactions could also lead to methanol formation that could be involved in other side reactions which may compete with lignin depolymerization or not depending on the solvent and/or system utilized in the process. These active released molecules could be the reason of the singular obtained products.

Compounds present in the obtained oils are the results of lignin interunit cleavage. Taking into account that the main lignin units are p-hydroxyphenyl alcohol (H),

guaiacyl alcohol (G) and syringyl alcohol (S), the origin of the monomeric products can be proposed. Thus, compounds 1, 5, 6 and 7 can be proposed to have a syringyl origin whereas compounds 2, 4, 9, 10, 11, 12 and 13 could be associated to be released from guaiacyl subunits. Pepper et al. (1963) stated that the higher prevalence of products with guaiacyl origin could be explained given the fact that syringyl units could undergo demethoxylation reactions to form guaiacyl derivatives (Pepper et al. 1963). In Table 5.5 it can be observed the concentrations and ratios of syringyl (S) and guaiacyl (G) derivatives for each solvent system. A transition to larger quantities of syringyl (S) was observed for all solvents employed which reached a maximum in the use of formic acid (5:1 syringyl to guaiacyl derivatives concentration ratio). These findings would suggest that typical demethoxylation reactions of syringilic intermediates do not take place when these solvent are used as hydrogen-donating solvent.

Interestingly, the profile of monomeric products was also found to be different from previous studies (Meier et al. 1992; Thring et al. 1996; Torr et al. 2011). As explained before, the origin of some of the obtained products was not very clear and could be hardly related to lignin degradation. However, these different results can be associated to the significantly different approach (heterogeneous catalysis, hydrogen donating solvents) as well as to the use of microwaves. Probably, this radiation could have promoted the release of active molecules. In principle, all solvents have varying natures with differing polarities and therefore different loss tangents, which lead to different interactions with microwave irradiation as well as different ways in the in-situ generation of hydrogen in the systems. These findings joined with the fact that each solvent is affected in a different way by the microwave irradiation should explain the different obtained phenolic monomeric products from lignin hydrogenolysis depolymerization. Since this is the first time that lignin hydrogenolytic depolymerization was developed in a microwave reaction system, no comparable

results in literature were found. In addition, the different mechanisms of each hydrogen-donor solvent used could also be responsible of this fact.

MALDI-TOF analyses of the oils have been depicted in Figure 5.13. These analyses were carried out with the purpose of evaluating molecular weight distribution of compounds present in the oil as GC-MS can only detect low boiling temperature compounds.

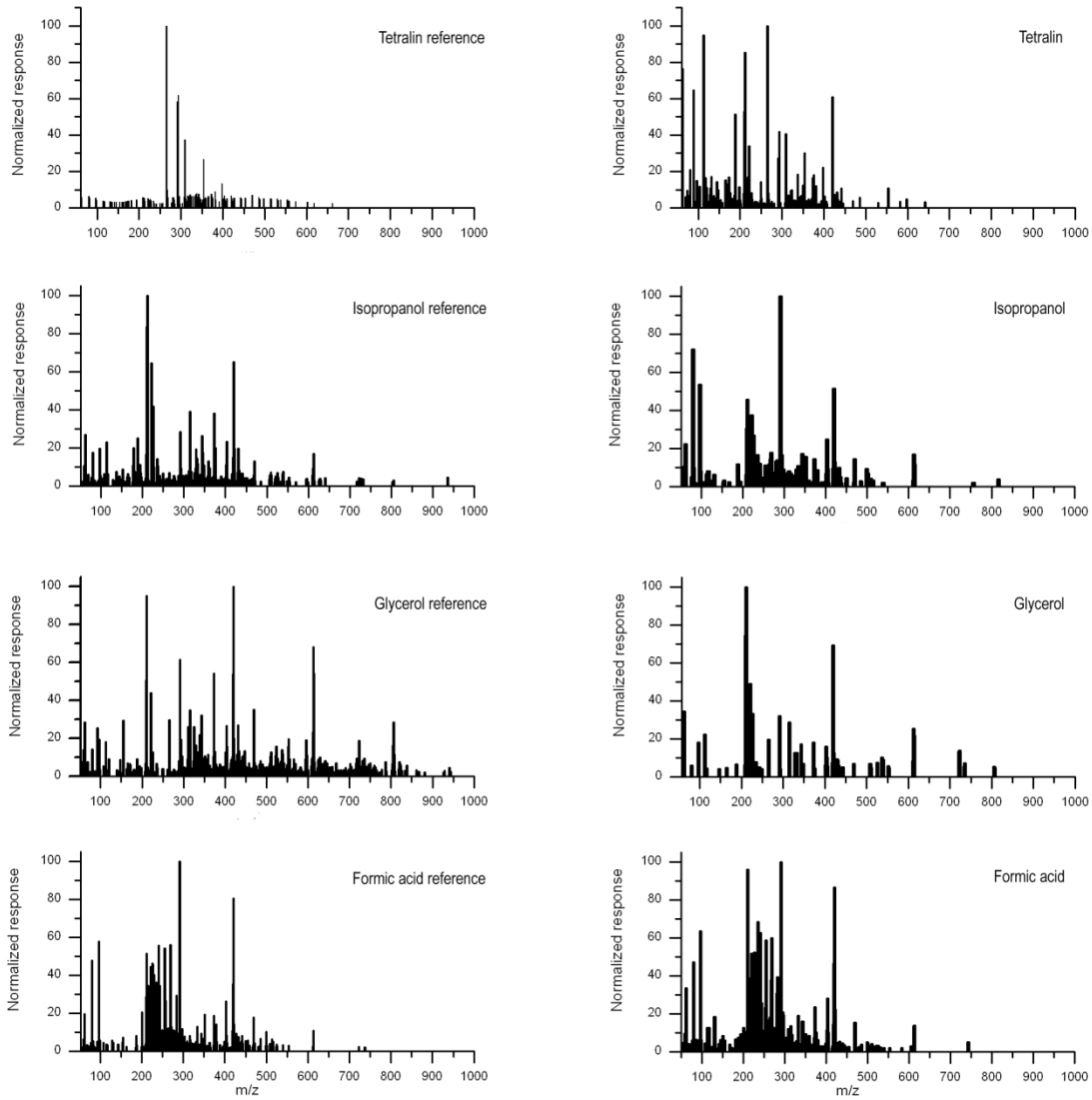


**Figure 5.13.** MALDI-TOF oil analyses of each hydrogen-donor solvent experiment.

Considering that a prototype lignin sub-unit (e.g. phenylpropane syringol unit) has a molecular weight around 150-200 g/mol, Figure 5.13 clearly demonstrates the majority of the obtained products in our proposed lignin depolymerization approach mainly correspond to monomers and dimers. These analyses were also useful to provide insights into the degree of lignin depolymerization. The use of Ni10%AlSBA15 as catalyst contributed positively to depolymerize lignin in the cases of tetralin and formic acid as hydrogen donating solvents. Comparably, the use of isopropanol and glycerol as hydrogen donating solvents combined with the Ni heterogeneous catalyst did not provide any appreciable degree of lignin depolymerization. In the range around 500-1000 g/mol, some signals could be detected that corresponded to trimers or oligomers. These signals were more intense, above all, in the case of the blank runs for glycerol and isopropanol, respectively. These two solvents were also those exhibiting the lowest content of phenolic monomeric compounds, which further confirms the poor lignin degree of depolymerization achieved in these systems even in the presence of an active Ni depolymerization catalyst.

### 5.4.3 Effect on char formation

Char is also produced as by-product in lignin depolymerization. Char yields showed in Figure 5.14 confirmed that the addition of Ni10%AlSBA15 increased the formation of carbonaceous deposits for studied systems, with the exception of the use of formic acid. Domburg et al. (1982) have noted that char formation from lignin under mild reaction conditions is a consequence of the cleavage of labile lignin bonds such as alkyl-aryl ether linkages and the resulting formation of more resistant condensed structures. Microwave irradiation could have possibly facilitated the formation of high radicals or unstable fragments that could not be saturated with hydrogen generated by the solvents, reacting between each other and forming complex structures.

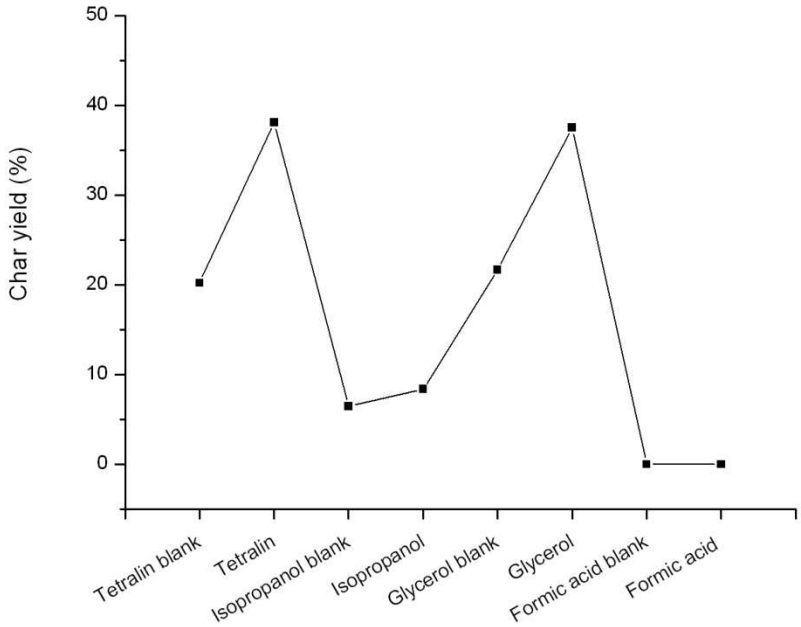


**Figure 5.14.** Obtained char yields (%, w/w) referred to initial lignin weight for each hydrogen-donor solvent.

However, the different pathways of in-situ hydrogen generation in the systems and thus generation of reactive intermediates (e.g. acetone, dihydroxiacetone, ect.), which are highly dependent on the type of hydrogen-donating solvent, are also believed to significantly influence the increasing formation of carbonaceous deposits in some cases via promotion of side reactions. Tetralin experiments yielded the highest amount of char (reaching a maximum value of 38%) in a similar way to glycerol. In the case of tetralin, these expected results may combine the production of char from the significant lignin depolymerization (Domburg et al. 1982) as well as some catalyzed formation of polycondensed aromatic rings from naphtalene generated in the microwave-assisted hydrogen-donating process.

Comparatively, the char contribution from glycerol is more likely to be mostly coming from side reactions from glycerol itself and its intermediates generated in the hydrogen-donating step catalyzed by the Ni10%AlSBA15 catalyst (e.g. dehydration to acrolein and polymerization, condensations and etherification/esterifications

catalysed by the aluminosilicate support, etc.). The use of isopropanol provided an unexpected low char content but this could be associated to the degree low depolymerization found in MALDI-TOF analyses as well as to a formation of lower molecular weight products (compared to glycerol) in the side reactions of isopropanol and acetone potentially promoted by the Ni catalyst. Formic acid experiments provided ideal results, with no coke formation at all, which are likely to be due to the decomposition of formic acid in the systems into $CO_2$ and $H_2$, in accordance with other reported work (Kleinert et al. 2008).

### 5.4.4 Effect on residual lignin

Last, the residual lignin results for all experiments with the different hydrogen-donor solvents are depicted in Figure 5.15. It can be observed that the percentage of recovered residual lignin was high values in most cases. Low residual lignin content does not however imply that all lignin has been transformed into monomers. Residual lignin contents obtained in the use of tetralin and glycerol showed a similar behavior, with blank runs in the absence of catalysts producing larger contents of residual lignin compared to those obtained with the Ni catalyst. However, this decreased in residual lignin content was associated in both cases to an increase in char yields rather than to increasing quantities of phenolic monomeric compounds. The blank isopropanol run gave low residual lignin values with respect to the catalytic experiment which produced high amounts of residual lignin. According to the MALDI-TOF analyses and to char yields, the addition of Ni10% SBA to isopropanol as solvent had a negative effect on lignin depolymerization. Experiments employing formic acid as hydrogen-donor solvent showed high residual lignin contents suggesting that lignin depolymerization by means of the proposed mild hydrogenolytic approach can be improved.

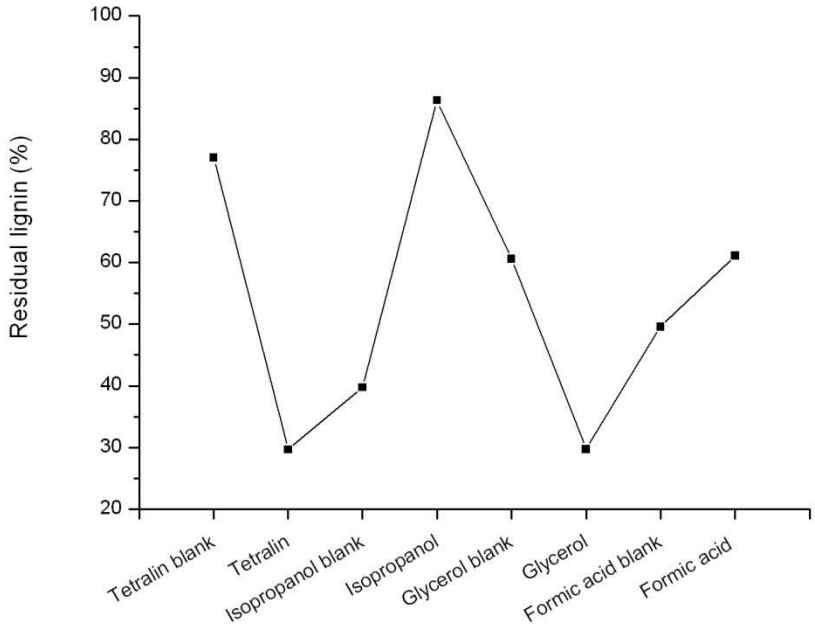


**Figure 5.15.** Residual lignin (%, w/w) referred to initial lignin weight for each hydrogen-donor solvent.

Figure 5.16 and Table 5.6 show molecular weight distributions of residual lignins and number-average (Mn), weight-average (Mw) molecular weight and polydispersity (Mw/Mn) of the analyzed samples. Rough lignin was also analyzed as reference. In all cases, two peaks could be observed related to unconverted lignin and to a lower molecular weight lignin as a result of the depolymerization process. In addition, some experiments exhibited more than one peak at high retention times suggesting the existence of oligomers or low molecular weight fractions of different molecular weights. Probably, these oligomers were dragged when precipitating the residual lignin and char at the first step of the separation procedure. Table 5.6 also clearly demonstrates that tetralin, isopropanol and glycerol blank runs (in the absence of catalyst) exhibited higher molecular weights to those of rough lignin, suggesting that lignin repolymerization had taken place. Microwave irradiation could have generated a pool of radicals and/or unstable fragments that could not be saturated with the in-

situ generated hydrogen by the hydrogen-donor solvents, which reacted with the parent lignin structure.

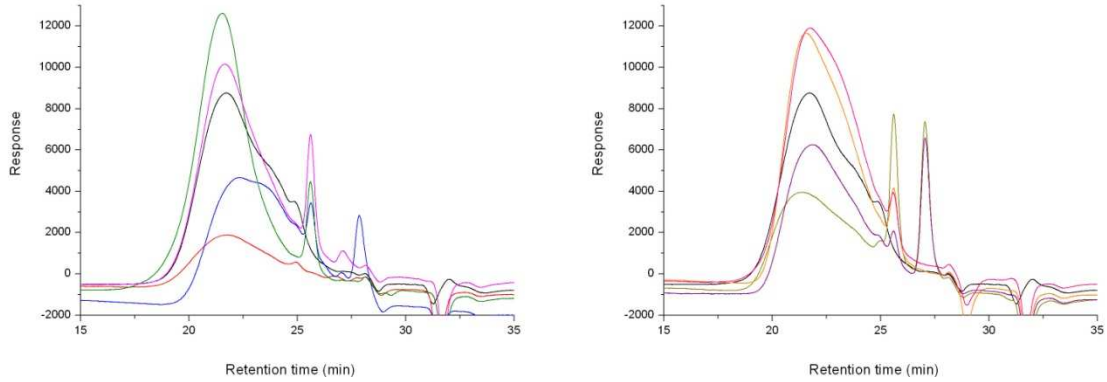


**Figure 5.16.** Residual lignin HPSEC results for each hydrogen-donor solvent. Left graphic: black (rough lignin), red (tetralin blank), blue (tetralin), olive green (isopropanol blank) and magenta (isopropanol). Right graphic: black (rough lignin), dark yellow (glycerol blank), purple (glycerol), orange (formic acid blank) and pink (formic acid).

Experiments using isopropanol possessed almost identical values to those of rough lignin, confirming again that the degree of depolymerization is very low. The residual lignin obtained in formic acid experiments showed a lower molecular weight with respect to rough lignin, proving that lignin depolymerization was successful in this case, in good agreement with previous results (Kleinert et al. 2008, 2009). However, the best depolymerization results were achieved when tetralin was used as hydrogen-donor solvent. These results indicated that tetralin could also be a good alternative compared to formic acid in lignin depolymerization practices, leading to an improved degree of depolymerization in lignin at the expense of producing large quantities of char in the reaction. A compromise between the undesirable product (char) and lignin depolymerization degree has to be reached when selecting the hydrogen-donor solvent.

| | Mw | Mn | Mw/Mn |
|---|---|---|---|
| Rough linin | 7232 | 2125 | 3.40 |
| Tetralin blank | 8549 | 2227 | 3.84 |
| Tetralin | 3984 | 1231 | 3.24 |
| Isopropanol blank | 10982 | 2982 | 3.68 |
| Isopropanol | 7296 | 1998 | 3.65 |
| Glycerol blank | 8231 | 2281 | 3.61 |
| Glycerol | 5696 | 1989 | 2.86 |
| Formic acid blank | 5664 | 1770 | 3.20 |
| Formic acid | 5865 | 1618 | 3.62 |

**Table 5.6.** Residual lignins number-average (Mn), weight-average (Mw) molecular weight and polydispersity (Mw/Mn) of residual lignin of each hydrogen-donor solvent experiment. Rough lignin was also characterized for comparative purposes

### 5.4.5 Conclusions

Lignin isolated from olive tree pruning by applying organosolv conditions could be efficiently depolymerize to produce simple aromatics using a facile and hydrogen-free heterogeneously catalyzed protocol under microwave irradiation. The use of a renewable derived hydrogen-donating solvent such as formic acid combined with a Ni based catalyst and microwaves could provide promising quantities of phenolic compounds including syringol, syringaldehyde, vanillin, desaspidinol and aspidinol, with larger quantities of syringyl as compared to guaiacyl derivatives.

Furthermore, as compared to other hydrogen-donating solvents employed in the depolymerization reaction, formic acid experiments minimized char production in the systems (no char generated). In general, the residual lignin content was high in all studied cases (with the best degrees of depolymerization obtained for tetralin and formic acid) indicating that these results can be improved. Although tetralin gave the

highest lignin depolymerization degree (residual lignins molecular weight results lower than initial lignin), the fact that employing formic acid as hydrogen donating solvent char formation is avoided and the acceptable depolymerization degree, led to continue this study of lignin hydrogenolytic depolymerization using formic acid as hydrogen-donor solvent.

## 5.5 Process proposal for lignin revalorization by hydrogenolytic depolymerization

This entire process proposal for lignin revalorization consists mainly of three stages: lignin extraction, lignin purification and lignin depolymerization by hydrogenolysis. The first two processes have been widely discussed in Chapter 2 and 3. This section presents the results of the third stage – lignin depolymerization by hydrogenolysis-. In this section, the relationship between lignin properties and hydrogenolytic depolymerization yields was studied.

Once the different studies for the optimization of lignin hydrogenolytic depolymerization (section 5.3 and 5.4) were concluded, the next step was to apply those optimized conditions to lignin ultrafiltered fractions (F1, F2, F3, F4, F5 and F6 -obtained in Chapter 3-) in order to study if there was a relationship between lignin properties and the obtained results from lignin depolymerization by hydrogenolysis. From the results obtained in section 5.3, the most desirable results were obtained when the highest concentration of nickel was supported on the aluminosilicates (Ni10%AlSBA15). Formic acid was the hydrogen-donor solvent (section 5.4) that

produced higher concentration of phenolic compounds from lignin and at the same time, no char (by-product) formation was observed.

### 5.5.1 . Materials and methods

Formic acid was used as hydrogen-donor solvent for in-situ hydrogen generation. Microwave power was set at 100 W, reaching an average temperature of 150 ºC. The applied power was determined taking into account the microwave temperature limit (200 ºC) and the solvent loss tangent (tan θ: 0.722). After reaction, the final mixture was filtered off to separate solids (catalyst). The liquid was treated in order to precipitate the residual lignin. The precipitate was isolated by filtration. The acidic liquid solution was extracted with ethyl acetate so as to isolate the phenolic compounds produced during lignin depolymerization. Ethyl acetate was evaporated to obtain the phenolic oil. The yield of every phenolic product obtained in the systems was calculated gravimetrically referring to the initial lignin. Other aspects of the reaction conditions, product separation and products analysis have been already discussed in section 5.2. The results are presented below.

### 5.5.2 Effect on oil yield and composition

Figure 5.17 depicts the oil yield obtained (referred to initial lignin weight) for the different lignin ultrafiltered fractions. The highest value was obtained for fraction 6 (membrane cut-off <5 KDa; ~ 37%) and the lowest oil yield (approximately 12%) for lignin fraction 3 (membrane cut-off between 50 and 150 KDa). Experiments seemed to follow a trend of increasing oil yields at decreasing the molecular weight of lignin (from fractions 1 to 6) but, unexpectedly, fraction 3 and 5 exhibited lower oil yields. This may suggest that the quantities of oil obtained were not directly related

to lignin properties such as molecular weight distribution or composition. Beside, the excess of formic acid added to the mixture may not have decomposed, and thus partially remained in the phenolic oil.

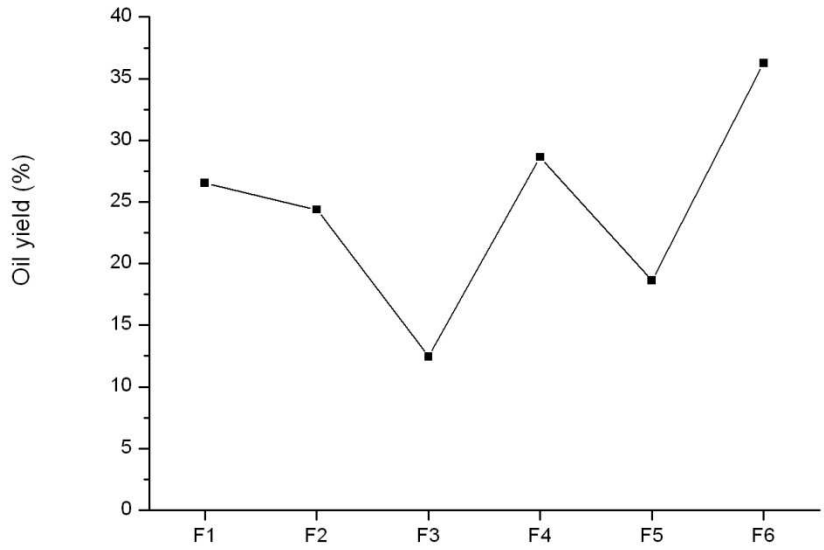


**Figure 5.17.** Obtained oil yields (%, w/w) referred to initial lignin weight for each lignin fraction.

The phenolic oil was further analyzed by GC-MS in order to determine the nature and concentration of the isolated phenolic monomeric compounds (Table 5.7 and Figure 5.18). The main compound found in oil was desaspidinol (12) proving that the applied mild-hydrogenolysis conditions were able to produce simple phenolic monomers. Fractions 1 and 2 (with larger molecular weights) yielded the highest concentrations of this compound. This fact suggested that the molecular weight of lignin can significantly influence lignin depolymerization practices. 4-hydroxyacetyl-2-methoxyphenol (5) and acetosyringone (7) were compounds obtained in low concentration in the oil. The ether linkage between carbon α, β and γ-carbon atoms of a side chain and the 4-position of a phenolic ring in an adjacent unit is said to be the principal reaction in the hydrogenolysis of lignins. Depending on the reaction

conditions, carbon-carbon linkages may also be ruptured during hydrogenolysis especially at α-β and β-γ sites (Sakakibara 1992). However, the applied mild-hydrogenolysis conditions did not seem to favor this type of cleavage since guaiacol and syringol were the only generated structures.

| Compound | Rt (min) | F1 | F2 | F3 | F4 | F5 | F6 |
|---|---|---|---|---|---|---|---|
| Guaiacol (1) | 7.44 | 0.19 | 0.31 | 0.09 | 0.16 | 0.11 | 0.30 |
| Syringol (2) | 14.01 | 0.62 | 1.47 | 0.31 | 0.65 | 0.47 | 0.74 |
| Vanillin (3) | 15.18 | 0.31 | 0.18 | 0.16 | 0.25 | 0.27 | 0.24 |
| Guaiacylacetone (4) | 17.70 | 0.25 | 0.35 | 0.08 | 0.20 | 0.09 | 0.15 |
| 4-hydroxyacetyl-2-methoxyphenol (5) | 18.60 | 0.11 | 0.10 | 0.06 | 0.09 | 0.09 | 0.09 |
| Syringaldehyde (6) | 18.67 | 1.66 | 0.76 | 0.76 | 1.10 | 1.19 | 0.87 |
| Acetosyringone (7) | 18.79 | 0.11 | 0.10 | 0.05 | 0.08 | 0.09 | 0.08 |
| Desaspidinol (8) | 19.60 | 2.43 | 3.31 | 0.88 | 2.25 | 0.70 | 1.10 |
| Aspidinol (9) | 20.54 | 0.51 | 0.65 | 0.32 | 0.52 | 0.37 | 0.30 |
| G derivatives (1, 3, 4, 5) | | 0.86 | 0.94 | 0.39 | 0.70 | 0.56 | 0.78 |
| S derivatives (2, 6, 7, 8) | | 4.82 | 5.64 | 2.00 | 4.08 | 2.45 | 2.79 |

**Table 5.7.** Compounds present in the obtained oil for each ultrafiltered lignin fraction. Compounds yields concentration in mg of each compound per gram of lignin.

The obtained results suggested that the main reactions taking place were α-O-4 cleavage in the connections between the oxygen and the carbon at the 4-position of a phenolic ring. Compounds 3, 4, 5, 6, 7 and 8 presented a carbonyl group in α position (ketone or aldehyde) that could have been originated in further reactions of the intermediate formed during the ether linkage cleavage between an aliphatic carbon (α) and the oxygen (generally, at position 4). Demethoxylation reactions could also lead to methanol formation that could be involved in other type of

chemistries (e.g. etherifications, esterifications, etc.), taking into account the acidic nature of the support.

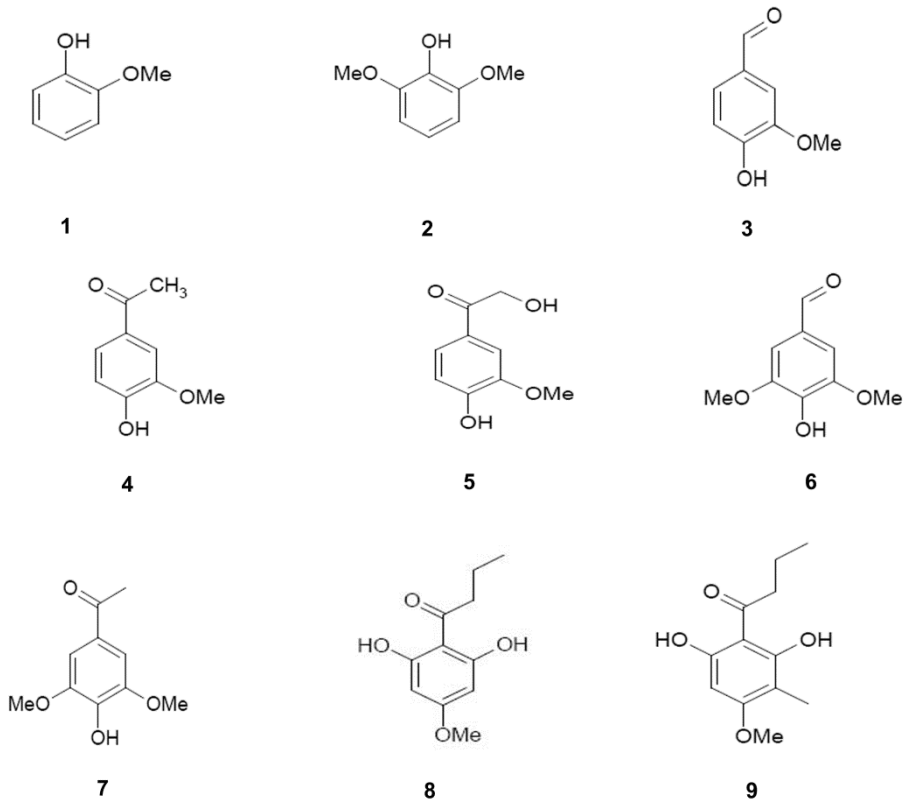


**Figure 5.18.** Simple phenolics obtained after heterogeneously catalyzed depolymerization of lignin fractions. (1) Guaiacol (2) Syringol (3) Vanillin (4) Guaiacylacetone (5) 4-hydroxyacetyl-2-methoxyphenol (6) Syringaldehyde (7) Acetosyringone (8) Desaspidinol (9) Aspidinol.

Compounds present in the obtained oils are the results of cleavage reactions between lignin interunits. Taking into account that the main lignin units are p-hydroxyphenyl alcohol, guaiacyl alcohol and syringyl alcohol, the monomeric products could be grouped together depending on their origin. Compounds 1, 3, 4 and 5 are believed to have guaiacyl origin whereas compounds 2, 6, 7 and 8 could be associated to be released from syringyl units. The origin of aspidinol could not be clearly confirmed. Table 5.7 also summarizes concentrations of syringyl and guaiacyl derivatives. Pepper et al. (1963) stated that the higher prevalence of products with guaiacyl origin could be explained from demethoxylation reactions of syringyl units that form

guaiacyl derivatives (Pepper et al. 1963). Interestingly, all lignin fractions exhibited higher concentrations of syringyl compared to guaiacyl derivatives, indicating that demethoxylation reactions are minimized when formic acid is used as hydrogen-donating solvent. The profile of monomeric products was also found to be different from related lignin hydrogenolysis studies (Meier et al. 1992; Thring et al. 1996; Kleinert et al. 2008; Torr et al. 2011). These findings were likely to be associated, as mentioned before, to the combination of microwaves with the heterogeneous supported metal nanoparticle catalyst in a similar way to that previously reported by other authors (Pineda et al. 2012; Balu et al. 2012).

The relatively low concentration observed of phenolic monomers suggested that there were more products in the oil that could not be detected by GC-MS (which can only detect compounds low molecular weight and low boiling point compounds). MALDI-TOF analyses were subsequently carried out to complement GC/MS data. Considering that a prototype lignin subunit (e.g. phenylpronane syringol) has a molecular weight of 197 g/mol, Figure 5.19 clearly shows that most of the obtained products were mainly monomers and dimers. The poor intensity of the signals for all lignin fractions suggested that the employed mild-hydrogenolysis conditions did not produced large quantities of low molecular weight phenolic compounds.

The presence of trimers and oligomers (500-700 g $mol^{-1}$ signals) was noticeable in fractions 2, 3 and 5, while fractions 1 and 2 possessed more abundant and intense signals at lower m/z values (200-400 g $mol^{-1}$) which relate to a higher concentration of lower molecular weight phenolic compounds with larger membrane cut-offs (in the 300-150 KDa range). These results were in good agreement with data shown in Table 5.7, confirming the higher quantities of monomers produced in experiments of fractions 1, 2 and 4.

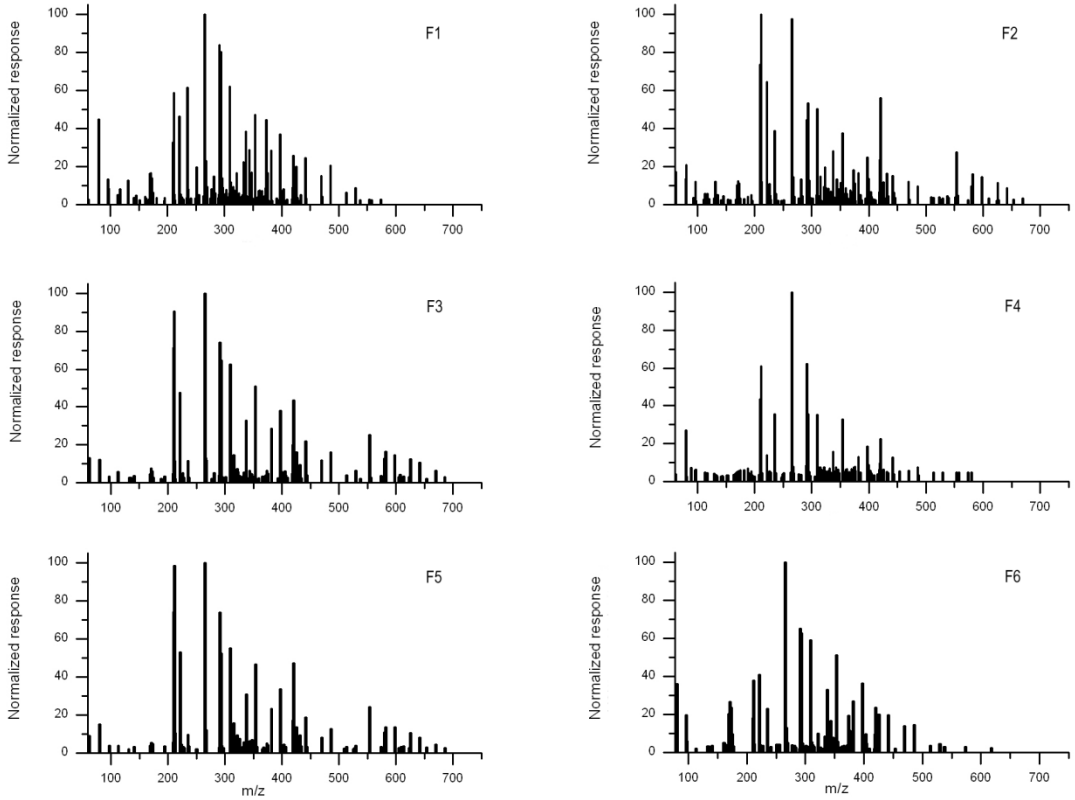


**Figure 5.19.** MALDI-TOF oil analyses of each lignin ultrafiltered fraction.

### 5.5.3 Effect on residual lignin

Figure 5.20 depicts contents of residual lignin for the different hydrogenolysis experiments carried out with F1 to F6 fractions. It is readily apparent that the content of residual lignin content was high in most cases, reaching a maximum of 65% for lignin fraction 5. The high residual lignin was connected to a low concentration of monomers in the phenolic oil. This residual lignin content clearly increased with smaller membrane cut-offs used to obtain the lignin fractions. The difference to 100 observed taking into account the results in Figure 5.17 and 5.20 corresponded to gaseous products. Interestingly, lignin fractions of low molecular weight (F6) prevented the formation of gaseous products by promoting the formation of larger quantities of phenolic oil, with the exception of fraction F5 (for which almost

15% of gaseous products were obtained). Such gaseous products were not recovered for further identification or quantification.

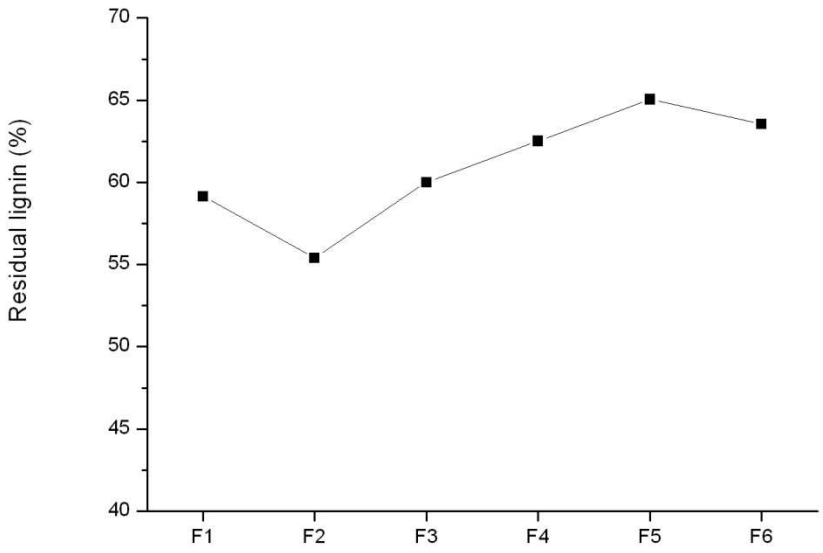


**Figure 5.20.** Residual lignin (%, w/w) referred to initial lignin weight for each lignin fraction.

Table 5.8 summarizes number-average (Mn), weight-average (Mw) molecular weight and polydispersity (Mw/Mn) values of residual lignins from the different ultrafiltrated fractions and of the original ultrafiltered lignin fractions. The molecular weight of residual lignins decreased, in all cases, with respect to those of the parent organosolv ultrafiltered fractions. These findings indicate that lignin depolymerization took place to some extent under the investigated conditions. However, all experiments presented a different extension in depolymerization. Interestingly, this degree of depolymerization was found to be higher for fractions with higher molecular weight (F1 and F2), correlated with a larger difference between the molecular weight of residual lignin versus its corresponding parent lignin fraction. These differences decreased along with the molecular weight of the lignin fractions to the point of giving similar results for both F6 and its parent ultrafiltrated fraction (Table 5.8, indicating that depolymerization does not occur). These data were in good agreement

with the obtained concentrations of phenolic monomers in the experiments and may suggest that the applied mild-hydrogenolytic conditions with the utilized Ni10% catalyst were truly effective only in the case of high molecular weight lignins as starting material. Comparing polydispersity values (Mw/Mn) between lignin fractions and their obtained residual lignins upon reaction, these values decreased for the higher molecular weight fractions F1 to F3 (Table 5.8) indicating the degradation of the biopolymer in these experiments.

| | **Ultrafiltered fractions** | | | **Residual lignin** | | |
|---|---|---|---|---|---|---|
| | **Mw** | **Mn** | **Mw/Mn** | **Mw** | **Mn** | **Mw/Mn** |
| **F1** | 12798 | 3060 | 4.18 | 7210 | 2021 | 3.57 |
| **F2** | 9302 | 2489 | 3.74 | 5261 | 1591 | 3.30 |
| **F3** | 7882 | 2183 | 3.61 | 5820 | 1758 | 3.31 |
| **F4** | 6555 | 2165 | 3.03 | 5748 | 1781 | 3.23 |
| **F5** | 5184 | 1686 | 3.07 | 5346 | 1776 | 3.01 |
| **F6** | 4527 | 1567 | 2.89 | 4436 | 1466 | 3.02 |

**Table 5.8.** HPSEC results. Number-average (Mn), weight-average (Mw) molecular weight and polydispersity (Mw/Mn) of ultrafiltered lignin samples and residual lignin of ultrafiltrated hydrogenolysis processes.

### 5.5.4 Ultrafiltration and hydrogenolysis as the pathway to revalorize lignin

A schematic representation of the proposed lignin valorization methodology to high value-added product is depicted in Figure 5.21. This process involves different stages including pretreatment (organosolv), purification (ultrafiltration), lignin depolymerization (hydrogenolysis) and recovery processes so as to recycle the reagents used.

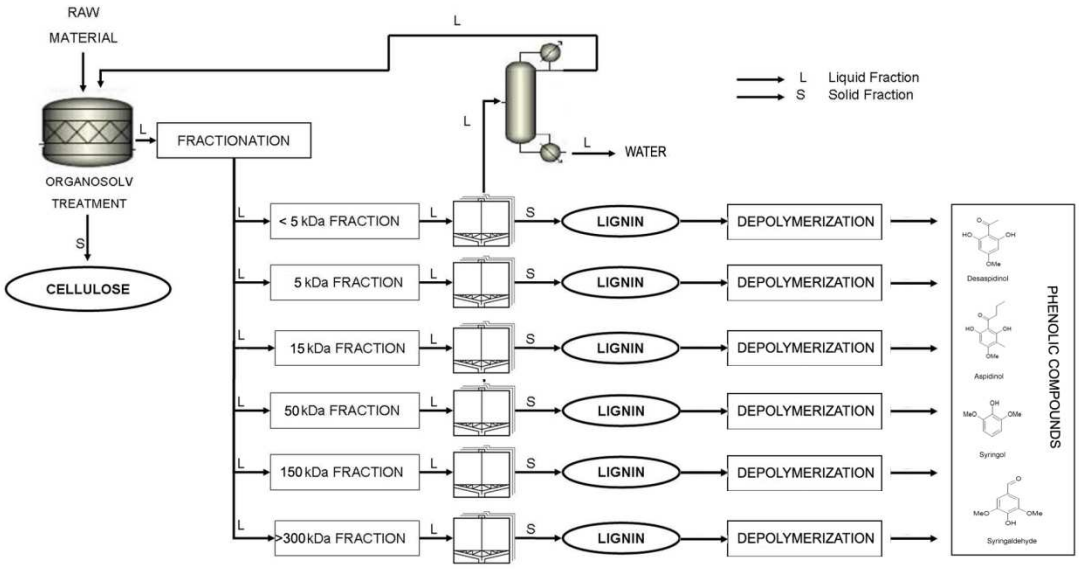


**Figure 5.21.** Schematic representation of the novel cascade-type lignin valorization approach.

As mentioned in section 4.5.4, the first step (pretreatment) has been proved to be an effective process to extract the lignin from the raw material. The purification process (ultrafiltration) has been confirmed not only to purify lignin fractions but also to be an effective technique to obtain specific molecular weight lignin fractions. The economy of the whole process was evaluated by Gonzalez-Alriols et al. (2010), concluding that high added value lignin application was needed to be found in order to afford the increase in the process economy. In these sense, lignin heterogeneous hydrogenolysis depolymerization was studied in order to evaluate the suitability of this process to produce high value added chemicals from lignin.

A major problem when using heterogeneous catalysts is related to side reactions and recombination of the highly reactive radical reaction intermediates (e.g. repolymerization, C-C couplings, etc.) formed during the thermal treatment that generate char (e.g. condensed oligomeric products of increased molecular weight, including tars or solid chars) therefore reducing activity and/or reusable properties of

the catalyst as well as potentially blocking the reactor (Kleinert et al. 2009). The applied mild reaction conditions allowed considering microwave irradiation as the main cause of that kind of undesirable reactions. One of the remarkable novelties of this study was the negligible formation of coke in the hydrogenolytic experiments carried out. The presence of formic acid as hydrogen donating compound leads to higher yields of desired monophenols and no char formation via prevention of the recombination of reactive radical species by the in-situ generated active hydrogen in the systems. The efficient decomposition of formic acid into $CO_2$ and $H_2$ (Kleinert et al. 2008) also minimizes the production of any carbonaceous species from the hydrogen donating solvent after reaction.

The main obtained phenolic products were desaspidinol, syringaldehyde and syringol. Desaspidinol is an anthelmintics drug utilized to treat infections with parasitic worms and also used as flavoring and food additive (Socolsky et al. 2003). In addition, Syringol (2) and Syringaldehyde (6) were also produced in large quantities but very similar between the ultrafiltrated lignin fractions. These findings would indicate that such syringyl derivatives were easily produced from lignin regardless of the molecular weight or purity of the employed feedstock. Syringaldehyde is largely employed as pharmaceutical precursor as well as dye agent (Eckert et al. 2007), while syringol finds uses as flavoring and natural preservative due to its antioxidant capacity (Maga 1978; Ikegami et al. 1998; Loo et al. 2008).

### 5.5.5 Conclusions

A complete approach for lignin valorization has been proposed with the purpose of isolating lignin from lignocellulosic residues and subsequent production of valuable compounds promoted by a mild-hydrogenolytic depolymerization assisted by

microwave irradiation. The main phenolic monomers obtained from lignin were desaspidinol, syringaldehyde and syringol, with concentration in phenolics generally increasing at increasing membrane cut offs. Syringyl-derived compounds were produced in larger quantities as compared to guaiacyl derivatives. The proposed lignin depolymerization conditions do not generate any undesirable products such as chars or tars in the process, with residual lignin and HPSEC technique further confirming that lignin depolymerization takes place in a large extension for higher molecular weight lignin fractions (typically F1 and F2) under the investigated reaction conditions with the investigated catalyst.

## 5.6 Hydrogenolytic depolymerization conclusions

Lignin transformation into phenolic monomers is a promising process to revalorize lignin in order to complete the total utilization of lignocellulosic raw material components. In this chapter, hydrogenolysis has been studied as the pathway to produce interesting phenolic bulk chemicals from lignin. To this end, optimization studies were conducted to improve obtained results and to better understand lignin depolymerization by hydrogenolysis.

A catalyst screening study for lignin hydrogenolytic depolymerization was developed. Different metal nanoparticles (nickel (Ni), palladium (Pd), platinum (Pt) and ruthenium (Ru)) were supported on an acidic aluminosilicate (Al-SBA15). The nature of the obtained depolymerization products was confirmed to vary depending on the employed catalyst. Interestingly, the main phenolic products were diethyl phthalate, mesitol and syringaldehyde. Obtained products were found to be produced by two

main processes, carbon-carbon linkage breakdown or demethoxylation reactions. The obtained products were different from the expected ones and that fact was attributed to the used microwave system reaction. Repolymerization phenomena were proved to take place except for Ni-based catalysts. Repolymerization reactions prevent reaction intermediates to produce simple phenolic monomeric products. The use of the highest concentration of Ni (Ni10%AlSBA) led to the highest depolymerization degree.

Different hydrogen donating solvents were employed in order to improve depolymerization yields. The use of isopropanol and the catalyst produced a negative effect on lignin hydrogenolytic depolymerization. As expected, the phenolic monomeric products profile was very different depending on the employed hydrogen source. Formic acid presented the highest concentration of those products obtained by all solvents (syringol, syringaldehyde and vanillin). Tetralin and formic acid presented the higher depolymerization degree. However, formic acid was confirmed to produce the widest profile and most concentrated products, with no char formation and repolymerization avoiding was reached.

Once optimized the hydrogenolysis reaction conditions, ultrafiltered lignin fractions were subjected to hydrogenolytic depolymerization. The main conclusion arose from this study was that lignin properties affected depolymerization reactions. In particular, lignin molecular weight had a strong effect on lignin depolymerization degree. As the lignin molecular weight was higher, the production of simple phenolic compounds was enhanced as well as the recovered residual lignin was higher. In these sense, HPSEC results were very enlightened. The main obtained compounds were desaspidinol, syringaldehyde and syringol.

## 5.7 References

Balu, A.M; Dallinger, D.; Obermayer, D.; Campelo, J.M.; Romero, A.A.; Carmona, D.; Balas, F.; Santamaria, J.; Yohida, K.; Gai, P.L.; Vargas, C.; Kappe, C.O.; Luque, R. 2012. Insights into the microwave-assisted preparation of supported iron oxide nanoparticles on silica-type mesoporous materials. Green Chem 14, 393–402.

Baruwati, B.; Polshettiwar, V.; Varma, R.S. 2009. Magnetically recoverable supported ruthenium catalyst for hydrogenation of alkynes and transfer hydrogenation of carbonyl compounds. Tetrahedron Lett. 50, 1215–1218.

Binder, J.B.; Gray, M.J.; White, J.F.; Zhang, Z.C.; Holladay, J.E. 2009. Reaction of lignin model compounds in ionic liquids. Biomass Bioenergy 33, 1122–1130.

Connors, W.J.; Johanson, L.N.; Sarkanen, K.V.; Winslow, P. 1980. Holzforschung 34, 29–37.

Couto, G.G.; Klein, J.J.; Schreiner, W.H.; Mosca, D.H.; de Oliveira, A.J.A.; Zarbin, A.J.G. 2007. Nickel nanoparticles obtained by a modified polyol process: synthesis, characterization and magnetic properties. J Colloid Interface Sci 311, 461–468.

Domburg, G.; Sharapova, T.E. 1982. Khim Drev 54–65

Eckert, C.; Liotta, C.; Ragauskas, A.; Hallett, J.; Kitchens, C.; Hill E.; Draucker, L. 2007. Tunable solvents for fine chemicals from the biorefinery. Green Chem 9, 545–548.

Fang, Z.; Qiu, X.; Chen, J.; Qiu, X. 2011. Debromination of polybrominated dephenyl ethers by Ni/Fe bimetallic nanoparticles: influencing factors, kinetics and mechanism. J Hazard Mater 185, 958–969.

Gandarias, I.; Arias, P.L.; Requies, J.; El Doukkali, M.; Güemez, M.B. 2011. Liquid-phase glycerol hydrogenolysis to 1,2-propanediol under nitrogen pressure using 2-

propanol as hydrogen source. J Catal 282, 237–247

Gracia, M.J.; Campelo, J.M.; Losada, E.; Luque, R.; Marinas, J.M.; Romero, A.A. 2009. Microwave-assisted versatile hydrogenation of carbonyl compounds using supported metal nanoparticles. Org Biomol Chem 7, 4821–4824.

Harris, E.E.; Adkins, H. 1938. Reactions of lignin with hydrogen. Paper Trade J 107, 38–40.

Horacek, J.; Homola, F.; Kubickova, I.; Kubicka, D. 2012. Lignin to liquid over sulfide catalysts. Catal Today 179, 191–198.

Hrutfiord, B. F. 1971. Reduction and hydrogenolysis (of lignin), In Lignin. Wiley-Interscience, New York, Chapter 12.

Ikegami, F.; Sekine, T.; Fuji, Y. 1998. Anti-dermatophyte activity of phenolic compounds in "Mokusaku-Eki". J Pharm Soc Japan 118, 27.

Johnstone, R.A.W.; Wilby, A.H.; Entwistle, I.D. 1985. Heterogeneous catalytic transfer hydrogenation and its relation to other methods for reduction of organic compounds. Chem Rev 85, 129-170.

Kleinert, M.; Barth, T. 2008. Phenols from lignin. Chem Eng Technol 31 (5), 736–745.

Kleinert, M.; Gasson, J.R.; Barth, T. 2009. Optimizing solvolysis conditions for integrated depolymerisation and hydrodeoxygenation of lignin to produce liquid biofuel. J Anal Appl Pyrol 85, 108–117.

Ko, J.; Shimizu, Y.; Ikeda, K.; Kim, S.; Park, C.; Matsui, S. 2009. Biodegradation of high molecular weight lignin under sulfate reducing conditions: Lignin degradability and degradation by-products. Bioresour Technol 100, 1622–1627.

Li, C.; Zheng, M.; Wang, A; Zhang, T. 2012. One-pot catalytic hydrocracking of raw woody biomass into chemicals over supported carbide catalysts: simultaneous conversion of cellulose, hemicelluloses and lignin. Energy Environ Sci 5, 6383–6390.

Liguori, L.; Barth, T. 2011. Palladium-Nafion SAC-13 catalysed depolymerisation of lignin to phenols in formic acid and water. J Anal Appl Pyrol 92, 477–484.

Loo, A.Y.; Jain, K.; Darah, I. 2008. Antioxidant activity of compounds isolated from the pyroligneous acid, *Rhizophora apiculata*. Food Chem 107, 1151–1160.

Maga, A.J. 1978. Simple phenol and phenolic compounds in food flavor, in E.T. Furia (Ed.), Critical Reviews in Food Science and Nutrition, CRC Press, Boca Raton 323–345.

Meier, D.; Ante, R.; Faix, O. 1992. Catalytic hydropyrolysis of lignin: influence of reaction conditions on the formation and composition of liquid products. Bioresour Technol 40, 171–177.

Pandey, M.P.; Kim, C.S. 2011. Lignin depolymerization and conversion: a review of thermochemical methods. Chem Eng Technol 34 (1), 29–41.

Pepper, J. M.; Steck, W. 1963. The effect of time and temperature on the hydrogenation of aspen lignin. Can J Chem 41 (11), 2867–2875.

Pepper, J.M.; Lee, Y.W. 1969. Lignin and related compounds. I. A comparative study of catalysts for lignin hydrogenolysis. Can J Chem, 47, 723–727.

Percival Zhang, Y.-H. 2008. Reviving the carbohydrate economy via multi-product lignocellulose biorefineries. J Ind Microbiol Biotechnol 35, 367–375.

Pineda, A.; Balu, A.M.; Campelo, J.M.; Luque, R.; Romero, A.A.; Serrano-Ruiz, J.C. 2012. High alkylation activities of ball-milled synthesized low-load supported iron oxide nanoparticles on mosoporous aluminosilicates. Catal Today DOI:10.1016/j.cattod.2012.02.028

Pineda, A.; Balu, A.M.; Campelo, J.M.; Romero, A.A.; Carmona, D.; Balas, F.; Santamaria, J.; Luque, R. 2011. A dry milling approach for the synthesis of highly active nanoparticles supported on porous materials. ChemSusChem 4, 1561–1565.

Roberts, V.M.; Knapp, R.T.; Li, X.; Lercher, J.A. 2010a. Selective hydrolysis of

diphenyl ether in supercritical water catalyzed by alkaline carbonates. ChemCatChem 2, 1407–1410.

Roberts, V.M.; Knapp, R.T.; Li, X.; Lercher, J.A. 2010b. Influence of alkali carbonates on benzyl phenyl ether cleavage pathways in supercritical water. Appl Catal B 95, 71–77.

Roberts, V.M.; Stein, V.; Reiner, T.; Lemonidou, A.; Li, X.; Lercher, J.A. 2011. Towards quantitative catalytic lignin depolymerization. Chem Eur J 17, 5939–5948.

Sakakibara, A. 1992. Hydrogenolysis in Methods in Lignin chemistry. (Eds. V.S.Y. Lin C.W. Dence), Springer-Verlag, Berlin Heidelberg, 350–368.

Sergeev, A.G.; Hartwig, J.F. 2011. Selective nickel-catalyzed hydrogenolysis of aryl ethers. Science 332, 439–442.

Socolsky, C.; Salvatore, A.; Asakawa, Y.; Bardón, A. 2003. Bioactive new bitter-tasting p-hydroxystyrene glycoside and other constituens from *Elapholossum spthulatum*. Arkivoc (x), 347–355

Su, F.Z.; He, L.; Ni, J.; Cao, Y.; He, H.Y.; Fan, K.N. 2008. Efficient and chemoselective reduction of carbonyl compounds with supported gold catalysts under transfer hydrogenation conditions. Chem Commun 3531–3533.

Thring, R.W.; Breau, J. 1996. Hydrocracking of solvolysis lignin in a batch reactor. Fuel 75, 795–800.

Torr, K.M.; van de Pas, D.J.; Cazeils, E.; Suckling, I.D. 2011. Mild hydrogenolysis of in-situ and isolated *Pinus radiata* lignins. Bioresour Technol 102, 7608–7611.

van Haveren, J.; Scott, E.L.; Sanders, J. 2008. Bulk chemicals from biomass. Biofuel Bioprod Bioref 2, 41–57.

Wolfson, A.; Dlugy, C.; Shotland, Y.; Tavor, D. 2009. Glycerol as solvent and hydrogen donor in transfer hydrogenation–dehydrogenation reactions. Tetrahedron Lett. 50, 5951–5953.

Yan, N.; Zhao, C.; Dyson, P.J.; Wang, C.; Liu, L.; Kou, Y. 2008. Selective degradation of wood lignin over noble-metal catalysts in a two-step process. ChemSusChem 1, 626–629.

Zakzeski, J.; Bruijnincx, P.C.A.; Jongerius, A.-L.; Weckhuysen, B.M. 2010. The Catalytic valorization of lignin for the production of renewable chemicals. Chem Rev 110 (6), 3552–3599.

# 6. CONCLUSIONS

## 6.1 Conclusions

In this chapter the summary of the main conclusions drawn from the developed research work are presented. The first idea of the whole thesis was to change the common point of view of the biorefinery process. All biomass industrial processes are focused on taking profit of the cellulosic fractions and the novelty of this study was to first think about lignin stream. Bearing this in mind, an entire lignin revalorization process was designed. The proposed process for lignin valorization consists of three stages: lignin extraction, lignin purification and in the end, lignin depolymerization.

The study concerning lignin extraction was focused on the influence of the extraction conditions on lignin structure and on the optimization of the reaction conditions in order to enhance lignin production.

As lignin structure strongly depends on the raw material and the applied pretreatment to extract it, this relationship was studied. Olive tree pruning was subjected to three different sulfur-free pretreatments (alkali, autohydrolysis and ethanol organosolv) to extract the lignin. The obtained lignins (AL, HL and OL) were deeply characterized in order to evaluate which pretreatment yielded the highest quality lignin. The applied alkali pretreatment produced very impure lignin (AIL < 5%). The contamination was mainly due to hemicellulosic sugars and inorganic salts. Authohydrolysis lignin was also contaminated by hemicellulosic sugars but interestingly, the molecular weight of that lignin was low. Organosolv treatment yielded the purest lignin (66%) with very interesting physicochemical properties (highly functionalities). Taking into account all obtained results, ethanol organosolv conditions were selected as the ones that yielded the highest quality lignin.

Once selected the ethanol organosolv pretreatment, the reaction conditions were varied and optimized in order to improve lignin production. An experimental design was used for the enhancement of lignin production from olive tree pruning by organosolv pretreatment. The maximization of lignin concentration in the liquid fraction entailed using high temperatures and low ethanol concentration ensuring also, low lignin content in solid fraction. Reaction temperature and ethanol concentration were the most significant variables for organosolv extraction process. High concentrated liquid fractions were treated to isolate lignin in order to evaluate its purity. Almost all lignins presented hemicellulosic contamination but the percentage of these sugars was different depending on the applied conditions to extract the lignin. Experiment 24 conditions (200 ºC, 90 minutes and 70% ethanol concentration) were selected to produce high concentrated liquid fractions with high quality lignin.

Lignin purification is an interesting issue to overcome lignin non-homogeneity problems. In this chapter, the previously obtained results concerning different purification techniques were presented. Differential precipitation and ultrafiltration were considered as purification processes. Obtained results comparison allow selecting ultrafiltration purification since it produce defined molecular weight and less contaminated lignin fractions than employing differential precipitation. These fractions were more adequate for the last objective of this thesis, lignin depolymerization.

The liquid fraction resulted from applying organosolv conditions of experiment 24 to olive tree pruning, was subjected to ultrafiltration. The isolated ultrafiltered lignin fractions were deeply characterized. Obtained results lead to confirm that ultrafiltration is not only a good purification process but also it constitutes an

excellent fractionation process since ultrafiltered lignin fractions presented clearly different molecular weight. As the used membrane cut-off was smaller, the obtained lignin fractions presented lower molecular weight and lower hemicellulosic content (contamination). In addition, functional groups content (carboxyl, carbonyl and total phenolic content) in ultrafiltered lignin fractions have been confirmed to be associated to the lignin fraction molecular weight. The most obvious and interesting finding to emerge from this study is that controlling the membrane cut-off used allows producing the desire lignin physicochemical properties or composition.

This thesis comprises two catalytic processes for lignin revalorization. The difference between them was the lignin depolymerization strategy, hydrolysis or hydrogenolysis. Comparing the results obtained when applying the different depolymerization conditions to ultrafiltered lignin fractions, many differences and similarities were observed.

Concerning oil obtaining, hydrogenolysis depolymerization reached the maximum oil yield (> 35%) although there was not a clear tendency related with the molecular weight of the lignin fraction. Unexpectedly, hydrothermal depolymerization presented an oil obtaining limitation (20-23%). The obtained phenolic monomers detected by GC-MS were different depending on the depolymerization approach. The compounds obtained by hydrolysis were phenol, cresols, guaiacol (low concentration), catechol and 4-methylcatechol. Their formation mechanism involved two steps: syringol and guaiacol released and their further transformation (via demethoxylation, demethylation, methylation, dealkylation… reactions). Comparatively, hydrogenolysis yielded different products such as guaiacol, syringol, vanillin, guaiacylacetone, syringaldehyde, desaspidinol and asipidinol as main products. Hydrothermal depolymerization allowed obtaining simpler phenolic products than hydrogenolytic

depolymerization. Moreover, these products concentration in the isolated oil was higher when using hydrothermal condition for lignin depolymerization. It should be notice that hydrogenolytic products concentration was presented as mg of compound per g of lignin since its percentage concentration referred to oil yield was so low that it was difficult to compare between the different catalysts and solvents studied. Comparing MALDI-TOF analyses of the obtained phenolic oil when subjecting ultrafiltered lignin fractions to each depolymerization approach, it was clearly observed that hydrothermal conditions provided more concentration of monomeric-dimeric compounds than hydrogenolytic conditions.

The relationship between the lignin molecular weight and depolymerization yields was completely different depending on the depolymerization conditions. While the phenolic monomer content increased as the ultrafiltrated lignin fraction presented lower molecular weight (F6>F5>…>F1) for the hydrothermal lignin depolymerization, the hydrogenolytic conditions affected yields in the opposite. Monomers compounds concentration was higher as the lignin molecular weight was higher (F1>F2>…>F6)) for the hydrogenolysis experiments.

Char is a typical subproduct when trying to depolymerize lignin. Regarding char formation, hydrogenolytic optimized conditions avoided totally char formation, above all, because of using formic acid as hydrogen-donor solvent. The optimization of the reaction conditions in the hydrothermal lignin depolymerization allowed the minimization of char formation (< 8%).

Recovered residual lignin was high for both approaches suggesting that these depolymerization processes still needs for more accurate optimization. For hydrolysis

experiments, it was found that the residual lignin was lower as the lignin molecular weight was smaller, as expected taking into account oil obtaining tendency. This was not the case of the residual lignin of the experiments carried out under hydrogenolytic conditions where residual lignin percentage increased as the lignin molecular weight was smaller. Depolymerization degree could have also been evaluated by determining residual lignin molecular weight. While hydrothermal lignin depolymerization did not show any trend toward the molecular weight of lignin fractions, hydrogenolytic conditions provided higher depolymerization degree as the lignin molecular weight was higher (F1>F2>…>F6).

The major difference concerning residual lignin was the occurrence of repolymerization phenomena. Lignin hydrothermal depolymerization favored reactions between instable fragments and original lignin. These instable fragments reacted with the original lignin instead of forming final phenolic monomeric products (repolymerization). Thus, these reactions limited obtained phenolic yields of lignin hydrothermal depolymerization. Differently, employed hydrogenolysis optimized conditions (formic acid + Ni10%AlSBA15) did not prompt this undesirable phenomenon.

Lignin hydrothermal depolymerization yielded more interesting compounds and the reaction produced more concentrated in simple monomers oil. However, repolymerization phenomenon constituted an important limitation that should be overcome. In that sense, the addition of a capping agent was study in order to improve lignin hydrothermal depolymerization. Two capping agents were studied and compared, namely boric acid and phenol, to determine their effect on lignin base catalyzed depolymerization. The studied capping agents presented totally different behaviors. Phenol experiments yielded high quantities of monomeric phenolic

compounds (cresols, catechols, ferulic acid...) that could be considered for further applications in material science or pharmaceutical industries, while boric acid yielded, above all, complex dimers. Boric acid prevented in some extent repolymerization phenomenon by increasing char formation. Phenol capping agent yielded low char content and its residual lignin slightly decreased. The main action of phenol capping agent was to prevent oligomerization reaction by not avoiding demethoxylation, dealkylation... reactions and that is why monomeric compounds concentration in oil rose dramatically comparing to the blank experiment. Repolymerization phenomenon was avoided in some extent at low capping agents' concentrations.

## 6.2 Future work

To continue the work in this field, the following lines of research could be tackled.

- Valorization of cellulose fraction to prove that the entire process could be considered for being adopted by lignocellulosic biorefinery. Cellulose fraction could be used for bioethanol production, paper manufacturing or fibers obtaining.

- Hydrothermal depolymerization optimization by studying the accurate amount of phenol that improves the process. Also, more knowledge about reaction mechanism would help to overcome yields limitation.

- Hydrogenation depolymerization should be deeply studied in order to improve oil yields and to better understand the reaction mechanism.

- Other lignin depolymerization processes involving enzymes could be considered to obtain simple monomeric compounds.

- Other lignin valorization processes such as liquefaction, pyrolysis or gasification could be regarded with lignin stream valorization objective.

- Scaling up the process is an interesting matter, considering energetic studies…

- Product separation is a challenging issue since the phenolic oil contains a mixture of these products.

## 6.2 List of publications and presentations

The work carried out along this thesis has led to numerous scientific articles. In addition, different studies contained in the thesis have also been presented at various conferences and international working group meetings. Bellow, the different contributions are listed.

### 6.2.1 Publications

6.2.1.1 Scientific articles

| | |
|---|---|
| **Authors** | **A. Toledano**, X. Erdocia, L. Serrano, J. Labidi |
| **Title** | Influence of extraction treatment on olive tree (Olea europaea) pruning lignin structure |
| **Journal** | Environmental Progress & Sustainable Energy. |

| | |
|---|---|
| | doi:10.1002/ep.11725. |
| **Year** | 2012 |
| **Impact factor** | 1.649 (JRC 2011) |
| **Rank** | 47/133 (Chemical Engineering) (JRC 2011) |

| | |
|---|---|
| **Authors** | **A.Toledano**, L. Serrano, A. Pineda, A.M. Balu, R. Luque, J. Labidi |
| **Title** | Fractionation of organosolv-lignin from olive tree pruning and its valorisation to simple phenolic compounds |
| **Journal** | ChemSusChem. Accepted. |
| **Year** | 2012 |
| **Impact factor** | 6.325 (JRC 2010) |
| **Rank** | 15/147 (Chemistry Multidisciplinary) (JRC 2010) |

| | |
|---|---|
| **Authors** | **A.Toledano**, L. Serrano, J. Labidi, A. Pineda, A.M. Balu, R. Luque |
| **Title** | Heterogeneously catalysed mild hydrogenolytic depolymerisation of lignin under microwave irradiation using hydrogen-donating solvents. |
| **Journal** | ChemCatChem. doi:10.1002/cctc.201200616 |
| **Year** | 2012 |
| **Impact factor** | 5.207 (JRC 2011) |
| **Rank** | 24/134 (Chemistry, Physics) (JRC 2011) |

| | |
|---|---|
| **Authors** | **A. Toledano**, L. Serrano, A. Pineda, A.A. Romero, R. Luque, J. Labidi |
| **Title** | Microwave-assisted depolymerisation of crude lignin via mild hydrogen-free hydrogenolysis: catalyst screening |
| **Journal** | Applied Catalysis B: Environmental. doi: |

| | |
|---|---|
| | 10.1016/j.apcatb.2012.10.015 |
| **Year** | 2012 |
| **Impact factor** | 5.625 (JRC 2011) |
| **Rank** | 6/133 (Chemical Engineering) (JRC 2011) |

| | |
|---|---|
| **Authors** | **A. Toledano**, L. Serrano, J. Labidi |
| **Title** | Process for olive tree pruning lignin revalorisation |
| **Journal** | Chemical Engineering Journal. DOI: 10.1016/j.cej.2012.04.068 |
| **Year** | 2012 |
| **Impact factor** | 3.074 (JRC 2010) |
| **Rank** | 10/135 (Chemical Engineering) (JRC 2010) |

| | |
|---|---|
| **Authors** | **A. Toledano**, L. Serrano, J. Labidi |
| **Title** | Effect of capping agents on base catalyzed lignin depolymerization |
| **Journal** | Fuel. Under Revision. |
| **Year** | 2012 |
| **Impact factor** | 3.248 (JRC 2011) |
| **Rank** | 13/133 (Chemical Engineering) (JRC 2011) |

| | |
|---|---|
| **Authors** | **A. Toledano**, L. Serrano, J. Labidi |
| **Title** | Extraction and revalorization of olive tree (Olea Europea) pruning lignin |
| **Journal** | Journal of the Taiwan Institute for Chemical Engineers. Accepted. |
| **Year** | 2012 |
| **Impact factor** | 2.110 (JRC 2011) |
| **Rank** | 34/133 (Chemical Engineering) (JRC 2011) |

| | |
|---|---|
| **Authors** | **A. Toledano**, L. Serrano, J. Labidi |
| **Title** | Organosolv lignin depolymerization with different base catalyst |
| **Journal** | Journal of chemical technology and biotechnology. DOI 10.1002/jctb.3799 |
| **Year** | 2012 |
| **Impact factor** | 1.818 (JRC 2010) |
| **Rank** | 37/135 (Chemical Engineering) (JRC 2010) |

| | |
|---|---|
| **Authors** | **A. Toledano**, L. Serrano, J. Labidi. |
| **Title** | Enhancement of lignin production from olive tree pruning integrated in a Green Biorefinery |
| **Journal** | Industrial & Engineering Chemical Research 50, 6573–6579 |
| **Year** | 2011 |
| **Impact factor** | 2.072 (JRC 2010) |
| **Rank** | 29/135 (Chemical Engineering) (JRC 2010) |

| | |
|---|---|
| **Authors** | A. García, **A. Toledano**, M.A. Andrés, J. Labidi. |
| **Title** | Study of the antioxidant capacity of Miscanthus sinensis lignins |
| **Journal** | Process Biochemistry 45 (6), 935-940 |
| **Year** | 2010 |
| **Impact factor** | 2.648 (JRC 2010) |
| **Rank** | 17/135 (Chemical Engineering) |

| | |
|---|---|
| **Authors** | **A. Toledano**, L. Serrano, A. García, I. Mondragon, J. Labidi. |
| **Title** | Comparative study of lignin fractionation by ultrafiltration and selective precipitation. |
| **Journal** | Chemical Engineering Journal 157, 93–99 |

| | |
|---|---|
| **Year** | 2010 |
| **Impact factor** | 3.074 (JRC 2010) |
| **Rank** | 10/135 (Chemical Engineering) (JRC 2010) |

| | |
|---|---|
| **Authors** | **A. Toledano**, A. García, I. Mondragon, J. Labidi. |
| **Title** | Lignin separation and fractionation by ultrafiltration. |
| **Journal** | Separation and purification technology 71, 38–43 |
| **Year** | 2010 |
| **Impact factor** | 2.775 (JRC 2010) |
| **Rank** | 14/135 (Chemical Engineering) (JRC 2010) |

| | |
|---|---|
| **Authors** | A. García, **A. Toledano**, L. Serrano, I. Egüés, M. González, F. Marín, J. Labidi |
| **Title** | Characterization of lignins obtained by selective precipitation |
| **Journal** | Separation and purification technology 68, 193–198 |
| **Year** | 2009 |
| **Impact factor** | 2.879 (JRC 2009) |
| **Rank** | 11/135 (Chemical Engineering) (JRC 2009) |

#### 6.2.1.2 Book chapters

| | |
|---|---|
| **Authors** | L. Serrano, **A. Toledano**, A. García, J. Labidi |
| **Chapter** | Obtaining of lignins for specific applications |
| **Book** | Lignin: Properties and Applications in Biotechnology and Bioenergy |
| **Year** | 2012 |
| **Editorial** | Nova Science Publishers |

**ISBN** 9781611229073

### 6.2.2 Communications

**Authors** **A. Toledano**, X. Erdocia, L. Serrano, J. Labidi

**Title** Proposal of catalytic process for lignin valorization

**Congress** Advances in catalysis for biomass valorization

**Participation** Poster

**Year** 2012

**Place** Thesalonik, Greece

**Authors** **A. Toledano**, L. Serrano, A. Sequeiros, X. Erdocia, J. Labidi

**Title** Enhacement of lignin production olive tree pruning by organosolv treatment

**Congress** International congress of chemical engineering. ANQUEICCE

**Participation** Oral presentation

**Year** 2012

**Place** Sevilla, Spain

**Authors** **A. Toledano**, L. Serrano, X. Erdocia, J. Labidi

**Title** From organosolv olive tree pruning lignin to chemicals: screening catalyst

**Congress** COST FP0901 - Analytical techniques for Biorefineries

**Participation** Poster

**Year** 2012

**Place** Tulln, Austria

**Authors** **A. Toledano**, L. Serrano, J. Labidi

**Title** Enhancement of lignin production from olive tree pruning by organosolv treatment

**Congress** WOODCHEM

**Participation** Poster

**Year** 2011

**Place** Strasbourg, France

**Authors** **A. Toledano**, L. Serrano, J. Labidi

**Title** Homogeneous catalytic pathway to produce chemicals from organosolv olive lignin.

**Congress** 8th European Congress of Chemical Engineering.

**Participation** Oral presentation

**Year** 2011

**Place** Berlin, Germany

**Authors** **A. Toledano**, L. Serrano, I. Egües, C. Sanchez

**Title** Alternative feedstock for biorefinery

**Congress** COST FP0602 meeting – Biotechnical processing of lignocellulosic raw material.

**Participation** Poster

**Year** 2010

**Place** Çesme, Turkey.

**Authors** **A. Toledano**, I. Egues, M.A. Andres. R. Llano-Ponte, J. Labidi

**Title** Lignocellulosic Biorefinery approach: a challenge for a new world

| | |
|---|---|
| **Congress** | Pres10 13th International Conference. Process Integration, Modeling and Optimisation for Energy Saving and Pollution Reduction |
| **Participation** | Poster |
| **Year** | 2010 |
| **Place** | Prague, Czech Republic |
| **Authors** | **A. Toledano**, A. García, M. González, J. Labidi |
| **Title** | Obtaining of lignin for specific applications |
| **Congress** | COST CM0903 meeting (UBIOCHEM) - Utilisation of Biomass for Sustainable Fuels & Chemicals |
| **Participation** | Poster |
| **Year** | 2010 |
| **Place** | Córdoba, Spain |

| | |
|---|---|
| **Authors** | **A. Toledano**, A. Garcia, R. Llano-ponte, J. Labidi |
| **Title** | Lignin fractionation. Comparative study between two different methods: ultrafiltration and selective precipitation |
| **Congress** | COST FP0901 meeting – Analytical techniques for Biorefineries |
| **Participation** | Poster |
| **Year** | 2010 |
| **Place** | Viena, Austria |

| | |
|---|---|
| **Authors** | **A. Toledano**, A. García, L. Serrano, R. Llano-Ponte, J. Labidi. |
| **Title** | Characterization of key functional groups of lignin |
| **Congress** | ITALIC. 5th Italian meeting on lignocellulosic chemistry |
| **Participation** | Oral presentation |
| **Year** | 2009 |
| **Place** | Varena, Italy |

| | |
|---|---|
| **Authors** | A. García, **A. Toledano**, I. Egües, R. Briones, M. A. Andrés, J. Labidi |
| **Title** | Study of the antioxidant capacity of Miscanthus Sinensis lignin |
| **Congress** | ITALIC. 5th Italian meeting on lignocellulosic chemistry |
| **Participation** | Poster |
| **Year** | 2009 |
| **Place** | Varena, Italy |

| | |
|---|---|
| **Authors** | **A. Toledano**, A. García, I. Egües, R. Llano-Ponte, J. Labidi. |
| **Title** | Study of fractionation of lignin by ultrafiltration and selective precipitation |
| **Congress** | ISWFPC 2009. 15th International Symposium on Wood, Fibre and Pulping Chemistry |
| **Participation** | Poster |
| **Year** | 2009 |
| **Place** | Oslo, Norway |

| | |
|---|---|
| **Authors** | **A. Toledano**, I. Egües, A. García, M. González, Mª. A. Andrés, R. Llano-Ponte, J. Labidi. |
| **Title** | Lignin separation and fractionation by ultrafiltration |
| **Congress** | ACHEMA. 29th International Exhibition-Congress on Chemical Engineering, Environmental Protection and Biotechnology |
| **Participation** | Oral presentation |
| **Year** | 2009 |
| **Place** | Frankfurt, Germany |

| | |
|---|---|
| **Authors** | M. González, A. García, **A. Toledano**, R. Llano-Ponte, M. A. de Andrés, J. Labidi. |
| **Title** | Lignocellulosic feedstock biorefinery processes. Analysis and design. |

| | |
|---|---|
| **Congress** | I-Cheap9 - Ninth International Conference on Chemical & Process Engineering |
| **Participation** | Oral presentation |
| **Year** | 2009 |
| **Place** | Rome, Italy |

| | |
|---|---|
| **Authors** | A. García, I. Egües, **A. Toledano**, M. González, L. Serrano, J. Labidi . |
| **Title** | Biorefining of lignocellulosic residues using ethanol organosolv process. |
| **Congress** | Pres09 12th International Conference. Process Integration, Modeling and Optimisation for Energy Saving and Pollution Reduction |
| **Participation** | Poster |
| **Year** | 2009 |
| **Place** | Rome, Italy |

# APPENDIX

# APPENDIX I. PROCEDURES FOR THE CHARACTERIZATION OF RAW MATERIAL AND SOLID FRACTIONS

The raw material and solid fractions were characterized using the procedures described in the standards developed by Technical Association of Pulp and Paper Industries (TAPPI), as detailed below:

**Sample preparation (TAPPI T257-cm85)**

The objective of this standard is to set the conditions suitable size of the raw material or sample so that it is homogeneous and suitable for the chemical treatments which will be performed to determine the chemical composition of the fibers.

The sample preparation consists of grinding the sample in a mill Restch 2000, neglecting the fraction with a size less than 0.25 mm. In the sieve (Controls) placed the ground raw material to separate the fractions suitable for further analysis. Raw material is selected with a size between 0.4 and 0.25 mm, ie, those that remain on the sieve of 0.25 mm.

**Moisture content (TAPPI T264-cm97, 8.2 section)**

This moisture corresponds to the equilibrium moisture content of the sample, and will be taken into account in subsequent analyzes. The procedure to determine the moisture consists of:

- Carefully clean the empty crucible and ignite in an oven at 105 ± 3 °C for 30-60 minutes. Cool slightly and then place in a desiccator. When cooled to

room temperature, weigh the ignited crucible on the analytical balance to the nearest 0.1 mg.

- Accurately weigh 2.00 ± 0.001 g of sample (m)
- Place in the oven at 105 ± 3 °C for 24 hours.
- After that time, samples were transferred to a desiccator until cool. After cooling the sample, weighing until the weight of the sample is constant to ± 0.2 mg.

The moisture is determined as follows:

$$\text{Moisture}, \% = \left[\frac{\text{A}}{\text{B}}\right] \text{x } 100$$

where A moisture-free weight of sample (g) and B is weight of the sample (g).

**Ash content at 525 ºC (TAPPI T211-om93)**

The ash content of the sample may consist of: (1) various residues from chemicals used in its manufacture, (2) metallic matter from piping and machinery, (3) mineral matter in the pulp from which the paper was made, and (4) filling, coating, pigmenting and/or other added materials. The amount and composition of the ash is a function of the presence or absence of any of these materials or others singly or in combination.

The procedure to determine the ash content at 525 ºC consists of:

- The test specimen, 1 g moisture free, shall be weighed on an analytical balance to the nearest 0.1 mg.
- Carefully clean the empty crucible and ignite in a muffle furnace at 525 ± 25 °C for 30-60 minutes. After ignition, cool slightly and then place in a dessicator. When cooled to room temperature, weigh the ignited crucible on the analytical balance to the nearest 0.1 mg.

- Transfer the test specimen to the crucible. Place the crucible, with lid removed, in a furnace at about 100 °C. Raise the temperature to 525 °C slowly so that the sample becomes carbonized without flaming. Sample must be charred, not burned so that the temperature of the sample does not exceed 525 °C. When the residue has ceased to char, place the crucible with specimen into the furnace at 525 ± 25 °C and remove the lid after the crucible seems to have reached the temperature of the furnace.
- When the specimen is completely combusted as indicated by the absence of black particles, remove the crucible from the furnace, replace the cover, and allow to cool somewhat; then place in a dessicator containing indicating grade anhydrous alumina and cool to room temperature. Weigh the crucible with ash to the nearest 0.1 mg. Repeat the ignition and weighing until the weight of the ash is constant to ± 0.2 mg.

The ash content at 525 ºC is determined as follows:

$$\text{Ash content}, \% = \left[\frac{\text{A}}{\text{B}}\right] \text{x } 100$$

where A initial weight of ash (g) and B is weight of the test specimen after extraction (g).

**Hot-water solubility (TAPPI T207-om93)**

This test method describes procedures for the determination of the hot water soluble materials in wood and pulp. Most of the inorganic components of the fibers, as well as gums, tannins, starches, sugars, dyes and compounds from the partial degradation of the holocellulose are solubilized.

The procedure to determine the hot-water solubility consists of:

- Weigh duplicate 2.0 ± 0.1 g specimens (moisture-free weight) to the nearest milligram, for cold-water solubility, or two similar specimens for hot-water solubility.
- Transfer the specimen to a 250 mL Erlenmeyer flask, add 100 mL of hot distilled water and place in a boiling water bath. Attach the reflux condenser and digest for 3 h, making certain the water level of the bath is held above the stock level in the flask.
- After this time, transfer the contents of the flask to a tared filtering crucible which has been previously dried to a constant weight at 105 ± 2 °C, wash with 200 mL of hot water and dry to constant weight at 105 ± 3 °C.

The hot-water solubility is determined as follows:

$$\text{Hot} - \text{water solubility}, \% = \left[\frac{\text{A}}{\text{B}}\right] \text{x } 100$$

where A initial weight of the test specimen (g, oven dry) and B is weight of the test specimen after extraction (g).

**NaOH solubility (TAPPI T212-om98)**

Hot alkali solution extracts low-molecular-weight carbohydrates consisting mainly of hemicelluloses and degraded cellulose in wood and pulp. The solubility of wood could indicate the degree of fungus decay or of degradation by heat, light, oxidation, etc.

The procedure to determine the solvent extractives consists of:

- Allow the sample to come to moisture equilibrium in the atmosphere near the balance; then weigh out two test specimens of 2.0 ± 0.1 g to the nearest 1.0 mg. Place the test specimens in 200 mL tall-form beakers.
- Add 100 ± 1 mL of 1% NaOH solution and stir with a glass rod.

- Cover the beaker with a watch glass and place in a water bath maintained at 97-100 °C for a period of 60 minutes. Keep the water in the bath boiling and its level above that of the alkali solution in the beaker. Stir the pulp with a rod for about 5 s at 10, 15, and 25 minutes after placing in the bath.
- At the end of 60 minutes, transfer the material to a tared filtering crucible and wash with 100 mL of hot water. Then add 25 mL of 10% acetic acid and allow soaking for 1 minute before removal. Repeat this step with a second 25 mL portion of 10% acetic acid. Wash the material finally with hot water until acid free.
- Dry the crucible and contents in an oven at 105° ± 3 °C to a constant weight, cool in a dessicator, and weigh.

The NaOH solubility is determined as follows:

$$1\%\ \text{NaOH solubility}, \% = \left[\frac{\text{A} - \text{B}}{\text{A}}\right] \text{x}\ 100$$

where A is oven-dry weight of the test specimen before extraction (g) and B oven-dry weight of the test specimen after extraction (g).

**Solvent extractives (TAPPI T204-cm97)**

This method describes a procedure for determining the amount of solvent-soluble, non-volatile material in wood and pulp. Since the pulping process usually removes most water-soluble and volatile compounds that are also soluble in organic solvents, the solvent extractable material in pulp may be considered to consist primarily of resin and fatty acids and their esters, waxes, and unsaponifiable substances. The procedure to determine the solvent extractives consists of:

- Place 4.0 ± 0.1 g (m) (accurately weight) of dry raw material on a extraction thimble (cellulose cartridge). Cap the cartridge with another cartridge to prevent sample losses.

- Place the extraction thimble and specimen in position in the Soxhlet apparatus. Fill the extraction flask with 150 mL of toluene-ethanol mixture (1:2 v/v).
- Connect the flask to the extraction apparatus, and start water flow to the condenser section. Adjust the heaters to provide a boiling rate which will cycle the specimens for not less than 24 extractions over a 4-5-h period. If the extraction is left unattended, a provision should be made to shut off the heat if the water and/or the electricity shut off unexpectedly.
- Remove the flask from the apparatus and partially evaporate the solvent in the extraction flask to a volume of 20-25 mL. Transfer the extract to the tared weighing dish by washing with small amounts of fresh solvent. Handle the weighing dish with forceps or tongs.
- Dry the dish and contents in an oven for 1 h at 105 ± 3ºC, cool in a dessicator, and weigh to the nearest 0.1 mg.

The percentage of extractives. is determined as follows:

$$\text{Extractives}, \% = \left[\frac{W_e - W_b}{W_p}\right] \text{x } 100$$

where $W_e$ is oven-dry weight of extract (g), $W_p$ is oven weight of wood or pulp (g) and $W_b$ is oven-dry weight of blank residue (g).

**Acid-insoluble lignin (TAPPI T-222-om98)**

Some of the lignin dissolves in acid solution during the test and is not included in the test result. In softwoods (coniferous woods) and in sulfate pulps, the amount of soluble lignin is small, about 0.2 to 0.5%. In hardwoods (deciduous woods), non-wood fibers, and in sulfite pulps, the content of soluble lignin is about 3 to 5%. The carbohydrates in wood and pulp are hydrolyzed and solubilized by sulfuric acid.

The procedure to determine the acid-insoluble lignin consists of:

- Weigh out two test specimens to the nearest 0.1 mg as follows: for wood, 1.0 ± 0.1 g; for pulp, 2.0 ± 0.1 g, equivalent to oven-dry weight. Place the test specimens in 100-mL beakers. Samples should be previously extracted.
- Add to the beakers containing the test specimens cold (10 to 15 °C) 72% sulfuric acid, 15.0 mL for a wood and 40.0 mL for a pulp specimen. Add the acid gradually in small increments while stirring and macerating the material with a glass rod. Keep the beaker in a bath at 20 ± 1 °C for 2 h. Stir the material frequently during this time to ensure complete solution.
- Add about 300 to 400 mL of water to a flask and transfer the material from the beaker to the flask. Rinse and dilute with water to 3% concentration of sulfuric acid, to a total volume of 575 mL for wood, and to 1540 mL for pulps.
- Boil the solution for 4 h, maintaining constant volume either by using a reflux condenser or by frequent addition of hot water.
- Allow the insoluble material (lignin) to settle, keeping the flask in an inclined position. If the lignin is finely dispersed, it may require an "overnight" or a longer period to settle. Without stirring up the precipitate, decant or siphon off the supernatant solution through a filtering crucible. Then transfer the lignin quantitatively to the filter, using hot water and a rod with rubber policeman. Wash the lignin free of acid with hot water.
- Dry the crucible with lignin in an oven at 105 ± 3°C to constant weight. Cool in a dessicator and weigh.

The percentage of acid-insoluble lignin is determined as follows:

$$\text{Acid} - \text{insoluble lignin}, \% = \left[\frac{\text{A}}{\text{W}}\right] \text{x } 100$$

where A is weight of lignin (g) and W is the oven-dry weight of test specimen (g).

**Holocellulose content (Wise et al. 1946)**

Holocellulose is defined as the fraction of water-insoluble carbohydrate present in plant raw materials, grouping cellulose and hemicelluloses present in the fibers. The method of Wise et al. [35] is based on chlorine dioxide which emerges in successive treatments with sodium chlorite dissolved lignin while carbohydrates remain unchanged.

The procedure to determine holocellulose consists of:

- Weigh 2.5 ± 0.1 g of sample (m) and placed in a beaker. Add 80 mL of hot distilled water (70-80 °C). The mixture was immersed in a bath at 70 °C and stirred periodically to homogenize.
- Every 60 min, add 0.5 mL of glacial acetic acid and 2.6 mL of 25% sodium chlorite to the beaker. Repeat these additions till cover a total period of 6-8 h.
- After that time the mixture is kept in the bathroom for 12 h without further additions.
- The vessel contents were poured over the filter (previously dried and tared) and filtered under vacuum, washing with hot water until neutral pH.
- Dry the crucible with lignin in an oven at 105 ± 3°C to constant weight. Cool in a dessicator and weigh.

The percentage of holocellulose is determined as follows:

$$\text{Holocellulose}, \% = \left[\frac{\text{A}}{\text{W}}\right] \text{x } 100$$

where A is weight of the isolated holocellulose (g) and W is the oven-dry weight of initial sample (g).

**α-cellulose content (Rowell et al. 1983)**

Since the TAPPI T203-om93 ("Determination of α, β and γ cellulose pulp") is defined only for paper pulp, and places special emphasis on it, it was decided to use the protocol proposed by Rowell et al. to determine the content of α-cellulose and hemicelluloses in wood samples. The term "hemicelluloses" is defined in this method as components of plant cell wall that are solubilized by treatment with sodium hydroxide and acetic acid, while the α-cellulose corresponds to the fraction remaining insoluble holocellulose after such treatment.

The procedure to determine α-cellulose consists of:

- Accurately weigh 2 ± 0.1 g of sample (m) of dry holocellulose free extracts, extracted from the fibers by the method described in the previous section (Wise method) in a beaker.
- Add 10 mL of 17.5% NaOH solution with stirring. Subsequently, add 5 mL of 17.5% NaOH solution every 5 minutes until reaching 15 mL of NaOH solution (3 additions of 5 mL). Wait for 30 minutes to the alkali solution to react with the sample at room temperature.
- Then, add 33 ml of distilled water at room temperature while stirring. Keep the solution at room temperature for 1 hour.
- The vessel contents were poured over the filter (previously dried and tared) and filtered under vacuum.
- The solid residue (α-cellulose) is washed with 100 ml 8.3 % of NaOH solution after which it is washed with distilled water two more times.
- Then, add 15 ml of 10% acetic acid allowing it to react 3 minutes before connecting the vacuum. Finally washed with distilled water until the filtrate is free from acid (pH neutral).
- Dry the filter at 105 ± 3 °C, cooled in dessicator and weighed (mf). Hemicelluloses are calculated by difference from the initial sample.

The percentage of α-cellulose is determined as follows:

$$\alpha - \text{cellulose}, \% = \left[\frac{\text{A}}{\text{W}}\right] \text{x } 100$$

where A is weight of the isolated α-cellulose (g) and W is the oven-dry weight of initial sample (g).

and the hemicelluloses content as follows:

% Hemicelluloses = % Holocellulose - % α-celullose

**REFERENCES**

Wise, L.E.; Murphy, M.; D'Adieco, A.A. 1946. Chlorite holocellulose, its fractionation and bearing on summative wood analysis and on studies on the hemicelluloses. Paper Trade J 122, 35-43.

Rowell, R. 1983. The chemistry of solid wood. Based on short course and symposium sponsored by the Division of Cellulose, Paper and Textile Chemistry at the 185th meeting of the American Chemical Society, Seattle, Washington, USA.

# APPENDIX II. PROCEDURES FOR LIGNIN CHARACTERIZATION

The obtained lignin by different pretreatments and ultrafiltered lignin fractions were characterized using the procedures described in the standards developed by International Lignin Institute (ILI) and internal procedures adapted to our facilities, as detailed below:

## Acid-insoluble lignin

Acid insoluble lignin (AIL) was determined by subjecting lignin to an acid hydrolysis process consisting in two stages. The first acidic hydrolysis was carried out adding 3.75 mL of sulphuric acid 72% to 0.375 g of lignin. The mixture was left for 1 hour at 30 ºC. Then it was diluted with 36.25 mL of deionized water for 3 hours at 100 ºC. After this time, the solution was cooled for 15 minutes and then filtered using filters over G4 glass filter crucible. The remaining solid is the acid insoluble lignin.

The acid-insoluble lignin is determined as follows:

$$\mathrm{AIL}, \% = \left[\frac{\mathrm{B} - \mathrm{A}}{\mathrm{C}}\right] \mathrm{x}\, 100$$

where A weight glass filter crucible (g), B weight glass filter crucible + dried residue (g) and C initial weight sample (g).

## Acid-soluble lignin

Acid soluble lignin (ASL) was determined by spectrophotometry (UV absorption at 205 nm). Filtrate samples had to be diluted with 1M $H_2SO_4$ until the absorbance was between 0.1 to 0.8 $cm^{-1}$.

The acid-soluble lignin is determined as follows:

$$\text{ASL}, \% = \left[\frac{\text{A} * \text{B} * \text{C}}{\text{D} * \text{E}}\right]$$

where A is the absorbance at 205 nm, B is dilution factor, C is filtrate volume (L), D is extinction coefficient of lignin (110 $g \cdot L^{-1} \cdot cm^{-1}$) and E is the initial lignin weight (g).

**Sugars content**

Sugars content was determined injecting the obtained filtrate from AIL analysis into a high performance liquid chromatography (Jasco LC Net II /ADC with a ROA Organic Acid (00H-0138-K0) column (Phenomenex) equipped with a refractive index detector (RI-2031Plus) and a photodiode array detector (MD-2018Plus)). 0.005 N $H_2SO_4$ prepared with 100 % deionized and degassed water was used as mobile phase (0.35 mL/min flow, 40 ºC and injection volume 20 µL). High purity standards of D-(+)-glucose, D-(+)-xylose and D-(-)-arabinose (provided by Fluka, with ≥99% of purity) were used for calibration.

The sugars content is determined as follows:

$$\text{Sugars content}, \% = \left[\frac{\text{A} * \text{B}}{1000 * \text{C}}\right] \text{x } 100$$

where A is obtained concentration by HPLC (ppm), B is filtrate volume (L), C is the initial lignin weight (g).

**Ash content**

A Thermogravimetric Analysis (TGA) was carried out in a TGA/SDTA RSI analyzer of Mettler Toledo to determine the ash content. The samples of approximately 7 mg were heated from 25 ºC up to 800 ºC at a rate of 10ºC/min in air atmosphere.

**Infrared spectroscopy**

Chemical structure of the different lignins was characterized by attenuated-total reflection infrared spectroscopy (ATR-IR) by direct transmittance in a single-reflection ATR System (ATR top plate fixed to an optical beam condensing unit with ZnSe lens) with an MKII Golden Gate SPECAC instrument. Transmittance spectra were recorded over 20 scans in the wavelength range from 4000 to 600 $cm^{-1}$, with a resolution of 4 $cm^{-1}$.

**Nuclear magnetic resonance**

NMR spectra were recorded at 30 ºC on a Bruker Avance 500 MHz equipped with a z-gradient BBI probe. Tipically, 40 mg of sample were dissolved in DMSO-d6. 2D-NMR (HSQC) spectra were recorded with a relaxation delay of 1.43 over 32 scans. The spectral widths were 5000 and 25000 Hz for the $^{1}H$ and $^{13}C$ dimensions, respectively.

**Molecular weight determination**

Lignins were subjected to High Performance Size Exclusion Chromatography (HPSEC) to evaluate lignin molecular weight (MW) and molecular weight distribution (MWD) using a JASCO instrument equipped with an interface (LC-NetII/ADC) and a reflex index detector (RI-2031Plus). Two PolarGel-M columns (300 x 7.5 mm) and PolarGel-M guard (50 x 7.5 mm) were employed. Dimethylformamide + 0.1% lithium bromide was the eluent. The flow rate was 0.7 mL/min and the analyses were carried out at 40 ºC. Calibration was made using polystyrene standards (Sigma-Aldrich) ranging from 266 to 70000g/mol. Therefore, the obtained values are relative to the employed polystyrene standards.

**Alkali nitrobenzene oxidation**

The chemical phenolic compositions were determined by alkaline nitrobenzene oxidation. 50 mg of lignin were placed in a tube with sodium hydroxide solution and nitrobenzene and left at 175 ºC for 2.5 hours. The oxidation products were analyzed by HPLC JASCO instrument equipped with an interface (LC-NetII/ADC) and a photodiode array detector (MD-2018). A Teknokroma Mediterranean Sea18 column (25 x 0.46 cm) was used for the experiments and a mixture of acetonitrile and water (1:8, m/m) with 1% of acetic acid was used a mobile phase. The flow rate was 0.5 mL/min and the analyses were carried out at 40 ºC. Calibration was made using pure compounds standards (Sigma-Aldrich) –vanillic acid, syringic acid, p-hydroxybenzoic acid, p-hydroxybenzaldehyde, vanillin, syringaldehyde, acetovanillone and ferulic acid-.

**Carboxyl groups' content**

Carboxyl groups were studied by aqueous titration. A weight of lignin sample (0.25 g) was suspended in 12.5 mL of 0.05 M sodium hydroxide. After stirring for approximately 3 hours until the complete dissolution of the lignin sample, the solution was potentiometrically titrated with 0.1 M hydrochloride acid until reaching a pH 7. Carboxyl groups were calculated as the difference between the added NaOH and the consumed.

The carboxyl groups' content is determined as follows:

$$\mathrm{COOH}, \% = \left[\frac{(\mathrm{N_{NaOH}} * \mathrm{V_{NaOH}} - \mathrm{N_{HCl}} * \mathrm{V_{HCl}}) * 4500}{\mathrm{m_{lignin}}}\right] \mathrm{x}\ 100$$

where $N_{NaOH}$ is the NaOH concentration, $V_{NaOH}$ is the added volumen of NaOH solution, $N_{HCl}$ is the hydrochloric acid concentration, $V_{HCl}$ is the volume consumed by the sample and $m_{lignin}$ is the initial lignin weight.

**Carbonyl gropus content**

Oximation reaction was used to determine lignin carbonyl content. Lignin was dissolved in 2 mL of DMSO. Once dissolved, 5 mL of oximating mixture were added to the solution and the mixture was heated at 80 ºC for two hours. After that time, the solution was potenciometrically titrated with hydrochloric acid.

The acid-insoluble lignin is determined as follows:

$$\mathrm{CO},\% = \left[\frac{(\mathrm{V_O} - \mathrm{V}) * \mathrm{C} * 2.801}{\mathrm{m}}\right] \mathrm{x}\ 100$$

where $V_0$ is the blank volume (mL), V is the volumen consumed by the sample (mL), C is the real concentration of hydrochloric acid solution (M), 2.801 is carbonyl group mass equivalent to 1 mL of 0.1 N HCl (mg) and m is the initial lignin weight (mg).

**Total phenolic groups content**

The total phenolic content in the analyzed lignin samples was determined by the Folin-Ciocalteau spectrophotometric method using gallic acid as reference compound and dimethyl sulfoxide as solvent. Each lignin solution (2 g/L in DMSO) was prepared for total phenolic content assay (0.5 mL of sample + 2.5 mL of Folin-Ciocalteau reagent + 5 mL of $Na_2CO_3$ 20% + distillate water up to 50 mL). The preparations were kept in a thermostatic bath at 40 ºC for 30 min, and afterwards the absorbance of the samples at 750 nm was registered, and the percentage of total phenolics in the lignin, as % of gallic acid equivalent, was calculated.

The total phenolic groups content is determined as follows:

$$\mathrm{OH},\% = \frac{\mathrm{C} * \mathrm{V} * 4 * 17}{170.12 * \mathrm{m}} \mathrm{x}\ 100$$

where C is the gallic equivalent concentration (ppm), 4 are the OH mmol in 1 gallic mmol, V is the solution volume (L), 170.12 is the gallic molecular weight and m is the initial lignin weight (ash free) (mg).

# APPENDIX III. PROCEDURES FOR THE CHARACTERIZATION OF LIQUID FRACTIONS

The obtained liquid fractions were physicochemically characterized using internal procedures, as detailed below:

## pH

The pH of the liquid fractions was determined using a pH meter "pH-2005 SELECTA".

## Density

Density was calculated gravimetrically by measuring the weight of the known volume of a volumetric flask filled with the liquid fraction.

## Total dissolved solids

The method for determining the content of total dissolved solids (TDS) in the liquid fraction is based on the procedure described in TAPPI Standard T264 cm-97, for the equilibrium moisture content of wood and pulp. Total dissolved solids were determined following an adaption of the procedure by the National Renewable Energy Laboratory NREL in standard LAP-012.

5 ± 0.001 g of the liquid fraction (m) are weight in a crucible free of moisture and a tared ($m_i$). The filled crucible is placed in an oven at 105 ± 3 °C for 24 hours. After cooling in a dessicator, the crucible is weighed ($m_f$) until constant weight.

The total dissolved solids are determined as follows:

$$\mathrm{TDS}, \% = \left[\frac{(\mathrm{m_f} - \mathrm{m_i})}{\mathrm{m}}\right] \mathrm{x}\, 100$$

where $m_f$ is the weight of the dried crucible (g), $m_i$ is the weight of the crucible (g) and m is the weight of the liquid fraction (g).

**Inorganic and organic matter**

The inorganic fraction of the liquid fraction can be determined after combustion of the sample, adapted procedure of TAPPI standard T211 om-93 (ashes at 525 °C).

The crucible assembly - solid residue obtained in the previous experiment (Total dissolved solids determination) is combusted in the oven at 525 °C for 3 hours. Subsequently, after cooling in a dessicator, the crucible is weighed assembly ($m_f$).

The inorganic matter (IM) is determined as follows:

$$\mathrm{IM}, \% = \left[\frac{(\mathrm{m_f} - \mathrm{m_i})}{\mathrm{m}}\right] \mathrm{x}\, 100$$

where $m_f$ is the weight of the dried crucible (g), $m_i$ is the weight of the crucible (g) and m is the weight of the liquid fraction (g).

The organic matter (OM) is determined as follows:

OM % = TDS % - IM %

**Lignin concentration**

The method for determining lignin concentration in the liquid fraction varies depending on the pretreatment applied to the raw material for lignin extraction. Nevertheless, the principle that governs all isolated procedures is the same, the insolubility of lignin in acid media.

A known volume of liquid fraction is treated with the corresponding lignin isolation procedure. Previously, the centrifuge tubes have to be dried over night at 50 ± 1 °C and then tared. Lignin suspensions are separated by centrifugation at 4000 rpm for 20 minutes. The liquid is removed and the centrifuge tubes with the isolated lignin are dried at 50 ± 1 °C till the lignin gets dried. Once dried, samples were transferred to a dessicator until cool. After cooling the sample, weighing until the weight of the sample is constant to ± 0.2 mg.

The lignin concentration is determined as follows:

$$\text{Lignin concentration } ({}^{g}/_{L}) = \left[\frac{(m_f - m_i)}{V}\right] \text{x } 100$$

where $m_f$ is the weight of the dried centrifuge tube + lignin (g), $m_i$ is the weight of the centrifuge tube (g) and V is the liquid fraction volume (L).

## LIST OF FIGURES


*Page*

**Figure 1.1.** Key crude oil spot prices in USD/barrel (IEA). 3

**Figure 1.2.** Biomass biorefiney scheme. Biorefinery inputs and outputs (Ragauskas et al. 2006). 5

**Figure 1.3.** Biomass schematic utilization possibilities (www.extension.org). 6

**Figure 1.4.** Schematic of plant cell wall utilization of lignin, hemicelluloses and cellulose. Adapted from (Sannigrahi et al. 2010). 8

**Figure 1.5.** Example of LCF Biorefinery products scheme (Kamm et al. 2006). 9

**Figure 1.6.** Schematic view of the components of cellulose fiber (Gandini 2008). 10

**Figure 1.7.** a) Structure of *O*-acetyl-(4-OMe-glucurono)xylan from hardwood. b) Structure of *O*-acetyl-galactoglucomannan. c) Structure of xylan from annual plants (Spiridon 2008). 12

**Figure 1.8.** Most common monolignols in lignin. H: p-coumaryl alcohol. G: conyferil alcohol. S: sinapyl alcohol. 13

**Figure 1.9.** Structural model of spruce lignin proposed by Adler 1977. 14

**Figure 1.10.** Current applications of lignosufonates (Bozel et al. 2007) 16

**Figure 1.11.** Lignin production and potential lignin derived product market and value (Gosselink 2011). 17

**Figure 1.12.** New product opportunities from lignin (Bozel et al. 2007). 18

**Figure 1.13.** Summary of lignin catalytic transformations to high added value products (Bozel et al. 2007). 18

**Figure 1.14.** Olive tree cultivation field with olive tree pruning. 19

**Figure 1.15.** Scheme of the objectives of this thesis. 21

**Figure 2.1.** Schematic of goals of pretreatment on lignocellulosic material (Mosier et al. 2005). 29

**Figure 2.2.** Olive tree pruning lignins ATR-IR spectra (4000-600 $cm^{-1}$). AL (black), HL (red) and OL (blue). 38

**Figure 2.3.** Olive tree pruning lignins magnified ATR-IR spectra (1800-800 $cm^{-1}$). AL (black), HL (red) and OL (blue). 39

**Figure 2.4.** HSQC spectra of extracted lignins from olive tree pruning. AL (alkali lignin), HL (autohydrolysis lignin) and OL (organosolv lignin). 40

**Figure 2.5.** Molecular weight distributions (HPSEC) of extracted lignins. AL (black), HL (red) and OL (blue) 44

**Figure 2.6.** Variation of lignin concentration (g/L) in the liquid fraction (LL) a) with the reaction time (normalized) and the ethanol concentration (normalized) at the central temperature point; b) with the temperature (normalized) and the ethanol concentration (normalized) at the central time point; c) with the temperature (normalized) and the reaction time (normalized) at the central ethanol concentration point. 55

**Figure 2.7.** Variation of lignin content (%, w/w) in pulp (LP) a) with the reaction time (normalized) and the ethanol concentration (normalized) at the central temperature point; b) with the temperature (normalized) and the ethanol concentration (normalized) at the central time point; c) with the temperature (normalized) and the reaction time (normalized) at the central ethanol concentration point. 57

**Figure 2.8.** ATR-IR spectra of the analyzed lignins isolated from most concentrated liquid fractions. 59

**Figure 2.9.** Scheme of the optimized lignin production process carried out. 63

**Figure 2.10.** ATR-IR spectrum of the organosolv olive tree pruning lignin (200ºC, 70% EtOH and 90 min.) 66

**Figure 2.11.** HSQC spectrum of the organosolv olive tree pruning lignin (200ºC, 70% EtOH and 90 min.) 67

**Figure 3.1**. Schematic operation of ultrafiltration membranes (Baker 2004). 84

**Figure 3.2.** Scheme of the used ultrafitration system. 85

**Figure 3.3.** Detail of the tubular ceramic ultrafiltration membrane section used in this work. 86

**Figure 3.4.** ATR-IR spectra of the obtained ultrafiltered organosolv olive tree pruning lignin. Black (F1), red (F2), blue (F3), green (F4), dark yellow (F5) and pink (F6). 89

**Figure 3.5.** Influence of molecular weight on lignin functionality. 93

**Figure 4.1.** Scheme of the products separation procedure carried out in the lignin depolymerization by hydrolysis. 105

**Figure 4.2.** Obtained oil yield by processing lignin with different bases that act as catalyst. Oil yields (%, w/w) referred to initial lignin weight. 109

**Figure 4.3.** MALDI-TOF analyses of the oil obtained by processing lignin with different bases that act as catalyst. 112

**Figure 4.4.** Obtained char yield by processing lignin with different bases that act as catalysts. Char yields (%, w/w) referred to initial lignin weight. 114

**Figure 4.5.** Recovered residual lignin after processing lignin with different bases that act as catalyst. Residual lignin (%, w/w) referred to initial lignin weight. 115

**Figure 4.6.** Molecular weight distributions of residual lignins recovered after processing lignin with different bases that act as catalyst (HPSEC). Left graphic: black (rough lignin), red (blank, $H_2O$), green (NaOH) and blue (KOH). Right graphic: black (rough lignin), purple (LiOH), dark yellow ($Ca(OH)_2$) y light blue ($K_2CO_3$). 116

**Figure 4.7.** Solids recovered in the first step of the separation procedure, composed by residual lignin and char. 119

**Figure 4.8.** Obtained oil yield by applying different severity factors. Oil yield (%, w/w) referred to initial lignin weight. 122

**Figure 4.9.** Proposed sequential reactions in base-catalyzed lignin depolymerization. (S) Syringol, (G) Guaiacol, (1) Phenol, (2) 4-Methylcatechol, (3) Catechol, (4) p-Cresol, (5) m-Cresol y (6) o-Cresol. 125

**Figure 4.10.** MALDI-TOF analyses of the obtained oil by applying different severity factors. 127

**Figure 4.11.** Obtained char yields by applying different severity factors. Char yields (%, w/w) referred to initial lignin weight. 128

**Figure 4.12.** Recovered residual lignin after applying different severity factors. Residual lignin (%, w/w) referred to initial lignin weight. 129

**Figure 4.13.** Molecular weight distributions of residual lignins recovered after applying different severity factors. Black (Rough lignin), red ($LogR_o$ 6.4), blue ($LogR_o$ 6.9), green ($LogR_o$ 7.3), dark yellow ($LogR_o$ 7.5) and magenta ($LogR_o$ 7.7). 130

**Figure 4.14.** Obtained oil yield of ultrafiltered lignin fractions. Oil yields (%, w/w) referred to initial lignin weight. 134

**Figure 4.15.** Suggested lignin intermediates mechanism during base catalyzed depolymerization. 136

**Figure 4.16.** MALDI-TOF oil analyses of each ultrafiltered lignin fractions. 137

**Figure 4.17.** Obtained char of ultrafiltered lignin fractions. Char yields (%, w/w) referred to initial lignin weight. 139

**Figure 4.18.** Recovered residual lignin of ultrafiltered lignin fractions. Residual lignin (%, w/w) referred to initial lignin weight. 140

**Figure 4.19.** Lignin revalorization process scheme. 141

**Figure 4.20.** Chemicals recovery scheme from BCD separation procedure. 143

**Figure 4.21.** Obtained oil yields after adding different capping agents. Oil yields (%, w/w) referred to initial lignin weight. 147

**Figure 4.22.** Chromatograms of experiments carried out using phenol as capping agent. Above (phenol 1:0.75), middle (phenol 1:1) and bottom (phenol 1:2). 152

**Figure 4.23.** MALDI-TOF oil analyses of each capping agent experiment. 154

**Figure 4.24.** Obtained char yields after adding different capping agents. Char yields (%, w/w) referred to initial lignin weight. 155

**Figure 4.25.** Recovered residual lignin after adding different capping agents. Residual lignin (%, w/w) referred to initial lignin weight. 157

**Figure 4.26.** Molecular weight distributions of residual lignins recovered after adding different capping agents. Left graphic: black (rough lignin), red (blank), blue ($H_3BO_3$ 1:0.75), green ($H_3BO_3$ 1:1) and magenta ($H_3BO_3$ 1:2). Right graphic: black (rough lignin), red (blank), blue (phenol 1:0.75), green (phenol 1:1) and magenta (phenol 1:2). 158

**Figure 5.1.** Scheme of products separation in hydrogenolysis screening experiments. 180

**Figure 5.2.** XRD patterns of 2 wt.% materials; from bottom to top A) Ni2%AlSBA; B) Pd2%AlSBA; C) Pt2%AlSBA; D) Ru2%AlSBA. 182

**Figure 5.3.** TEM micrographs of A) Ni2%AlSBA; B)Ni10%AlSBA (Ni nanoparticles can be spotted as little black dots) and C) Ni10%AlSBA showing some NP aggregates. 184

**Figure 5.4.** Obtained oil yields (%, w/w) referred to initial lignin weight for each catalyst. 185

**Figure 5.5.** Compounds found in isolated oils. (1) Tetralin (solvent) (2) Mesitol (3) 2,3,6-trimethylphenol (4) 6-ethyl-o-cresol (5) 4-ethyl-m-cresol (6) 3,4-dimethoxyphenol (7) Vanillin (8) Diethyl phthalate (9) Syringaldehyde (10) Butyl Octyl Ester Phthalate. 188

**Figure 5.6.** MALDI-TOF oil analyses of all catalysts in the depolymerization of lignin. 190

**Figure 5.7.** Obtained char yields (%, w/w) referred to initial lignin weight for each catalyst. 191

**Figure 5.8.** Residual lignin (%, w/w) referred to initial lignin weight for each catalyst. 193

**Figure 5.9.** Residual lignin HPSEC results for each catalyst. Left graphic: black (rough lignin), red (blank), blue (Ni2% SBA15), olive green (Ni5%AlSBA) and magenta (Ni10% AlSBA). Right graphic: black (rough lignin), purple (Pd2%AlSBA), dark yellow (Pt2%AlSBA) and light green (Ru2%AlSBA). 194

**Figure 5.10.** Elemental analyses of recovered residual lignins for each catalyst. 196

**Figure 5.11.** Obtained oil yields (%, w/w) referred to lignin weight for each 200

hydrogen-donor solvent.

**Figure 5.12.** Compounds found in isolated oils. (1) Guaiacol (2) Mesitol (3) 2,3,6-trimethylphenol (4) Syringol (5) Vanillin (6) Guaiacylacetone (7) 2,4'-dihydroxy-3'-methoxyacetophenone (8) Diethylphthalate (9) Methoxyeugenol (10) Syringaldehyde (11) Acetosyringone (12) Desaspidinol (13) Aspidinol (14) Butyl Octyl Ester Phthalate. 203

**Figure 5.13.** MALDI-TOF oil analyses of each hydrogen-donor solvent experiment. 206

**Figure 5.14.** Obtained char yields (%, w/w) referred to initial lignin weight for each hydrogen-donor solvent. 208

**Figure 5.15.** Residual lignin (%, w/w) referred to initial lignin weight for each hydrogen-donor solvent. 210

**Figure 5.16.** Residual lignin HPSEC results for each hydrogen-donor solvent. Left graphic: black (rough lignin), red (tetralin blank), blue (tetralin), olive green (isopropanol blank) and magenta (isopropanol). Right graphic: black (rough lignin), dark yellow (glycerol blank), purple (glycerol), orange (formic acid blank) and pink (formic acid). 211

**Figure 5.17.** Obtained oil yields (%, w/w) referred to initial lignin weight for each lignin fraction. 215

**Figure 5.18.** Simple phenolics obtained after heterogeneously catalyzed depolymerization of lignin fractions. (1) Guaiacol (2) Syringol (3) Vanillin (4) Guaiacylacetone (5) 4-hydroxyacetyl-2-methoxyphenol (6) Syringaldehyde (7) Acetosyringone (8) Desaspidinol (9) Aspidinol. 217

**Figure 5.19.** MALDI-TOF oil analyses of each lignin ultrafiltered fraction. 219

**Figure 5.20.** Residual lignin (%, w/w) referred to initial lignin weight for each lignin fraction. 220

**Figure 5.21.** Schematic representation of the novel cascade-type lignin valorization approach. 222

## LIST OF TABLES


*Page*

**Table 1.1.** Types and frequencies of interunitary linkages by some authors. 15

**Table 2.1.** Chemical (sulfur-free) lignocellulosic pretreatments. (Brodeur et al. 2011, Fengel et al. 1984) 31-32

**Table 2.2.** Physicochemical properties of the liquid fractions (dissolved lignin) obtained after applying different pretreatments to olive tree pruning. 36

**Table 2.3.** Yields (%, w/w) of the detected phenolic acids and aldehydes compounds released from olive tree pruning lignins by alkaline nitrobenzene oxidation. S corresponded to the sum of syringic acid and syringaldehyde yields. G corresponded to the sum of vanillic acid, vanillin and acetovanillone yields. 43

**Table 2.4.** Olive tree pruning lignins compositions extracted by different treatments. Weight-average (Mw), number-average (Mn) molecular weight and polydispersity (Mw/Mn) of the different lignins. 45

**Table 2.5.** Functional groups contents (%, w/w) of alkali lignin (AL), autohydrolysis lignin (HL) and organosolv lignin (OL). 48

**Table 2.6.** Experimental conditions applied to olive tree pruning. $X_T$ normalized temperature; $X_t$ normalized time; $X_C$ normalized ethanol concentration. 51

**Table 2.7.** Lignin content in pulp (LP) and lignin concentration in liquid fraction (LL) of the experimental design runs. 53

**Table 2.8.** Snedecor's F values for the terms in the obtained equations (3-4) for the lignin in liquor (LL) and lignin content in pulp (LP). $R^2$y adjusted-$R^2$ values obtained from the adjusted model equations (3) and (4). 54

**Table 2.9.** Thermogravimetric analyses data of the analyzed lignins isolated from most concentrated liquid fractions. T (temperature, ºC); WL (weight loss, %); R (residue, %). 61

**Table 2.10.** Chemical composition of the raw material (olive tree pruning) and the solid fraction derived from the optimized organosolv treatment. 64

**Table 2.11.** Physicochemical properties of the liquid fraction derived from the optimized organosolv treatment. 65

**Table 2.12.** Optimized organosolv lignin properties. Weight-average (Mw), number-average (Mn) molecular weight, polydispersity index (Mw/Mn), yields (%, w/w) of the detected phenolic acids and aldehydes compounds released from rough lignin alkaline nitrobenzene oxidation, rough lignin composition and functional groups contents (%, w/w). 68

**Table 3.1.** Molecular weight of obtained lignin fractions by the studied fractionation processes, ultrafiltration and selective precipitation. 80

**Table 3.2.** Common operating conditions and applications of different membrane separation processes (Mulder 1991). 83

**Table 3.3.** Lignin ultrafiltered fractions after using different membrane cut-offs. 87

**Table 3.4.** Physicochemical properties of obtained retentates by ultrafiltration. Density (g/L); TDS: total dissolved solids (%); OM: organic matter (%); IM: inorganic matter (%) and lignin concentration (g/L). 88

**Table 3.5.** Ultrafiltered lignin fractions composition. Composition (%, w/w). 90

**Table 3.6.** Weight-average (Mw), number-average (Mn) molecular weight and polydispersity (Mw/Mn) of the obtained ultrafiltered lignin fraction. 91

**Table 3.7.** Functional groups (%, w/w) of the ultrafiltered lignin fractions. 92

**Table 4.1.** Oil phenolic compounds obtained by processing lignin with different base catalysts. Compounds yields (%, w/w) referred to oil weight. 110

**Table 4.2.** HPSEC results of the first peak of the recovered residual lignins related to repolymerization phenomena. 117

**Table 4.3.** Studied conditions in the base catalyzed lignin depolymerization. 121

**Table 4.4.** Phenolic compounds obtained by applying different severity factors. Compound yields (%, w/w) referred to oil weight. 123

**Table 4.5.** HPSEC results of the first peak of the recovered residual lignins related to repolymerization phenomena for each severity factor. 131

**Table 4.6**. Phenolic compounds obtained from ultrafiltered lignin fractions. Compounds yields (%, w/w) referred to oil weight. 135

**Table 4.7.** HPSEC results of the first peak of the recovered residual lignins related to repolymerization phenomena for each ultrafiltered lignin fraction and their corresponding rough lignin. 140

**Table 4.8.** Initial pH of the resulting reaction mixtures composition (w/w). All experiments were carried out adding 4% (w/w) of sodium hydroxide as catalyst. 146

**Table 4.9.** Phenolic compounds obtained after adding different capping agents. Compounds yields (%, w/w) referred to oil weight. 148

**Table 4.10.** Dimers present in the obtained oil using phenol as capping agent. Compounds yields (%) referred to oil weight (w/w). 151

**Table 4.11.** HPSEC results of the first peak of the recovered residual lignins related to repolymerization phenomena for each capping agent ratio. 159

**Table 5.1.** Textural properties, metal content and nanoparticle sizes of the various investigated supported metal nanoparticles in the depolymerization of rough lignin. 181

**Table 5.2.** XPS data of the prepared catalysts including the main lines for the different metal nanoparticles. 183

**Table 5.3.** Compounds present in the obtained oil in screening catalyst study. Compounds yields concentration in mg of each compound per gram of lignin. 187

**Table 5.4.** Residual lignins number-average (Mn), weight-average (Mw) molecular weight and polydispersity (Mw/Mn) of residual lignin of screening catalyst study. Rough lignin was also characterized for comparative purposes. 195

**Table 5.5.** Compounds present in the obtained oil for each hydrogen-donor solvent. Compounds yields concentration in mg of each compound per gram of lignin. TL (tetralin), IP (isopropanol), GLY (glycerol) and FA (formic acid). 202

**Table 5.6.** Residual lignins number-average (Mn), weight-average (Mw) molecular weight and polydispersity (Mw/Mn) of residual lignin of each hydrogen-donor solvent experiment. Rough lignin was also characterized for 212

comparative purposes.

**Table 5.7.** Compounds present in the obtained oil for each ultrafiltered lignin fraction. Compounds yields concentration in mg of each compound per gram of lignin. 216
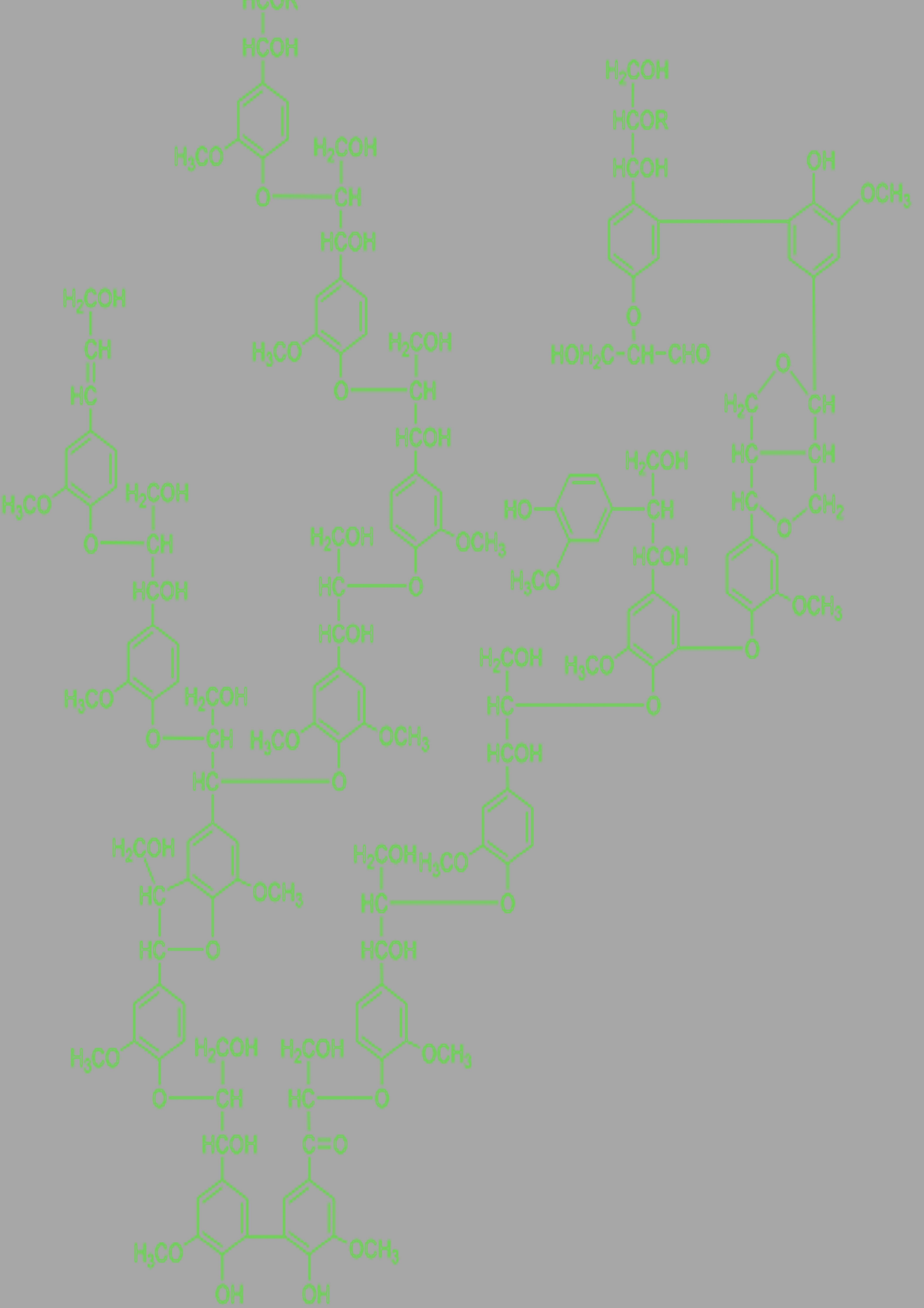
**Table 5.8.** HPSEC results. Number-average (Mn), weight-average (Mw) molecular weight and polydispersity (Mw/Mn) of ultrafiltered lignin samples and residual lignin of ultrafiltrated hydrogenolysis processes. 221